How light competition between plants affects trait optimization and vegetation-atmosphere feedbacks

Marloes P. van Loon

Thesis committee	Prof. dr. ir. P. M. van Bodegom Dr. C. Farrior Prof. dr. ir. B.J.J.M. van den Hurk Prof. dr. ir. G.A. Kowalchuk Prof. dr. ir. M.J. Wassen

Citation:	Van Loon, M.P. (2016) How light competition between plants affects trait optimization and vegetation-atmosphere feedbacks. PhD thesis, Utrecht University, The Netherlands.
Cover design and photo:	M.P. van Loon
ISBN:	978-90-393-6467-3
Printed by:	GVO drukkers & vormgevers B.V. | Ponsen & Looijen

How light competition between plants affects trait optimization and vegetation-atmosphere feedbacks

Hoe competitie tussen planten om licht de optimalisatie van planteneigenschappen en vegetatie-atmosferische terugkoppelingen beïnvloedt
(met een samenvatting in het Nederlands)

Proefschrift

ter verkrijging van de graad van doctor aan de Universiteit Utrecht op gezag van de rector magnificus, prof.dr. G.J. van der Zwaan, ingevolge het besluit van het college voor promoties in het openbaar te verdedigen op maandag 11 januari 2016 des middags te 2.30 uur

door

Marloes Petronella van Loon
geboren op 18 oktober 1988 te Kaatsheuvel

Promotoren:	Prof. dr. ir. N.P.R. Anten
	Prof. dr. ir. M. Rietkerk
Copromotor:	Dr. S.C. Dekker

Table of contents

Chapter 1

General introduction

1.1 Research context

The climate has changed drastically over the past century and is expected to continue to change in the future (IPCC 2014). The atmospheric CO_2 concentration is predicted to rise (Fig 1.1a), and partly as a result of this, global temperature will further increase (Fig 1.1b). It is also predicted that the nitrogen deposition rates will change; the magnitude of this change will depend on the region of the world (Fig 1.1c) (Lamarque *et al.* 2013; IPCC 2014). It is important to know how plants respond to these changes, as this determines future biodiversity and food production. Besides, plants have a large influence on atmospheric processes that influence the climate (Bonan 2008) through regulating the flows of water, nitrogen, carbon and energy (Sellers *et al.* 1997). So there is a two-way interaction between vegetation and the atmosphere, meaning that there are vegetation-atmosphere feedbacks. More explanation on vegetation-atmosphere feedbacks are provided in Box 1.1. In addition, it has been argued that these feedbacks at multiple scales are relevant for the functioning of the climate system as a whole (Rietkerk *et al.* 2011).

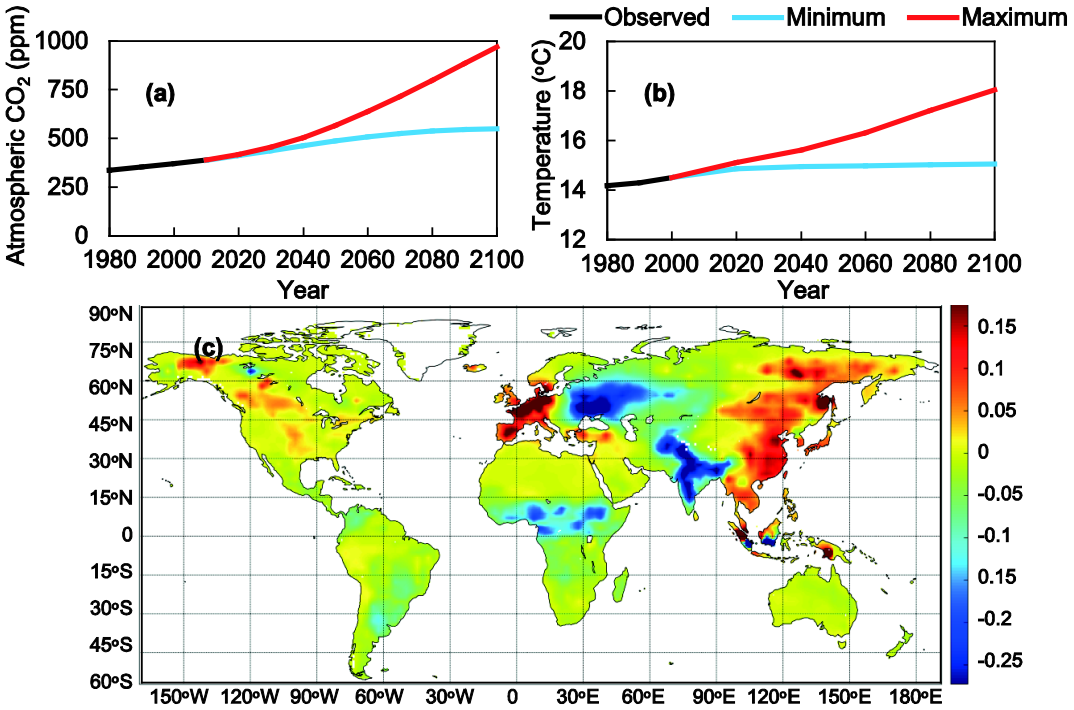

Fig 1.1 Global average atmospheric CO_2 concentration (a) and temperature (b) as observed (black line) and projected according to the IPCC scenarios of either the lowest (minimum, blue line) or the highest increase (maximum, red line). Panels a and b are modified from IPCC (2014). Spatial nitrogen deposition change from 1985 to 2005 in g m^{-2} yr^{-1} (c), source Lamarque *et al.* (2013)

Vegetation responses to elevated CO_2 are thought to have an important influence on atmospheric processes. For example, vegetation influences the carbon cycle by altering the CO_2 exchange. As plants take up CO_2 they reduce the carbon in the atmosphere and this uptake will counterbalance the expected increase in atmospheric CO_2, which thus entails a

negative vegetation-atmosphere feedback. Another example of a vegetation response to elevated CO_2, which might have an important influence on atmospheric processes, is the expected reduction of the stomatal conductance (Long *et al.* 2004) that results in an increased plant water use efficiency (WUE, ratio of carbon gain to water loss) (Keenan *et al.* 2013). This could lead to a reduced leaf transpiration rate and thereby to a rise of leaf temperature, resulting in more energy available for the sensible heat flux than for the latent heat flux as leaf temperature balances the energy budget (e.g. Bernacchi *et al.* 2007). This reduction in stomatal conductance could potentially contribute to increasing temperature and decreasing recycling of the precipitation (Field, Jackson & Mooney 1995). If a sufficient amount of plants exhibit this stomatal closure, this can have regional or even global effects on the climate. Contrary to this scenario, other studies predict that reduced stomatal conductance under elevated CO_2 will not affect the water cycle (e.g. Tor-ngern *et al.* 2015). These studies stress that elevated CO_2 reduces stomatal conductance and thus transpiration per unit leaf area, but that it will also result in the production of more leaf area and that the latter will compensate for the former (Tor-ngern *et al.* 2015). So, it is still unclear how plant responses to climate change will influence atmospheric processes.

Box 1.1 Modelling vegetation-atmospheric responses

The relationships and feedbacks between vegetation and the atmosphere can be studied with a coupled soil-water-atmosphere-plant model; Fig B1.1 shows a simplified representation of the main processes involved. In the model the atmosphere consists of the surface, mixed, boundary and free layers. It is assumed that the atmospheric boundary layer (ABL) is well mixed, therefore one value for the potential temperature and specific humidity can be used throughout the whole layer; the interface between the top of the ABL and the free atmosphere is characterized by a jump in potential temperature and specific humidity (Fig B1.1, blue arrows). Changes in the boundary layer height depend on the surface fluxes of heat and moisture.

In the soil-water-atmosphere-plant model radiation is the main driver that brings energy into the system. This energy has both a shortwave and longwave radiation component (Fig B1.1, black dashed arrows).

$$R_n = S_{in} - S_{out} + L_{in} - L_{out} \quad \text{(B1)}$$

where R_n is the incoming net surface radiation; S_{in} and S_{out} are the incoming and outgoing shortwave radiation respectively; L_{in} and L_{out} are the incoming and outgoing longwave radiation respectively. The amount of shortwave and longwave radiation is dependent on the properties of the surface and on the degree of cloud cover. For example, the outgoing shortwave radiation is a function of both the incoming shortwave radiation and the surface albedo.

Box 1.1 Continued

This net radiation determines the available energy for the sensible heat flux (H), the latent heat flux (LE) and the ground heat flux (G) (Fig B1.1, black continuous arrows).

$R_n = H + LE + G$ (B2)

The sensible heat flux involves heat diffusion between surface and the atmosphere, and depends on the aerodynamic resistance and the difference between surface and mixed layer temperature. The latent heat flux is associated with evapotranspiration (or condensation) and is the sum of the latent heat flux of the vegetation, soil and wet surfaces and its partitioning depends on the fractional vegetation coverage.

The exchange of CO_2 between land surface and the atmosphere (Fig B1.1, red arrows) is calculated according to

$NEE = -P_{nT} + Resp$ (B3)

where NEE is the net ecosystem CO_2 exchange; P_{nT} is the total net canopy photosynthesis rate (note that it is a negative flux, as it is the uptake of CO_2 from the atmosphere); Resp is the soil respiration rate.

Thus the land surface and the atmosphere are in this way coupled through the stomata, as stomata regulate the exchange of CO_2 into the plant and water vapour out of the plant.

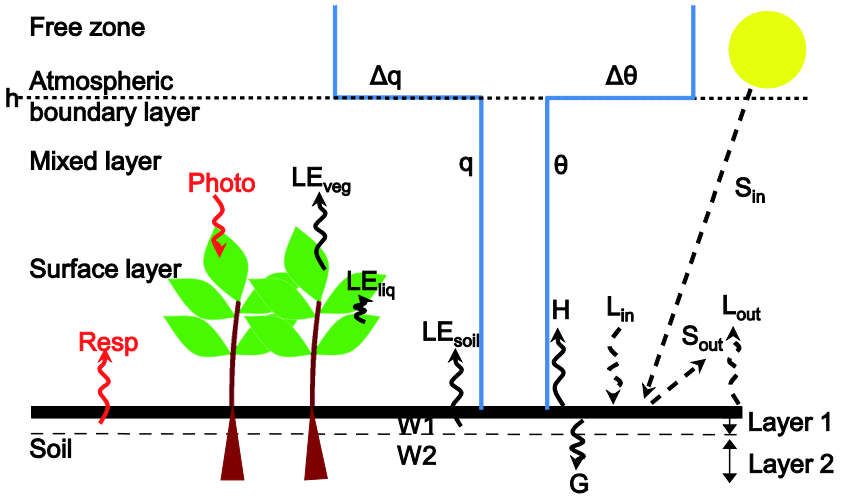

Fig B1.1 Representation of a soil-water-atmosphere model (modified from Van Heerwaarden *et al.* 2010). The atmosphere consists of the surface, mixed, boundary and free layers, and the atmospheric boundary layer height (h) which is the top of the atmospheric boundary layer (dotted line). The radiation budget consists of the shortwave and longwave incoming and outgoing radiation (S_{in}, S_{out}, L_{in}, L_{out}; black dashed arrows). Soil (G), latent (LE) and sensible heat (H) energy balance fluxes (black continuous arrows) and their interaction with specific humidity (q) and temperature (θ) (blue lines). The total latent heat flux (LE) is the sum of LE from vegetation (LE_{veg}), soil (LE_{soil}) and wet leaves (LE_{liq}). LE_{soil} depends on the water content of the top soil layer (layer 1, W1) and the soil temperature. LE_{veg} depends among others on the water content of the deeper soil layer (layer 2, W2). Free tropospheric conditions are represented by Δq and Δθ. Carbon content of the atmosphere depends on the soil respiration flux (Resp) and on the canopy photosynthesis rate (Photo). Black arrows indicate heat fluxes. Red arrows indicate carbon fluxes

In addition, the responses of plants to climate change and associated atmosphere feedbacks will depend on the environmental conditions in which plants grow. For instance, more nitrogen and less water available were found to increase plant growth responses to elevated CO_2 (McMurtrie *et al.* 2008). It is in general thought that plant traits, i.e. attributes that have the potential to significantly influence plant performance (establishment, survival, fitness) (Reich *et al.* 2003; Violle *et al.* 2007), determine the functioning of vegetation and that of ecosystems (Diaz *et al.* 2004). For example, the availability of soil nutrients has a large influence on plant traits (e.g. rooting depth, leaf area) and is therefore one of the main factors in determining vegetation functioning (Ordoñez *et al.* 2009). Furthermore, plant competition may also strongly influence plant responses to climate change (Ziska 2011), as some plants may benefit more from climate change than others. Therefore it is thought that certain traits (e.g. stomatal conductance, leaf photosynthetic capacity) are modified by competition and these traits are therefore determining vegetation functioning (Reich *et al.* 2003). So, it is very important to know how plants respond to changes in the climate and how this is affected by plant competition to identify how strong the associated feedbacks with the climate are.

1.2 Optimality hypothesis

To study the effect of plant responses on climate change and the potential effect on the coupling between vegetation and the atmosphere, (simple) optimization theory can be a good approach. See Box 1.2 for more explanation on optimization models. With this approach one can scale from individual physiological processes to vegetation functioning (Schymanski *et al.* 2007; Dewar *et al.* 2009; Sterck *et al.* 2011; Dekker, Vrugt & Elkington 2012). These simple optimization models take an evolutionary viewpoint and assume that natural selection favours plants with the highest performance (Parker & Maynard-Smith 1990). From this perspective one could predict that plants respond optimally to changes in the climate in a way that would maximize their performance.

Optimization can be done at the scale of a single leaf, whole canopy, new offspring or new generations. On the leaf scale for example, it is thought that nitrogen is distributed optimally among different parts of the photosynthetic apparatus to acclimate to environmental changes (Harley *et al.* 1992; Evans & Poorter 2001). N is assumed to be used optimally, because it is a limiting resource in many ecosystems (Field 1983), while it is an important component of photosynthetic enzymes and chlorophyll and is thereby directly involved in the photosynthetic process (Field 1983). For instance, with elevated CO_2 less Rubisco is needed to catalyse photosynthesis, therefore the N invested in Rubisco is redundant and can be invested in other plant components (Woodrow 1994). The degree to which this modifies whole canopy carbon uptake is unknown (Long *et al.* 2004) and thereby the potential effect on carbon cycling remains unclear.

Box 1.2 Optimization: simple and competitive

Optimization models state a goal or objective function that is maximized with respect to one or more plant functional traits (e.g. leaf area, stomatal conductance, photosynthetic capacity). The maximization of the objective function is most of the times subjected to several (physiological or environmental) constraints (Dewar *et al.* 2009). The underlying assumption is that natural selection led to optimized plant functional traits that maximize fitness under a given set of conditions (Franklin *et al.* 2012). As real fitness, i.e. the transfer of genes to the next generation, is hard to quantify most models use a performance measure that can be assumed to be a proxy for fitness.

Optimization can be simple or competitive (Parker & Maynard-Smith 1990). Simple optimization requires for its solution only one differential equation to be solved (Maynard-Smith 1978), and is frequency-independent, as the optimum is not dependent on what other individuals do (Parker & Maynard-Smith 1990). So to optimize plant functional traits (*f*, examples that are generally used are LAI, stomatal conductance, canopy N content) fitness is maximized (F, generally net growth rate or net photosynthesis rate are used as proxies for fitness). Therefore, for simple optimization the following equation should be solved: $dF(f)/df = 0$.

Competitive optimization can be determined by applying evolutionary game theory. Here the optimum for an individual is affected by what other individuals do and it is therefore frequency-dependent (Parker & Maynard-Smith 1990). With this approach one can assess the extent to which a population of organisms (in my case plants) playing a given strategy (i.e., with a given trait value) can be invaded by an individual (e.g. a mutant or another genotype) that plays a different strategy (i.e., that has a different trait value). Such an invasion would be possible if the invader has a higher fitness than the resident population. A strategy that is used in a population and cannot be invaded anymore by an alternative strategy, because this alternative strategy would not give a higher fitness for the mutant, is an (evolutionarily) stable strategy (ESS) (Parker & Maynard-Smith 1990). An ESS is not always the strategy that maximizes fitness in a population sense (see main text). Two conditions should be met for an ESS (Riechert & Hammerstein 1983).

1) No mutant strategy (J) should have a higher fitness than the strategy (I) played by the ESS population.
   $F(I,I) \geq F(J,I)$ for all strategies J
   where F(I,I) is the payoff to a single I strategy in a population of I strategists and F(J,I) is the payoff of a mutant playing strategy J in the same population.
2) If the strategy J is as successful as strategy I in a population of I strategists, then J should be at a selective disadvantage as it increases in frequency for I to be an ESS.
   When $F(I,I) = F(J,I)$, then $F(I,J) > F(J,J)$

At the whole canopy scale, plants are also thought to use their N optimally. For instance, plants invest most N in leaves that receive most light and less in more shaded leaves (Field 1983) resulting in an increased canopy photosynthesis compared to the situation where all leaves have the same N content. The pattern of N distribution is thus supposed to follow the light distribution within a canopy (Hirose *et al.* 1988). The relative advantage of an optimal N distribution within a canopy has been shown to increase when N availability increases (Hirose & Werger 1987). Rates of N deposition are expected to change, in some regions it is expected to increase (Galloway *et al.* 2004; IPCC 2014). So, in these regions predictions of optimality would result in a more positive contribution to photosynthesis and could thus impact the carbon cycle.

Another example of optimization that relates to light distribution within the canopy is optimal canopy architecture (e.g. plant height, and leaf angle, length, width, curvature). To maximize canopy photosynthesis an optimal light environment within the canopy is needed, which is determined by the canopy architecture (Song, Zhang & Zhu 2013). For example under high light conditions, plants with more vertical leaves would be favoured in terms of photosynthesis, as it allows for a better distribution of light; less light being captured by upper leaves that tend to be light saturated and light penetrating to lower leaves that tend to be light limited (Hikosaka & Hirose 1997; Falster & Westoby 2003a). Vertical leaves are also more favourable in morning hours when the sun is close to the horizon (Falster & Westoby 2003a).

Another example of optimal responses at the whole canopy scale is the regulation of stomatal conductance. The stomatal apparatus determines both diffusion of CO_2 into the leaf, which is essential for photosynthesis, and water loss from the leaf. It is thought that plants maximize their carbon gain while minimizing water loss by optimizing stomatal conductance (e.g. Cowan 1978; Katul *et al.* 2010). From this perspective it is expected that plants decrease their stomatal conductance when atmospheric CO_2 increases (Ainsworth & Long 2005) as CO_2 is less limiting and therefore are the opportunity costs of minimizing water loss smaller. If enough plants respond in this way this reduction can result in alteration of the hydrological cycle (De Boer *et al.* 2011). The ultimate outcome of this response however is strongly influenced by interactions between vegetation and atmosphere. Decreased stomatal conductance and associated transpiration could result in a reduced atmospheric humidity. As a consequence the specific humidity gradient between land surface and the atmosphere becomes stronger, stimulating opening of the stomata (Van Heerwaarden *et al.* 2009). However, when the stomatal conductance is predicted to adjust optimally to elevated CO_2 it was shown to significantly weaken the hydrological cycle compared to a non-optimal response (Friend & Cox 1995). Additionally, the lower stomatal conductance also leads to a lower potential increase in the photosynthesis rate with elevated CO_2, as a result this contributes to relatively less carbon being invested in vegetation and consequently a smaller mitigating effect of plants on the rise of atmospheric CO_2 (Katul *et al.* 2010). There are many more similar vegetation-

atmosphere feedbacks than described here that could influence this dynamics, but in general it is found that most of the feedbacks are negative (Van Heerwaarden *et al.* 2009). So, acclimation responses of plants to climate change could have significant feedbacks on climate that are difficult to predict.

For a given amount of N it is also thought that plants optimize their LAI (Leaf Area Index, i.e., the leaf area per unit soil area) to maximize carbon gain (Anten *et al.* 1995). The LAI is strongly determined by N availability (Anten *et al.* 1995), more available N correlates with a higher LAI (Hirose *et al.* 1997). Rates of N deposition are expected to change and the magnitude of this change will differ considerably between different parts of the world (Fig 1.1c) (Lamarque *et al.* 2013; IPCC 2014). This heterogeneity in N deposition will contribute to variations in LAI response to climate change, while LAI in turn plays an important role in vegetation-atmosphere feedbacks. The latter is primarily, because the LAI affects the albedo and indirectly the rate of evapotranspiration and consequently this will change the energy partitioning between the latent and sensible heat flux.

One of the approaches used in this thesis, to study the effect of plant responses to climate change and the potential effect on the coupling between vegetation and the atmosphere, is simple optimization (the other being competitive optimization that I will discuss below). The assumption of simple optimization models is that natural selection led to optimization of plant functional traits to maximize fitness (Franklin *et al.* 2012), see Box 1.2 for more explanation. I have chosen to use whole-plant net photosynthesis as a proxy for fitness, the argument being that photosynthesis supplies the energy for growth and reproduction (Bowes, Ogren & Hageman 1972). However, I do note that the use of plant photosynthesis as fitness proxy makes simplifying assumptions, as many other processes than photosynthesis determine fitness (see also General discussion, Chapter 6). Plant photosynthesis is mainly determined by the total leaf area (Sitch *et al.* 2003), because it defines light interception. The leaf area index (LAI) is of great importance in this thesis, because next to its influence on photosynthesis, climate models often use the LAI to characterize vegetation (Van den Hurk, Viterbo & Los 2003); as the LAI influences the surface albedo and thereby the available radiative energy and its partitioning between the latent and the sensible heat flux. So, in this thesis the optimal LAI that maximizes whole-plant photosynthesis for a given amount of N is determined (Schieving, Werger & Hirose 1992; Anten *et al.* 1995).

Models that use simple optimality principles successfully predicted plant responses to among others elevated CO_2 (e.g. Franklin 2007; McMurtrie *et al.* 2008); for example, predictions of leaf N per unit leaf area in trees at ambient and elevated CO_2 (Franklin 2007), and acclimation of stomatal conductance to elevated CO_2 (McMurtrie *et al.* 2008; Medlyn *et al.* 2011). However, while optimization models make qualitatively good predictions, quantitatively the predictions tend to deviate from the observations. For example, predictions

of optimization models often underestimate measured LAIs and overestimate canopy photosynthesis (Anten, Werger & Medina 1998; Anten 2005). Several reasons can be the cause of this deviation, for instance, in the formulating of the objective function. In general, the net photosynthesis is used as a proxy for fitness (Makela *et al.* 2002), but additional carbon costs for among others root production are commonly not considered (Dekker, Vrugt & Elkington 2012). Although predictions of optimization models might deviate from observed values, optimization can still predict the general observed trends well and can therefore be very useful in predicting plants theoretical maximum carbon gain under future climate scenarios (Dewar *et al.* 2009).

1.3 Competition between plants

With the simple optimization approach it is implicitly assumed that the optimal trait values of one plant are independent of the trait values of its neighbours. However, this ignores the fact that plants strongly compete for resources (Anten 2002). Competition between plants for resources, such as light, water and nutrients, commonly occurs, as plants often grow in dense communities (e.g. forests or grasslands). Competition for these resources is thus an important selective force, and competition therefore strongly determines vegetation functioning (McNickle & Dybzinski 2013), and as a consequence it also largely determines vegetation structure (Anten & Hirose 2001); meaning that natural selection results in vegetation stands that are dominated by the best competitors and not necessarily by the best inherent performers (McNickle & Dybzinski 2013). Nevertheless, on the leaf scale simple optimality can still be a valid approach, as on this scale there is no influence of competition between plants (Franklin *et al.* 2012), though there might be competition between leaves of plants.

To study the effect of competition on plant responses, evolutionary game theory, or competitive optimization, can be used. This is a "game" where the strategy of an individual plant depends on the strategy "played" by its competitors (Parker & Maynard-Smith 1990). The game can be played, because the fitness of the individual can be both influenced by its own strategy, the strategy of its neighbours and by the environmental conditions. A certain strategy of a population that cannot be invaded anymore by an alternative strategy, because this strategy would not give a higher fitness for the competitors, is an (evolutionarily) stable strategy (Parker & Maynard-Smith 1990). More information on competitive optimization and the difference with simple optimization can be found in Box 1.2.

The competitive optimization approach will be used in this thesis to find (evolutionarily) stable LAIs (Fig 1.2). In a high density stand consisting of plants with all the same LAI, which is the optimal LAI for maximizing whole-stand photosynthesis (Fig 1.2a), a plant with a larger LAI can invade (Fig 1.2b). This plant can invade, because it receives a

larger fraction of the available light and thereby obtains a higher photosynthesis rate. But at the same time it reduces the light intercepted by its neighbouring plants, as they are shaded by the individual plant, and thus also diminishes the photosynthesis rate of these neighbouring plants. However, increasing LAI also comes with extra costs to the plant itself, for example a higher respiration rate. So, the individual plant increases its photosynthesis rate at expense of its neighbours. However, once it has invaded (i.e., its offspring dominate the vegetation stand) whole-stand photosynthesis is reduced due to the extra costs in leaf area investment. A plant with a larger LAI will not invade anymore if the extra returns of photosynthesis are smaller than the costs of extra leaf area, which is then the stable LAI (Fig 1.2d) (Falster & Westoby 2003b). So, the end result is that (evolutionarily) stable stands have larger LAIs than optimal ones, and therefore have lower maximum photosynthesis. This can be interpreted as a tragedy of the commons (Hardin 1968), because all individuals would have a higher performance if they would have a lower LAI, but they are outcompeted by plants with a higher LAI (Anten 2002; Lloyd *et al.* 2010). This tragedy of the commons may occur for other traits as well. It was shown theoretically that competition for resources would select for plants that are taller (Falster & Westoby 2003b), have more horizontally projected leaves (Hikosaka & Hirose 1997), produce more roots (Riechert & Hammerstein 1983; Gersani *et al.* 2001; Dybzinski *et al.* 2011), have larger specific leaf area (ratio of leaf area to leaf mass) (Schieving & Poorter 1999), and flower later (Vincent & Brown 1984; Vermeulen 2015) than would be optimal in terms of maximum performance of the population.

Competitive optimization is therefore a good approach to determine the LAI under different environmental conditions, as the LAI is an emergent outcome and in addition interaction between neighbouring plants is taken into account. By comparing the competitive optimization approach with the simple optimization approach the effect of competition can be determined.

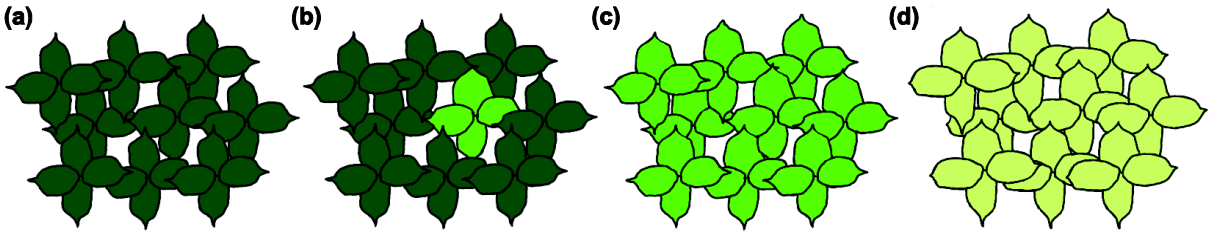

Fig 1.2 Conceptual figure on obtaining the evolutionarily stable leaf area. (a) A resident stand consisting of plants with all the same LAI, which is the optimal LAI for maximizing photosynthesis. (b) A mutant with a larger LAI invades (indicated by the lighter green colour), because of its larger leaf area it receives a larger fraction of the available light and thereby obtains a higher photosynthesis rate; while at the same time it reduces the light intercepted by its neighbouring plants as they are shaded by the individual plant and thus also diminished the photosynthesis rate of its neighbouring plants. (c) The resident population also "plays" this strategy and they increase their LAI. (d) This process continues until a plant with a larger LAI cannot invade anymore, this is if the extra returns of photosynthesis are smaller than the costs of extra leaf area, which is then the stable LAI

1.4 Knowledge Gaps

1.4.1 Response to climate change

It is essential to know how plants respond to changes in the climate, because among others the coupling between vegetation and the atmosphere could influence the climate system as a whole. As noted, this is particularly so for LAI as this trait determines light interception and thus photosynthesis, and because it has a very important role in vegetation-atmosphere feedbacks. Yet, it is still unclear in which direction the LAI will change with elevated CO_2 (Anten *et al.* 2004). An increase in LAI is expected, as leaves at lower light levels can be maintained, due to their higher photosynthesis rate at elevated CO_2 (Long 1991). However, previous experimental studies show contradictory results, in some cases the LAI increased (Luo *et al.* 2001) while other experiments showed no change (DeLucia, George & Hamilton 2002) or LAI decreased (Lutze & Gifford 1998). This is probably the result of differences in environmental conditions; the effect of CO_2 is modified by environmental conditions, like the availability of water and nitrogen. So, in spite of a fair amount of experiments having been done, it is unclear in what direction LAIs may change with climate change. In addition, most experiments that investigate plant responses to elevated CO_2 ran for a maximum of 10 years (Ainsworth *et al.* 2003) and only few studies investigated longer term responses (De Boer *et al.* 2011; Nakamura *et al.* 2011). Therefore using an optimality model can be useful to develop quantitative hypotheses on how adaptive responses of plants to climate change will shape vegetation structure and functioning. In addition, it can assess how these responses may be mediated by variation in environmental conditions. It is therefore needed to investigate optimal leaf and whole-stand acclimation to climate change under different environmental conditions, to define the theoretical maximum influence it has on the atmospheric processes and thereby how it potentially could impact the climate system as a whole.

1.4.2 Effect of competition under future climate

While, as noted above, it is generally accepted that competition will likely modify vegetation responses to climate change, little investigation has been done on the direction and magnitude of this effect. Under current climate conditions it was already shown that predictions of LAI by game theoretical models, which account for competition, result in closer fits to real values compared to predictions from models that do not account for competition (Anten 2002; Lloyd *et al.* 2010). However, the outcome of competition under elevated CO_2 is difficult to predict (Bazzaz & McConnaughay 1992), because an increase in atmospheric CO_2 increases plant growth and thereby likely increases competition for light and soil nutrients between plants. Only few modelling studies included plant competition when investigating plant responses to climate change (e.g. Friend, Schugart & Running 1993; Farrior *et al.* 2015). The use of competitive optimization models to investigate vegetation functioning under future climate scenarios may provide a useful approach in this regard, as it can be used to assess what future

vegetation stands would look like, if they would become dominated by the best competitors. By comparing these outcomes with outcomes from a simple optimization model and to data from climate change experiments, it is possible to give an indication of the extent and direction in which competition modifies responses to climate change. So, it is important to know how plants respond to climate change and how this is potentially modified by competition, in order to define the impact of competition on plant responses to climate change.

1.4.3 Time scale of plants responses to climate change

Plant responses to climate change could be plastic, i.e. changes in traits that occur during the lifetime of a plant and are on a relatively short timescale. Nevertheless, these responses may still be slow compared to short-term environmental fluctuations that can act on very short time scales (i.e., a matter of days, hours or seconds depending on the factor involved). For a plastic trait response to be fully effective it should not lag too far behind the environmental changes. For example, some changes like stomatal opening and closure are relatively fast and reversible processes (Katul *et al.* 2010), so it seems reasonable that plants notice short term fluctuations in environmental conditions and respond fast to this, although it is known that stomatal responses in understory forest plants can lag behind the occurrence of light flecks that may last only a few seconds (Pearcy 1999). Other changes are more structural and less reversible, like leaf thickness and N allocation (Frak *et al.* 2001; Oguchi, Hikosaka & Hirose 2003), and thus take longer to realize. Therefore, plants are thought to respond to long term average environmental conditions. Models that use optimality principles optimize for a specific time interval, while the response time of plants to changes in environmental conditions might deviate from this time interval (Chen *et al.* 1993).The effect of this time scale of response is not yet investigated by optimization models, while it might have a large impact on the predicted outcomes.

Plants could also respond to climate change genotypically, i.e. over several generations through natural selection. All plants are exposed to increasing CO_2 concentrations, and are therefore exposed to a high selection pressure of elevated CO_2 (Onoda, Hirose & Hikosaka 2009). Due to the high selection pressure under climate change, plants with high levels of plastic and genotypic adaptations are thought to be favoured (Parmesan 2006). This means that the level of plastic and genotypic responses has a major influence on vegetation level processes. In contrast, research investigating plant plastic and genotypic responses does not clearly investigate the potential mediating effect of plant competition. As noted, the mediating effect of competition can be analysed using game theoretical models. However, current game theoretical models in plant ecology do not state whether trait responses occur through plastic or genotypic responses (McNickle & Dybzinski 2013), while this distinction is important. If trait changes occur primarily through plasticity, a

community may rapidly arrive at an evolutionarily stable state. Conversely, if such changes are mostly genotypic then communities will have to undergo several generations of natural selection before they arrive at the evolutionarily stable state (McNickle & Dybzinski 2013). Given the fact that current climate change is occurring on a relatively short time scale, i.e. decades, predictive ability of game theoretical models could strongly depend on the relative contribution of plastic and genotypic changes. Therefore it is important to define the level of plastic and genotypic responses of plants and how this is potentially mediated by plant competition.

1.4.5 Vegetation-atmosphere feedbacks

It is important to know how plants respond to changes in the climate, and how this is potentially modified by competition. This is because plant competition could strongly influence vegetation responses to changes in environmental conditions. This in turn, could have a large impact on climate predictions due to the existence of vegetation-atmosphere feedbacks (more information about vegetation-atmosphere feedbacks can be found in Box 1.1). However, even though inclusion of plant competition in atmospheric models has frequently been called for (e.g. Farrior 2014; Zhang *et al.* 2015), currently it is generally not included in atmospheric models (Sitch *et al.* 2003; Boussetta *et al.* 2013). It is therefore needed to investigate how the coupling between vegetation and the atmosphere is affected by competition.

1.5 Research Questions

Based on the knowledge gaps described in section 1.4, I will address several research questions in this thesis:

- *How are optimal leaf- and whole-canopy responses influenced by climate change?*
    - *How are these responses modified by plant competition?*
    - *To which degree can these responses be attributed to plastic or to genotypic adaptations?*
- *What is the impact of the time scale of optimization?*
- *How is the coupling between vegetation and the atmosphere affected by plant competition?*

1.6 Thesis outline

The research presented in this thesis follows a logical pattern from lower towards higher aggregation scales: starting at the leaf, then the vegetation canopy and ultimately the coupling between vegetation and the atmosphere. A conceptual diagram on the outline of this thesis is given in Fig 1.3.

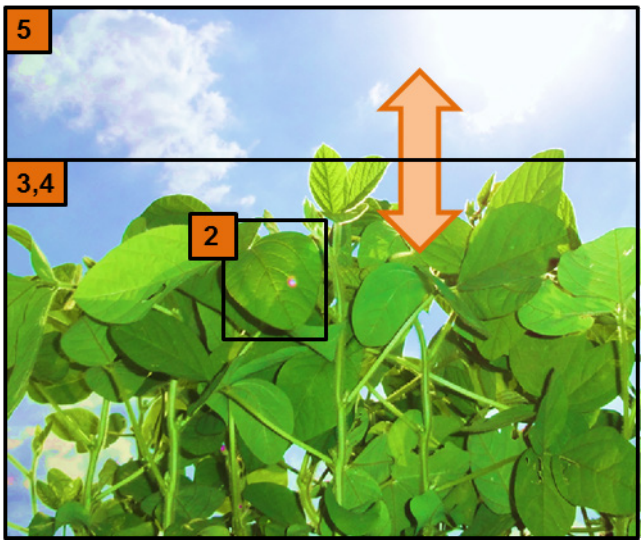

Fig 1.3 A conceptual picture on the scales of aggregation of thesis chapters, the numbered boxes relate to the chapters involved. Chapter 2: leaf scale responses to changes in environmental conditions. Chapters 3 and 4: canopy scale responses to changes in environmental conditions. Chapter 5: canopy scale responses and the coupling with the atmosphere

In **Chapter 2** of this thesis we focus on optimal leaf level responses to environmental changes by using the simple optimality approach. More specifically, we analyse optimal N allocation between RuBP regeneration and RuBP carboxylation. An analytical solution of this optimal partitioning is provided, it is shown how different environmental factors influence this optimal allocation, and it is discussed how this relates to experimental results. In the end of this chapter, the impact of different time scales of optimization is shown.

In **Chapter 3** we investigate how vegetation functioning and structure is influenced by climate change and to which extent competition may modify these effects. We investigate this with a vegetation model. To study the effect of competition between plants in a canopy, a comparison of the simple optimality with the competitive optimality approach is made. Validation was done by comparing the model outcomes against a large data set from several Free air CO_2 enrichment (FACE) experiments.

In **Chapter 4** we experimentally determine the relative contribution of plastic versus genotypic responses to elevated CO_2 on plant performance and define the extent to which these patterns are modified by competition. To investigate this we use *Plantago asiatica* seeds originating from three different natural CO_2 springs and seeds originating from ambient CO_2 collected in nearby areas. Furthermore, we create mono stands of plants originating from either elevated CO_2 areas or from ambient CO_2 areas and mixed stands with both origins. The plants grow in CO_2 controlled walk-in climate rooms, under different CO_2 levels. Next to this,

we use a model for scaling up from leaf to whole-plant photosynthesis and to estimate the influence of plastic and genotypic responses.

In **Chapter 5** we investigate how the coupling between vegetation and the atmosphere is influenced by competition. We use a coupled vegetation-atmosphere model and include a game theoretical procedure to incorporate competition. Validation was done by comparing the model outcomes against diurnal data from the Ameriflux Bondville site over a growing season.

In Chapter 6 I provide a discussion of my results, give recommendations for future research, followed by some concluding remarks.

Chapter 2

Optimization of nitrogen-use for leaf photosynthesis with co-limitation between RuBP regeneration and RuBP carboxylation: an analytical solution

Marloes P. van Loon, Feike Schieving, Frank Sterck, Xinyou Yin, Daniel S. Falster and Niels P.R. Anten

Abstract

In the widely used biochemical model of Farquhar, Von Caemmerer & Berry (1980), photosynthesis is either limited by ribulose-1,5-bisphosphate (RuBP) regeneration (P_{jl}) or by RuBP carboxylation (P_{cl}). It is believed that plants optimize allocation of nitrogen, a key component of the photosynthetic machinery, between P_{cl} and P_{jl} to maximize photosynthesis; which occurs when P_{cl} and P_{jl} co-limit photosynthesis. Here, we present an analytical solution for the optimal N distribution and provide a code for this solution in both MATLAB and R. We show that the simulated response of leaf photosynthesis to changes in atmospheric CO_2 concentration and temperature differ substantially when plants are allowed to distribute N optimally within the leaf, compared to the situation where allocation is assumed to be constant. Simulating increase of CO_2 reduced the fraction of N allocated to P_{cl}, while increasing temperature increased the N fraction allocated to P_{cl}. These findings are consistent with literature data. The simulated increase in leaf photosynthesis with CO_2 elevation was considerably higher when N allocation responded optimally than when this allocation was fixed. A similar but weaker trend was found for warming. Our simulations also show that the rate of acclimation, the time lag between environmental change and trait optimization, may strongly affect predicted photosynthesis, indicating that more research on this time lag and variation therein is needed. Finally, we show that use of our analytical solution substantially reduces the computation effort required to calculate leaf assimilation compared to a numerical methods that are used elsewhere. We suggest that incorporation of our analytical solution for the optimal allocation of N among leaf components will add to our conceptual biological understanding of leaf photosynthetic responses to environmental changes, in addition to greatly increasing model speed.

Key words: model, optimal N allocation, N partitioning, J_{max}, V_{cmax}, ribulose-1,5-bisphosphate regeneration, ribulose-1,5-bisphosphate carboxylation, atmospheric CO_2, temperature

2.1 Introduction

2.1.1 Biochemical model of leaf photosynthesis

Photosynthesis is the main process underlying carbon acquisition, carbon sequestration, and growth and survival of plants, and it is thus an important driver of the global carbon cycle, ecosystem productivity and crop and timber yields (Lambers, Chapin III & Pons 2008). A wide variety of scientific fields, such as forestry, agronomy, ecology, and global change biology use the same biochemical model (Farquhar, Von Caemmerer & Berry 1980) to calculate photosynthesis of leaves (Farquhar, Von Caemmerer & Berry 1980; Lloyd & Farquhar 2008), whole plants (Tuzet, Perrier & Leuning 2003; Sterck & Schieving 2011), stands (Anten 2005; Dewar *et al.* 2009), or crops (Yin & Struik 2010). Consequently, most predictions about changes in leaf photosynthesis, plant growth, vegetation dynamics, as well as timber production and crop yields in response to different climate or soil conditions rely on the same underlying biochemical photosynthesis model.

This basic photosynthesis model considers that photosynthesis is limited by one of two processes (Fig 2.1). The first process is electron transport $P_{jl,}$ which transforms light energy into the high energy compounds ATP and NADPH, and limits ribulose-1,5-bisphosphate (RuBP) regeneration. The second process is RuBP carboxylation P_{cl}, which uses high-energy compounds to bind atmospheric carbon into complex sugar compounds. The compounds associated with P_{cl} and P_{jl} account for a large fraction of N within the leaf (Evans & Poorter 2001), while N is acting as a limiting resource in many ecosystems, and it is costly for plants to acquire even when it is available (Aerts & Chapin III 1999). From an evolutionary standpoint, we therefore expect selection to favour plants achieving the greatest uptake of carbon per unit leaf N, as this would provide advantages in growth, competition and ultimately seed production. So, one would expect that N is distributed among the components of the photosynthetic system such that photosynthesis is maximized (Hikosaka & Terashima 1996; Evans & Poorter 2001). It has been shown that this optimal distribution of leaf N for maximizing photosynthesis occurs when P_{cl} and P_{jl} both co-limit photosynthesis (e.g. Hikosaka & Terashima 1996; Niinemets & Anten 2009; Westoby, Cornwell & Falster 2012) (Fig 2.1).

2.1.2 Factors affecting acclimation to optimal nitrogen partitioning between RuBP regeneration and RuBP carboxylation

Various environmental factors may influence the balance between P_{jl} and P_{cl}, such as atmospheric CO_2 concentration (Fig 2.1a-c), temperature (Fig 2.1d-f) and light intensity (Fig 2.1g-i), with first two being projected to increase considerably in association with climate change (IPCC 2007). Plants would thus be expected to acclimate in the N partitioning between electron transport and carboxylation in response to changes in these environmental factors (e.g. Medlyn 1996; Hikosaka *et al.* 2006). Plants have indeed been found to acclimate

to various environmental changes by optimizing their N partitioning among the photosynthetic components (Harley *et al.* 1992; Evans & Poorter 2001).

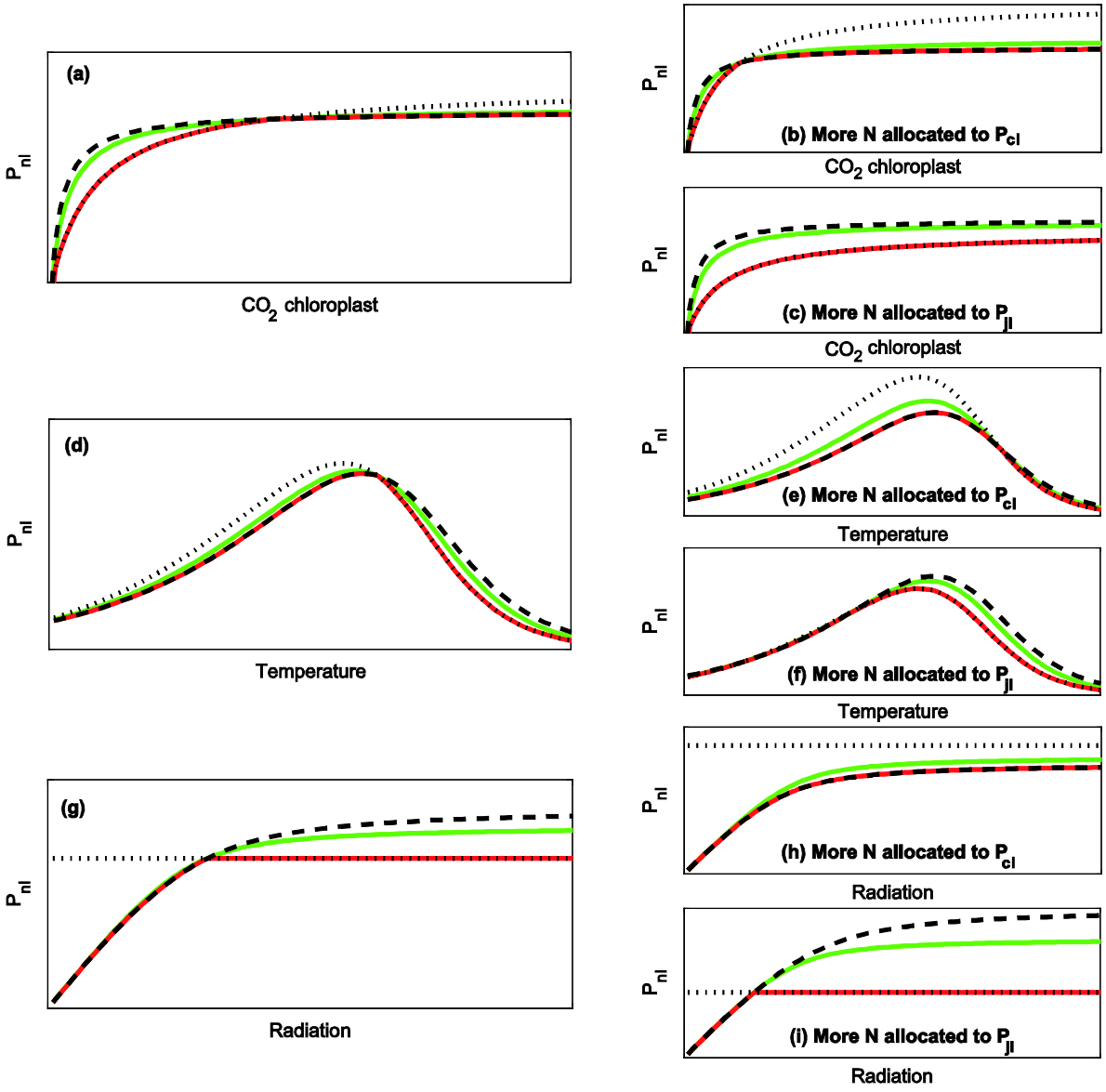

Fig 2.1 Schematic representation of photosynthesis rate (P_{nl}) versus CO_2 concentration in the chloroplast (a-c), temperature (d-f) and radiation (g-i). The green line represents photosynthesis with optimal partitioning of nitrogen, while the red line represents photosynthesis with constant partitioning and it is the minimum of the RuBP regeneration limited photosynthesis rate (P_{jl}, black dashed line) and the RuBP carboxylation limited photosynthesis rate (P_{cl}, black dotted line). More nitrogen can be allocated to P_{cl} (b,e,h) or to P_{jl} (c,f,i), but the optimal allocation always results in a higher photosynthesis rate compared to constant partitioning (green versus red line)

In addition to the overall magnitude of responses in N partitioning between RuBP regeneration and RuBP carboxylation, the time lag between the environmental change and the response may also affect photosynthetic performance. For acclimation to be beneficial, the response time of the leaves should be sufficiently fast such that it can track environmental

changes (Pearcy & Sims 1994). An environmental factor such as temperature typically fluctuates on a seasonal (i.e., over periods of several weeks) and on a diurnal scale, while light availability also fluctuates much faster. The time scale of acclimation in N partitioning among photosynthetic compounds differs per species. Full acclimation to an increase in irradiance can take 4 to 7 days for herbaceous plants (e.g. Oguchi, Hikosaka & Hirose 2003; Trouwborst *et al.* 2011), while for woody plants it can take around 2 to 5 weeks (e.g. Frak *et al.* 2001; Oguchi, Hikosaka & Hirose 2005). Furthermore, the time scale of acclimation also depends on the age of the leaf (Frak *et al.* 2001; Oguchi, Hikosaka & Hirose 2003). As far as we know, the impact of these acclimation time lags on plant photosynthetic responses to environmental change are not well known primarily because they are currently not incorporated in most photosynthesis models.

2.1.3 Inclusion of the co-limitation of RuBP regeneration and RuBP carboxylation in models

Many vegetation models include the co-limitation of RuBP regeneration and RuBP carboxylation (Medlyn 1996; Hikosaka 1997; Hikosaka & Hirose 1998; Sterck & Schieving 2011; Westoby, Cornwell & Falster 2012; Xu *et al.* 2012; Buckley, Cescatti & Farquhar 2013). However, with few exceptions (Westoby, Cornwell & Falster 2012), these models use numerical methods to solve for the optimal N distribution. Analytical solutions bypass the problem of having to find numerical solutions, and can thus greatly increase the computing speed of vegetation models when the optimization has to be repeated over and over. This is especially important as vegetation models are often complex and contain many processes and thus involve many computation steps. Such models can include algorithms, for example for incoming radiation, leaf turnover, (dynamic) plant architecture and respiration in addition to leaf photosynthesis. Furthermore, vegetation models are increasingly used to predict ecosystem and climate dynamics under climate change (Cramer *et al.* 2001; Sitch *et al.* 2003), as well as agronomic production (Van Ittersum *et al.* 2003), and there is increasing recognition that plant acclimation to changing environmental conditions should be included (Corlett 2011). Fast analytical models are therefore the key to modelling vegetation dynamics at the global scale. Finally, analytical solutions can improve our conceptual understanding of biological systems by explicitly formalizing the relationships between underlying elements.

In this chapter, we present an analytical solution for the optimal N distribution between RuBP regeneration and RuBP carboxylation. We then use this model to show how plants may adjust the partitioning of N between the two types of photosynthetic components, and thus photosynthesis rates, in response to increase in atmospheric CO_2 concentration and to increase in temperature. Furthermore, we show the impact of optimization on different time scales and discuss these.

In Table 2.1 we present and describe all the parameters and variables mentioned in the main text, and their units. To improve the accessibility of our model we provide the code of the analytical solution, both in R (A2.1 Methods) and MATLAB (A2.2 Methods), which can be compared with the numerical solution (MATLAB code, A2.3 Methods). In Appendix A2.4 Methods we describe the temperature relationships of the parameters of the model, used in one of the examples below.

Table 2.1 List of symbols, a description and the unit for the model variables and parameters.

Symbol	Unit	Explanation	Input value	Source	Equation
C_c	μmol mol^{-1}	CO_2 concentration in the chloroplast	350		
I_l	μmol m^{-2} s^{-1}	Total amount of intercepted radiation by a leaf	1500		
J	μmol m^{-2} s^{-1}	Potential electron transport rate			2.5
J_{max}	μmol m^{-2} s^{-1}	Maximum electron transport rate			2.9
k_c	μmol C mmol N^{-1} s^{-1}	Carboxylation capacity per nitrogen mass	0.91	1	
K_c	μmol mol^{-1}	Michaelis-Menten constant for carboxylation	402[a]	1	
k_j	μmol e mmol N^{-1} s^{-1}	Electron transport capacity per nitrogen mass	0.91	1	
K_o	μmol mol^{-1}	Michaelis-Menten constant for oxygenation	560900[a]	2	
N_l	mmol m^{-2}	Total nitrogen content allocated to J_{max} and V_{cmax}	270		2.7
N_{lc}	mmol m^{-2}	Leaf nitrogen content for carboxylation			2.12
N_{lj}	mmol m^{-2}	Leaf nitrogen content for electron transport			2.7, 2.12
O	μmol mol^{-1}	Oxygen concentration	205000	2	
P_{cl}	μmol m^{-2} s^{-1}	Rubisco limited photosynthesis rate			2.2
P_{gl}	μmol m^{-2} s^{-1}	Leaf gross photosynthesis rate			2.1
P_{jl}	μmol m^{-2} s^{-1}	Electron transport limited photosynthesis rate			2.3
V_{cmax}	μmol m^{-2} day^{-1}	Maximum carboxylation rate			2.8
y	-	Light absorption to electron transport capacity ratio			2.6
Γ^*	μmol mol^{-1}	CO_2 compensation point in absence of mitochondrial respiration	51[a]	2	
θ	-	Curvature factor	0.9	3	
Φ	μmol $μmol^{-1}$	Quantum yield (μmol electrons per photon)	0.25		

[a] Input value if it is 25°C, for other temperatures see A2.4 Methods

Literature sources:

1) Anten, Schieving & Werger (1995)
2) Cai & Dang (2002)
3) Dermody, Long & DeLucia (2006)

2.2 The Analytical solution

2.2.1 Photosynthesis rate

According to the widely-accepted Farquhar-von-Caemmerer-Berry biochemical model, the gross photosynthesis rate of a leaf under a given incoming radiation is given by the minimum of two biochemical processes: RuBP carboxylation (P_{cl}) and RuBP regeneration (P_{jl}) (2.1), which are given by equations:

$$P_{cl} = V_{cmax} \cdot \frac{C_c - \Gamma^*}{C_c + K_c \cdot \left(1 + \frac{O}{K_o}\right)}, \tag{2.2}$$

and

$$P_{jl} = J/4 \cdot \frac{C_c - \Gamma^*}{C_c + 2 \cdot \Gamma^*} \tag{2.3}$$

where V_{cmax} is the maximum rate of carboxylation rate; C_c is the CO_2 concentration in the chloroplast; Γ^* is the CO_2 compensation point in the absence of mitochondrial respiration; K_c and K_o are respectively the Michaelis-Menten constants for carboxylation and oxygenation and O is the oxygen concentration (Farquhar, Von Caemmerer & Berry 1980). J is the irradiance-dependent potential electron transport rate, as described by Eqns (2.4) and (2.5).

2.2.2 Light limiting effects on photosynthesis

The following equation was used to link J to irradiance:

$$\theta \cdot J^2 - \left(J_{max} + \Phi \cdot I_1\right) \cdot J + J_{max} \cdot \Phi \cdot I_1 = 0 \tag{2.4}$$

where θ is a curvature factor for a non-rectangular hyperbola, Φ is the quantum yield, J_{max} is the maximum electron transport rate under saturating irradiance, and I_1 is the total amount of light absorbed by leaf photosynthetic-pigments (Farquhar, Von Caemmerer & Berry 1980).

Solving Eqn (2.4) for J gives:

$$J = J_{max} \cdot \frac{(1+y) - \sqrt{(1+y)^2 - 4 \cdot \theta \cdot y}}{2 \cdot \theta} \tag{2.5}$$

where y is $\Phi I_1 / J_{max}$ (2.6).

2.2.3 Effect of nitrogen on the photosynthesis

Let N_l be the amount of leaf N that can be allocated to electron transport components (N_{lj}) and carboxylation components (N_{lc}), so: $N_l = N_{lj} + N_{lc}$ (2.7). We therefore describe J_{max} and V_{cmax} as a linear function of N_{lj} and N_{lc}, respectively (Harley *et al.* 1992), as:

$$V_{cmax} = k_c \cdot N_{lc} \tag{2.8}$$

$$J_{max} = k_j \cdot N_{lj} = k_j \cdot \left(N_l - N_{lc}\right) \tag{2.9}$$

where k_c is the carboxylation capacity per N mass, and k_j is the electron transport capacity per N mass.

Note that there is also N invested in other photosynthetic and non-photosynthetic protein components, in addition to the protein components for RuBP carboxylation and RuBP regeneration. We assume that leaf N invested in other components is constant, and therefore does not play a role in our analysis.

2.2.4 Optimal nitrogen partitioning RuBP regeneration, RuBP carboxylation

Mathematically, it can be shown that photosynthesis is maximized when leaf N is distributed in such a way that the RuBP carboxylation and RuBP regeneration both co-limit the photosynthesis (Westoby, Cornwell & Falster 2012). This means that:

$$P_{cl} = P_{jl}. \tag{2.10}$$

Substituting Eqns (2.2) to Eqn (2.9) into Eqn (2.10) yields:

$$4 \cdot k_c \cdot N_{lc} \cdot \delta \cdot \left(4 \cdot \theta \cdot k_c \cdot \delta + k_j\right) \cdot N_{lc}{}^2 - \left(4 \cdot k_j \cdot k_c \cdot \delta \cdot N_l + 4 \cdot k_c \cdot \delta \cdot \Phi \cdot I_l + k_j \cdot \Phi \cdot I_l\right) \cdot N_{lc} + k_j \cdot \Phi \cdot I_l \cdot N_l = 0 \tag{2.11}$$

where δ is:

$$\delta = \frac{C_c + 2 \cdot \Gamma^*}{C_c + K_c \cdot \left(1 + \frac{O}{K_o}\right)}.$$

Solving N_{lc} from Eqn (2.8) yields:

$$N_{lc} = \frac{-b - \sqrt{b^2 - 4 \cdot a \cdot c}}{2 \cdot a}, \tag{2.12}$$

in which

$$a = 4 \cdot k_c \cdot \delta \cdot \left(4 \cdot \theta \cdot k_c \cdot \delta + k_j\right)$$

$$b = -\left(4 \cdot k_c \cdot k_j \cdot \delta \cdot N_l + 4 \cdot k_c \cdot \Phi \cdot \delta \cdot I_l + k_j \cdot \Phi \cdot I_l\right)$$

$$c = k_j \cdot \Phi \cdot I_l \cdot N_l.$$

Using Eqn (2.12) for the calculation of the maximum carboxylation capacity [Eqn (2.8)] and the maximum electron transport rate [Eqn (2.9)], results into an optimal distribution of N in which the photosynthesis is co-limited by the RuBP carboxylation [Eqn (2.2)] and the RuBP regeneration [Eqn (2.3)]; and thereby we found with Eqn (2.12) a method to solve the optimal distribution of N analytically (Fig 2.1).

2.3 Results and Discussion

Here we illustrate the defined leaf photosynthesis model with simulations for optimized acclimation in N partitioning in response to changing atmospheric conditions. Acclimating leaves are expected to tune their N partitioning between RuBP carboxylation and RuBP regeneration to maximize net carbon gain (McMurtrie *et al.* 2008; Sterck & Schieving 2011). We show simulations where leaves are allowed to acclimate N partitioning and compare this with simulations where leaves have a fixed N partitioning, concentrating on responses to increase in atmospheric CO_2 and to increase in temperature. For all simulations we use the same parameter values as described in Table 2.1, unless specified otherwise (for parameter values related to the temperature equations see Table A2.1). Parameter values of Soybean (*Glycine max* (L.) Merr) are used, as this is grown extensively over the world and as it is frequently being studied in its response to elevated CO_2 (Ainsworth *et al.* 2002). We compare our simulation results to real observations and show and discuss different timescales of optimization. In the second section, we compare the performance of our analytical model to that of a numerical model, similar to those used in other existing vegetation models.

2.3.1 Responses to CO_2 changes

We investigated leaf-level responses to an increase in atmospheric CO_2 from 350 μmol mol^{-1} to 700 μmol mol^{-1} (we assume a fixed ratio of CO_2 in the chloroplast to external CO_2 of 0.7, as it was shown that this ratio will stay the same despite changes in environmental conditions (Wong, Cowan & Farquhar 1979)). We expected reduced N investment in RuBP carboxylation, as CO_2 elevation and the associated increase in CO_2 in the chloroplast reduces the constraints on RuBP carboxylation.

With an increase in atmospheric CO_2 from 350 to 700 μmol mol^{-1}, the N allocation to RuBP carboxylation decreased by 24% with optimal N partitioning (Fig 2.2a). This finding is in agreement with our expectation, and experimental data also show this effect (Harley *et al.* 1992; Medlyn 1996). Experimental data show a reduction of 13% with an increase of atmospheric CO_2 from 350 μmol mol^{-1} to 700 μmol mol^{-1} for 39 tree species (Medlyn 1996). For cotton there was a reduction of 12%, when the atmospheric CO_2 increased from 350 μmol mol^{-1} to 650 μmol mol^{-1} (Harley *et al.* 1992); for the same increases in CO_2, our model results show a reduction of 22% in N allocated to RuBP carboxylation. Furthermore, the model developed by Xu *et al.* (2012) predicted a potential decrease in investment of N allocated to RuBP carboxylation of 15% for deciduous trees, evergreen trees, and herbaceous plants for an increase in atmospheric CO_2 from 370 to 550 μmol mol^{-1} (Xu *et al.* 2012). For the same increases in CO_2, our model results also show a reduction of 15% in N allocated to RuBP carboxylation.

The increase in leaf photosynthesis with elevated CO_2 was simulated to be considerably larger (i.e. 34%) when N allocation is optimized compared to constant

partitioning (Fig 2.2b). So, while many models assume a constant allocation of N between RuBP carboxylation and RuBP regeneration (Chen *et al.* 1993; Peltoniemi, Duursma & Medlyn 2012), our results suggest that this may lead to an underestimation of the effect of CO_2 elevation on leaf photosynthesis. Conversely, as acclimation in N partitioning in response to CO_2 has been shown to vary between species – maybe not all species respond optimally – therefore our model may in some cases lead to overestimation.

2.3.2 Responses to temperature changes

We investigated leaf-level responses to an increase in temperature from 15°C to 25°C (see A2.4 Methods for the temperature relationships of the model parameters). We expected there to be less investment of N in RuBP regeneration, as higher temperatures differentially increase the rates of electron transport and carboxylation (Lambers, Chapin III & Pons 2008), such that the increase in RuBP regeneration is higher than the increase in RuBP carboxylation, and to compensate for this misbalance, more N needs to be allocated to RuBP carboxylation (or V_{cmax}).

Fig 2.2c shows the predicted optimal changes in ratio of N investment in RuBP carboxylation to RuBP regeneration (N_{lc}/N_{lj}) with increasing temperature from 15°C to 25°C; for which an increase of 7% in N allocation of V_{cmax} was found (Fig 2.2c). This finding is in agreement with our expectation and experimental studies also show this trend (e.g. Onoda, Hikosaka & Hirose 2005; Yamori *et al.* 2010). For *Polygonum cuspidatum* and *Fagus crenata* an increase of 16% was found when the temperature increased from 15°C to 25°C (Onoda, Hikosaka & Hirose 2005). Results of another experiment on 11 herbaceous crop species show an increase of 19% when the temperature increased from 15°C to 30°C (Yamori *et al.* 2010); for the same increase in temperature our model results show an increase of 17% in N allocated to RuBP carboxylation. Furthermore, our model showed that the change in leaf photosynthesis across the simulated temperature range would be 10% more positive if N allocation is optimized compared to constant partitioning (Fig 2.2d).

Plants have indeed been found to acclimate to for example growth temperature changes by optimizing their N partitioning among the photosynthetic components (Yamori *et al.* 2009). However, these temperature-induced changes in the N partitioning seem to differ between species (Hikosaka 1997). For example, annual plants exhibit smaller acclimation responses to changes in temperature compared to evergreen woody species. This difference has been attributed to the fact that herbaceous plants experience a smaller seasonal change in growth temperature (Hikosaka 1997). Interestingly, cold tolerant plants tend to have a higher capacity for acclimation to temperature compared to cold sensitive species (Yamori *et al.* 2010), suggesting that this capacity can be associated with adaptations to extreme temperatures.

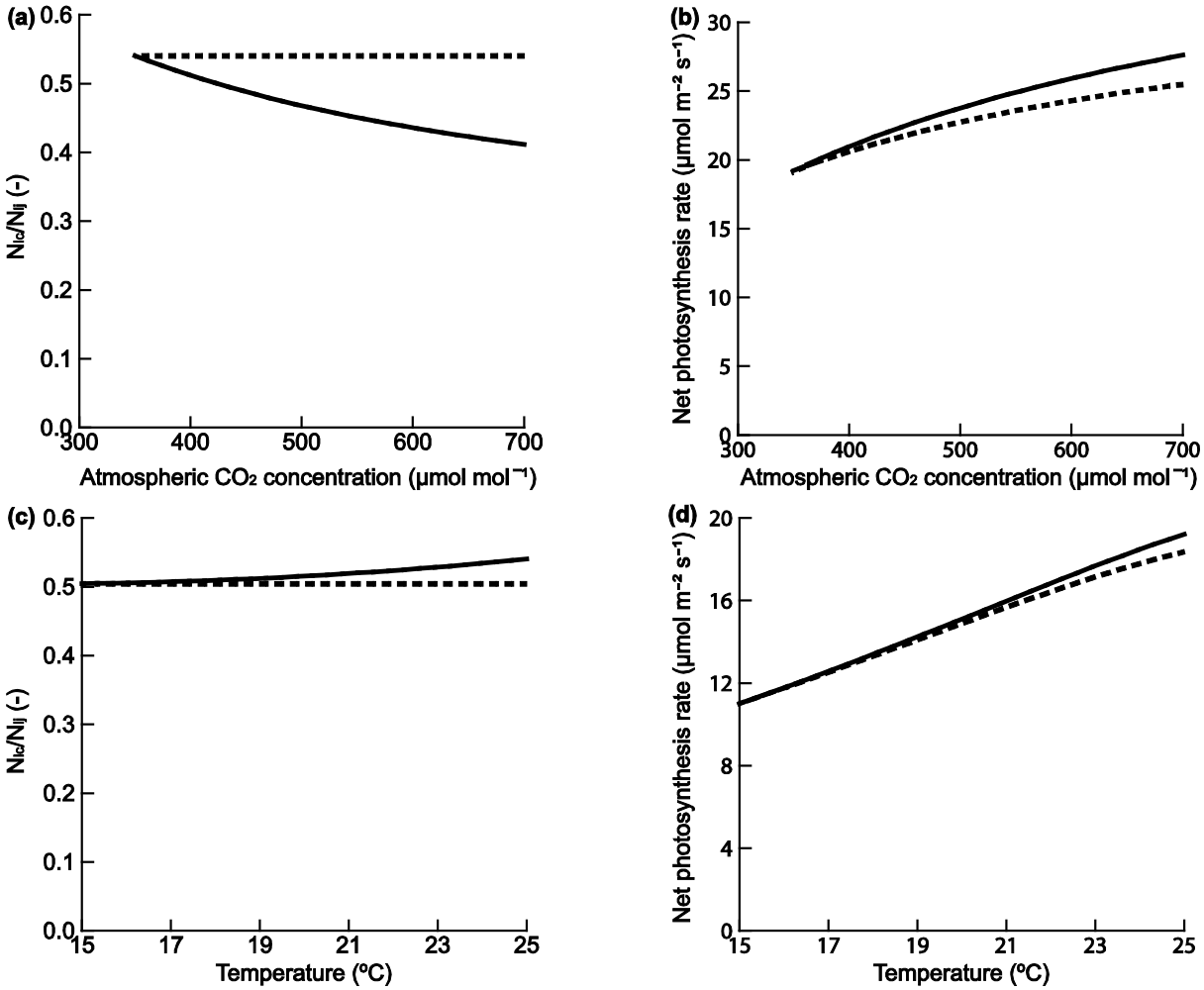

Fig 2.2 Nitrogen allocated to V_{cmax} divided by nitrogen allocated to J_{max} (N_{lc}/N_{lj}) (left panels: a, c) and net photosynthesis rate (right panels: b, d) for the optimal nitrogen allocation between J_{max} and V_{cmax} (continuous lines) and for constant nitrogen allocation between J_{max} and V_{cmax} (dashed lines) for different CO_2 concentrations (a, b) and temperatures (c, d) (parameter values are provided in Table 2.1)

2.3.3 Optimization time scale

Here we analyse the extent to which the time scale over which optimization is calculated relative to the variation in environment affects simulated rates of photosynthesis. The effect of daily temperature and radiation changes on photosynthesis were examined for three weeks in a year. Weather data from 24 July until 13 August 1998, Bondville Champaign Illinois USA (40° latitude, -88° longitude) was used. We chose this climate station as it is close to the soybean FACE experiment; the largest climate change experiment for soybean (Ainsworth *et al.* 2002) the species for which the model version presented here was calibrated. We studied the effect of different timescales of N optimization between RuBP carboxylation to RuBP regeneration. We used hourly data of radiation and temperature (Fig 2.3a). Optimal N allocation was determined according to three scenarios: 1) N allocation was optimized per hour, 2) N allocation was optimized for average daily conditions and 3) N allocation was

optimized for average weekly weather conditions. A constant atmospheric CO_2 of 350 μmol mol^{-1} was assumed.

The effect of increasing the time step of optimization of N allocation (Fig 2.3b) was the largest from hour (scenario 1) to day (scenario 2); it reduced estimated total photosynthesis by 13% over the three weeks (Fig 2.3c-e). Further reduction of the time step of optimization had less effect, if the time step was increased from per hour to per week (scenario 3) the reduction on the photosynthesis became 15% (Fig 2.3c-e). Interestingly, the difference in simulations 2 and 3 depended on the dynamics of light availability. When light intensity and temperature on a certain day are higher than the weekly average, the calculated daily net photosynthesis is higher for scenario 2 than for scenario 3. The reverse holds when the daily light availability is below the weekly average (Fig 2.3c,d). This is, because under low light conditions the advantage of optimal N partitioning decreases with increase in N, as limitation of photosynthesis by N decreases, and therefore there is less advantage of optimal partitioning (Hikosaka & Hirose 1998). So, plants adjusted to long-term average light conditions have to cope with daily light fluctuations that are strongly deviating from average light conditions, but optimal partitioning of N may be restricted by temporal and anatomical limitations (Oguchi, Hikosaka & Hirose 2003). In this respect, it is interesting to note that herbaceous species exhibit faster acclimation to changing light conditions, than woody species (Niinemets 2007). It has been shown for several plant species that they change N partitioning optimally to maximize their net carbon gain under changing irradiance (Evans & Poorter 2001) and temperature (Yamori *et al.* 2009). However, next to the time scale of optimization, the degree to which species acclimate to changes in light intensity differs per species. For example, shade species are able to acclimate to the shade, but their ability to acclimate to full sun is more limited, and this could be associated with their general adaptation to shade (Hikosaka & Terashima 1995).

The degree and rate of acclimation to temperature is also species dependent (Hikosaka 1997). For example, annual plants show less acclimation to variation in temperature than evergreen species, and this has been attributed to the fact that herbaceous plants experience a smaller seasonal change in growth temperature (Hikosaka 1997). Furthermore, shade species are able to acclimate to the shade, but their ability to acclimate to full sun is more limited, probably due to specialization to a particular ecological niche (Hikosaka & Terashima 1995). Together, these simulations show that the time lag of optimization of N allocation and its potential variation across species should be taken into account in vegetation models, which currently not being done (Medlyn 1996; Hikosaka 1997; Hikosaka & Hirose 1998; Sterck & Schieving 2011; Westoby, Cornwell & Falster 2012; Xu *et al.* 2012; Buckley, Cescatti & Farquhar 2013). This may at first make predictions of photosynthesis more accurate, and second it can be used as a means to help assess the adaptive significance of variation in the rate of acclimation.

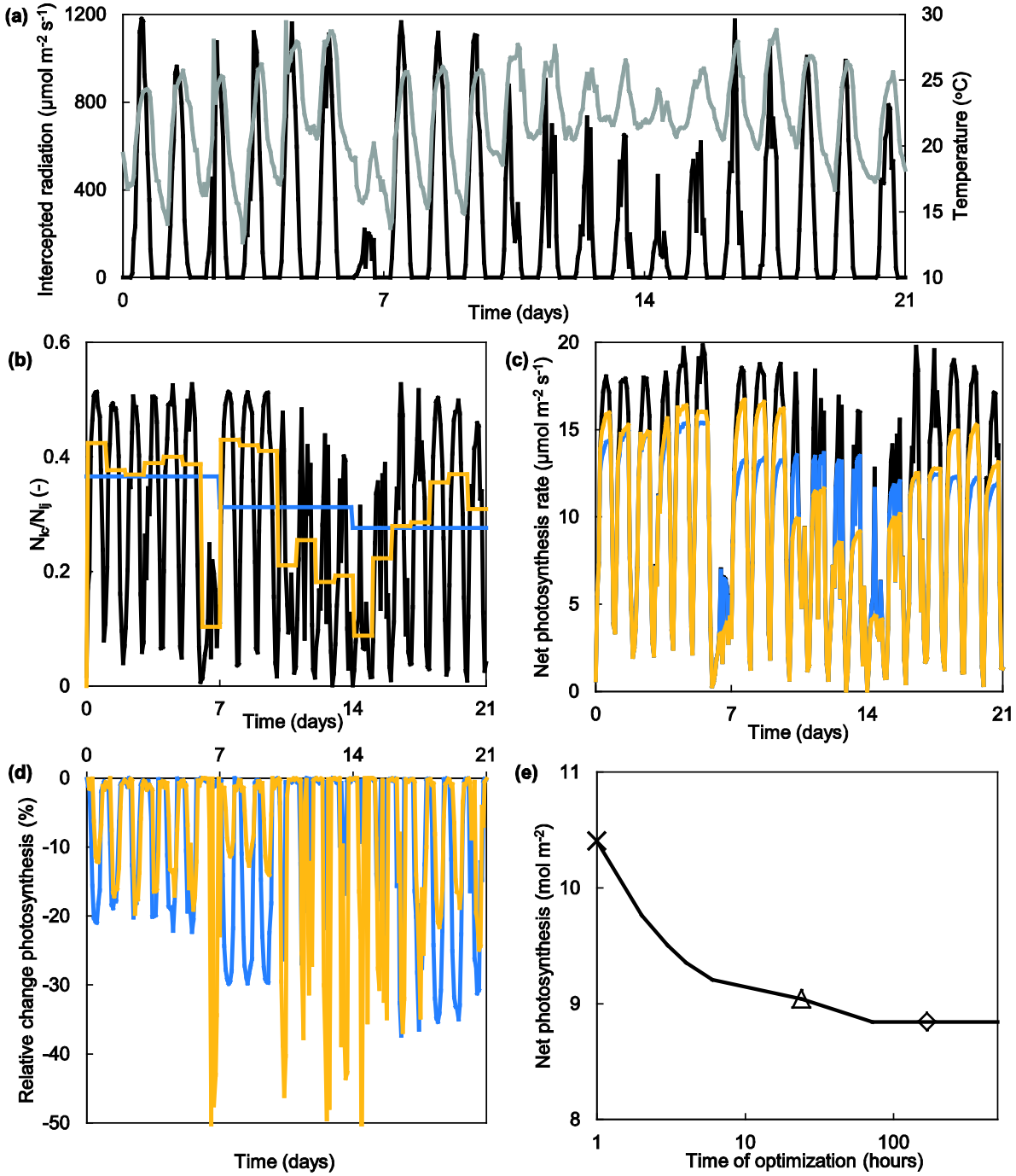

Fig 2.3 Varying timescale of leaf acclimation. We used temperature (grey line) and radiation (black line) data from Bondville Champaign Illinois USA, 40°-88°, day 0 until 21 (24 July until 13 August 1998) to drive leaf photsynthesis (a). Panels (b-d) show results when leaves acclimated on different timescales over the three weeks: per hour (black line, scenario 1), per day (orange line, scenario 2) or per week (blue line, scenario 3). For these different scenarios we show: (b) the ratio of nitrogen allocation between V_{cmax} and J_{max} (N_{lc}/N_{lj}), (c) the total photosynthesis, (d) the relative change in photosynthesis of the scenario of optimizing per day (orange line) and per week (blue line) compared to optimizing per hour, and (e) integration of the hourly photosynthesis rate over the three weeks versus different time scales of acclimation: the cross indicates scenario 1, the triangle scenario 2, and the diamond scenario 3

2.3.4 Comparison of the analytical and numerical optimal nitrogen allocation model

Vegetation models are gradually becoming embedded within larger, more complex models, like General Circulation Models (Sitch *et al.* 2003). These larger models contain many processes that often involve a very large number of computations. So, there is a need for analytical solutions, which improve computational efficiency. In our case, our analytical model for N allocation between RuBP carboxylation and RuBP regeneration reduces the computation time for estimating photosynthesis with optimal N allocation by about 4 times (A2.2, A2.3 Methods for the analytical solution and the numerical solution respectively). Most models execute hundreds of optimizations, therefore it is very important to reduce the modelling time. In addition, the analytical calculation yielded the same solution as the numerical calculation of the optimal N distribution between RuBP carboxylation and RuBP regeneration. The analytical solution and the numerical solution were developed in MATLAB, the numerical solution is solved by using the fzero function in MATLAB (root solver function) (see A2.2, A2.3 Methods for the analytical solution and the numerical solution respectively).

2.4 Concluding remarks

In this chapter we presented an analytical solution for the optimal N distribution between RuBP regeneration and RuBP carboxylation. Based on this, we showed the impact of variation in temperature and CO_2 on the optimal N partitioning within the leaf. Our results showed (i) that acclimation at the level of N allocation between components of RuBP carboxylation and RuBP regeneration may strongly impact leaf-level responses to climate change, particularly rising CO_2, (ii) that the assumption of an optimal allocation provides patterns that are in agreement with observations, (iii) that the time-step of optimization in association with the rate at which plants acclimate to changing conditions is an important element to consider and (iv) that our analytical model provides a much faster yet accurate alternative to the numerical models currently in use.

Acknowledgement

We thank Kouki Hikoska and Ülo Niinemets for their valuable comments on the manuscript.

Appendix – A2.1 Methods. R code analytical solution

```
#################################################################
#Here we define the functions related to temperature

getDefaultTempPars<- function(){

  #Default leaf pars
  par<- NULL
  par$R <- 8.315  #Gas constant (J /K mol)

  #Parameter values for the temperature functions
  par$HaKcmm <- 59400  #Activation energy of the Michaelis Menten constant for carboxylation (KJ /mol)
  par$HaKomm <- 36000  #Activation energy of the Michaelis Menten constant for oxygenation (KJ /mol)
  par$HaGamma <- 20970  #Activation energy of the CO2 compensation point (KJ /mol)

  par$HaJmax <- 58936  #Activation energy of the maximum electron transport rate (KJ /mol)
  par$HdJmax <- 199233  #Deactivation energy of Jmax (KJ /mol)
  par$dSJmax <- 647  #Entropy term of Jmax (KJ /mol)

  par$HaVcmax <- 75794  #Activation energy of the maximum rate of carboxylation (KJ /mol)
  par$HdVcmax <- 202022  #Deactivation energy of Vcmax (KJ /mol)
  par$dSVcmax <- 657  #Entropy term of Vcmax (KJ /mol)

  par
}

celsiusToKelvin<-function(tempCelsius){
  #Convert temperature from Celsius to Kelvin
  tempCelsius + 273
}

tempAdjustArrehniusResponse <- function(fromTempC, toTempC, Ha, R){
  # Arrhenius equation
  # Args:
  #   Ha: Activation energy (KJ /mol)
  #   R: Gas constant (J /K mol)
  #   tempc: Temperature in degrees C
  #
  # Returns:
  #   Adjusted rate

  fromTempK <- celsiusToKelvin(fromTempC)
  toTempK <- celsiusToKelvin(toTempC)

  exp((Ha * (toTempK - fromTempK)) /(fromTempK * R * toTempK))
}

tempAdjustPeakModel <- function(fromTempC, toTempC, Ha, Hd, dS, R){
  # Temperature effect according to a peak model
  #
  # Args:
  #   toTempC: temperature in degrees C
  #   Ha: Activation energy (KJ /mol)
  #   Hd: Deactivation energy (KJ /mol)
  #   dS: Entropy term (J /mol)
  #   R: Gas constant (J /K mol)
  #
  # Returns:
```

```
  #   adjusted rate

  fromTempK <- celsiusToKelvin(fromTempC)
  toTempK <- celsiusToKelvin(toTempC)
  exp((Ha * (toTempK - fromTempK)) /(fromTempK * R * toTempK)) *
    (1 + exp((fromTempK * dS - Hd) /(fromTempK * R))) /
    (1 + exp((dS * toTempK - Hd) /(toTempK * R)))
}

adjustLeafsParsToTemp<-function(basePars, toTempC, tempPars=getDefaultTempPars()){
  newPars<-  basePars
  fromTempC <-basePars$tempC

  #CO2 compensation point adjusted with Arrhenius equation
  newPars$Gamma = newPars$Gamma *
     tempAdjustArrehniusResponse(fromTempC, toTempC, tempPars$HaGamma, tempPars$R)

  #Michaelis Menten constant for carboxylation adjusted with Arrhenius equation
  newPars$cKcmm = newPars$cKcmm *
    tempAdjustArrehniusResponse(fromTempC, toTempC, tempPars$HaKcmm, tempPars$R)

  #Michaelis Menten constant for oxygentation adjusted with Arrhenius equation
  newPars$cKomm = newPars$cKomm *
    tempAdjustArrehniusResponse(fromTempC, toTempC, tempPars$HaKomm, tempPars$R)

  #Temperature effect on Jmax adjusted with peak model
  newPars$kj = newPars$kj * tempAdjustPeakModel(fromTempC, toTempC, tempPars$HaJmax,
                                  tempPars$HdJmax, tempPars$dSJmax, tempPars$R)
  #Temperature effect on Vcmax adjusted with peak model
  newPars$kc = newPars$kc * tempAdjustPeakModel(fromTempC, toTempC, tempPars$HaVcmax,
                                  tempPars$HdVcmax, tempPars$dSVcmax, tempPars$R)
  newPars
}

#####################################################################
#Here we define the functions

setDefaultLeafPars<- function(){
  #Default leaf pars
  #Parameter values
  par <- NULL
  par$tempC <- 25  #Temperature at which parameters are measured (degree Celsius)

  par$CcCa <- 0.7  #Ratio of internal CO2 to atmospheric CO2 ( - )
  par$Gamma <- 51  #CO2 compensation point (mu mol/ mol)
  par$q <- 0.25  #Quantum efficiency (mu mol/ mol)
  par$cv <- 0.9  #Curvature factor ( - )
  par$O2 <- 205000  #Oxygen concentration (mu mol/ mol)
  par$cKomm <- 560900  #Michaelis-Menten constant for oxygenation (mu mol/ mol)
  par$cKcmm <- 402  #Michaelis-Menten constant for carboxylaton (mu mol/ mol)

  #Parameter values related to nitrogen
  par$kc <- 0.83  #Carboxylation capacity per N mass (mu mol C/ mmol N/ s)
  par$kj <- 0.83  #Electron transport capacity per N mass (mu mol C/ mmol N/ s)
  par$Nb <- 30  #Leaf N concentration not associated with the photosynthesis (mmol/ m2)

  par
}

#Effective Michaelis Menten constant for carboxylation,  including the effect of temperature (mu mol/ mol)
```

```
Km <- function(par){
  par$cKcmm * (1 + (par$O2 / par$cKomm ))
}

#Nitrogen needed for Vcmax (mmol/ m2)
Nlc <- function(par, Ca, Nl, Il){
  Ccij = (Cc(par, Ca) + 2 * par$Gamma) / (Cc(par, Ca) + Km(par))
  a = 4 * par$kc * Ccij * (4 * par$cv * Ccij * par$kc + par$kj)
  b =  - (4 * par$kj * par$kc * Ccij * (Nl - par$Nb) + 4 * par$kc * Ccij * Il * par$q + par$kj * Il * par$q)
  c = par$kj * Il * par$q * (Nl - par$Nb)

  (- b - sqrt((b^2) - (4 * a * c))) / (2 * a)
}

#Vcmax with optimal partitioning of N (mu mol/ m2/ s)
Vcmax <- function(par, Ca, Nl, Il){
  par$kc * Nlc(par, Ca, Nl, Il)
}

#Jmax with optimal partitioning of N (mu mol/ m2/ s)
Jmax <- function(par, Ca, Nl, Il){
  par$kj  * (Nl - Nlc(par, Ca, Nl, Il) - par$Nb)
}

#effect of light on the electron transport rate ( - )
ELight <- function(par, Ca, Nl, Il){
  E = ((par$q * Il)) / Jmax(par, Ca, Nl, Il)

  ((1 + E) - sqrt(((1 + E)^2) - (4 * par$cv * E))) / (2 * par$cv)
}

####Co - limitation of the photosynthesis by RuBP regeneration and RuBP carboxylation####
#Photosynthesis limited by RuBP regeneration (mu mol/ m2/ s)
ElectronLim <- function(par, Ca, Nl, Il){
  (Cc(par, Ca) - par$Gamma) /
  (Cc(par, Ca) + 2 * par$Gamma) *
  ELight(par, Ca, Nl, Il) * (Jmax(par, Ca, Nl, Il) / 4)
}

#Photosynthesis limited by RuBP carboxylation (mu mol/ m2/ s)
CarboxLim <- function(par, Ca, Nl, Il){
  Vcmax(par, Ca, Nl, Il) *
  (Cc(par, Ca) - par$Gamma) /
  (Cc(par, Ca) + Km(par))
}

#CO2 concentration in chloroplast (mu mol/ mol)
Cc <- function(par, Ca){
  Ca * par$CcCa
}

#Nitrogen to RuBP regeneration (mmol/ m2)
Nlj <- function(par, Ca, Nl, Il){
  Nl - par$Nb - Nlc(par, Ca, Nl, Il)
}

#Program that gives the analytical solution for N investment in RuBP regeneration
#and the RuBP carboxylation to have co-limitation of the photosynthesis
#####################################################################
```

```
rm(list=ls(all=TRUE))
source("aci-fun.R")
source("temperatureResponse-fun.R")

#Environmental circumstances
Ca <- 350  #Atmospheric CO2 concentration (mu mol/ mol)

#Variable of the plant
Nl <- 300  #Total amount of leaf N (mmol/ m2)
Il <- 1000  #Total amount of light intercepted by a leaf (mu mol/ m2/ s)
leafPars <- setDefaultLeafPars()

#####################################################################
##Getting the results, ElectronLim should be equal to CarboxLim for co-limitation
#Results for 25 degree Celsius
ElectronLim(par=leafPars, Ca=Ca,Nl=Nl,Il=Il)
CarboxLim(par=leafPars, Ca=Ca,Nl=Nl,Il=Il)

#Nitrogen to RuBP carboxylation (mmol/ m2)
Nlc(par=leafPars, Ca=Ca,Nl=Nl,Il=Il)

#Nitrogen to RuBP regeneration (mmol/ m2)
Nlj(par=leafPars, Ca=Ca,Nl=Nl,Il=Il)

#adjust parameters to temp
newPars <- adjustLeafsParsToTemp(leafPars, 30)
ElectronLim(par=newPars, Ca=Ca,Nl=Nl,Il=Il)
CarboxLim(par=newPars, Ca=Ca,Nl=Nl,Il=Il)
Nlc(par=newPars, Ca=Ca,Nl=Nl,Il=Il)
Nlj(par=newPars, Ca=Ca,Nl=Nl,Il=Il)
```

Appendix – A2.2 Methods. MATLAB code analytical solution

```
function Parameters_temp(parT,tempCelsius)

  parT.TempC=tempCelsius.TempC;

  %Parameter values for the temperature functions
  parT.R = 8.315;  %Gas constant (J /K mol)

  parT.HaKcmm = 59400;  %Activation energy of the Michaelis Menten constant for carboxylation
(KJ /mol)
  parT.HaKomm = 36000;  %Activation energy of the Michaelis Menten constant for oxygenation
(KJ /mol)
  parT.HaGamma = 20970;  %Activation energy of the CO2 compensation point (KJ /mol)

  parT.HaJmax = 58936;  %Activation energy of the maximum electron transport rate (KJ /mol)
  parT.HdJmax = 199233;  %Deactivation energy of Jmax (KJ /mol)
  parT.dSJmax = 647;  %Entropy term of Jmax (KJ /mol)

  parT.HaVcmax = 75794;  %Activation energy of the maximum rate of carboxylation (KJ /mol)
  parT.HdVcmax = 202022;  %Deactivation energy of Vcmax (KJ /mol)
  parT.dSVcmax = 657;  %Entropy term of Vcmax (KJ /mol)

  parT.celsiusToKelvin = parT.TempC + 273;  %to convert from degrees Celsius to Kelvin

  %Functions to relate Kcmm, Komm, Gamma to temperature (Arhenius model)
  parT.KcmmT = exp((parT.HaKcmm * (parT.celsiusToKelvin - 298)) /...
              (298 * parT.R * parT.celsiusToKelvin));

  parT.KommT = exp((parT.HaKomm * (parT.celsiusToKelvin - 298)) /...
               (298 * parT.R * parT.celsiusToKelvin));

  parT.GammaT = exp((parT.HaGamma * (parT.celsiusToKelvin - 298)) /...
                (298 * parT.R * parT.celsiusToKelvin));

  %Functions to relate Vcmax, Jmax to temperature (peak model)
  parT.VcmaxT = exp((parT.HaVcmax * (parT.celsiusToKelvin - 298)) /(298 * parT.R *
parT.celsiusToKelvin)) * ...
                (1 + exp((298 * parT.dSVcmax - parT.HdVcmax) /(298 * parT.R))) / ...
                (1 + exp((parT.dSVcmax * parT.celsiusToKelvin - parT.HdVcmax)
/(parT.celsiusToKelvin * parT.R)));

 parT.JmaxT = exp((parT.HaJmax * (parT.celsiusToKelvin - 298)) /(298 * parT.R *
parT.celsiusToKelvin)) * ...
              (1 + exp((298 * parT.dSJmax - parT.HdJmax) /(298 * parT.R))) / ...
              (1 + exp((parT.dSJmax * parT.celsiusToKelvin - parT.HdJmax)
/(parT.celsiusToKelvin * parT.R)));

end
```

```
function Parameters_aci(par)
  %Parameter values A-Cc curve
  par.CcCa = 0.7;  %Ratio of internal CO2 to atmospheric CO2 ( - )
```

```
  par.Gamma = 51;  %CO2 compensation point (at 25 oC) (mu mol/mol)
  par.q = 0.25;  %Quantum efficiency (mu mol/ mol)
  par.cv = 0.9;  %Curvature factor ( - )
  par.O2 = 205000;  %Oxygen concentration (mu mol/mol)
  par.cKomm = 560900;  %Michaelis-Menten constant for oxygenation (at 25 oC) (mu mol/mol)
  par.cKcmm = 402;  %Michaelis-Menten constant for carboxylaton (at 25 oC) (mu mol/mol)

  %Parameter values related to nitrogen
  par.kc = 0.83;  %Carboxylation capacity per N mass (mu mol C/ mmol N/ s)
  par.kj = 0.83;  %Electron transport capacity per N mass (mu mol C/ mmol N/ s)
  par.Nb = 30;  %Leaf N concentration not associated with the photosynthesis (mmol/ m2)
end
```

```
classdef aci_class < handle
    %Here we define the functions

    properties (SetAccess=public, GetAccess=public)
        %Parameters A-Cc curve (25oC)
        CcCa, Gamma , q, cv, O2, cKomm, cKcmm
        kc, kj, Nb

        %Parameters needed for other temperatures
        TempC, celsiusToKelvin
        R
        HaKcmm, HaKomm, HaGamma
        HaJmax, HdJmax, dSJmax
        HaVcmax, HdVcmax, dSVcmax
        KcmmT, KommT, GammaT, VcmaxT, JmaxT
    end

    methods (Access=public)
        Parameters_aci(par)
        Parameters_temp(parT,tempCelsius)

        function Km = KmFu(par, parT)
            Km = par.cKcmm * parT.KcmmT * (1 + (par.O2 / (par.cKomm* parT.KommT)));
        end

%Nitrogen allocated to Vcmax for optimal partitioning of N (mmol/ m2)
        function Nlc = NlcFu(par, parT, Ca, Nl, Il)
            kc_=par.kc * parT.VcmaxT;
            kj_=par.kj * parT.JmaxT;
            Ccij = (CcFu(par, Ca) + 2 * par.Gamma * parT.GammaT) / (CcFu(par, Ca) + KmFu(par,
parT));
            a = 4 * kc_ * Ccij * (4 * par.cv * Ccij * kc_ + kj_);
            b =  - (4 * kj_ * kc_ * Ccij * (Nl - par.Nb) + 4 * kc_ * Ccij * Il * par.q + kj_ *
Il * par.q);
            c = kj_ * Il * par.q * (Nl - par.Nb);

            Nlc = (- b - sqrt((b^2) - (4 * a * c))) / (2 * a);
        end

%Vcmax with optimal partitioning of N (mu mol/ m2/ s)
        function Vcmax = VcmaxFu(par, parT, Ca, Nl, Il)
            Vcmax = par.kc * parT.VcmaxT * NlcFu(par, parT, Ca, Nl, Il);
```

```
        end

%Jmax with optimal partitioning of N (mu mol/ m2/ s)
        function Jmax = JmaxFu(par, parT, Ca, Nl, Il)
            Jmax =  par.kj * parT.JmaxT  * (Nl - NlcFu(par, parT, Ca, Nl, Il) - par.Nb);
        end

%Effect of light on the electron transport rate ( - )
        function ELight = ELightFu(par, parT, Ca, Nl, Il)
            E = ((par.q * Il)) / JmaxFu(par, parT, Ca, Nl, Il);
            ELight = ((1 + E) - sqrt(((1 + E)^2) - (4 * par.cv * E))) / (2 * par.cv);
        end

%%Co - limitation of the photosynthesis by RuBP regeneration and RuBP carboxylation
%Photosynthesis limited by RuBP regeneration (mu mol/ m2/ s)
        function ElectronLim = ElecFu(par, parT, Ca, Nl, Il)
            ElectronLim = (CcFu(par, Ca) - par.Gamma * parT.GammaT) / (CcFu(par, Ca) + 2 *
par.Gamma * parT.GammaT)...
                           * ELightFu(par, parT, Ca, Nl, Il) * (JmaxFu(par, parT, Ca, Nl, Il) /
4);
        end

%Photosynthesis limited by RuBP carboxylation (mu mol/ m2/ s)
        function CarboxLim = CarboxyLimFu(par, parT, Ca, Nl, Il)
            CarboxLim =  VcmaxFu(par, parT, Ca, Nl, Il) * (CcFu(par, Ca) - par.Gamma *
parT.GammaT)...
                         / (CcFu(par, Ca) + KmFu(par, parT));
        end

%CO2 concentration in chloroplast (mu mol/mol)
        function Cc = CcFu(par, Ca)
            Cc =  Ca * par.CcCa;
        end

%Nitrogen to RuBP regeneration (mmol/ m2)
        function Nlj = NljFu(par, parT, Ca, Nl, Il)
            Nlj =  Nl - par.Nb - NlcFu(par, parT, Ca, Nl, Il);
        end

    end
end
```

```
%MainAnalysis.m
% Program for analytical solution of optimal N investment in Pjl and Pcl
%Program that gives the analytical solution for optimal N investment in
%RuBP regeneration (Pjl) and the RuBP carboxylation (Pcl), such that
%both are co-limiting
%%%%%%%%%%%%%%%%%%%%%%%%%%%%%%%%%%%%%%%%%%%%%%%%%%%%%%%%%%%%%%%%%%%%%%%%%%%%%%%
clc,clear all, close all, clear classes
name_simulation='Analytical solution of optimal N investment in RuBP regeneration and RuBP
carboxylation';
%%%%%%%%%%%%%%%%%%%%%%%%%%%%%%%%%%%%%%%%%%%%%%%%%%%%%%%%%%%%%%%%%%%%%%%%%%%%%%%
aci25=aci_class;
aci25.Parameters_aci;
T_Celsius25.TempC=25;
```

```
aci25.Parameters_temp(T_Celsius25)

aci=aci_class;
aci.Parameters_aci;
T_Celsius.TempC=30;
aci.Parameters_temp(T_Celsius);

%%%%%%%%%%%%%%%%%%%%%%%%%%%%%%%%%%%%%%%%%%%%%%%%%%%%%%%%%%%%%%%%%%%%%%%%%%%%%%%
%Environmental circumstances
Ca=350;  %Atmospheric CO2 concentration (mu mol/mol)

%Variable of the plant
Nl=300;  %Total amount of leaf N (mmol/ m2)
Il=1000;  %Total amount of light intercepted by a leaf (mu mol/ m2/ s)

display('Getting the results, ElectronLim should be equal to CarboxLim for co-limitation')
display('Results for 25 degree Celsius')

ElectromLim25 = aci25.ElecFu(aci25, Ca, Nl, Il)
CarboxLim25 = aci25.CarboxyLimFu(aci25, Ca, Nl, Il)

Nlj25 = aci25.NljFu(aci25, Ca, Nl, Il)
tic
Nlc25 = aci25.NlcFu(aci25, Ca, Nl, Il)
display('Computation time of the model')
Time=toc   %Measures time of the model run
display('Results for 30 degree Celsius')
ElectromLim = aci.ElecFu(aci, Ca, Nl, Il)
CarboxLim = aci.CarboxyLimFu(aci, Ca, Nl, Il)
Nlj = aci.NljFu(aci, Ca, Nl, Il)
Nlc = aci.NlcFu(aci, Ca, Nl, Il)

display(['Simulation: ' name_simulation ', is finished'])
```

```
Getting the results, ElectronLim should be equal to CarboxLim for co-limitation
Results for 25 degree Celsius

ElectromLim25 =
   18.5825

CarboxLim25 =
   18.5825

Nlj25 =
  178.3770

Nlc25 =
   91.6230

Computation time of the model
Time =
   1.3645e-04

Results for 30 degree Celsius
ElectromLim =
   19.9004

CarboxLim =
```

```
   19.9004

Nlj =
  174.5647

Nlc =
   95.4353

Simulation: Analytical solution of optimal N investment in RuBP regeneration and RuBP
carboxylation, is finished
```

Published with MATLAB® R2013a

Appendix – A2.3 Methods. MATLAB code numerical solution

```
function Parameters_temp(parT,tempCelsius)

  parT.TempC=tempCelsius.TempC;

  %Parameter values for the temperature functions
  parT.R = 8.315;  %Gas constant (J /K mol)

  parT.HaKcmm = 59400;  %Activation energy of the Michaelis Menten constant for carboxylation
(KJ /mol)
  parT.HaKomm = 36000;  %Activation energy of the Michaelis Menten constant for oxygenation
(KJ /mol)
  parT.HaGamma = 20970;  %Activation energy of the CO2 compensation point (KJ /mol)

  parT.HaJmax = 58936;  %Activation energy of the maximum electron transport rate (KJ /mol)
  parT.HdJmax = 199233;  %Deactivation energy of Jmax (KJ /mol)
  parT.dSJmax = 647;  %Entropy term of Jmax (KJ /mol)

  parT.HaVcmax = 75794;  %Activation energy of the maximum rate of carboxylation (KJ /mol)
  parT.HdVcmax = 202022;  %Deactivation energy of Vcmax (KJ /mol)
  parT.dSVcmax = 657;  %Entropy term of Vcmax (KJ /mol)

  parT.celsiusToKelvin = parT.TempC + 273;  %to convert from degrees Celsius to Kelvin

  %Functions to relate Kcmm, Komm, Gamma to temperature (Arhenius model)
  parT.KcmmT = exp((parT.HaKcmm * (parT.celsiusToKelvin - 298)) /...
              (298 * parT.R * parT.celsiusToKelvin));

  parT.KommT = exp((parT.HaKomm * (parT.celsiusToKelvin - 298)) /...
               (298 * parT.R * parT.celsiusToKelvin));

  parT.GammaT = exp((parT.HaGamma * (parT.celsiusToKelvin - 298)) /...
                (298 * parT.R * parT.celsiusToKelvin));

  %Functions to relate Vcmax, Jmax to temperature (peak model)
  parT.VcmaxT = exp((parT.HaVcmax * (parT.celsiusToKelvin - 298)) /(298 * parT.R *
parT.celsiusToKelvin)) * ...
                (1 + exp((298 * parT.dSVcmax - parT.HdVcmax) /(298 * parT.R))) / ...
                (1 + exp((parT.dSVcmax * parT.celsiusToKelvin - parT.HdVcmax)
/(parT.celsiusToKelvin * parT.R)));

 parT.JmaxT = exp((parT.HaJmax * (parT.celsiusToKelvin - 298)) /(298 * parT.R *
parT.celsiusToKelvin)) * ...
              (1 + exp((298 * parT.dSJmax - parT.HdJmax) /(298 * parT.R))) / ...
              (1 + exp((parT.dSJmax * parT.celsiusToKelvin - parT.HdJmax)
/(parT.celsiusToKelvin * parT.R)));


end
```

```
function Parameters_aci(par)
  %Parameter values A-Cc curve
```

```
  par.CcCa = 0.7;  %Ratio of internal CO2 to atmospheric CO2 ( - )
  par.Gamma = 51;  %CO2 compensation point (at 25 oC) (mu mol/mol)
  par.q = 0.25;  %Quantum efficiency (mu mol/ mol)
  par.cv = 0.9;  %Curvature factor ( - )
  par.O2 = 205000;  %Oxygen concentration (mu mol/mol)
  par.cKomm = 560900;  %Michaelis-Menten constant for oxygenation (at 25 oC) (mu mol/mol)
  par.cKcmm = 402;  %Michaelis-Menten constant for carboxylaton (at 25 oC) (mu mol/mol)

  %Parameter values related to nitrogen
  par.kc = 0.83;  %Carboxylation capacity per N mass (mu mol C/ mmol N/ s)
  par.kj = 0.83;  %Electron transport capacity per N mass (mu mol C/ mmol N/ s)
  par.Nb = 30;  %Leaf N concentration not associated with the photosynthesis (mmol/ m2)
end
```

```
classdef aci_class < handle
    %Here we define the functions

    properties (SetAccess=public, GetAccess=public)
        %Parameters A-Cc curve (25oC)
        CcCa, Gamma , q, cv, O2, cKomm, cKcmm
        kc, kj, Nb

        %Parameters needed for other temperatures
        TempC, celsiusToKelvin
        R
        HaKcmm, HaKomm, HaGamma
        HaJmax, HdJmax, dSJmax
        HaVcmax, HdVcmax, dSVcmax
        KcmmT, KommT, GammaT, VcmaxT, JmaxT
    end

    methods (Access=public)
        Parameters_aci(par)
        Parameters_temp(parT,tempCelsius)

        function Km = KmFu(par, parT)
            Km = par.cKcmm * parT.KcmmT * (1 + (par.O2 / (par.cKomm* parT.KommT)));
        end

%Vcmax with optimal partitioning of N (mu mol/ m2/ s)
        function Vcmax = VcmaxFu(par, parT, Nl, alpha)
            Vcmax = par.kc * parT.VcmaxT * alpha * Nl;
        end

%Jmax with optimal partitioning of N (mu mol/ m2/ s)
        function Jmax = JmaxFu(par, parT, Nl, alpha)
            Jmax =  par.kj * parT.JmaxT  * (Nl - alpha * Nl - par.Nb);
        end

%effect of light on the electron transport rate ( - )
        function ELight = ELightFu(par, parT, Nl, alpha, Il)
            E = ((par.q * Il)) ./ JmaxFu(par, parT, Nl, alpha);
            ELight = ((1 + E) - sqrt(((1 + E).^2) - (4 * par.cv * E))) / (2 * par.cv);
        end
```

```
%%Co - limitation of the photosynthesis by RuBP regeneration and RuBP carboxylation
%Photosynthesis limited by RuBP regeneration (mu mol/ m2/ s)
        function ElectronLim = ElecFu(par, parT, Ca, Nl, alpha, Il)
            ElectronLim = (CcFu(par, Ca) - par.Gamma * parT.GammaT) / (CcFu(par, Ca) + 2 *
par.Gamma * parT.GammaT)...
                          * ELightFu(par, parT, Nl, alpha, Il) .* (JmaxFu(par, parT, Nl,
alpha) / 4);
        end

%Photosynthesis limited by RuBP carboxylation (mu mol/ m2/ s)
        function CarboxLim = CarboxyLimFu(par, parT, Ca, Nl, alpha)
            CarboxLim =  VcmaxFu(par, parT, Nl, alpha) * (CcFu(par, Ca) - par.Gamma *
parT.GammaT)...
                         / (CcFu(par, Ca) + KmFu(par, parT));
        end

%CO2 concentration in chloroplast (mu mol/mol)
        function Cc = CcFu(par, Ca)
            Cc =  Ca * par.CcCa;
        end

%Solving for which fraction of the leaf N to Vcmax the RuBP regeneration equals the RuBP
carboxylation
    function Intersect=IntersectFu(par, parT, Ca, Nl, alpha, Il)
           ZeroRes=fzero(@Diff,[0,600]);
           Intersect=ZeroRes;
             function ZeroRes=Diff(alpha)
                ZeroRes=ElecFu(par, parT, Ca, Nl, alpha, Il) - CarboxyLimFu(par, parT, Ca, Nl,
alpha);
             end
    end

    end
end
```

```
%MainAnalysis.m
%Program for numerical solution of optimal N investment in Pjl and Pcl
%
%Program that gives the numerical solution for optimal N investment in
%RuBP regeneration (Pjl) and the RuBP carboxylation (Pcl), such that
%both are co-limiting
%
%%%%%%%%%%%%%%%%%%%%%%%%%%%%%%%%%%%%%%%%%%%%%%%%%%%%%%%%%%%%%%%%%%%%%%%%%%%%%%%%%%%%%%%
clc,clear all, close all, clear classes
name_simulation='Numerical solution of optimal N investment in RuBP regeneration and RuBP
carboxylation';
%%%%%%%%%%%%%%%%%%%%%%%%%%%%%%%%%%%%%%%%%%%%%%%%%%%%%%%%%%%%%%%%%%%%%%%%%%%%%%%%%%%%%%%
aci25=aci_class;
aci25.Parameters_aci;
T_Celsius25.TempC=25;
aci25.Parameters_temp(T_Celsius25)

aci=aci_class;
aci.Parameters_aci;
```

```
T_Celsius.TempC=30;
aci.Parameters_temp(T_Celsius);

%%%%%%%%%%%%%%%%%%%%%%%%%%%%%%%%%%%%%%%%%%%%%%%%%%%%%%%%%%%%%%%%%%%%%%%%%%%%
%Vector of the possible fraction of Nl to Vcmax
alphaBgn=0.01; alphaEnd=0.99;StpNb=1000;
alphaStpSz=(alphaEnd-alphaBgn)/StpNb;
alpha=alphaBgn:alphaStpSz:alphaEnd;

%%%%%%%%%%%%%%%%%%%%%%%%%%%%%%%%%%%%%%%%%%%%%%%%%%%%%%%%%%%%%%%%%%%%%%%%%%%%
%Environmental circumstances
Ca=350;  %Atmospheric CO2 concentration (mu mol/mol)

%Variable of the plant
Nl=300;  %Total amount of leaf N (mmol/ m2)
Il=1000;  %Total amount of light intercepted by a leaf (mu mol/ m2/ s)

display('Getting the results, ElectronLim should be equal to CarboxLim for co-limitation')
display('Results for 25 degree Celsius')

alphaIntersect25 = aci25.IntersectFu(aci25, Ca, Nl, alpha, Il);
ElectromLim25 = aci25.ElecFu(aci25, Ca, Nl, alphaIntersect25, Il)
CarboxLim25 = aci25.CarboxyLimFu(aci25, Ca, Nl, alphaIntersect25)

Nlj25 = Nl - aci25.Nb - alphaIntersect25 * Nl
tic
Nlc25 = alphaIntersect25 * Nl
display('Computation time of the model')
Time=toc   %Measures time of the model run
display('Results for 30 degree Celsius')
alphaIntersect = aci.IntersectFu(aci, Ca, Nl, alpha, Il);
ElectromLim25 = aci.ElecFu(aci, Ca, Nl, alphaIntersect, Il)
CarboxLim25 = aci.CarboxyLimFu(aci, Ca, Nl, alphaIntersect)

Nlj25 = Nl - aci.Nb - alphaIntersect * Nl
Nlc25 = alphaIntersect * Nl


display(['Simulation: ' name_simulation ', is finished'])
```

```
Getting the results, ElectronLim should be equal to CarboxLim for co-limitation
Results for 25 degree Celsius

ElectromLim25 =
   18.5825

CarboxLim25 =
   18.5825

Nlj25 =
  178.3770

Nlc25 =
   91.6230

Computation time of the model
Time =
   5.0191e-04
```

```
Results for 30 degree Celsius
ElectromLim25 =
   19.9004

CarboxLim25 =
   19.9004

Nlj25 =
  174.5647

Nlc25 =
   95.4353

Simulation: Numerical solution of optimal N investment in RuBP regeneration and RuBP
carboxylation, is finished
```

Published with MATLAB® R2013a

Appendix – A2.4 Methods. Temperature relationships

Here we describe the temperature relationship of the parameters of the Farquhar model of photosynthesis; in Table A2.1 we present and describe all parameters mentioned in the text, their units and input values.

The solution for the optimal nitrogen distribution between RuBP regeneration and RuBP carboxylation can also be applied for different temperatures. By multiplying the carboxylation capacity per N mass (k_c) by the temperature dependency of V_{cmax} [Eqn (A2.1)] we obtain a capacity that is temperature dependent. This can be substituted for k_c in the N allocation equation to find the optimal solution. The same holds for J_{max}, here the electron transport capacity per N mass (k_j) multiplied by the temperature dependency of J_{max} is the substitute of k_j in the N allocation equation [Eqn (A2.1)].

The temperature dependency of V_{cmax} and J_{max} is according to a peak model (Johnson, Eyring & Williams 1942)

$$g = \frac{\left(e^{\frac{H_a(T-25)}{298\cdot R\cdot(T+273)}}\right)\left(1+e^{\frac{298\cdot\Delta S - H_d}{298\cdot R}}\right)}{1+e^{\frac{\Delta S\cdot(T+273)-H_d}{(T+273)\cdot R}}} \qquad \text{(A2.1)}$$

In which g could either be for V_{cmax} or J_{max}, and g should be multiplied with k_c or k_j respectively; ΔS is an entropy term and H_d is the energy of deactivation of g.

For the temperature dependencies of K_c, K_o and Γ^* the Arrhenius model was used (Farquhar, Von Caemmerer & Berry 1980)

$$f = f(25°C)\cdot e^{\frac{H_a\cdot(T-25)}{298\cdot R\cdot(T+273)}} \qquad \text{(A2.2)}$$

In which f could be either K_c, K_o, Γ^*; $f(25°C)$ is the value of f at 25°C; H_a is the activation energy of f; R is the universal gas constant and T is the temperature.

Table A2.1 List of symbols, a description, input value and the unit for the model variables and parameters mentioned in the text.

Symbol	Explanation	Input value	Unit	Source
H_a (of J_{max})	Activation energy of J_{max}	58936	J mol^{-1}	2
H_a (of K_c)	Activation energy of K_c	59400	J mol^{-1}	2
H_a (of K_o)	Activation energy of K_o	36000	J mol^{-1}	2
H_a (of V_{cmax})	Activation energy of V_{cmax}	75794	J mol^{-1}	2
H_a (of Γ^*)	Activation energy of Γ^*	20970	J mol^{-1}	2
H_d (of J_{max})	Deactivation energy of J_{max}	199233	J mol^{-1}	2
H_d (of V_{cmax})	Deactivation energy of V_{cmax}	202022	J mol^{-1}	2
J_{max}	Maximum electron transport rate		µmol m^{-2} s^{-1}	
k_c	Carboxylation capacity per nitrogen mass	0.83	µmol C mmol N^{-1} s^{-1}	
K_c	Michaelis-Menten constant for carboxylation		µmol mol^{-1}	
K_c(25°C)	Michaelis-Menten constant for carboxylation at 25°C	402	µmol mol^{-1}	2
k_j	Electron transport capacity per nitrogen mass	0.83	µmol e mmol N^{-1} s^{-1}	1
K_o	Michaelis-Menten constant for oxygenation		µmol mol^{-1}	
K_o(25°C)	Michaelis-Menten constant for oxygenation at 25°C	560900	µmol mol^{-1}	2
R	Universal gas constant	8.315	J K^{-1} mol^{-1}	2
ΔS (of J_{max})	Entropy term of J_{max}	647	J mol^{-1}	2
ΔS (of V_{cmax})	Entropy term of V_{cmax}	657	J mol^{-1}	
T	Temperature		°C	
V_{cmax}	Maximum carboxylation rate		µmol m^{-2} day^{-1}	
Γ^*	CO_2 compensation point in absence of mitochondrial respiration		µmol mol^{-1}	
Γ^*(25°C)	CO_2 compensation point in absence of mitochondrial respiration at 25°C	51	µmol mol^{-1}	2

Literature sources:
1) Anten, Schieving & Werger (1995)
2) Cai & Dang (2002)

Chapter 3

How light competition between plants affects their response to climate change

Marloes P. van Loon, Feike Schieving, Max Rietkerk, Stefan C. Dekker, Frank Sterck and Niels P.R. Anten

Published as: Van Loon M.P., Schieving F., Rietkerk M., Dekker S.C., Sterck F. & Anten N.P.R. (2014) How light competition between plants affects their response to climate change. *New Phytologist* 203, 1253–1265.

Abstract

How plants respond to climate change is of major concern, as plants will strongly impact future ecosystem functioning, food production and climate. Here we investigate how vegetation structure and functioning may be influenced by predicted increases in annual temperatures and atmospheric CO_2 concentration, and modelled the extent to which local plant-plant interactions may modify these effects. A canopy model was developed, which calculates photosynthesis as a function of light, nitrogen, temperature, CO_2 and water availability, and considers different degrees of light competition between neighbouring plants through canopy mixing; soybean (*Glycine max*) was used as a reference system. The model predicts increased net photosynthesis and reduced stomatal conductance and transpiration under atmospheric CO_2 increase. When CO_2 elevation is combined with warming, photosynthesis is increased more, but transpiration is reduced less. Intriguingly, when competition is considered the optimal response shifts to producing larger leaf areas, but with lower stomatal conductance and associated vegetation transpiration than when competition is not considered. Furthermore, only when competition is considered are the predicted effects of elevated CO_2 on LAI well within the range of observed effects obtained by Free Air CO_2 Enrichment (FACE) experiments. Together, our results illustrate how competition between plants may modify vegetation responses to climate change.

Key words: canopy, FACE data, gas exchange, Leaf Area Index, modelling, optimality principle, photosynthesis, soybean

3.1 Introduction

Atmospheric CO_2 concentration is predicted to rise in the future, and partly as a result of this, global temperature will increase (IPCC 2007). It is of major concern how plants respond to changing climate, as this strongly affects basic vegetation functions such as crop production in the future. Vegetation in turn may modify climate change through climate-vegetation feedbacks (Claussen 1997; Brovkin *et al.* 1998; Bonan 2008; Dekker *et al.* 2010), because vegetation affects the radiative flow, water balance and carbon in the atmosphere itself (Scheffer *et al.* 2005). These vegetation-climate feedbacks necessitate the inclusion of vegetation into climate models.

Currently, in many climate models vegetation functioning is directly linked to LAI (Leaf Area Index, i.e., the leaf area per unit soil area). This is because LAI, being the amount of light intercepting tissue, is a key trait driving exchange of CO_2, water vapour and energy between vegetation and atmosphere (Running & Coughlan 1988; Sellers *et al.* 1997; Van den Hurk, Viterbo & Los 2003). But LAI is highly variable and can differ as a function of vegetation type, climatic and soil conditions (Asner, Scurlock & Hicke 2003; Iio *et al.* 2013). Climate models are often used for climate change predictions and studying climate-vegetation feedbacks. However, these models generally ignore local interactions between plants. In fact, there is a frequent call for the inclusion of the role of the interactions between plants in modifying the effects of climate change on plant structure and functioning, and on species composition (e.g. Dewar *et al.* 2009; Lloyd *et al.* 2010), but so far it has rarely been done. Incorporating local interactions between plants into climate-vegetation models can result in different predictions of transpiration rates and net primary production, which are likely to have major but largely unknown consequences for the future climate (Nicotra *et al.* 2010).

Optimization theory can be a good addition to climate-vegetation models, as it is a simple but elegant way to scale from individual physiological processes to vegetation functioning, and has been applied to different natural forest stands (Schymanski *et al.* 2007; Dewar *et al.* 2009; Sterck *et al.* 2011; Dekker, Vrugt & Elkington 2012). Optimization models assume that plants optimize their traits as to maximize performance (usually canopy photosynthesis or net primary production) at the whole-stand level. Thus, they implicitly quantify the maximum contribution of trait acclimation to whole-stand performance (Anten & During 2011). Several optimization models have been developed that predict the response of plants to elevated CO_2 (e.g. Franklin 2007; McMurtrie *et al.* 2008). However, while these optimization models make qualitatively good predictions, because there is usually a strong positive correlation between predicted and observed LAI, quantitatively they often underestimate measured LAIs, and overestimate canopy photosynthesis (Anten, Werger & Medina 1998; Anten 2005).

By defining performance maximization at the level of vegetation stands rather than at the individual level, optimization models implicitly assume that the optimal trait values of one

plant are independent of the trait values of its neighbours. This in turn ignores the fact that plants strongly compete for resources (Anten 2002). Competitive optimization (also known as density-dependent optimization, Maynard Smith (1974)) may overcome this problem as this assesses the payoff of a given set of trait values in relation to the characteristics of neighbour plants (Riechert & Hammerstein 1983; Anten 2002). Through this approach, stable strategies can be defined (also known as evolutionarily stable strategies), whereby a population adopting such a strategy cannot be invaded by individual adopting any other strategy, because this will not increase the payoff of the individual (Parker & Maynard-Smith 1990). This approach can for example be used to predict the allocation of biomass to leaves, wood and roots (Dybzinski *et al.* 2011; Farrior *et al.* 2013). In the current study we apply this approach to analyse the effects of climate change on LAI and associated vegetation functioning, because, as noted already, the LAI is a key trait in driving exchange of CO_2, water vapour and energy between vegetation and atmosphere. Application of the evolutionarily stable strategies approach to analyse vegetation structure and functioning under current climate conditions resulted in a closer fit of predicted stable LAI to real values compared to predictions from simple optimization, in which only the total stand is optimized (Anten 2002; Lloyd *et al.* 2010). However, although adding competitive optimization at the individual level provides a relatively simple means of assessing how competition may modify plant responses to climate change, very few studies (e.g. Friend, Schugart & Running 1993; Friend *et al.* 1997; Medvigy *et al.* 2010) have used it to investigate vegetation functioning under future climate scenarios.

The aim of this study is therefore to analyse how vegetation structure and functioning may be influenced by climate change and to what extent competition for light through canopy overlap may modify these effects. We will develop a canopy model in which we use soybean (*Glycine max*) as a reference system. This choice for soybean is because this species is widely grown all over the world and is one of the most studied species for response to elevated CO_2 (Ainsworth *et al.* 2002) and therefore ample experimental data are available. Here, the effect of CO_2 on vegetation structure and functioning predicted by the model will be validated against a large data set from several Free Air CO_2 Enrichment (FACE) experiments on soybean. In addition, the model predictions of seasonal dynamics in LAI at current and elevated CO_2 concentrations were are validated against data from a detailed study on this (Dermody, Long & DeLucia 2006). The canopy model we will develop, calculates the canopy photosynthesis of soybean as a function of light, nitrogen, temperature, CO_2 and water. A water balance was included in the model in which we can calculate water transport through the plant and transpiration of the plant.

There are three different versions of the canopy model. The first model version is the baseline version (hereafter called NoOpt), assuming the LAI will remain constant under climate change. The second model version uses simple optimization (hereafter called SimOpt) where plants optimize their LAI to maximize the performance at the whole-stand level (so

competition is not included). The last version uses competitive optimization (hereafter called ComOpt) where plants optimize their LAI in a competitive setting. SimOpt is included as because comparison of its results with those of the ComOpt version, allow us to determine the effect of competition separate from that of acclimation itself (included in the SimOpt version). With these model versions we study the effects of the predicted gradual increased temperature and elevated CO_2 on soybean, and how these effects differ if competition is included.

3.2 Materials and Methods

3.2.1 Introduction of the canopy model

To answer our main research question; a canopy model is developed. This canopy model is based on steady state assumptions of water transport and of CO_2 inflow and consumption, and these are solved with the given parameters (Table A3.1) and for the given constraints (for a given amount N that plants allocate to leaves, water availability as reflected by soil water potential, incident light, temperature, atmospheric CO_2 concentration). The model uses parameter values obtained from experimental studies on soybean (*Glycine max* (L.) Merr) from Anten, Schieving & Werger (1995) and Dermody, Long & DeLucia (2006) (Table 1). Parameter values given in Table A3.1 were used for all simulation unless otherwise specified. All variables names with units are supplied in Table A3.2. Here we present a short description of the canopy model, a full description can be found in the Appendix (Methods A3.1). After presenting the canopy model, a description is given of the three different model versions, the climate change scenarios and a description of how we compared the model outcomes with experimental data.

Table 3.1 Parameters used in the model which are obtained from experimental studies on soybean, with their units, description of the parameter and input value.

Symbol	Unit	Explanation	Input value
c_{rl}	µmol m^{-2} s^{-1}	Intercept of the R_l N_l relation[1]	0.388 [2]
F_T	-	Leaf area index	6.58 [3,4]
h_t	m	Top height of the canopy	0.66 [3]
K_{df}	-	Extinction coefficient for diffuse PFD	0.747 [2]
K_n	-	Extinction coefficient for nitrogen	0.298 [2]
N_b	mmol m^{-2}	Leaf N content not associated with photosynthesis	29.0 [2]
N_T	mmol m^{-2}	Total canopy leaf N	526.6 [3]
x_c	µmol CO_2 mmol N^{-1} s^{-1}	Slope of the V_{cmax} N_l-N_b relation[1]	0.17 [2]
x_j	µmol CO_2 mmol N^{-1} s^{-1}	Slope of the J_{max} N_l-N_b relation[1]	1.03 [2]
x_r	µmol CO_2 mmol N^{-1} s^{-1}	Slope of the R_l N_l relation[1]	0.0099 [2]
θ	-	Curvature factor	0.9 [3]

[1] J_{max}, V_{cmax} and R_l are assumed to be linearly related to leaf nitrogen content per unit leaf area
[2] Source: Anten, Schieving & Werger (1995)
[3] Source: Dermody, Long & DeLucia (2006)
[4] This value was only used for NoOpt version of the model. For the SimOpt and CompOpt leaf area index is an emerging property.

3.2.2 Plant structure

From a whole-stand (Fig 3.1a) a target plant is defined (Fig 3.1b), whose leaves are confined within area, *A*. The total leaf area of the target plant (f_i) per unit of ground area (*A*) is the Leaf Area Index (F_i), since we standardized A to 1 m^2. Neighbouring plants can also have leaves within *A* thereby influencing the light climate of the target plant (Fig 3.1f). Our competitive optimization criterion is defined as maximization of an individual plant's photosynthesis in the presence of neighbours, but does not consider the photosynthesis of those neighbours. The number of neighbour plants having part of their leaves in *A* does therefore not affect the calculation, only their combined total leaf area in *A* matters. The interaction between the target and the neighbouring plants through canopy mixing was modelled following Anten (2002). A summary of this approach is given here.

The total LAI (F_T) is a summation of the LAI of the target plant (F_i) and of the neighbouring plants (F_n) in the same area A (Fig 3.1f). All plants are assumed to be identical (same height, LAI etc.). The leaf area of the target plant and neighbours are assumed to be uniformly distributed, horizontally and vertically.

The ratio of the target plant's leaf area to the total leaf area (β) in the area A describes the degree to which canopies of plants are mixed, which in turn determines the degree to which plants influence each other's light climate.

$$\beta = \frac{F_i}{F_T} \qquad (3.1)$$

A value of β = 1 means that the leaves of the target plant in area A are not mixed with leaves of neighbouring plants, and the target plant only influences its own light climate through self-shading (Fig 3.1b). Conversely decreasing values of β indicate an increased degree of mixing and thus mutual shading between the plants (Fig 3.1f). It should be noted that β values approaching zero are unrealistic as β = 0 entails a target plant has no leaf area, which is evidently impossible.

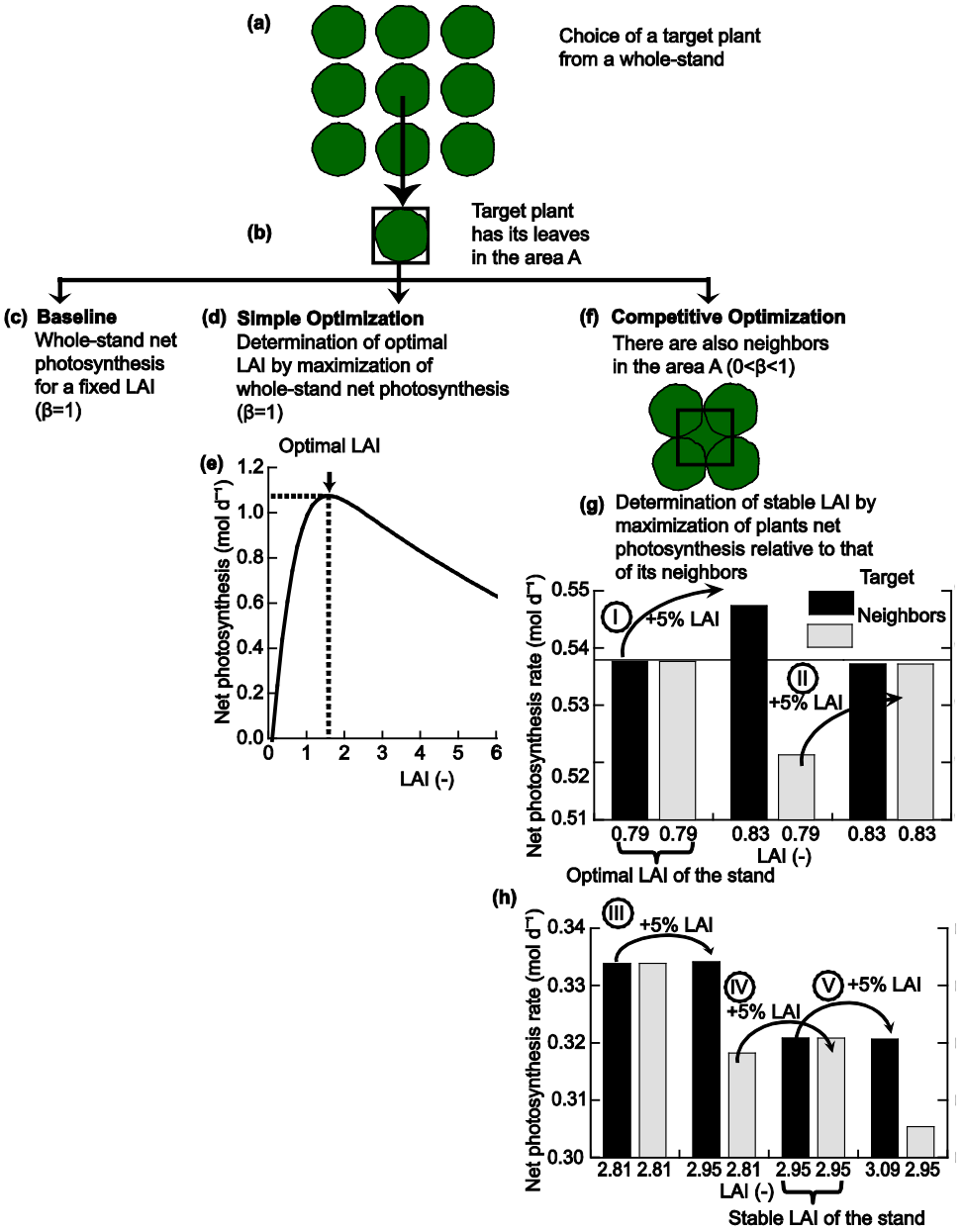

Fig 3.1 Overview of determination of optimal LAI and stable LAI. (a) From a whole-stand is a target plant defined (top down view). (b) The target plant has its leaves in a specified area (area *A*, A is 1 m^2). (c) If there are no neighbours in the area *A*, then the simple optimization is performed (β = 1; β is the ratio of targets leaf area to the total leaf area in the area *A*) (d), by maximization of whole-stand net photosynthesis to determine the optimal LAI. (e) If there are next to the target's plant neighbours in the area *A* (0 < β < 1), then competitive optimization is performed (f). The stable LAI is defined by maximization of the plants net photosynthesis rate relative to that of its neighbours. To determine this several steps are necessary. (Step I) Increase the LAI of the target plant to 5% above the optimal LAI (which maximizes net photosynthesis for the whole-stand, indicated by a black line). By unilaterally increasing its leaf area, the target plant captures a larger fraction of the available light, resulting in an increase in net photosynthesis rate of the target plant. (Step II) The neighbour increases its LAI also by 5%, and as such the LAI of the whole-stand was also increased by 5%. Increasing the LAI of the stand above its optimal LAI will reduce the net photosynthesis of the whole stand (g). This process was repeated (Step III and IV), until a value of the LAI of the stand was found at which a further change in the LAI of the target plant did not increase the net photosynthesis rate of the target plant (Step V), which then is the stable LAI (h)

3.2.3 Light distribution

Calculation of the light interception of the leaves was done with the model of Spitters, Toussaint & Goudriaan (1986), which distinguishes between direct light (i.e., direct beam irradiance) and diffuse light (i.e., radiation from the sky dome as well as radiation that is scattered by leaves in the canopy). Furthermore, two leaf classes were distinguished: shaded leaf area and sunlit leaf area. This model has been shown to be sufficiently accurate for estimates of canopy photosynthesis (De Pury & Farquhar 1997).

3.2.4 Nitrogen distribution

The nitrogen content of the leaves (N_l) in the canopy is calculated as a negative exponentially declining function of depth in the canopy (i.e. similar in shape but less steep than the light distribution) following Anten *et al.* (1995). Plants are assumed to have a fixed total amount of leaf N (N_T); thus increasing the leaf area results in a reduced leaf N content.

3.2.5 Photosynthesis

The net photosynthesis of a leaf per unit area (P_{nl}) was calculated with the Farquhar photosynthesis model (Farquhar, Von Caemmerer & Berry 1980). Where the net photosynthesis is calculated as the gross photosynthesis rate of a leaf per unit ground area (P_{gl}) minus the leaf respiration rate (R_l); and P_{gl} is the minimum of the carboxylation or Rubisco limited photosynthesis rate P_{cl} and the electron transport limited photosynthesis rate P_{jl} (Farquhar, Von Caemmerer & Berry 1980).

Gross- and net daily photosynthesis rates of a plant (P_{gT} and P_{nT}, respectively) are obtained by integration of the leaf gross and net photosynthetic rates over the cumulated LAI of the canopy (thus taking account of variation in light and N between leaves) and over the time of the day (yielding whole-vegetation value with area *A*) and subsequently multiplying the integrands by β.

$$P_{nT} = \beta \int_{t=0}^{t=24} \int_{f_i=0}^{f_i=F_T} P_{nl}\, df\, dt \qquad (3.2)$$

$$P_{gT} = \beta \int_{t=0}^{t=24} \int_{f_i=0}^{f_i=F_T} P_{gl}\, df\, dt \qquad (3.3)$$

where t is the time (in hours).

The photosynthetic parameters are dependent on temperature. The temperature dependency of the maximum carboxylation rate (V_{cmax}) and of the maximum electron transport rate (J_{max}) were calculated according to a peak model (Johnson, Eyring & Williams 1942), for all other photosynthetic parameters we used an Arrhenius model (Farquhar, Von Caemmerer & Berry 1980).

J_{max}, V_{cmax} and R_l are assumed to be linearly related to leaf nitrogen content per unit leaf area N_l (Harley *et al.* 1992). Thus due to the fixed total amount of leaf N (N_T), increasing the leaf area results in a reduced leaf N content and associated lower photosynthetic capacity per leaf.

3.2.6 Steady state flow of CO_2 and water transport

We assume that there is a steady state of inflow of CO_2 for the photosynthesis and consumption of CO_2. Solving the steady state condition for the internal CO_2, results in the net photosynthesis rate. The inflow of CO_2 is determined by the stomatal conductance (G_{sT}) and the difference between the atmospheric and the internal CO_2 concentration (C_a and C_i respectively), in which both G_{sT} and C_i are calculated according to Tuzet, Perrier & Leuning (2003). This means that both G_{sT} and C_i are a function of the leaf water potential (Ψ_l). Furthermore, we assume a steady state of plant transpiration E_T and plant water transport through the stem W_T, i.e., $E_T = W_T$ (Sterck & Schieving 2011). Calculation of the water transport is done for the whole plant. This assumes that all leaves have the same leaf water potential. The transpiration depends on canopy stomatal conductance of the plant (G_{sT}) and on the vapour pressure difference between leaf and air (VPD). The VPD depends on the relative humidity (RH) and on the temperature (Tetens 1930). We assume that the RH remains constant with a change in temperature, resulting in an increased VPD with increased temperature. The plant water transport through the stem depends on a constant stem conductance and on the difference in base water potential, gravity potential and leaf water potential.

So the steady state of both water transport and CO_2 inflow and consumption should hold. Then we can solve these steady states for Ψ_l with the given parameters (Sterck & Schieving 2011) (Table A3.1) and for the given constraints (constant total canopy N, base water potential, temperature, atmospheric CO_2 concentration, RH; we assume for all simulations a fixed and relatively high base water potential, see Fig A3.1 for results of a wide range water availabilities and total canopy N contents). With this Ψ_l, we can calculate C_i of the plant and thus the net photosynthesis.

3.2.7 Model versions: baseline model, simple optimization model, competitive optimization model

Three model versions are developed to show effects of competition on vegetation functioning. All model versions use the same canopy model, the only difference is the way the LAI is calculated (Fig 3.1). The first model version is the baseline version (NoOpt) where we show responses of plants with a fixed LAI (Fig 3.1c). For the LAI a measured value of soybean was used of 6.58 (Table 1), this value was obtained for an atmospheric CO_2 of 37 Pa and a temperature of 24˚C (Dermody, Long & DeLucia 2006), i.e. the 'current climate' treatment

(representing the year 2000). The LAI was kept constant if simulations were done for different climate conditions.

The second model version is the simple optimization model (SimOpt). Here the optimization procedure determines the optimal-LAI that maximizes the whole-stand net photosynthesis (P_{nT}), and it assumes that plants do not compete for light ($\beta = 1$, leaves of target plant are not mixed with neighbours; Fig 3.1d). An optimal LAI at which net photosynthesis is maximized exists, as light interception increases with LAI but with decreasing marginal returns (i.e., for LAI = 1 about 50% of available light is captured, for LAI = 2, 75% etc.) while increasing LAI also entails a reduction in leaf N content and thus in leaf photosynthetic capacity (Anten *et al.* 1995) (Fig 3.1e). Thus, the underlying assumption of the simple optimization is that trait acclimation to climate change will be such that whole-stand performance is maximized (Fig 3.1d).

The third model version is the competitive optimization model (ComOpt) where plants are able to change their LAI and individual plants are assumed to interact with neighbouring plants ($\beta<1$, leaves of target plant are mixed with neighbours; Fig 3.1f). With this model the stable LAI of the stand, i.e. the LAI at which no individual can increase its performance with a change of its leaf area (often denoted as the evolutionarily stable state, Maynard Smith (1974)), is determined (Fig 3.1g). Thus, plant-plant interactions are taken into account to determine the optimal trait values of individuals plants (Fig 3.1g).

In order to find the stable LAI of a stand, we followed the same approach as Anten (2002), which is shortly described here. We defined a certain degree of mixture between a target plant and other plants in the same area (β, Eqn 3.1; $\beta = 1$ is no mixture, the closer β is to zero, the higher the degree of mixture) (Fig 3.1f). Then the LAI of the target plant (F_i) was increased by 5%, while the LAI of the neighbours (F_n) was kept constant (Fig 3.1g, step I). This 5% increase in F_i not only increased the total LAI of the stand (F_T), but also β. That is, by increasing its leaf area, the target plant captures a larger fraction of the available light. When this resulted in an increase in net photosynthesis rate of the target plant (Fig 3.1g), LAI of neighbours was also increased by 5% (all plants have the same leaf area and β was thus restored to its original value), and as such the LAI of the whole-stand (F_T) was also increased by 5% (Fig 3.1g, step II). This process was repeated (Fig 3.1h, step III and IV) until a value of F_T was found at which a further change in F_i did not increase the net photosynthesis rate of the target plant (Fig 3.1h, step V), which then is the stable LAI for a certain value of β (Fig 3.1h). In all simulations with the ComOpt model we used a value of β of 0.5. This value was based on the results from an independent study (Anten 2002) which found that this $\beta = 0.5$ gave good predictions of real LAIs for a variety of herbaceous species grown under ambient conditions (Anten 2002); that is, for a wide range of LAI values there was both a strong correlation between predicted and observed LAI value ($r^2 = 0.8$) and the slope of the regression line (1.09 +/- 0.178) was not significantly different from 1.

Note that neither SimOpt and ComOpt specify whether changes in trait values occur through plasticity, genotypic adaptation or the replacement of less optimal genotypes by more optimal ones that come from elsewhere. This issue will be discussed further in the discussion section. By comparing ComOpt and SimOpt we can show the extent to which competition modifies the vegetation structure and functioning.

3.2.8 Climate change scenarios

For the climate change scenarios we assume an increase in atmospheric CO_2 concentration from 37 Pa until 97 Pa (IPCC 2007) between the years 2000 and 2100. In the first climate change scenario we assume that the temperature stays constant (24˚C, average over the experiments) over this period, while for the second scenario we assume a temperature increase of 4˚C over this period (A1Fl scenario of the Special Report on Emissions Scenarios (SRES), IPCC 2007). We assume that the RH remains constant with increasing temperature, which means that there is an increase in VPD. Consequently, the stomatal conductance has to decrease to keep the same rate of transpiration. Thus, an increase in temperature causes a certain degree of water stress.

3.2.9 Model validation against experimental data

We first tested the extent to which SimOpt and ComOpt can predict the seasonal dynamics in LAI using data from Dermody, Long & DeLucia (2006). Dermody, Long & DeLucia (2006) measured the total canopy leaf N content and the LAI under ambient and elevated CO_2 concentrations at different times during the season. For our model we use the total canopy leaf N content as an input value and compare the resulting LAI obtained under ambient and elevated CO_2 with those of Dermody, Long & DeLucia (2006).

Secondly, we tested the extent to which three model versions (NoOpt, SimOpt and ComOpt) could correctly predict measured effects of elevated CO_2 on LAI, leaf photosynthesis and stomatal conductance in soybean obtained in a wide range of field-applied elevated CO_2 (FACE) experiments. The data were taken from Rogers *et al.* (2004); Bernacchi *et al.* (2005; 2006); Dermody, Long & DeLucia (2006); Leakey *et al.* (2006); Ainsworth *et al.* (2007); A.D.B. Leakey (unpublished); and J.M. McGrath (unpublished). These experiments compare plants grown under an atmospheric CO_2 from around 37.5 Pa with plants under atmospheric CO_2 of around 55.0 Pa. We will specifically compare the relative changes of simulated and measured LAI (107 measurements), as well as the net photosynthetic rate (186 measurements on the topmost leaves in the canopy) and stomatal conductance (258 measurements on the topmost leaves in the canopy) under saturating light conditions with our simulations over the same increase in CO_2. Here we compare relative changes as the total canopy N content is not known for all studies. To assess the impact of variation in the assumed total canopy N we ran the model for the range in canopy N (45-1023 mmol N m^{-2}).

3.3 Results

3.3.1 The effect of β on the competitive optimization-model version

First we analysed the degree to which the predicted plant traits depended on the assumed plant-plant interaction (indicated by the parameter β; β = 1, simple optimization model SimOpt, Fig 3.1d; reduction in β from 1 towards zero, competitive optimization model ComOpt, Fig 3.1f) under current climate conditions (year 2000: temperature of 24˚C, atmospheric CO_2 of 37 Pa). The stable LAIs were found to be clearly larger than the optimal LAI (β = 1) and the predicted stable LAIs increased as β values became lower (Fig 3.2a). Predicted canopy photosynthesis in turn showed the opposite trend becoming lower with decreasing values of β (Fig 3.2b). Both canopy-level stomatal conductance (Fig 3.2c) and transpiration rate (Fig 3.2d) decreased with increasing β. As with a fixed canopy N, LAI is increased beyond the optimum for maximizing whole-stand net photosynthesis, so leaf photosynthesis and associated conductance decrease. The nonlinear responses to β (Fig 3.2) are the result of the non-linearity of the empirical logistic function [Eqn (A27), this function determines the stomatal conductance which influences the rate of transpiration and therefore the leaf water potential and the internal CO_2]. Thus our model results reveal that including competition, results in higher predicted values of LAI, but with a lower total transpiration rate. However, even though transpiration is reduced with a higher degree of mixture (Fig 3.2d), the reduction in photosynthesis is even stronger such that WUE becomes lower (Fig 3.2e). Since the amount of nitrogen in the canopy is the same for the two model versions, predicted whole-plant photosynthetic nitrogen-use efficiency also decreases with increasing mixture (data not shown). But model results are highly sensitive to β (Eqn 3.1), indicating that this is a key parameter in the model (Fig 3.2).

3.3.2 Climate change

By the year 2100 SimOpt (β = 1) and ComOpt (constant β = 0.5) predicted that with constant temperature and increased CO_2 concentration LAI would increase by 0.3% and 14%, respectively, and with increases in both temperature and CO_2 concentration LAI would increase by 14% and 4%, respectively, while for NoOpt a constant LAI was assumed (Fig 3.3a). For ComOpt the LAI increases, because due to increase of CO_2 leaf photosynthesis becomes more electron-transport limited, and thus indirectly light limited. When light is limiting, the benefits of investing in leaf area and the associated ability to compete for light increase. There is less increase in LAI when temperature also increased, because increase in temperature results in increase in vapour pressure difference between leaf and air (VPD)[Eqn (A30), we assumed constant relative humidity] which causes a certain degree of water stress causing lower LAI. However, for SimOpt increase in temperature resulted in more leaf area as the negative effects of water stress are much smaller due to the lower initial leaf area and therefore increasing LAI will result in higher photosynthesis. Given the fact that total canopy

N was assumed to be constant, the model predicts a small reduction in leaf N content per unit leaf area (see Fig A3.1 for results for a wide range of total canopy N contents and water availabilities).

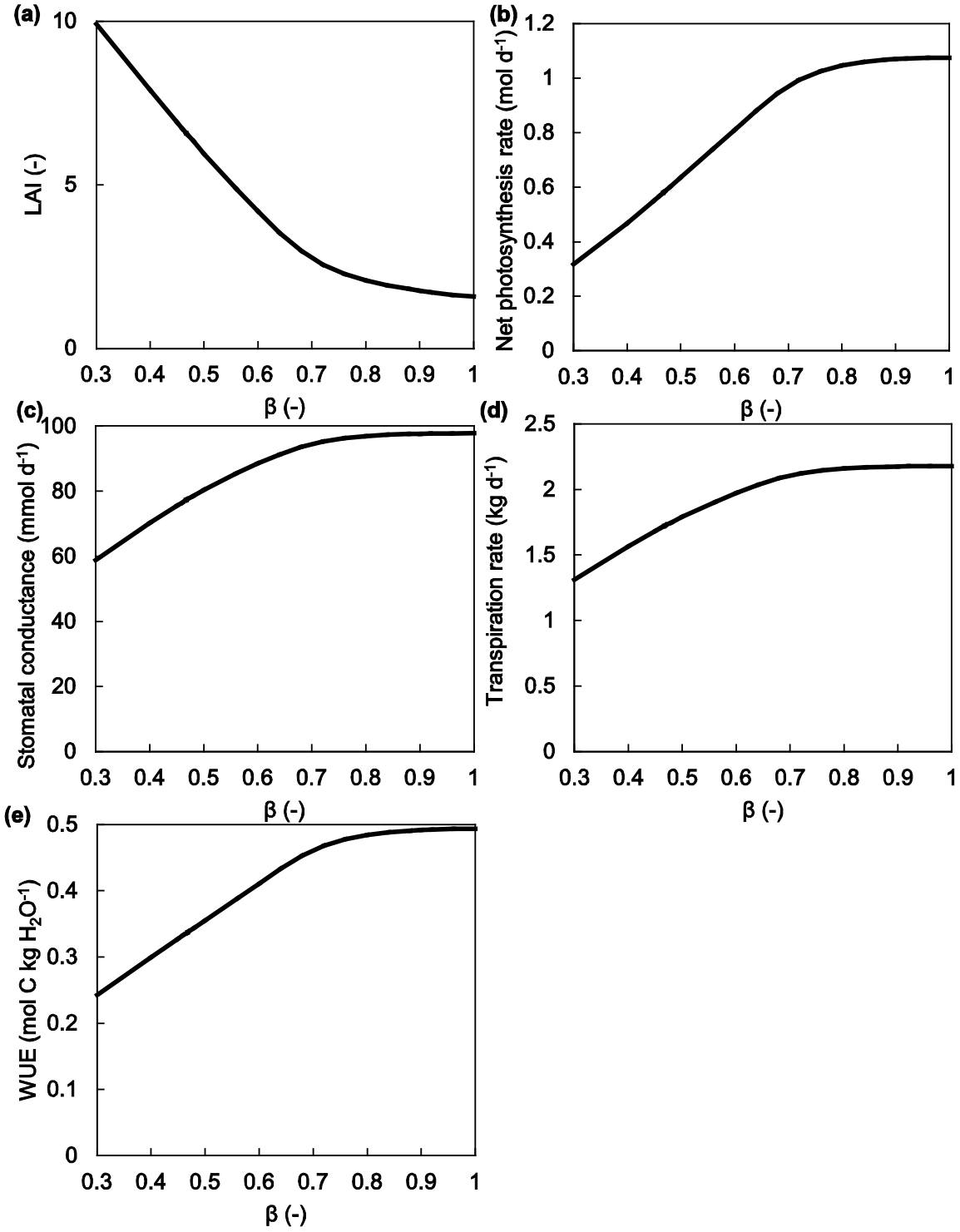

Fig 3.2 Total LAI (a), net photosynthesis rate (b), stomatal conductance (c), transpiration rate (d) and water use efficiency (WUE) (e) for different degrees to which canopies are mixed (β; β = 1 is no mixture, the closer β is to zero, the higher the degree of mixture)

All three models predict an increase in net photosynthesis rate from 2000 to 2100 (Fig 3.3b). With a constant temperature, NoOpt, SimOpt and ComOpt predict an increase of 58%, 61% and 40% respectively. All models predict a stronger increase if the temperature increased over time, due to the increase in efficiency of the photosynthesis (64%, 68% and 58% for NoOpt, SimOpt and ComOpt respectively) (Fig 3.3b).

All three models predict a reduction in the stomatal conductance with increasing CO_2 over the simulation period (2000 to 2100), but this is smaller for both ComOpt and NoOpt when temperature is also assumed to increase over this period. The latter is because temperature increases the rate of photosynthesis and thus the demand for CO_2. For SimOpt this decrease is larger, as a consequence of the stronger increase in LAI with increase in temperature. The CompOpt version predicts a larger reduction (41% and 48% with and without warming, respectively) than the NoOpt version (41% and 45%) and SimOpt (33% and 31%) (Fig 3.3c).

The transpiration rate decreased with increasing CO_2 according to all model versions, with the largest reduction in ComOpt (Fig 3.3d). With a constant temperature NoOpt predicts a reduction of 45%, SimOpt 31% and ComOpt 48% reduction. These reductions mirror the reductions in stomatal conductance because there is no change in VPD. If the temperature also increases there is relatively less reduction of the transpiration rate than in stomatal conductance, NoOpt predicts a reduction of 25%, SimOpt 15% and ComOpt 25% reduction (Fig 3.3d). The smaller reduction in transpiration rate with increase in temperature is because VPD increases (we assumed constant relative humidity), and because of the mentioned positive effect of temperature on stomatal conductance.

The WUE (i.e., the net photosynthetic rate divided by the transpiration rate of the whole canopy) will increase under elevated CO_2 conditions as a result of the increase in net photosynthesis and the decrease in transpiration rate (Fig 3.3e). The temperature rise increased the VPD, which increases transpiration rate. This increase in transpiration rate with rise in temperature is relatively greater than the increase in net photosynthesis, so WUE increased less if temperature also increased.

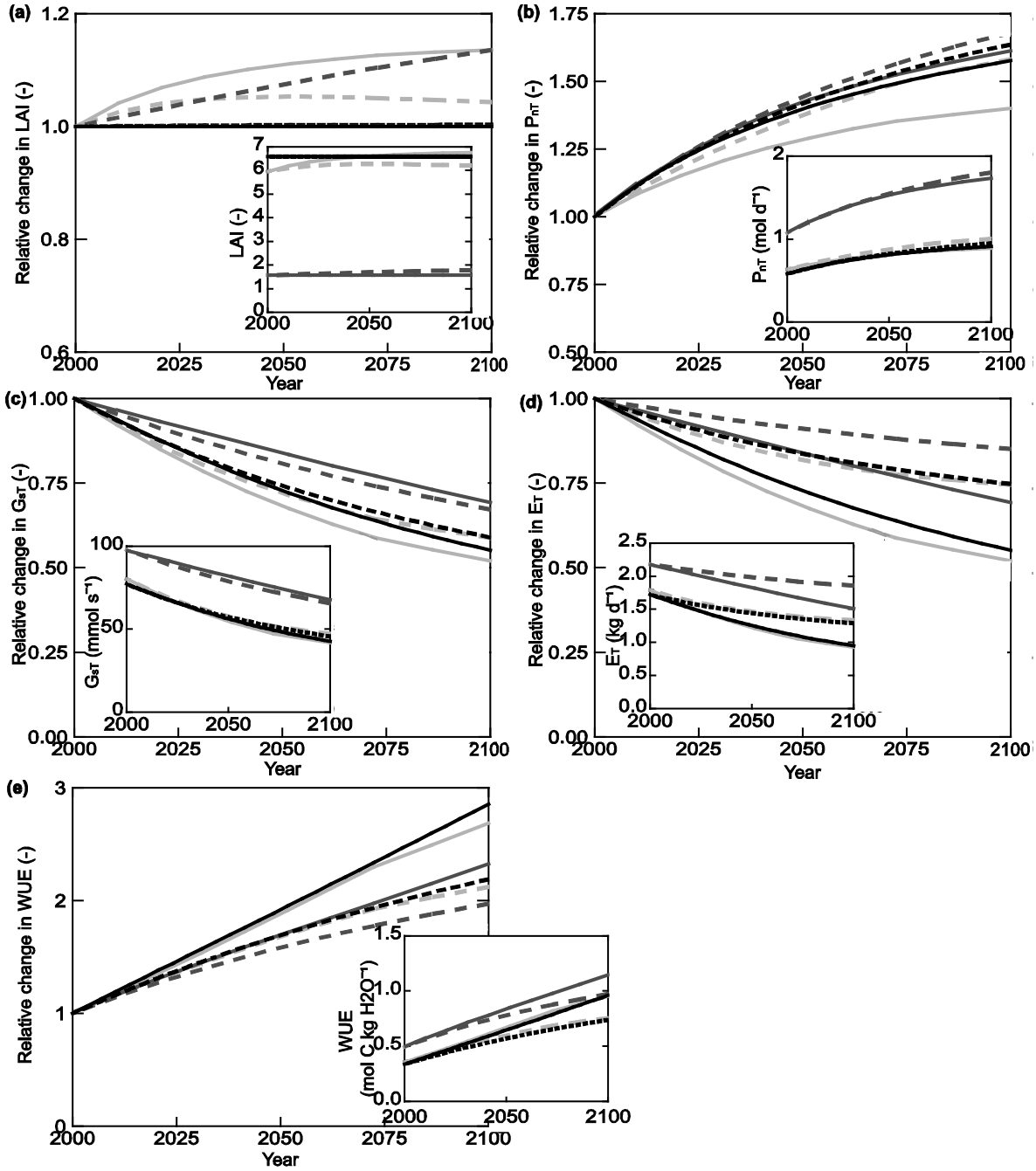

Fig 3.3 Fractional changes of total LAI (a), net photosynthesis rate (P_{nT}) (b), stomatal conductance (G_{sT}) (c) transpiration rate (E_T) (d), and water use efficiency (WUE) (e) as predicted by the baseline model (black lines), the simple optimization model (dark grey lines) and the competitive optimization model (light grey lines, $\beta = 0.5$), figure inserts show the absolute values. In 2000 is the atmospheric CO_2 concentration 37 Pa and it is assumed to increase linearly until 97 Pa in 2100. The temperature is in 2000 24˚C; the striped lines indicate the results for a linearly increase in temperature until 28˚C, the continuous lines indicate a constant temperature of 24˚C over the years

3.3.3 Model validation against experimental studies

The seasonal pattern in LAI development of the crop under both ambient and elevated CO_2 (Dermody, Long & DeLucia 2006) corresponded well with the predictions of the ComOpt model version (Fig A3.2). This was illustrated by the fact that predicted and measured values clustered around the 1:1 correspondence line, when plotted against all points. Conversely the simple optimization model (SimOpt: no competition, $\beta = 1$; optimal LAI) strongly underestimated the LAI values throughout the season values under both ambient and elevated CO_2 (Fig 3.4a, b; Fig A3.2).

Secondly, ComOpt predicted the relative change in LAI due to increase in CO_2 from 37.5 Pa to 55.0 Pa well within the wide range of data (107 observed values) obtained from a set of FACE experiments (Fig 3.5). The average increase in LAI across all these observation was 11% (95% confidence interval ranging from 2% to 19%). For the same increase in atmospheric CO_2, ComOpt predicted an 8% increase (0.5% lower bound, 17% higher bound; as a result of variation in observed canopy leaf N by Dermody, Long & DeLucia (2006)). Conversely, SimOpt predicted a very small change (0.2%) well below the observed range, and this was also the case if the sensitivity of the model is included (lower bound 0.15%, higher bound 0.30%); and for NoOpt there is no change in LAI by definition (Fig 3.5). The FACE experiments showed a mean increase in net photosynthesis rate of the top leaves in the canopy of 24% (20% lower bound, 28% higher bound). All model versions predicted changes that fell within this range (NoOpt 21%, SimOpt 26% and ComOpt 23%) (Fig 3.5). The experiments showed a mean reduction in stomatal conductance of 11% (lower bound -16%, higher bound -5%); NoOpt, SimOpt and ComOpt predict a decrease of 17%, 9% and 14% respectively (Fig 3.5). Across all simulations, higher values of total canopy N content resulted in a more positive relative responses to elevated CO_2; i.e., larger relative increases in LAI and photosynthesis and lower relative reductions in stomatal conductance (Fig 3.5, higher bounds; Fig A3.1). Thus, all three model version gave good predictions of the relative effects of CO_2 elevation on leaf fluxes. However, the absolute values of the fluxes for both ambient and elevated CO_2 were strongly overestimated by SimOpt (not shown). Similarly SimOpt strongly underestimated the absolute LAI values (Figs 3.4, 3.5). Thus ComOpt was the only model version of the three that well predicted the CO_2 effects on both LAI and leaf fluxes.

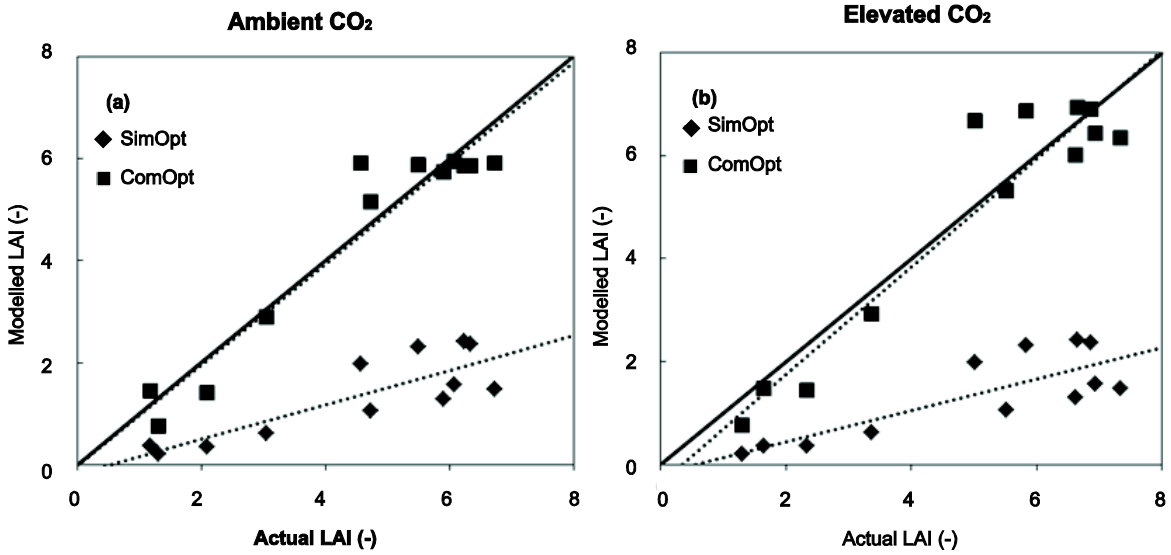

Fig 3.4 Predicted LAI by the simple optimization model (diamonds) and the competitive optimization model (squares) as a function of actual LAI (Dermody, Long & DeLucia 2006), for an atmospheric CO_2 concentration of 37 Pa (a) and 55 Pa (b). Solid lines indicate the 1:1 correspondence line and dashed lines the linear regressions

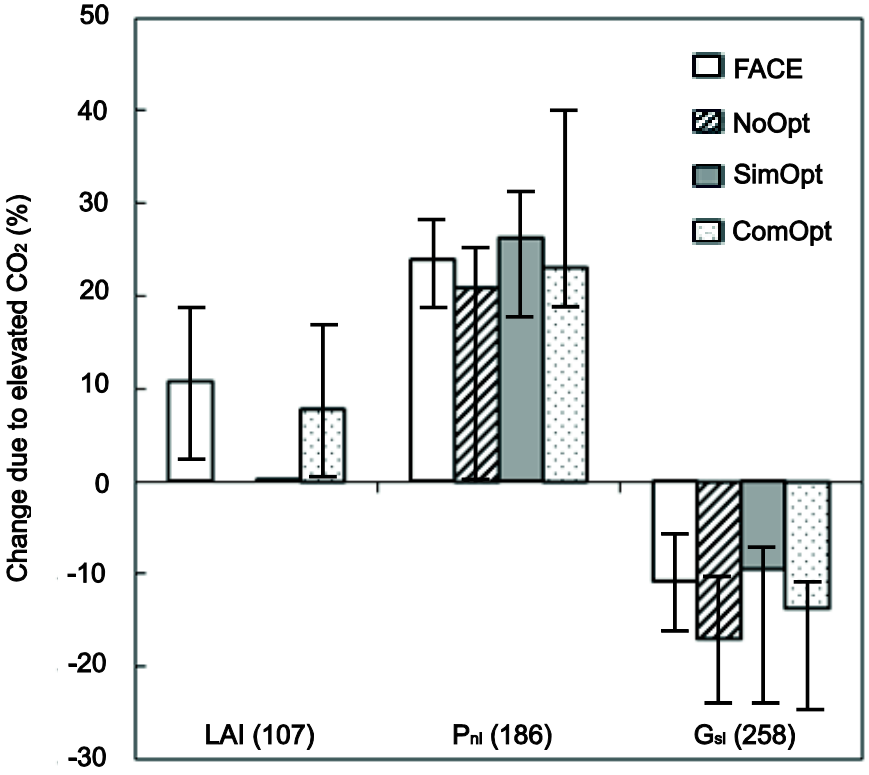

Fig 3.5 Percentage changes in LAI, leaf net photosynthesis rate (P_{nl}) and stomatal conductance (G_{sl}) of the topmost leaf due to increase of CO_2 from 37.5 Pa to 55 Pa. White bars represent the mean percentage change according to Free Air CO_2 enrichment (FACE) experiments with 95% confidence interval as error bar and sample size appears in parenthesis next to the symbol. Striped, grey and dotted bars represent the percentage change according to the baseline model (NoOpt), the simple optimization model (SimOpt) and the competitive optimization model (ComOpt) respectively; error bars are the result of changes in canopy leaf N content (45-1023 mmol N m^{-2})

3.4 Discussion

This study shows that it is important to consider local plant-plant interactions in models that predict vegetation structure and functioning under climate change. Our simulations reveal that including competition in the model (ComOpt; degree of interaction, $\beta<1$), results in predicted vegetation stands with higher LAIs, but with lower transpiration rates and lower photosynthesis rates compared to simple optimization (SimOpt; $\beta = 1$). As the reduction in photosynthesis is proportionally larger than the reduction in transpiration, inclusion of competition also results in lower predicted WUE. This finding is contrary to the simple positive relationship between LAI and transpiration often assumed by climate and ecology modellers (e.g. Van den Hurk, Viterbo & Los 2003). Thus, our results illustrate how competition between plants may modify vegetation responses to climate.

With the CO_2 elevation predicted for the 21st century, our model simulated an increase in both LAI and net canopy photosynthesis, while transpiration rates decreased. This CO_2 fertilization mechanism is known from many studies (e.g. Cao & Woodward 1998), and in turn, entails a considerable increase in photosynthetic WUE. However, with predicted increase in temperature, the transpiration is less reduced, but photosynthesis is more increased while LAI is less increased. The result is that plants are predicted to become more efficient with elevated CO_2, but due to temperature rise WUE increases less.

The competitive optimization model has been shown to be a good predictor of LAIs under current conditions (Anten 2002) and here we show here that it also accurately predicts the effects of elevated CO_2 on this trait observed in a large number of FACE experiments (Fig 3.5) as well as the seasonal dynamic in LAI over the season (Fig 3.4), at least in soybean. LAI is a key trait in driving vegetation climate feedbacks through its effects on CO_2 and water vapour exchange between vegetation and atmosphere and its effect on surface albedo.

3.4.1 Degree of interaction between plants

The ecological implications of light competition among plants has been the subject of extensive research (e.g. Weiner 1990; Schmitt, Dudley & Pigliucci 1999; Falster & Westoby 2003b; Niinemets 2010), but to our knowledge, the degree to which competition may mediate plant responses to climate change has not been quantitatively studied. Here we show that the degree to which canopies of neighbouring plants are mixed and thus influence each other's light climate, has a large influence on model outcomes. This was shown by the strong increase in LAI with the degree to which plants influence each other's light climate. This result suggests that the degree of plant-plant interaction may strongly affect vegetation responses to climate change and that more work is therefore needed to quantify this interaction. In this respect it is important to note that this degree of self to non-self interaction (β) in plant canopies probably differs between plant types. For example, trees have relatively broad canopies and probably a higher degree of self-interaction (larger β), than herbaceous plants

with much narrower canopies (Anten & During 2011). Clonal plants may also differ markedly in the degree of self/non-self interaction, depending on the spatial pattern in which they produce their vegetative offspring. If placed closely together such plants may produce large mono-clonal patches and competition between genetically different individuals is very limited which would be reflected in β values close to one. Thus we emphasize that if our approach would be extended to more plant types, careful consideration should be made regarding the assumptions of self/non-self interactions.

Our model predicts that with increasing interaction among plants in vegetation (decreasing β), the leaf area of plants increases while their stomatal conductance declines, resulting in both a larger LAI and a lower transpiration at the vegetation level. The pattern observed in our simulations can be explained as follows. If a plant is competing, increasing its LAI to more than the optimal LAI (determined for a given canopy nitrogen and water availability) will result in a relatively smaller increase in self-shading while the plant is able to capture a larger fraction of the available light. Thus, the individual plant can increase its carbon gain by increasing the LAI even if this reduces photosynthesis of the stand as a whole. It will thus have a higher relative fitness and can invade, resulting in a new population with a larger leaf area. Since canopy N remains unchanged this implies that plants reduce N use efficiency in order to shade competitors. So with an increase in the degree of mixture between plants, the LAI of the stand as a whole will increase while the net photosynthesis of the stand decreases. Due to the decreased consumption of CO_2 of the stand, this will decrease the stomatal conductance of the stand which results into a lower transpiration rate compared to plants which are not mixed.

3.4.2 Model compared with experimental studies

The correspondence between model predictions and observed values was dependent on the type of competition, the trait and whether absolute or relative effects were considered. However, ComOpt was the only model version that correctly predicted both the seasonal course in LAI under ambient and elevated CO_2 from Dermody, Long & DeLucia (2006) and the average relative effect of CO_2 elevation on LAI as determined by 107 FACE experiments. By contrast, SimOpt strongly underestimated absolute LAIs and the relative effects of elevated CO2 on LAI. This indicates that inclusion of competition into vegetation models may strongly improve predictions of LAI and effects of climate change thereupon. For the stomatal conductance and net photosynthesis rate, all three model versions simulated the relative changes with increasing CO_2 well within the range of observed effects obtained by FACE experiments. But in absolute terms SimOpt considerably overestimated net photosynthesis and stomatal conductance.

All three models showed an amplified response to elevated CO_2 with higher N contents, which is consistent with the general finding that growth stimulation by CO_2 is larger

at high than at low N availability (Rogers *et al.* 1996; Poorter 1998). In the model the mechanism that drives the stronger response to CO_2 at high N is that LAI and thus shading in the canopy increases with N availability and thus plants benefit more from the CO_2 stimulation of quantum yield (Anten *et al.* 2004). In addition, inhibition of photosynthesis by carbohydrate accumulation at high CO_2 tends to be weaker at high than at low N (Rogers *et al.* 1996).

3.4.3 Vegetation responses due to climate change

Plants were predicted to respond to climate change (i.e. warming and CO_2 elevation) by increasing LAI, and decreasing leaf N, stomatal conductance and transpiration rate. Plants decrease their stomatal conductance when the atmospheric CO_2 increases, in order to maintain the ratio of internal CO_2 to atmospheric CO_2 (Goudriaan & Unsworth 1990), resulting in a decrease in the transpiration rate. Increase in temperature resulted in a lower LAI for ComOpt compared to the situation where only CO_2 was increased. This can be explained by the optimality hypothesis of gas exchange. According to the optimality theory, plants maximize carbon gain while having minimum water loss (e.g. Cowan 1978; Katul *et al.* 2010). The increased temperature results in higher transpiration rates. To keep transpiration constant, LAI is reduced but photosynthesis increased due to increased efficiency of the photosynthetic apparatus. However, in the case of SimOpt this issue plays a much smaller role as this model version predicts much lower LAIs (since it does not consider competition).

The magnitude of the change in transpiration rate projected by the models strongly depends on the extent of future warming. We used the climate predictions of the A1Fl climate scenario of the IPCC; which predicts that the temperature increase by 4˚C from the year 2000 to 2100, and we had a scenario where the temperature stayed constant. This variation in temperature resulted in a broad range of predicted transpiration rates.

3.4.4 Limitations of the model and considerations for future work

Our main objective was to show that inclusion of competition in vegetation models may strongly affect predictions of vegetation structure and functioning in response to climate, and not to provide a tailor made predictive tool. We therefore used a canopy model that was based on a number of simplifications that more predictive studies should consider in the future. For example, while we did include leaf respiration costs, added costs of leaf construction and investments in stems and roots needed to support leaves were not taken into account. We also did not set an upper limit to the specific leaf area. These factors likely impose limitations on LAI particularly where LAI was predicted to be very high e.g. at very low values of β.

All three model versions predicted a decreased transpiration rate; this may affect climate predictions through effects of climate-vegetation feedbacks (e.g. Bonan 2008; Dekker *et al.* 2010). A decreased transpiration rate can cause a drying of the near surface atmosphere

as well as a warming of the canopy itself (due to less evaporative cooling), which subsequently increases the vapour pressure difference between leaf and air. Depending on soil water availability, this can lead to further stomatal closure or if stomatal opening remains unchanged, a relatively higher transpiration (Friend & Cox 1995; Bernacchi *et al.* 2007). The latter feedback likely occurred in the SoyFACE experiments as plants were well watered, but this was not considered in our model. Thus, while our predicted effect of CO_2 elevation on stomatal conductance were consisted with results from FACE experiments (Fig 3.5), it is possible that we overestimated the reduction in transpiration. Indeed other studies predicted smaller reductions in transpiration (e.g. Bernacchi *et al.* 2007; Drewry *et al.* 2010).

Our analysis was constrained at the canopy-level; as we addressed the question how plants compete for light given the amount of resources allocated to their leaves. As our model was developed for well-watered systems, biomass allocation to the root was not simulated. Therefore we did not extend the model with inclusion of acquisition and competition for belowground resources. Intriguingly, while game theoretical models exist analysing either above-ground traits (e.g. Hikosaka & Hirose 1997; Anten 2002; Falster & Westoby 2003a) or belowground traits (Gersani *et al.* 2001) separately, combined analyses of both components have not been done. Such analyses would constitute an important step forward.

We did not consider growth related processes that underlie leaf area production. LAI increment arises from the balance between leaf production with associated construction costs and senescence with associated losses of resources (e.g. Hikosaka 2005). In spite of this simplification, ComOpt is able to accurately simulate the seasonal dynamics in LAI. This indicates that if one knows the seasonal pattern in N uptake by the crop, which can be modelled fairly realistically (e.g. Franklin 2007), ComOpt can provide fairly accurate estimates of LAI.

In our approach of defining the stable LAI we assumed that there is a stand of identical plants and assess whether this stand can be invaded by a plant with a slightly different LAI. If this invader plant has a higher assimilation rate, it will invade resulting in a new situation in which all individuals have this different LAI. However, it is not shown whether these changes in LAI occur through plasticity, genotypic adaptation or replacement of less competitive resident genotypes by more competitive ones. Moreover, it is unlikely that such changes in canopy traits would occur completely through genotypic adaptation, given the short time-span of the predicted effects (100 years). Thus, the patterns as predicted by us could be the result of phenotypic plasticity or of invasions of existing populations by individuals from outside. Regarding the former, plant acclimation to elevated CO_2 (e.g. Sage 1994; Ainsworth & Long 2005) and temperature have been reported (e.g. Hikosaka *et al.* 2006; Yamori *et al.* 2009). Regarding the potential contribution of invasions from outside, this process is likely to take place with respect to increased temperature, as populations from warmer areas (i.e., lower latitudes or altitudes) could competitively replace those from cooler

habitats (e.g. Dukes & Mooney 1999; Parmesan & Yohe 2003). For CO_2 this seems to be an unlikely scenario, as the CO_2 is rather constant across the globe. Thus within this time-span it is most likely that plants show acclimation to elevated CO_2. So, although our model is relatively simple as it was not our objective to make a detailed model of vegetation functioning, our study does strongly imply that inclusion of trait acclimation in a competitive setting in vegetation models is both ecologically more realistic and it may improve predictions of climate change effects on vegetation structure and functioning.

Acknowledgement

We thank Elisabeth Ainsworth for the provision of the FACE data set. This work was financially supported by a Focus & Mass grant from Utrecht University awarded to NPRA MR and SD.

Appendix – A3.1 Methods

Here we present a full description of the canopy model. This canopy model is based on steady state assumptions of water transport and of CO_2 inflow and consumption and these are solved with the given parameters (Table A3.1) and for the given constraints (for a given N content, water availability, incident light, temperature, atmospheric CO_2 concentration). All parameter values used in this study can be found in Table A3.1 and all variables can be found in Table A3.2.

A3.1.1 Light distribution

Calculation of the light interception of the leaves was done with the model of Spitters, Toussaint & Goudriaan (1986), which distinguishes between direct light (i.e., direct beam irradiance) and diffuse light (i.e., radiation from the sky dome as well as radiation that is scattered by leaves in the canopy). This model has proven to be sufficiently accurate to model canopy photosynthesis in vegetation stands (De Pury & Farquhar 1997).

The profile of direct irradiance over the height of the canopy

$$I_{dr} = I_{odr} \cdot e^{-K_{bl}(1-\sigma)^{0.5} \cdot f_i/\beta} \quad \text{(A1)}$$

where I_{odr} is the daily course of direct PFD (photon flux density) above the canopy (described as a sinusoidal function, dependent on the solar constant and the atmospheric transmittance) σ is the leaf scattering coefficient (i.e., the sum of leaf reflectance and transmittance), f_i the cumulative leaf area index of the individual (total cumulative LAI, $f_T = f_i / \beta$) and K_{bl} is the extinction coefficient for direct light of 'black' non-scattering leaves.

$$K_{bl} = \frac{o}{\sin \gamma_s} \quad \text{(A2)}$$

where γ_s is the solar inclination angle (which depends on the time of the day) and o is the projection of leaves in the direction of a solar beam

$$o = \sin \gamma_s \cdot \cos \gamma_l \quad \text{(A3a)}$$

where γ_l is the leaf inclination angle, but if $\gamma_s < \gamma_l$ then the following equation is used

$$o = 2 \cdot \pi \cdot \left(\sin \gamma_s \cdot \cos \gamma_l \cdot \frac{\sin^{-1} \gamma_s}{\sin^{-1} \gamma_l} + (\sin \gamma_s{}^2 \cdot \sin \gamma_l{}^2)^{0.5} \right) \quad \text{(A3b)}$$

The profile of diffuse irradiance over the height of the canopy

$$I_{df} = I_{odf} \cdot e^{-K_{df} \cdot f_i / \beta} \quad \text{(A4)}$$

where I_{odf} is the daily course of diffuse PFD above the canopy and K_{df} is the extinction coefficient for diffuse PFD (-)

On its way through the canopy a part of the direct flux which is intercepted by the leaves is scattered by those leaves. Hence, the direct flux segregates into a diffused, scattered

component and another component which remains as direct uninterrupted beam. Extinction of the direct component of the direct flux proceeds equally to the decrease of light in a hypothetical canopy of black, non-scattering leaves.

Direct component of the direct PFD

$$I_{drdr} = I_{odr} \cdot e^{-K_{bl} \cdot f_i / \beta} \quad \text{(A5)}$$

Diffuse component of the direct PFD

$$I_{drdf} = I_{dr} - I_{drdr} \quad \text{(A6)}$$

Two leaf classes were distinguished: shaded leaf area and sunlit leaf area. The PFD incident on the shaded leaf area (I_{sh}) was derived by multiplying the sum of the diffuse flux and the diffused component of the direct flux by the extinction coefficient for diffuse light.

$$I_{sh} = \frac{K_{df}}{(1-\sigma)^{0.5}} \cdot (I_{df} + I_{drdf}) \quad \text{(A7)}$$

The sunlit leaf area (I_{sl}) receives diffuse and direct beam radiation.

$$I_{sl} = I_{sh} + \frac{o \cdot I_{odr}}{\sin \beta_s} \quad \text{(A8)}$$

The fraction of sunlit leaf area (f_{sl}) is equal to the fraction of direct beam reaching that layer.

$$f_{sl} = e^{-K_{bl} \cdot f_i / \beta} \quad \text{(A9)}$$

A3.1.2 Nitrogen distribution

The nitrogen content of the leaves (N_l) in the canopy is calculated following Anten *et al.* (1995)

$$N_l = \frac{K_n \cdot N_{TF}}{1-e^{-K_n \cdot F_i / \beta}} \cdot e^{-K_n \cdot f_i / \beta} + N_b \quad \text{(A10)}$$

where N_b is the minimum leaf N content (i.e., the amount of N that cannot be retranslocated), K_n is the coefficient of N distribution and N_{TF} is the amount of N in the canopy that is free for redistribution

$$N_{TF} = N_T - N_b \cdot \frac{F_i}{\beta} \quad \text{(A11)}$$

where N_T is the total leaf N.

A3.1.3 Photosynthesis

The net photosynthesis of a leaf per unit ground area (P_{nl}) was calculated as the gross photosynthesis rate of a leaf per unit ground area (P_{gl}) minus the leaf respiration rate (R_l) (Farquhar, Von Caemmerer & Berry 1980)

$$P_{nl} = P_{gl} - R_l \quad \text{(A12)}$$

The gross photosynthesis rate of a leaf on a certain height in the canopy per unit ground area was the minimum of the carboxylation or Rubisco limited photosynthesis rate P_{cl} and the electron transport limited photosynthesis rate P_{jl} (Farquhar, Von Caemmerer & Berry 1980).

$$P_{cl} = V_{cmax} \cdot \frac{C_i - \Gamma^*}{C_i + K_{cmm} \cdot \left(1 + \frac{O}{K_{omm}}\right)} \quad \text{(A13)}$$

$$P_{jl} = \frac{J_{max}}{4} \cdot \frac{C_i - \Gamma^*}{C_i + 2 \cdot \Gamma^*} \cdot \varphi \quad \text{(A14)}$$

where V_{cmax} is the maximum rate of carboxylation; C_i is the internal CO_2 concentration; Γ^* is the CO_2 compensation point in the absence of mitochondrial respiration; K_{cmm} and K_{omm} are respectively the Michaelis-Menten constants for carboxylation and oxygenation and O is the oxygen pressure in the crown. J_{max} is the maximum electron transport rate area and φ gives the effect of light on the electron transport path of the photosynthesis process

$$\varphi = \frac{(1+\xi) - \sqrt{(1+\xi)^2 - 4 \cdot \theta \cdot \xi}}{2 \cdot \theta} \quad \text{(A15)}$$

where θ is a curvature factor for a non-rectangular hyperbola and ξ is the ratio of the light absorption rate to the capacity for electron transport

$$\xi = \frac{q \cdot I_l}{J_{max}} \quad \text{(A16)}$$

where q is the quantum yield and I_l is either I_{sh} (the PFD incident on a shaded leaf) or I_{sl} (the PFD incident on a sunlit leaf).

The values for V_{cmax}, J_{max}, R_l, K_{cmm}, K_{omm} and Γ^* are dependent on temperature. For the temperature dependencies of R_l, K_{cmm}, K_{omm} and Γ^* the Arrhenius model was used (Farquhar, Von Caemmerer & Berry 1980)

$$f(T) = f(25℃) \cdot e^{\frac{H_a \cdot (T-25)}{298 \cdot R \cdot (T+273)}} \quad \text{(A17)}$$

where f could be either K_{cmm}, K_{omm}, Γ^* or R_l; f(25˚C) is the value of f at 25˚C; H_a is the activation energy of f; R is the universal gas constant and T is the temperature.

Temperature dependency of V_{cmax} and J_{max} are according to a peak model (Johnson, Eyring & Williams 1942)

$$z(T) = \frac{z(25°C) \cdot \left(e^{\frac{H_a (T-25)}{298 \cdot R \cdot (T+273)}}\right) \left(1 + e^{\frac{298 \cdot \Delta S - H_d}{298 \cdot R}}\right)}{1 + e^{\frac{\Delta S \cdot (T+273) - H_d}{(T+273) \cdot R}}} \quad \text{(A18)}$$

where z could either be J_{max} or V_{cmax}; z(25˚C) is the value of z at 25˚C; ΔS is an entropy term and H_d is the energy of deactivation of z.

J_{max}, V_{cmax} and R_l are assumed to be linearly related to leaf nitrogen content per unit leaf area N_l (Harley *et al.* 1992)

$$V_{cmax}(25℃) = x_c \cdot (N_l - N_b) \quad \text{(A19)}$$

where x_c is the slope of the V_{cmax} N_l-N_b relation.

$$J_{max}(25℃) = x_j \cdot (N_l - N_b) \quad \text{(A20)}$$

where x_j is the slope of the J_{max} N_l-N_b relation.

$$R_l(25^{\circ}C) = x_r \cdot (N_l - N_b) + c_{rl} \quad \text{(A21)}$$

Where x_r is the slope of the R_l N_l relation and c_{rl} the intercept of the R_l N_l relation.

The leaf photosynthesis at a certain height (assuming that the leaf area is uniformly distributed, horizontally and vertically) depends on the photosynthesis rate of the shade leaves and the sunlit leaves and the fraction of both on that height [Eqn (A9)].

$$P_{nl} = f_{sl} \cdot P_{nl\_sl} + (1 - f_{sl}) \cdot P_{nl\_sh} \quad \text{(A22)}$$

where P_{nl_sl} is the net photosynthesis rate of a sunlit leaf and P_{nl_sh} the net photosynthesis of a shaded leaf, obtained by substituting Eqns (A7) and (A8) respectively into Eqn (A16).

Integration of the leaf net photosynthesis rate and the leaf gross photosynthesis rate over the cumulated LAI of the canopy and over the time of the day resulted in the total canopy net photosynthesis rate (P_{nT}) and the total canopy gross photosynthesis rate (P_{gT}) respectively.

$$P_{nT} = \beta \int_{t=0}^{t=24} \int_{f_i=0}^{f_i=F_T} P_{nl}\, df\, dt \quad \text{(A23)}$$

$$P_{gT} = \beta \int_{t=0}^{t=24} \int_{f_i=0}^{f_i=F_T} P_{gl}\, df\, dt \quad \text{(A24)}$$

where t is the time (in hours).

A3.1.4 Steady state flow of CO_2

We assume that there is a steady state of inflow of CO_2 for the photosynthesis and consumption of CO_2. Solving the steady state condition for the internal CO_2 results in the total canopy gross photosynthesis rate. By applying Fick's law of diffusion, we write the steady state for CO_2 influx and CO_2 consumption of the canopy

$$G_{sT} \cdot \frac{C_a - C_i}{Pa} = P_{gT} \quad \text{(A25)}$$

where G_{sT} is the stomatal conductance of the plant to CO_2; C_a is the atmospheric CO_2 concentration, Pa is the atmospheric pressure (added to the equation, because C_i and C_a are expressed in pressure units) and P_{gT} is the total canopy gross photosynthesis rate.

In which G_{sT} is described as (Tuzet, Perrier & Leuning 2003)

$$G_{sT} = G_{s0} + \frac{a \cdot P_{gT}}{(C_i - \Gamma^*)/Pa} \cdot g_\Psi \quad \text{(A26)}$$

where G_{s0} is the residual stomatal conductance; a is a scaling parameter and g_Ψ is an empirical logistic function to describe the sensitivity of stomata to leaf water potential Ψ_l (Tuzet, Perrier & Leuning 2003)

$$g_\Psi(\Psi_l) = \frac{1 + e^{a\Psi \cdot \Psi_{ref}}}{1 + e^{a\Psi \cdot (\Psi_{ref} - \Psi_l)}} \quad \text{(A27)}$$

where a_Ψ is the slope parameter for the stomatal sensitivity function g_Ψ and Ψ_{ref} is the crown water potential at which the stomatal sensitivity function is half its maximum.

The internal CO_2 equation follows from substituting Eqn (A26) (stomatal conductance) into Eqn (A25) (steady state inflow and consumption of CO_2). We assume that $G_{s0} = 0$ and the result is therefore

$$C_i = \frac{C_a \cdot g_\Psi \cdot a + \Gamma^*}{1 + g_\Psi \cdot a} \quad \text{(A28)}$$

A3.1.5 Steady state water transport

Assumed is that there is a steady state of plant transpiration E_T and plant water transport through the stem W_T (Sterck & Schieving 2011). Calculation of the water transport is done for the whole plant. This assumes that all leaves have the same leaf water potential, and therefore thus the same C_i. However this does not mean that all leaves have the same photosynthesis rate, this depends on the light level and leaf N content [Eqns (A7)-(A22)].

E_T was calculated as

$$E_T = \frac{\Delta V}{Pa} \cdot G_{sw} \quad \text{(A29)}$$

where G_{sw} is the stomatal conductance for water vapour and is calculated as G_{sT} times the rate of water diffusivity over CO_2 diffusivity (1.6). ΔV is the vapour pressure difference between leaf and air. The vapour pressure in the leaf is assumed to be the same as the saturated vapour pressure v_s, which depends on the temperature (Tetens 1930):

$$v_s = 611.25 \cdot e^{\frac{17.502 \cdot T}{240.9 + T}} \quad \text{(A30)}$$

The vapour pressure of the air (v_a) depends on the saturated vapour pressure and the relative humidity (RH):

$$v_a = v_s \cdot \frac{RH}{100} \quad \text{(A31)}$$

Plant water transport through the stem (W_T)

$$W_T = K \cdot (\Psi_b - \Psi_g - \Psi_l) \quad \text{(A32)}$$

where Ψ_b is water potential at stem base (reflecting plant water availability; we assume for all simulations a fixed and relatively high Ψ_b, see Table A3.1); Ψ_g is the water potential loss at the focal point due to gravity and K is the stem conductance

The steady state condition of water transport is then

$$\frac{\Delta V}{Pa} \cdot G_{sw} = K \cdot (\Psi_b - \Psi_g - \Psi_l) \quad \text{(A33)}$$

The steady state of water transport (Eqn A33) and CO_2 inflow and consumption (Eqn A25) should both hold, we can solve these steady states for Ψ_l with the given parameters (Table A3.1) and for the given constraints (N_T, Ψ_b, T, C_a, RH, Table A3.2), and with this Ψ_l we can calculate C_i of the plant and thus the net photosynthesis rate.

Appendix – A3.2 Tables

Table A3.1 List of symbols for the model parameters mentioned in the main text, with their unit, description of the parameter, input value and the source of the input value. The parameters are given in alphabetic order.

Symbol	Unit	Explanation	Input value	Source
a	Pa	Scaling parameter for calculation of stomatal conductance	2	7
A	m^2	The area in which an individual plant has its leaf area	1	
a_Ψ	MPa^{-1}	Slope parameter for the stomatal sensitivity function	3.2	7
c_{rl}	$\mu mol\ m^{-2}\ s^{-1}$	Intercept of the R_l N_l relation	0.388	1
G_{s0}	$\mu mol\ d^{-1}$	Residual stomatal conductance per unit ground area	0	6
H_a (of J_{max})	$J\ mol^{-1}$	Activation energy of J_{max}	58936	3
H_a (of K_{cmm})	$J\ mol^{-1}$	Activation energy of K_{cmm}	59400	3
H_a (of K_{omm})	$J\ mol^{-1}$	Activation energy of K_{omm}	36000	3
H_a (of R_l)	$J\ mol^{-1}$	Activation energy of R_l	48294	3
H_a (of V_{cmax})	$J\ mol^{-1}$	Activation energy of V_{cmax}	75794	3
H_a (of Γ^*)	$J\ mol^{-1}$	Activation energy of Γ^*	20970	3
H_d (of J_{max})	$J\ mol^{-1}$	Deactivation energy of J_{max}	199233	3
H_d (of V_{cmax})	$J\ mol^{-1}$	Deactivation energy of V_{cmax}	202022	3
K	$kg\ MPa^{-1}\ d^{-1}$	Stem conductance	1.1832	5
$K_{cmm}(25^\circ C)$	Pa	Michaelis-Menten constant for carboxylation at 25˚C	40.2	3
K_{df}	-	Extinction coefficient for diffuse PFD	0.747	1
K_n	-	Coefficient of leaf N allocation in a canopy	0.298	1
$K_{omm}(25^\circ C)$	Pa	Michaelis-Menten constant for oxygenation at 25˚C	56090	3
N_b	$mmol\ m^{-2}$	Leaf N concentration not associated with photosynthesis	29	1
N_T	$mmol\ m^{-2}$	Total canopy leaf N	526.6	4
O	Pa	Oxygen pressure in crown	20500	
Pa	Pa	Atmospheric pressure	$1 \cdot 10^5$	
q	$\mu mol\ \mu mol^{-1}$	Quantum yield (µmol electrons per photon)	0.25	
R	$J\ K^{-1}\ mol^{-1}$	Universal gas constant	8.315	
RH	%	Relative humidity	70	
ΔS (of J_{max})	$J\ mol^{-1}$	Entropy term of J_{max}	647	3
ΔS (of V_{cmax})	$J\ mol^{-1}$	Entropy term of V_{cmax}	657	3
x_c	$\mu mol\ CO_2\ mmol\ N^{-1}\ s^{-1}$	Slope of the V_{cmax} N_l-N_b relation	0.74	2
x_j	$\mu mol\ CO_2\ mmol\ N^{-1}\ s^{-1}$	Slope of the J_{max} N_l-N_b relation	1.03	2

Table A3.1 Continued

Symbol	Unit	Explanation	Input value	Source
x_r	μmol CO_2 mmol N^{-1} s^{-1}	Slope of the R_l N_l relation	0.0099	1
γ_l	^{o}	Leaf inclination angle	26	
$\Gamma^*(25^\circ C)$	Pa	CO_2 compensation point in absence of mitochondrial respiration at 25˚C	5.1	3
θ	-	Curvature factor	0.9	4
λ_s	m^2 m^{-3}	Stem area density in the crown cylinder	$1.5 \cdot 10^{-5}$	
σ	-	Leaf scattering coefficient	0.2	
Ψ_b	MPa	Water potential at stem base	0	
Ψ_{ref}	MPa	Crown water potential at which the stomatal sensitivity function is half its maximum	-1.9	7

Literature sources:
1) Anten, Schieving & Werger (1995)
2) Anten *et al.* (1995)
3) Cai & Dang (2002)
4) Dermody, Long & DeLucia (2006)
5) Maherali, Pockman & Jackson (2004)
6) Sterck & Schieving (2011)
7) Tuzet, Perrier & Leuning (2003)

Table A3.2 List of symbols for the model variables mentioned in the main text, with their unit, description of the variable and their equation number as mentioned in the main text. The variables are given in alphabetic order.

Symbol	Unit	Explanation	Equation
C_a	Pa	Atmospheric CO_2 concentration	
C_i	Pa	Internal CO_2	A28
E_T	µmol d^{-1}	Transpiration rate	A29
f_i	-	Cumulative leaf area index from the top of the individual	
F_n	-	Leaf area index of a neighbour plant	
F_i	-	Leaf area index of the individual	
f_{sl}	-	Fraction of sunlit leaf area	A9
F_T	-	Total leaf area index per unit of ground area of a stand	1
f_t	-	Total cumulative leaf area index from the top of a canopy	
G_{sT}	µmol d^{-1}	Stomatal conductance of the plant to CO_2	A26
G_{sw}	µmol d^{-1}	Stomatal conductance of the plant to H_2O	
g_Ψ	-	Describes stomatal sensitivity to water pressure at the focal point in the crown (-)	A27
I_{df}	µmol m^{-2} s^{-1}	Profile of diffuse irradiance in the canopy	A4
I_{dr}	µmol m^{-2} s^{-1}	Profile of direct irradiance in the canopy	A1
I_{drdf}	µmol m^{-2} s^{-1}	Diffuse component of direct PFD	A6
I_{drdr}	µmol m^{-2} s^{-1}	Direct component of direct PFD	A5
I_l	µmol m^{-2} s^{-1}	Total amount of light intercepted by a leaf	A10
I_{sh}	µmol m^{-2} s^{-1}	PFD incident on the shaded leaf area	A7
I_{sl}	µmol m^{-2} s^{-1}	PFD incident on the sunlit leaf area	A8
J_{max}	µmol m^{-2} s^{-1}	Maximum electron transport rate	A18, A20
K_{bl}	-	Extinction coefficient for direct light	A2
N_l	mmol m^{-2}	Leaf N content	A10
N_{TF}	mmol m^{-2}	Amount of N in the canopy that is free for redistribution	A11
o	-	Projection of leaves in the direction of the solar beam	A3
P_{cl}	µmol m^{-2} d^{-1}	Rubisco limited photosynthesis rate per unit ground area	A13
P_{jl}	µmol m^{-2} d^{-1}	Electron transport limited photosynthesis rate per unit ground area	A14
P_{gl}	µmol m^{-2} d^{-1}	Leaf gross photosynthesis rate per unit ground area	
P_{gT}	µmol d^{-1}	Whole plant gross photosynthesis rate	A24
P_{nl}	µmol m^{-2} d^{-1}	Leaf net photosynthesis rate per unit ground area	A12, A22
P_{nT}	µmol d^{-1}	Whole plant net photosynthesis rate	A23
R_l	µmol m^{-2} d^{-1}	Leaf respiration rate	A17,A21
T	˚C	Temperature	
t	h	Time	
v_a	Pa	Vapour pressure of the air	A31
V_{cmax}	µmol m^{-2} d^{-1}	Maximum carboxylation rate	A18, A19
v_s	Pa	Saturated vapour pressure	A30
W_T	µmol d^{-1}	Plant water transport through stem	A32
β	-	The ratio of the leaf area index of an individual to the total leaf area	
ΔV	Pa	Vapour pressure difference between leaf and air	
ξ	-	Light absorption to electron transport capacity ratio	A16
Φ	-	Effect of light on the electron transport path of the photosynthesis process	A15

Table A3.2 continued

Symbol	Unit	Explanation	Equation
Ψ_b	MPa	Water potential at stem base	
Ψ_g	MPa	Water potential loss at the focal point due to gravity	
Ψ_l	MPa	Leaf water potential	

Appendix – A3.3 Figures

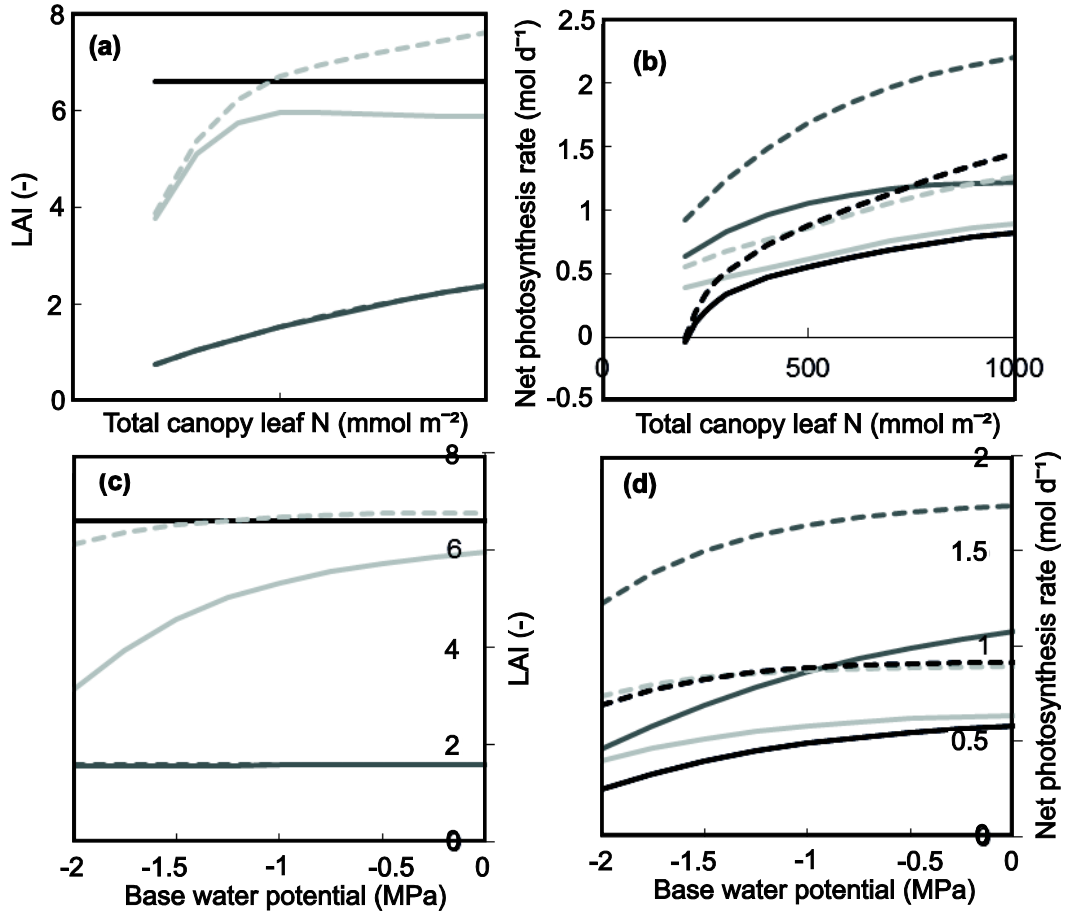

Fig A3.1 For different total canopy leaf N contents (a,b) and base water potentials (c,d) the LAI (a,c) and the net photosynthesis rate (b,d) for the baseline model (NoOpt, LAI is constant and no competition included) (black lines), the simple optimization model (SimOpt, optimal LAI for maximum photosynthesis, no competition included; $\beta = 1$) (dark grey lines) and the competitive optimization model (ComOpt, optimization of LAI in a competitive setting; $\beta = 0.5$) (light grey lines) for an atmospheric CO_2 concentration of 37 Pa (continuous lines) and for 97 Pa (striped lines) (temperature is 24ºC)

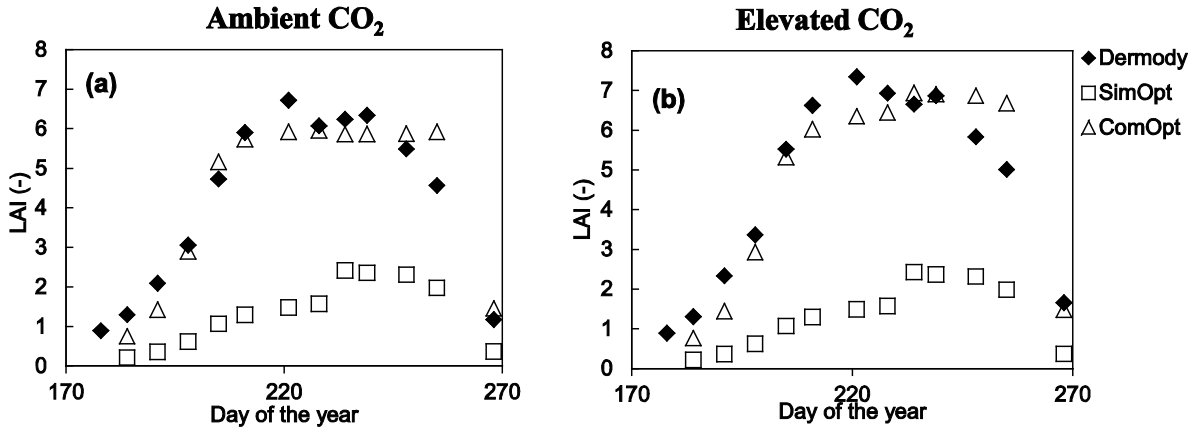

Fig A3.2 Predicted seasonal LAI by the simple optimization model (diamonds) and the competitive optimization model (squares) compared to the measurements of Dermody, Long & DeLucia (2006) (triangles), for ambient (a) and elevated CO_2 (b)

Chapter 4

Plant-plant interactions mediate the plastic and genotypic response of *Plantago asiatica* to CO_2: an experiment with plant populations from naturally high CO_2 areas

Marloes P. van Loon, Max Rietkerk, Stefan C. Dekker, Kouki Hikosaka, Miki U. Ueda and Niels P.R. Anten

(Manuscript is under review with Annals of Botany)

Abstract

The rising atmospheric CO_2 concentration ($[CO_2]$) is an ubiquitous selective force that may strongly impact species distribution and vegetation functioning. Plant-plant interactions could mediate the trajectory of vegetation responses to elevated $[CO_2]$, because some plants may benefit more from $[CO_2]$ elevation than others. We investigated the relative contribution of plastic (within lifetime) and genotypic (over several generations) responses to elevated $[CO_2]$ on plant performance and analysed how these patterns are modified by plant-plant interactions. We grew *Plantago asiatica* seeds originating from three independent natural $[CO_2]$ springs and from ambient $[CO_2]$ in mono stands of both origins as well as mixtures of both origins. In total 1944 plants were grown in $[CO_2]$ controlled walk-in climate rooms, under a $[CO_2]$ of 270, 450 and 750 ppm. A model was used for upscaling from leaf to whole-plant photosynthesis and for quantifying the influence of plastic and genotypic responses. We showed that changes in canopy photosynthesis, specific leaf area (SLA) and stomatal conductance in response to changes in growth $[CO_2]$ were mainly determined by plastic and not by genotypic responses. We further found that plants originating from high $[CO_2]$ habitats performed better in terms of whole-plant photosynthesis, biomass and leaf area, than those from ambient $[CO_2]$ habitats at elevated $[CO_2]$ only when both genotypes competed. Similarly, plants from ambient $[CO_2]$ habitats performed better at low $[CO_2]$, also only when both genotypes competed. No difference in performance was found in mono stands. Our results indicate that natural selection under increasing $[CO_2]$ will be mainly driven by competitive interactions. This supports the notion that plant-plant interactions have an important influence on future vegetation functioning and species distribution. Furthermore, plant performance was mainly driven by plastic and not by genotypic responses to changes in atmospheric $[CO_2]$.

Key words: canopy functioning, climate change, competition, elevated CO_2, evolutionary response, game theory, genotypic response, naturally high CO_2, *Plantago asiatica* L., plant-plant interactions, plastic response, selection pressure

4.1 Introduction

Since the industrial revolution there has been a rapid increase in atmospheric CO_2 concentration ($[CO_2]$), and it is predicted to further increase in the future. Understanding how plants respond to elevated $[CO_2]$ is important, because of the central role of plants in ecological and production processes and because plants have a large influence on the local climate itself. The latter is, among others, because plants have a negative feedback on the atmospheric $[CO_2]$, as they take up $[CO_2]$ (Bonan 2008). Hence, changes in $[CO_2]$ entail a global selective force due to their ubiquitous nature and importance for plant responses. Furthermore, plant-plant interactions may influence plant responses to elevated $[CO_2]$ as some plants may benefit more from rising $[CO_2]$ than others and their traits therefore determine vegetation functioning. For example, C_3 species may gain a competitive advantage over C_4 species at elevated $[CO_2]$ as C_3 species benefit more from elevated $[CO_2]$ (Ziska 2011), and this could lead to shifts in plant distribution patterns. So, it is important to know how plants respond to changes in the climate, and how this is potentially modified by plant-plant interactions.

When plants are placed in elevated $[CO_2]$ they respond immediately (instantaneous response hereafter, on the time scale of seconds to days), for example, through an increase in their assimilation rate (Ainsworth & Long 2005). On a time scale of days to weeks of exposure to elevated $[CO_2]$ plants will respond plastically (response within a plants lifetime), e.g. through reduction of leaf N content or changes in leaf area (Ainsworth & Long 2005). But it is still unclear what the magnitude of these responses is and how this impacts on whole-stand characteristics. For instance, leaf area responses to elevated $[CO_2]$ and their effect on whole-stand Leaf Area Index (LAI, leaf area per unit ground area) were found to differ between plant functional types. Increases in LAI were reported for young trees (Norby & Zak 2011), while crops and grasses exhibited little change in LAI (Hirose *et al.* 1997; Anten *et al.* 2004; Ainsworth & Long 2005). Most of the experiments that investigated plant responses to elevated $[CO_2]$ ran for a maximum of 10 years, while only a few studies investigated this on a longer time scale. One study investigated plastic responses within the lifespan of ferns, broadleaved trees and conifers in Florida that were likely associated with the last 150 years increase in $[CO_2]$ (Lammertsma *et al.* 2011) and found altered stomatal densities and reduced maximum pore size of the stomatal opening to reduce stomatal conductance (De Boer *et al.* 2011).

Genotypic responses of plant populations to elevated $[CO_2]$, which take place over several generations, can be studied with plants from natural CO_2 springs. In these natural elevated CO_2 areas, the atmospheric $[CO_2]$ has likely been elevated for hundreds of years (Körner & Miglietta 1994; Onoda, Hirose & Hikosaka 2007). The functioning of plants from these areas can be compared with ones from ambient $[CO_2]$ (Cook *et al.* 1998; Vodnik *et al.*

2002; Onoda, Hirose & Hikosaka 2007). Some studies (e.g. Fordham *et al.* 1997; Nakamura *et al.* 2011) show that plants originating from natural CO_2 springs have a higher relative growth rate compared to plants originating from ambient [CO_2] when grown at elevated [CO_2].

However, the few experimental studies investigating plant genotypic responses to elevated [CO_2], did not clearly investigate the potential mediating effect of plant-plant interactions. Plants often grow in dense communities where they share resources (e.g. light, water, nutrients) with their neighbouring plants, and therefore there is a high selective force on competition for those resources (Aerts 1999). Furthermore, it is likely that due to plant-plant interactions the species composition will change, because some plants may benefit more than others from the rise of [CO_2] (Owensby *et al.* 1999). For example, species with a high level of plastic and genotypic response are thought to benefit most (Parmesan 2006), and therefore those plants will determine vegetation functioning. This indicates that plant-plant interactions may strongly mediate the trajectory of vegetation responses to elevated [CO_2]. For instance, a study that included competition through natural selection (i.e. game theoretical principles) accurately predicted the LAI, net photosynthesis and stomatal conductance of soybean stands grown at elevated [CO_2] obtained in Free Air Carbon dioxide Enrichment (FACE) experiments, and this prediction was much better than a model that did not consider these interactions (Van Loon *et al.* 2014). This further suggests that plant-plant interactions may indeed play an important role in driving plant responses to elevated [CO_2]. However, the role of plant-plant interactions in mediated vegetation responses to elevated [CO_2] is still poorly understood (Bazzaz & McConnaughay 1992). This is at least in part, because an increase in atmospheric [CO_2] increases plant growth and thereby likely increases the competition for light and soil nutrients between plants.

The main aim of our study is therefore to determine the relative contribution of plastic versus genotypic responses to elevated [CO_2] on plant performance, and to determine the extent to which these patterns are modified by plant-plant interactions. To investigate this we use *Plantago asiatica* L., a perennial rosette herb. It was used in our experiment as it is known to adapt to a wide range of environments by genetic differentiation. This makes it particularly suitable for testing adaptation to increased [CO_2] (Onoda, Hirose & Hikosaka 2009). The seeds originate from populations growing near natural CO_2 springs where elevated [CO_2] levels have existed for hundreds of years (Onoda, Hirose & Hikosaka 2007), and from populations in control areas with normal [CO_2]. These are hereafter called spring and non-spring plants respectively, the [CO_2] of origin is called their 'native [CO_2] environment'. Mono stands and mixed stands of either or both spring and non-spring plants, respectively, were created, to test whether differences in responses also lead to a higher performance.

Plants were grown in walk-in growth chambers with low, intermediate and high [CO_2] (270, 450 and 750 ppm [CO_2] respectively; this is their growth [CO_2]) (Fig 4.1). During the experiment we measured leaf photosynthetic traits, plant dry weight, leaf area and total leaf N content. A model was used for scaling up from leaf to canopy photosynthetic traits to study the effect of the different treatments on canopy level and secondly to estimate the relative contribution of instantaneous responses, plastic responses within the lifetime of the plant and genotypic responses over several generations to elevated [CO_2] independently from competition.

We hypothesize that plants respond plastically to elevated growth [CO_2] through partial closure of the stomata (Long *et al.* 2004), increase of photosynthesis rate (Ainsworth & Long 2005) and reduction of leaf N content per unit area (Ainsworth & Long 2005). Furthermore, we expect that the genotypic response of plants to elevated growth [CO_2] will depend on the effect of plant-plant interactions. Here, we hypothesize two possible outcomes. The first one assumes that regardless of plant-plant interactions (between or within populations), plants would do best in their 'native [CO_2] environment' (i.e. elevated [CO_2] for spring and low [CO_2] for the non-spring). So, for both mono and mixed stands, the best performer would be the genotype of its native [CO_2] environment. The second possible outcome, with regard to the genotypic response of plants to elevated [CO_2], is that plants that would succeed under changing [CO_2] are not those that intrinsically perform best, but rather those that are the best competitors under those circumstances. This expectation is based on game theoretical principles, as according to this, selection under competition tends to result in being a better competitor rather than having the highest performance. So, this hypothesis predicts that the performance advantages of a given genotype in its native [CO_2] environment will be apparent only in the mixed stands and not in the mono stands.

4.2 Materials and Methods

4.2.1 Plant material and growth conditions

We used *P. asiatica*. This is a small (0.1-0.3m) perennial rosette plant, predominantly self-pollinating species (Huh 2013) where pollen dispersal of these plants is thought to be very limited (0.1-0.4 m) (Onoda, Hirose & Hikosaka 2009). The seeds originate from three independent natural CO_2 springs in Japan: Asahi (38.2° N, 140.0° E, 540 m asl, 2000 ppm in the elevated [CO_2] area), Kosaka (40.4° N, 140.8° E, 450 m asl, 560 ppm in the elevated [CO_2] area) and Yuno-Kawa (40.7° N, 140.9° E, 560 m asl, 530 ppm in the elevated [CO_2] area). In these CO_2 springs most of the CO_2 is emitted from spring water and not from the soil. We choose for three springs instead of a single CO_2 spring, to have more replications and to test if plant responses to elevated [CO_2] occur independently of the environmental factors from their original habitats (Osada, Onoda & Hikosaka 2010). Furthermore, we did choose for these three springs, because these springs did not emit toxic gasses. The springs also did not

have a significant effect on the air temperature; and the [CO_2] around these springs has been constantly high for hundreds of years (Onoda, Hirose & Hikosaka 2007). Seeds from normal [CO_2] were collected from plants in nearby areas (non-spring populations). In each location spring and non-spring populations were shown to be genetically distinct (Nakamura *et al.* 2011). In the present study, offspring of each population (i.e. from each elevated and ambient CO_2 site) were used for experiments to avoid maternal effects (i.e., the effects of environment of parent generation). To obtain offspring of each population, seeds obtained from field populations were separately sown in a common garden of Tohoku University (38.4° N, 140.6° E, Japan) in May 2010, and cultivated for two years. From July to September 2010, individuals germinated from seeds of the same population were mated. From October to December 2010 and 2011, offspring seeds were harvested.

Seeds originating from these three CO_2 springs (spring plants) and from their respective control areas (non-spring plants) were sown on 25 October 2013 on sandy soil. On 4 November 2013 the seedlings were transplanted to square (0.1 by 0.1 m) 0.15 L pots filled with sandy soil and 0.7 g of slow release fertilizer (N-P-K 16:9:12). Two plants were grown in each pot. Plants were grown in walk-in growth chambers (Reftech custom made, 20°C, 70% relative humidity, 10 hours light at 400 μmol $m^{-2}s^{-1}$) with three different CO_2 levels: 270 ppm (low [CO_2]), 450 ppm (intermediate [CO_2]) and 750 ppm (elevated [CO_2]). The low [CO_2] (270 ppm) chamber, was about equal to the pre-industrial levels that have more or less persisted for several thousand years until about the 1800s. The intermediate level indicates the [CO_2] that can be expected within the next 1 – 2 decades, and the elevated [CO_2] level is the level that is predicted for the end of this century. Plants were placed on an automatically watered irrigation mat.

Stands were established by putting three by three pots together for a total of nine pots and 18 plants (total stand size is 0.3 by 0.3 m, Fig 4.1a), the eight middle plants of each stand were used for measurements (total area for the measurements in a stand is 0.2 by 0.2 m, Fig 4.1b). Stands could be a mono stand of either only spring plants (Fig 4.1a) or non-spring plants (Fig 4.1b), or a mixed stand with both spring and non-spring plants with one of both in each pot (Fig 4.1c). This set up was repeated for all three localities. For each combination there were four replicate stands (Fig 4.1d). So, in total 1944 plants were grown from which 864 plants were used for measurements, as stands of 18 plants were established from which eight plants were used for measurements for a total of 27 different combinations of factors which were replicated four times.

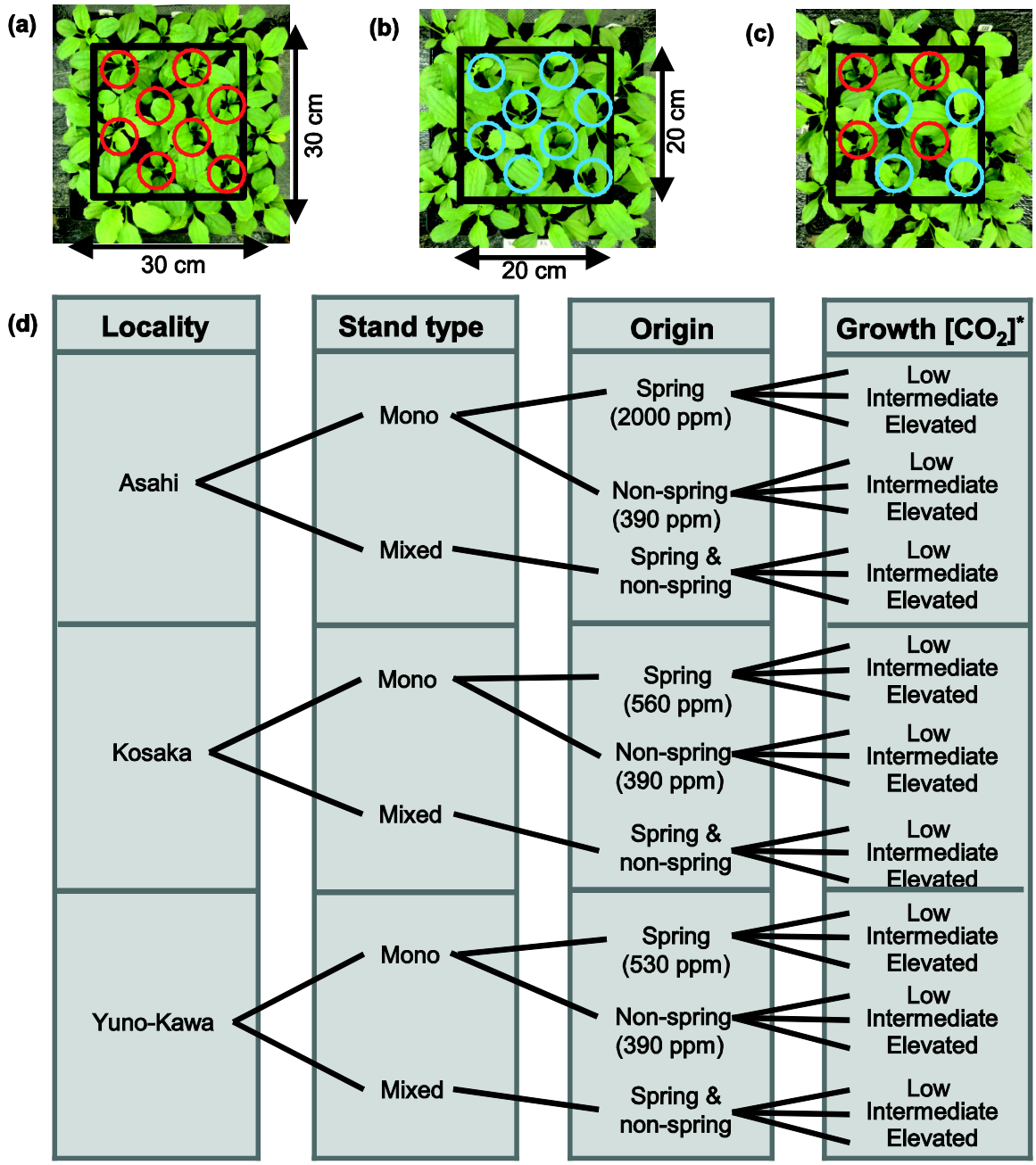

Fig 4.1 Experimental set-up. Stands were established by putting three by three pots together, the total size of a stand is 30 by 30 cm. Stands could be a mono stand of either only spring plants (originating from CO_2 spring) (a) or non-spring plants (originating from control area) (b), or a mixed stand with both spring and non-spring plants in one stand (c). The plants within the area of the dashed square (20 by 20 cm) were used for measurements, these are the 8 middle plants of a stand. Plants were grown under different CO_2 levels, this set-up was repeated for different localities. Photos (panels a-c) of the experiment were taken on 19 December 2013, 55 days after sowing. The different combinations of factors and their levels which were used in the experiment (d). * Low, intermediate and elevated growth [CO_2] are respectively 270, 450 and 750 ppm

4.2.2 Gas exchange measurements

From 23 December 2013 (59 days after sowing) and onwards, photosynthetic CO_2 response curves were made using a portable open gas exchange system (LI-6400, LiCor) on attached

fully expanded leaves. The system was equipped with an LED light source (LI-6400-02B, LiCor), which provided both red and blue light (the latter is important in controlling stomatal aperture). From every stand one young fully expanded leaf was measured and in case of a mixed stand two leaves were measured (one of a spring plant and one of a non-spring plant). Photon flux density during the measurements was 1500 µmol $m^{-2}s^{-1}$, vapour pressure deficit was <2 kPa and temperature was 25°C. For each leaf the photosynthesis was determined at a [CO_2] of 50, 90, 150, 270, 500, 700, 900, 1100, 1500 ppm.

The CO_2 response curves were fitted with the biochemical model of Farquhar, Von Caemmerer & Berry (1980). Below an intercellular [CO_2] (C_i) of 300 ppm the curve was fitted to the RuBP carboxylation limited photosynthesis rate (P_{cl}):

$$P_{cl} = V_{cmax} \cdot \frac{C_i - \Gamma^*}{C_i + K_c \cdot \left(1 + \frac{O}{K_o}\right)} - R_d$$

where V_{cmax} is the maximum carboxylation rate; Γ^* is the [CO_2] compensation point in the absence of mitochondrial respiration; K_c and K_o are respectively the Michaelis-Menten constants for carboxylation and oxygenation and O is the oxygen concentration. For K_c, K_o and O we assume a value of 404.9 µmol mol^{-1}, 278.4 mmol mol^{-1} and 205 mmol mol^{-1} respectively (Ishikawa, Onoda & Hikosaka 2007; for *P. asiatica*). R_d is the respiration rate in light and was assumed to be 10% of V_{cmax} (Von Caemmerer 2000).

Above an intercellular [CO_2] of 300 ppm the CO_2 response curve was fitted to RuBP regeneration limited photosynthesis rate (P_{jl}):

$$P_{jl} = J_{max} \cdot \frac{C_i - \Gamma^*}{4 \cdot C_i + 8 \cdot \Gamma^*} - R_d$$

where J_{max} is the maximum electron transport rate.

4.2.3 Canopy characteristics

Measurements of canopy structure, leaf area and biomass were done from 27 until 29 January 2014 (94-96 days after sowing). At this time the stands had formed a closed canopy and there was clear mutual shading among neighbouring plants (see also pictures of the stands in Fig 4.1a-c taken on 19 December 2013, more than one month before harvest). The height of each plant was measured from ground surface to the apex of the topmost leaf of all plants in the centre of the blocks (eight per stand, see Fig 4.1a-c). Leaf vertical inclination angles were measured with a protractor and then categorized in three leaf angle classes (0-30º; 30-60º; 60-90º), which were used as input in the model (see below and also Goudriaan (1988)). The shoots (i.e., in this rosette plant consisting of only leaves) were then cut at ground level and leaf area was determined with a LI3100 leaf area meter (LICOR, Lincoln NE, USA). The

Leaf Area Index (LAI, the leaf area of a plant divided by the ground area [in this case per plant half of the ground area of a pot]) was determined from the leaf area. We defined LAI of one individual to distinguish between the LAI of spring and non-spring plants in mixed stands. Leaves were dried at 70ºC for three days after which the dry weight per plant was determined. The leaf organic nitrogen content per plant was determined with a continuous flow analyser (SKALAR, the Netherlands) after Kjeldahl digestion.

4.2.4 Statistical analysis

Statistical analysis was performed using SPSS (version 21.0.0.1). A generalized linear model was applied to test the effects of growth [CO_2] (270, 450 and 750 ppm [CO_2]), origin (spring, non-spring) and stand type (mono stand, mixed stand), all as fixed factors. Location (Asahi, Kosaka and Yuno-Kawa) was treated as a random factor. A four-way ANOVA was used to test for significant differences. The average of a stand (average of eight spring or non-spring plants in a mono stand, the average of either the four spring or the non-spring plants in a mixed stand) was used for statistical analysis. For photosynthesis rate, stomatal conductance and leaf N, we measured one leaf in every mono stand and two leaves for every mixed stand (one of a spring plant and one of a non-spring plant).

4.2.5 Model analysis

Measured leaf photosynthetic traits were scaled up to canopy photosynthetic traits by using the canopy model of Van Loon *et al.* (2014). In short, this model calculates the light distribution within the canopy, following the approach of Spitters, Toussaint & Goudriaan (1986) that distinguishes between the distribution of direct solar beam and diffuse radiation. The canopy photosynthesis model (Farquhar, Von Caemmerer & Berry 1980) is a function of light (Spitters, Toussaint & Goudriaan 1986), nitrogen (logarithmic relationship for leaf nitrogen versus photosynthetic capacity), temperature (Johnson, Eyring & Williams 1942; Farquhar, Von Caemmerer & Berry 1980), [CO_2] and water (Tuzet, Perrier & Leuning 2003). Further, this canopy model is based on steady state assumptions of water transport (Sterck & Schieving 2011) and of [CO_2] inflow and consumption, and these were solved with plant-specific parameters (Appendix, Table A4.1) and for the measured experimental constraints (total canopy leaf N content, water availability, incident light, temperature, atmospheric [CO_2] [Table A4.1]). Details can be found in Van Loon *et al.* (2014).

The canopy photosynthesis model was used for two purposes. First, the model was used for scaling up from leaf to canopy photosynthetic traits to study the effect of the different treatments at the canopy level. This allowed us to assess effects of [CO_2], spring vs non-spring and competition on whole-plant carbon gain. Second, the model was used to estimate the relative contribution of three different types of responses to elevated [CO_2] on the canopy

photosynthesis rate independently from competition. For this objective, we therefore only conducted model calculations for the mono stands. The distinction between the three types of responses is based on the time scale: I) instantaneous – immediate, time scale of seconds to days, which assesses what the effect of [CO_2] elevation would have been if plants would not have exhibited any trait changes, II) plastic – within lifetime plant, days to weeks, and III) genotypic – over several generations, evolutionary time scale (Table 4.1). We will further explain these responses and how they are modelled.

I) Instantaneous response, was defined as the difference in canopy photosynthesis rate of plants that have been exposed to elevated [CO_2] for a short time because they are transferred from low to elevated [CO_2], and of plants that have never been exposed to elevated [CO_2] and thus grew whole their lifetime at low [CO_2]. In the model this is done by calculating the canopy photosynthesis rate of non-spring plants at elevated [CO_2] with the plants being given the same traits as measured from the non-spring plants growing in low [CO_2] (i.e., virtually transferring non-spring plants from low to elevated [CO_2]) (Table 4.1, model run 2) and subtracting the calculated canopy photosynthesis rate of non-spring plants grown in low [CO_2] (Table 4.1, model run 1).

II) Plastic response, was defined as the difference in canopy photosynthesis rate of plants that grew their whole lifetime at elevated [CO_2], and of plants that have been exposed to elevated [CO_2] for a short time because they are transferred from low to elevated [CO_2]. In the model this is done by calculating the canopy photosynthesis rate of non-spring plants at elevated [CO_2] with their trait values as measured under those conditions (Table 4.1 model run 3) and subtracting the calculated canopy photosynthesis rate of the virtually transferred plants from low to elevated [CO_2] (Table 4.1, model run 2).

III) Genotypic response, was defined as the difference in canopy photosynthesis rate of plants that are for several generations under elevated [CO_2], and of plants grew whole their lifetime at elevated [CO_2]. In the model this is done by subtracting the canopy photosynthesis rate of spring and non-spring plants grown at elevated [CO_2] with their trait values as measured under those conditions (Table 4.1 model run 4 and 3 respectively).

The traits that are changed for the model simulations to make the distinctions between the three different responses to elevated [CO_2] are plant height (see Appendix, Fig A4.1a), leaf angle determining the extinction coefficient (Fig A4.1b-d), LAI and plant leaf N content. Other parameter input values were kept constant for all simulations (Table A4.1, Figs A4.2, A4.3). The parameters that were changed were chosen, because we focus only on canopy photosynthesis. We used for those parameters the measured values from the three localities, i.e. Asahi, Kosaka and Yuno-Kawa, and from the four replicates in the model for one treatment separately for the model runs. So, the model outcome of one treatment is the average of twelve model runs.

Table 4.1. Three types of responses to elevated [CO_2] that act on different time scales (I-III), these are modelled by subtracting different types of model runs (1-4). NSpr are non-spring plants originating from ambient [CO_2] and Spr, are spring plants originating from naturally elevated [CO_2] areas

				In the model	
Time scale of response	Type of response		Time exposed to elevated [CO_2]	Growth [CO_2]	Traits
		2:	Seconds, transferred from low to elevated [CO_2]	Elevated	Low [CO_2]: NSpr
		1:	None, whole lifetime in low [CO_2]	Low	Low [CO_2]: NSpr
I) Immediate (seconds-days)	***Instantaneous***		**2-1**		
		3:	Lifetime exposure to elevated [CO_2]	Elevated	Elevated [CO_2]: NSpr
		2:	Seconds, transferred from low to elevated [CO_2]	Elevated	Low [CO_2]: NSpr
II) Within lifetime plant (days-weeks)	***Plastic***		**3-2**		
		4:	Several generations exposure to elevated [CO_2]	Elevated	Elevated [CO_2]: Spr
		3:	Lifetime exposure to elevated [CO_2]	Elevated	Elevated [CO_2]: NSpr
III) Several generations (evolutionary time scale)	***Genotypic***		**4-3**		

4.3. Results

4.3.1 Results of growth chamber experiment

No significant difference was found among the three localities (Asahi, Kosaka and Yuno-Kawa) for all measured traits, except for stomatal conductance (see further below).

Lumped for locality, origin and stand type, LAI significantly increased with increase in growth [CO_2]; this increase being stronger from low to intermediate than from intermediate to elevated [CO_2] (13.6% and 3.3% respectively) (Fig 4.2a). Notably, there was a significant three-way interaction of growth [CO_2] x origin x stand type. At low [CO_2] spring plants had larger LAIs than non-spring plants in the mono stand, but this was not the case at intermediate and elevated [CO_2]. Conversely, in the mixed stands non-spring plants had larger LAIs than spring plants under low [CO_2], while for intermediate and elevated growth [CO_2] spring plants had larger LAIs (Fig 4.2a). In other words, plants produced larger LAIs in their 'native [CO_2] environment' (non-spring at low [CO_2] and spring at intermediate and elevated [CO_2]) only if there was competition between the different populations of origin.

A similar pattern was observed for whole-plant dry weight (Fig 4.2b). Dry weight increased significantly with increasing growth [CO_2] lumped for locality, origin and stand type; a stronger increase was observed if [CO_2] increased from low to intermediate compared to intermediate to elevated (43.0% and 10.1% respectively) (Fig 4.2b). There was a significant three-way interaction of growth [CO_2] x origin x stand type. The dry weight of spring and non-spring plants in mono stands did not differ significantly. On the other hand, in mixed stands non-spring plants had a significant greater dry weight under low [CO_2]; while this held for spring plants at intermediate and elevated growth [CO_2] (Fig 4.2b).

Lumped for locality, origin and stand type there was a significant decrease in specific leaf area (SLA, leaf area divided by leaf dry weight) with increasing growth [CO_2], with a larger difference between low and intermediate [CO_2] than for intermediate and elevated levels (-19.6% and -6.7% respectively) (Fig 4.2c). A significant growth [CO_2] x origin interactive effect was observed. Although not significant, spring plants tended to have higher SLA compared to non-spring plants at low growth [CO_2]; while non-spring plants had significantly higher SLA compared to spring plants at intermediate [CO_2], this trend was also found for elevated [CO_2] (Fig 4.2c). In other words, the SLA reduction with [CO_2] appeared to be stronger in the spring than in the non-spring plants.

None of the effects (locality, growth [CO_2], origin and stand type) was significant for total leaf N content (i.e., total amount of N in the canopy of a plant), but the general pattern resembled that of LAI and dry mass. That is, the spring and non-spring plants in mono stands had no significantly different total N, but in mixture spring plants had a significantly greater total N compared to the non-spring plants under intermediate and elevated growth [CO_2] (Fig 4.2d). Total leaf N of plants was strongly and positively correlated to leaf area (Fig A4.4).

The measured leaf photosynthesis rate at growth [CO_2] (A_{growth}) significantly increased with increasing [CO_2] (lumped for locality, origin and stand type) (Fig 4.3a). There was a significant origin x stand type interactive effect. The non-spring plants tended to have a higher A_{growth} in mono stands, while in a mixed stand they tended to have a lower A_{growth} compared to spring plants a trend that appeared consistent across CO_2 levels (Fig 4.3a).

Stomatal conductance significantly decreased with increasing [CO_2] (lumped for locality, origin and stand type) (Fig 4.3b-d). There was a significant interaction of growth [CO_2] x origin. Spring plants had a higher stomatal conductance at low growth [CO_2] compared to non-spring plants for Kosaka and Yuno-Kawa, whereas this was the case for non-spring plants at intermediate [CO_2] for Kosaka (Fig 4.3c,d).

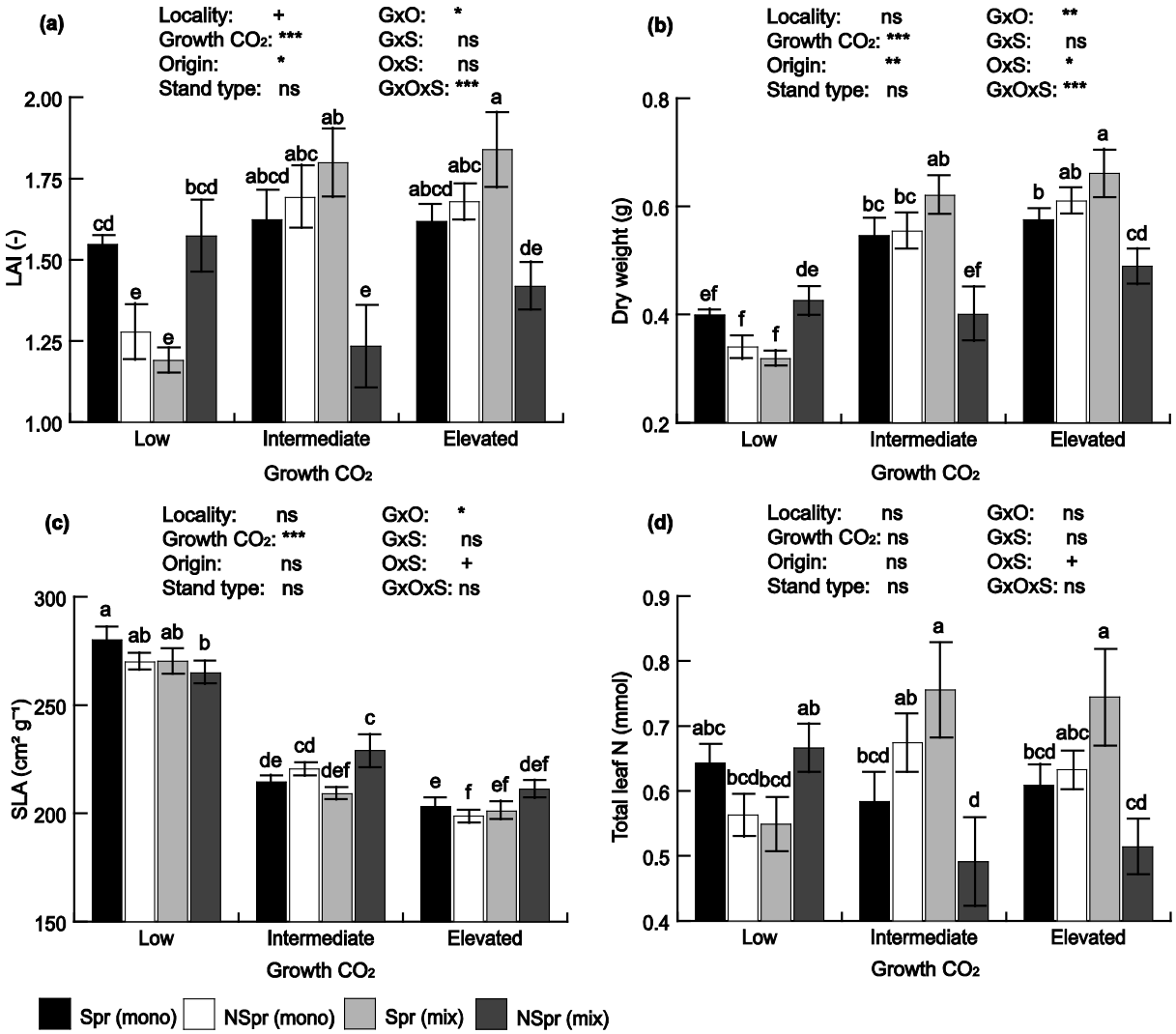

Fig 4.2 Leaf Area Index (LAI) (a), aboveground dry weight (b), Specific Leaf Area (SLA) (c) and total canopy leaf N content (d) of plants grown under low (270 ppm), intermediate (450 ppm) or high (750 ppm) [CO_2] and originating from either spring areas (Spr) or non-spring areas (NSpr) and these are either grown in mono stand (mono) or in mixed stand (mix) (n=12). Values are mean ± standard error. Different letters indicate significant differences between the treatments (P<0.05). Results of the generalized linear model are shown: *** P<0.001, ** P<0.01, * P<0.05, + P<0.1

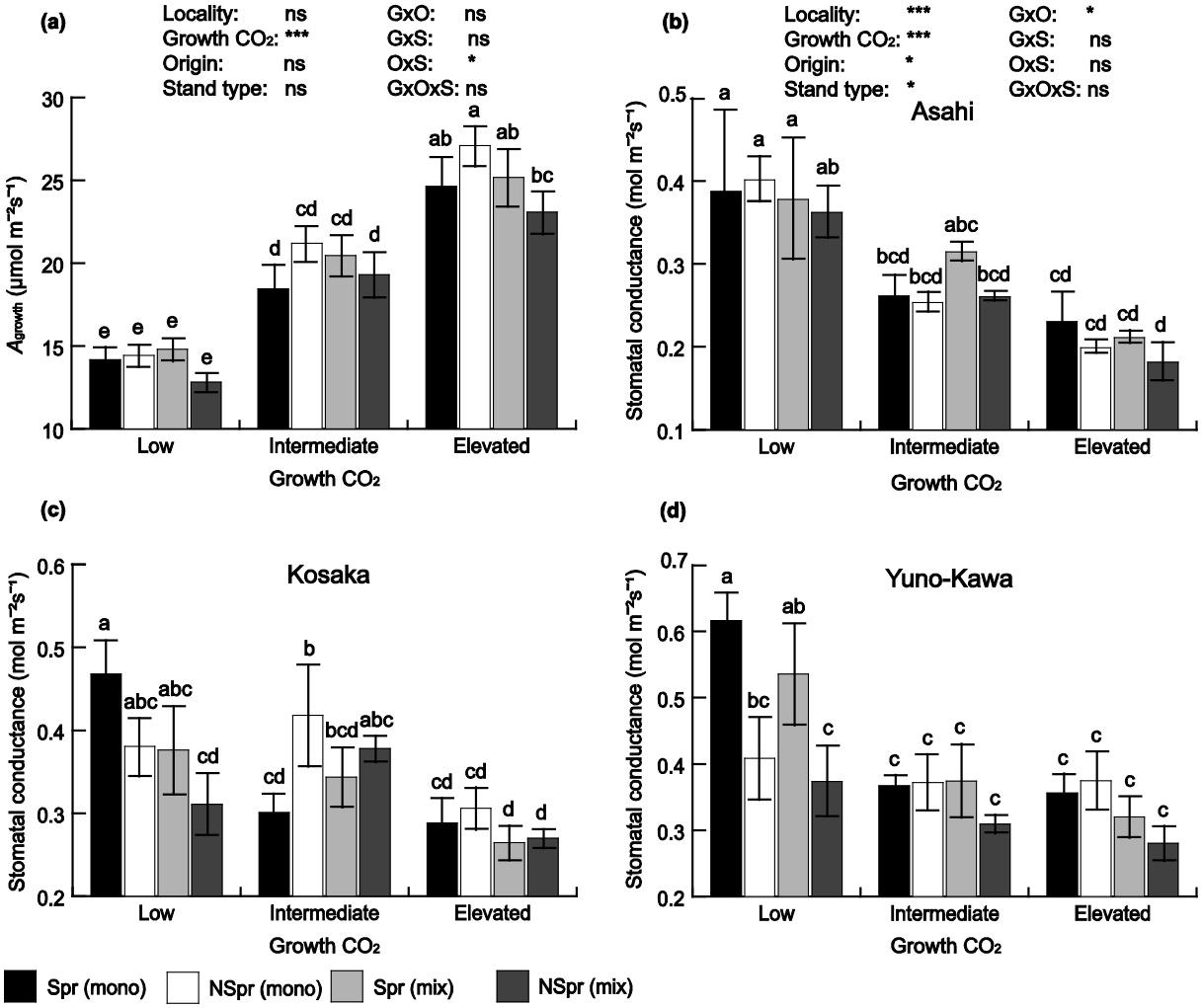

Fig 4.3 Photosynthesis at growth [CO_2] (A_{growth}) (n=12) (a) and stomatal conductance for the areas Asahi (b), Kosaka (c) and Yuno-Kawa (d) (n=4) of plants grown under low (270 ppm), intermediate (450 ppm) or high (750 ppm) [CO_2] and originating from either spring areas (Spr) or non-spring areas (NSpr) and these are either grown in mono stand (mono) or in mixed stand (mix). Values are mean ± standard error. Different letters indicate significant differences between the treatments (P<0.05). Results of the generalized linear model are shown: *** P<0.001, ** P<0.01, * P<0.05, + P<0.1

4.3.2 Results of canopy model

A canopy model was used for two different purposes. First, to scale up from leaf photosynthetic traits to plant and canopy photosynthetic traits, to study the effects of the different treatments at the canopy level. Second, to investigate the contribution of phenotypic trait responses to elevated [CO_2] and genotypic trait differences between spring and non-spring plants to canopy photosynthesis (Table 4.1). For this latter objective, we only conducted model calculations for the mono stands. The four parameters that were changed for the different scenarios of both modelling executions are the measured values of the extinction coefficient (determined from the leaf angle), plant height, plant leaf N content and LAI. Other parameter input values were kept the same for all model runs (Table A4.1, Figs A4.2 and A4.3).

Fig 4.4a shows the outcomes for the first modelling execution: the simulated average total canopy photosynthesis rates (with standard error) of the four replications of spring and non-spring plants in mono- or mixed stands per locality. For the total canopy net photosynthesis rate, a similar pattern was found as for LAI and whole plant aboveground dry weight. Canopy net photosynthesis rate increased significantly with increasing growth [CO_2] lumped for locality, origin and stand type (Fig 4.4a). A significant three-way interaction of growth [CO_2] x origin x stand type was found. There was no significant difference in canopy net photosynthesis rate of spring and non-spring plants in mono stands; while in mixed stands non-spring plants had a significant higher canopy photosynthetic rate under low [CO_2] and this held for spring plants at intermediate and elevated growth [CO_2] (Fig 4.4a).

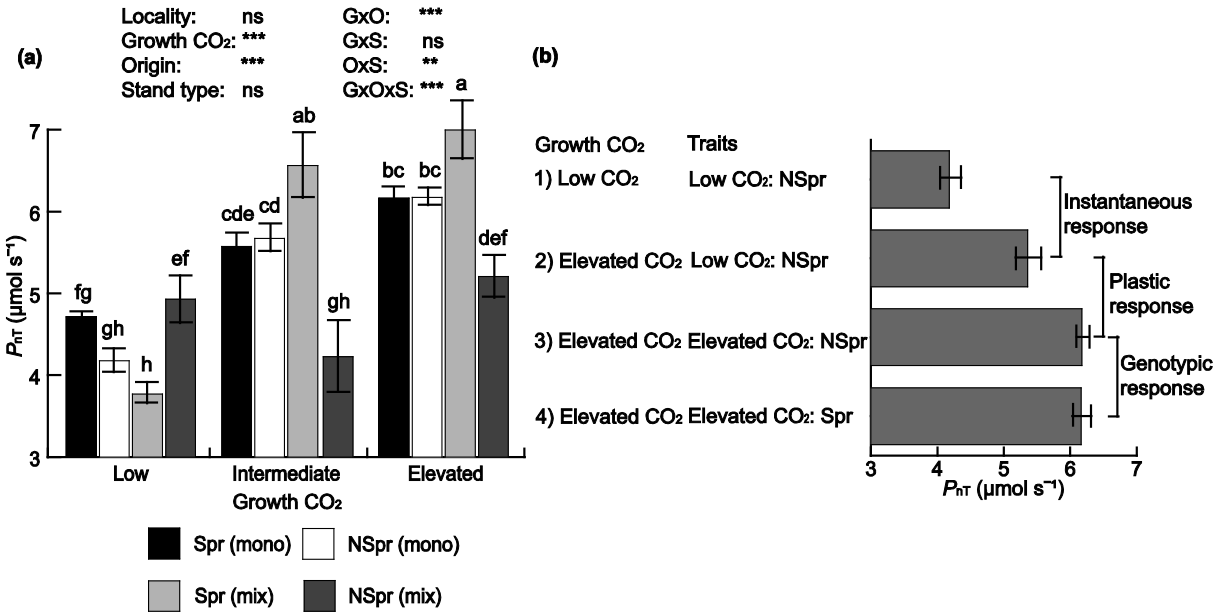

Fig 4.4 (a) Modelled canopy photosynthesis rate (P_{nT}) of plants grown under low (270 ppm), intermediate (450 ppm) or high (750 ppm) [CO_2] and originating from either spring areas (Spr) or non-spring areas (NSpr) and these are either grown in mono stand (mono) or in mixed stand (mix) (n=12). Values are mean ± standard error. Different letters indicate significant differences between the treatments (P<0.05). Results of the generalized linear model are shown: *** P<0.001, ** P<0.01, * P<0.05, + P<0.1. (b) Modelled canopy photosynthesis rate of 1) non-spring plants grown at low [CO_2], 2) non-spring plants grown at elevated [CO_2] which have the traits of those grown at low [CO_2] (transferred non-spring plants from low to elevated [CO_2]), 3) non-spring plants grown at elevated [CO_2], and 4) spring plants grown at elevated [CO_2]. Difference 1 and 2: instantaneous response; difference 2 and 3: plastic response; difference 3 and 4: genotypic response (see also Table 4.1). Values are mean ± standard error

Fig 4.4b shows the outcomes for the second modelling exercise: the relative contribution of the different type of responses to elevated [CO_2] on the simulated canopy photosynthesis rate. Canopy photosynthesis rate was simulated to increase with 28% by an instantaneous response, i.e. plants that were grown in low [CO_2] were virtually transferred to

elevated [CO_2] (Fig 4.4b). Plastic response resulted in an additional 15% increase in photosynthesis at elevated [CO_2] compared to transferred plants (Fig 4.4b). Conversely the simulation showed that non-spring plants had similar canopy photosynthesis rate as spring plants at elevated [CO_2] indicating that in mono stands the genotypic differences contributed little to whole-stand photosynthesis (Fig 4.4b). So, both the direct effect of elevated [CO_2] and the plastic response to this condition contributed to increased whole-plant photosynthesis, but effects of the genotypic response were negligible.

4.4 Discussion

In our study, we showed that changes in whole-stand photosynthetic rate, specific leaf area (SLA) and stomatal conductance of *Plantago asiatica* to changes in growth [CO_2] were mainly driven by instantaneous responses and plastic responses within the lifetime of a plant and not by genotypic changes, which take place over several generations. We further found that plants native to high [CO_2] habitats (spring plants) performed better in terms of whole-stand photosynthesis, biomass and leaf area, than those from ambient [CO_2] habitats (non-spring plants) at elevated [CO_2] only when plants of the two [CO_2] habitats competed. Similarly, plants from ambient [CO_2] habitats performed better at preindustrial [CO_2] only when competing with plants from elevated [CO_2] habitats. Our results build upon the work of Manea & Leishman (2011) who illustrated the large role of plant competition in determining community-level outcomes under elevated [CO_2], by showing that the relative success of invasion by exotic species was increased under elevated [CO_2]. Together, our findings suggest that selection under changing [CO_2] is strongly mediated by competitive interactions between plants, as more competitive plants benefit more from elevated [CO_2], and this may have important consequences for species distribution and vegetation functioning.

Although we found an increase in whole-plant photosynthetic rate to elevated [CO_2] by both the direct effect and the plastic response, this increase was small compared to the [CO_2] increase. Yet, Free-Air CO_2 Enrichment (FACE) studies found similar results of responses to elevated [CO_2] (Ainsworth & Long 2005). An important cause could be the concave form of the photosynthesis-CO_2 response curve, as photosynthesis tends to saturate at high [CO_2] (Leakey & Lau 2012). In addition, light levels in growth chambers were around 400 µmol $m^{-2}s^{-1}$ which is comparable to the light levels on moderately overcast day at our site, but which tends to be below the level that would saturate photosynthesis. So, the RuBP regeneration rate was probably limiting the photosynthesis rate resulting in a relatively moderate increase in photosynthesis by [CO_2] elevation. Additionally, this low photosynthetic response to [CO_2] elevation is also generally thought to be the result of photosynthetic down-regulation (e.g. Von Caemmerer *et al.* 2001). Poorter (1993) also found, by reviewing a large number of

studies, that on average an increase in [CO_2] only leads to small increases in growth due photosynthetic down-regulation, but this response is highly species dependent.

A decrease in SLA with elevated [CO_2] was found, and this might cause the induction of photosynthetic down-regulation. The decreased SLA was thought to be the result of the increase in leaf thickness (data not shown); which is often the result of the accumulation of non-structural carbohydrates at elevated [CO_2], and this might cause induction of photosynthetic down-regulation (Roumet, Laurent & Roy 1999).

A decrease in stomatal conductance with elevated [CO_2] was found, this was mostly resulting from instantaneous closure of the stomatal apparatus and to a lesser extent to decreased stomatal density across the populations from the different [CO_2] habitats (data not shown). No clear differences between spring and non-spring plants were observed, suggesting that there are no genotypic differences in stomatal response. This finding was contradictory to the results of Haworth, Elliott-Kingston & McElwain (2011), who found for the grass species *Agrostis canina* that spring plants had a higher stomatal conductance compared to non-spring plants when grown at ambient [CO_2], and spring plants reduced their stomatal conductance much less compared to non-spring plants when grown at elevated [CO_2] which increased the difference in stomatal conductance between spring plants and non-spring plants. The lack of genotypic differences in the stomatal responses to elevated [CO_2] in our study, may be caused by the costs of stomatal control (Haworth, Elliott-Kingston & McElwain 2011). There is possibly a trade-off between physiological and morphological control of stomatal conductance to changes in [CO_2] (De Boer *et al.* 2012; Haworth, Elliott-Kingston & McElwain 2013). Species with active control of stomatal apparatus generally show little reduction in stomatal density; while species with little or no active control of the stomatal apparatus are more likely to reduce their stomatal density (Haworth, Elliott-Kingston & McElwain 2013). Furthermore, many species show little or no response in stomatal density to [CO_2] elevation (Haworth, Elliott-Kingston & McElwain 2013).

Although the spring plants originated from three different localities in Japan (Asahi, Kosaka and Yuno-Kawa) with rather different natural CO_2 levels (530 – 2000 ppm), there was no location effect found for most of the measured traits. This might be due to the nonlinear photosynthetic response of plants to CO_2 and the concentration at which CO_2 is saturating (Leakey & Lau 2012). That is, above a certain [CO_2], photosynthesis only responds very little and thus variation in [CO_2] probably no longer exerts a strong influence on plant performance.

Our results confirm our second hypothesis regarding genotypic responses, that spring plants performed better under intermediate and elevated [CO_2] than non-spring plants only when the two competed and not when each was grown alone. The reverse also held, non-spring plants performed better under low [CO_2] only when they competed with spring plants and not when

grown alone. So, our findings clearly suggest that adaptation to changing [CO_2] can be strongly mediated by plant-plant interactions at least for our species. The study of Bazzaz *et al.* (1995) also supports this, as plants with the highest growth response to elevated [CO_2] in absence of competition did not have the highest growth response in competitive stands. Game theory could help to explain our findings, as it proposes that in vegetation stands where plants interact, natural selection would not favour plants with the highest performance (e.g. growth or reproduction) per se, but rather those that exhibit competitive advantages over neighbours (Anten & During 2011). For example, selection might favour plants with more leaf area or that grow taller than would be needed for maximized production (Anten 2002; Falster & Westoby 2003). Van Loon *et al.* (2014) showed that a game theoretical model, which assumed that the best competitors will prevail under elevated [CO_2], gave better predictions of LAI and photosynthesis in elevated [CO_2] experiments than models that assume that plants with the inherent highest photosynthesis will prevail. Together with the findings reported here, this also suggests that competition strongly mediates plant adaptations to elevated [CO_2] and this may have important consequences for future species distribution and vegetation functioning.

The higher performance of the competing plants in their native [CO_2] environment is the result of a higher dry weight and leaf area, but not of higher leaf photosynthetic rates per unit leaf area. Differences in dry mass allocation might explain the differences in dry weight and leaf area while having a similar photosynthetic rate per unit leaf area for the spring and non-spring plants in mixture. Several studies (e.g. Polle, McKee & Blaschke 2001; Nakamura *et al.* 2011) show that spring plants allocate more biomass to leaves than to roots, resulting in higher growth rates for spring plants (Nakamura *et al.* 2011). In addition, it has been shown that a larger leaf area is an important trait in plants' competitive ability under elevated [CO_2] (Ziska, Faulkner & Lydon 2004; Ziska, Reeves & Blank 2005), as competition for light becomes more intense (Hikosaka *et al.* 2003). This could explain why spring plants had a competitive advantage when competition would be primarily for light. However, this would not explain why in our study non-spring plants were competitively superior under pre-industrial [CO_2]. In addition, as spring and non-spring plants shared pots in the mixed stands, belowground interactions could also have contributed to the observed competitive differences. The fact that leaf area and biomass were correlated with whole-plant nitrogen suggests that differences in nitrogen uptake and thus competition for that resource may have partly driven our results. However, as we did not measure roots we cannot confirm these conclusions. So, more research is needed to identify the traits that may explain the competitive interactions observed in this study.

Due to its ubiquitous nature and importance for plant growth, changes in [CO_2] entail a global selective force. Although the selection pressure is high, changes in plant performance were

mainly determined by plastic responses, with genotypic differences contributing very little. However, our results also suggest that genotypic selection under changing [CO_2] is determined more strongly by differences in competitive ability, than by difference in performance per se. This is, because we found that *P. asiatica* plants originating from naturally high [CO_2] areas and from ambient [CO_2] areas responded the same to variations in [CO_2] when grown separately, but when grown together they appeared to differ in their competitive ability.

4.5 Acknowledgement

This work was supported financially by a Focus & Mass grant from Utrecht University awarded to NPRA MR and SCD. We thank Heinjo During for his valuable comments on the manuscript.

Appendix – A4.1 Tables

Table A4.1 Model parameters with input value and unit, which are the same for every treatment (mono stand or mixed stand, spring or non-spring plant).

Parameter	Input value	Unit
Scaling parameter for calculation of stomatal conductance	2	Pa
The area in which an individual plant has its leaf area	1	m^2
Slope parameter for the stomatal sensitivity function	3.2	MPa^{-1}
Intercept of the leaf respiration rate – leaf N per unit leaf area relation	0.5238	µmol m^{-2} s^{-1}
Residual stomatal conductance per unit ground area	0	µmol d^{-1}
Activation energy of the maximum electron transport rate (J_{max})	58936	J mol^{-1}
Activation energy of the Michaelis-Menten constant for oxygenation	59400	J mol^{-1}
Activation energy of the Michaelis-Menten constant for carboxylation	36000	J mol^{-1}
Activation energy of the leaf respiration rate	48294	J mol^{-1}
Activation energy of the maximum carboxylation rate (V_{cmax})	75794	J mol^{-1}
Activation energy of the CO_2 compensation point (Γ^*)	20970	J mol^{-1}
Deactivation energy of J_{max}	199233	J mol^{-1}
Deactivation energy of V_{cmax}	202022	J mol^{-1}
Petiole conductance	1.1832	kg MPa^{-1} d^{-1}
Michaelis-Menten constant for carboxylation at 25°C	40.49	Pa
Michaelis-Menten constant for oxygenation at 25°C	27840	Pa
Leaf N concentration not associated with photosynthesis (intercept of the V_{cmax}-N_l and of the J_{max}-N_l relation)	6.0	mmol m^{-2}
Oxygen pressure in crown	20500	Pa
Atmospheric pressure	$1 \cdot 10^5$	Pa
Quantum yield (µmol electrons per photon)	0.25	µmol $µmol^{-1}$
Universal gas constant	8.315	J K^{-1} mol^{-1}
Relative humidity	70	%
Temperature	20	°C
Entropy term of J_{max}	647	J mol^{-1}
Entropy term of V_{cmax}	657	J mol^{-1}
Slope of the V_{cmax} – leaf N per unit leaf area relation	33.026	µmol CO_2 mmol N^{-1} s^{-1}
Slope of the J_{max} – leaf N per unit leaf area relation	61.159	µmol CO_2 mmol N^{-1} s^{-1}
Slope of the leaf respiration rate – leaf N per unit leaf area relation	0.0015	µmol CO_2 mmol N^{-1} s^{-1}
Γ^* in absence of mitochondrial respiration at 25°C	2.7	Pa
Curvature factor	0.821	-
Petiole area density in the crown cylinder	$1.5 \cdot 10^{-5}$	m^2 m^{-3}
Leaf scattering coefficient	0.2	-
Water potential at petiole base	0	MPa
Crown water potential at which the stomatal sensitivity function is half its maximum	-1.9	MPa

Appendix – A4.1 Figures

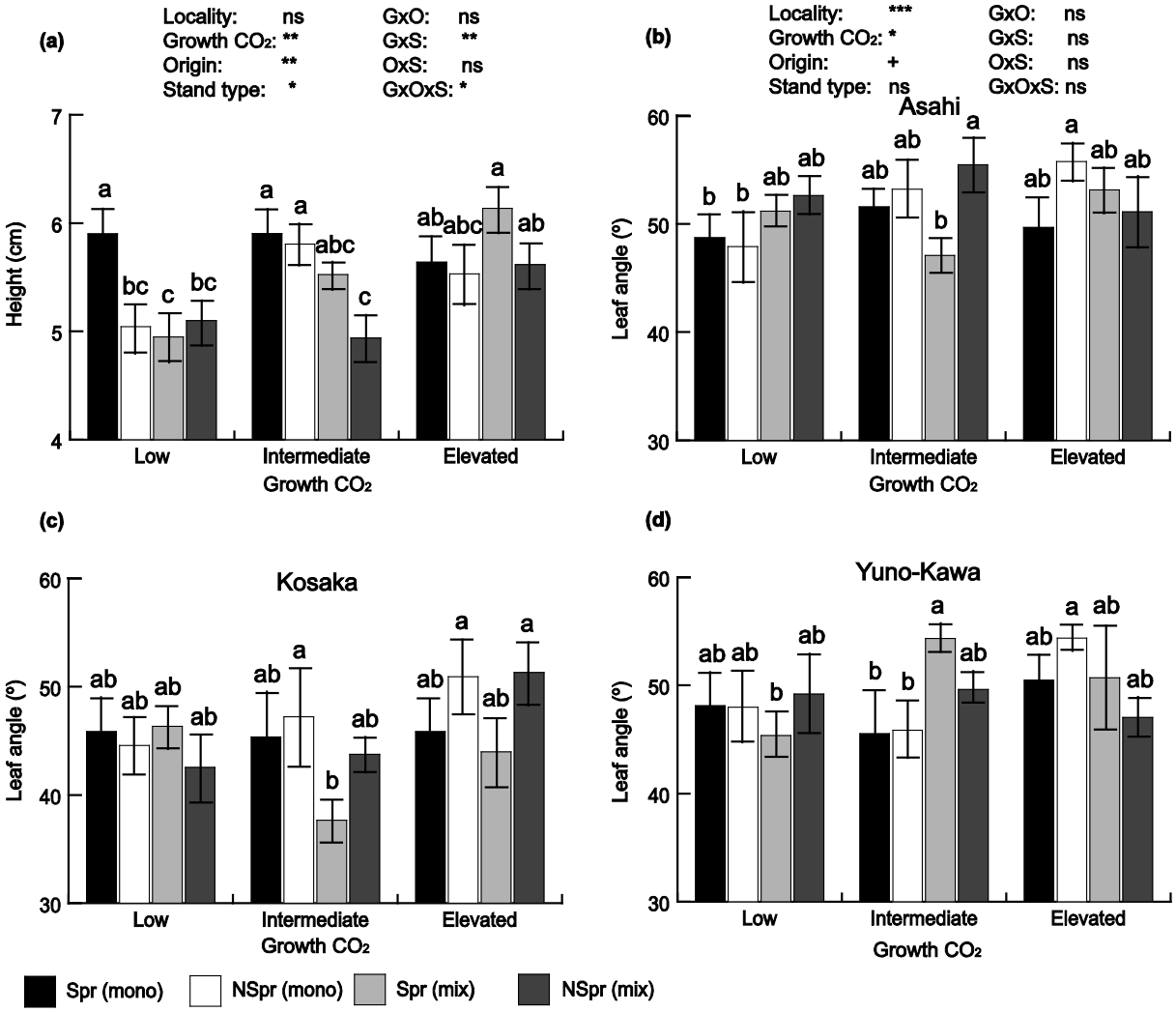

Fig A4.1 Canopy height (n=12) (a) and leaf angle for the areas Asahi (b), Kosaka (c) and Yuno-Kawa (d) (n=4) of plants grown under low (270 ppm), intermediate (450 ppm) or high (750 ppm) [CO_2] and originating from either spring areas (Spr) or non-spring areas (NSpr) and these are either grown in mono stand (mono) or in mixed stand (mix). Values are mean ± standard error. Different letters indicate significant differences between the treatments (P<0.05). Results of the generalized linear model are shown: *** P<0.001, ** P<0.01, * P<0.05, + P<0.1

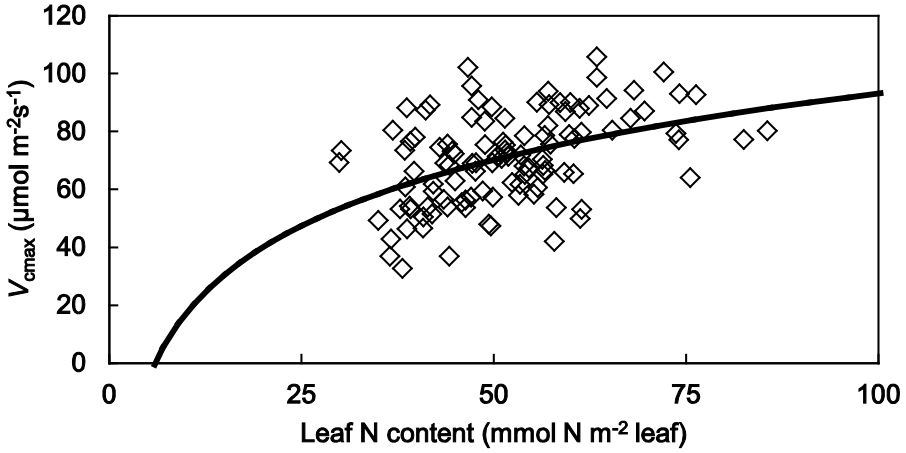

Fig A4.2 Maximum carboxylation capacity (V_{cmax}) versus leaf N content per unit leaf area. Black line indicates the logarithmic regression line of the leaf N-V_{cmax} relationship

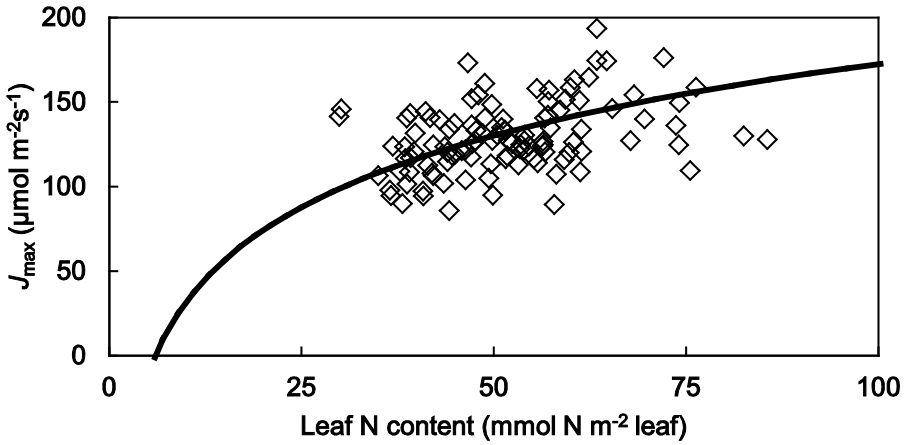

Fig A4.3 Maximum electron transport rate (J_{max}) versus leaf N content per unit leaf area. Black line indicates the logarithmic regression line of the leaf N-J_{max} relationship

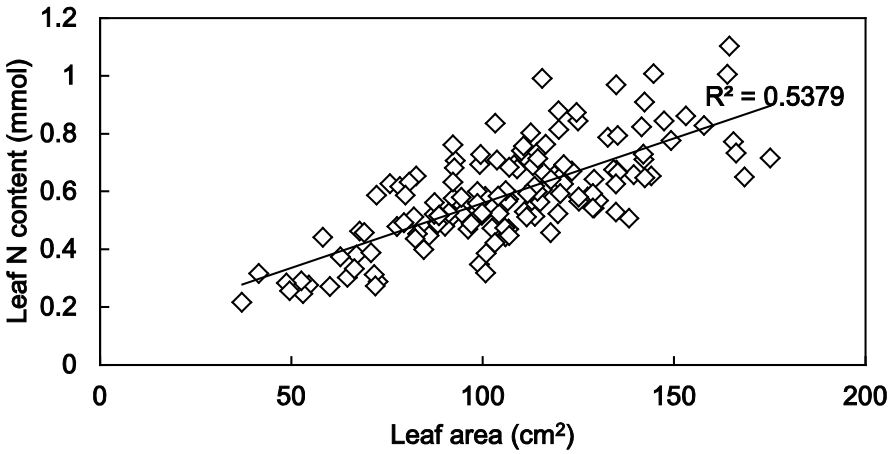

Fig A4.4 Total leaf area of a plant versus the N content of its leaves. Black line indicates the linear regression line of the leaf area-N relationship, R^2=0.538

Chapter 5

Understanding the impact of plant competition on the coupling between vegetation and the atmosphere

Marloes P. van Loon, Stefan C. Dekker, Niels P.R. Anten, Max Rietkerk and Jordi Vilà-Guerau de Arellano

Published as: Van Loon M.P., Dekker S.C., Anten N.P.R., Rietkerk M. & Vilà-Guerau de Arellano J. (2015) Understanding the impact of plant competition on the coupling between vegetation and the atmosphere. *Journal of Geophysical Research – Biogeosciences*, 120, doi:10.1002/2015JG003108

Abstract

Competition between plants for resources is an important selective force. As a result competition through natural selection determines vegetation functioning and associated atmospheric interactions. However, currently most coupled vegetation-atmosphere models do not consider this. Our aim is to investigate how the coupling between vegetation and atmosphere is influenced by plant competition. We used a coupled vegetation-atmosphere model and included a new representation of plant competition. We compared the model results with diurnal data from Ameriflux Bondville site over a growing season, and showed that inclusion of competition improved LAI (Leaf Area Index) and net ecosystem exchange of CO_2 (NEE) predictions; while if competition was not considered, there were strong deviations from observations. Remarkably, competition increased LAI while it reduced whole stand photosynthesis, resulting in a less negative NEE. Finally, independent of competition, our model results of latent heat flux, surface temperature, specific humidity and atmospheric CO_2 are in good agreement with observations. Only the sensible heat flux was overestimated, due to the representation of the surface energy balance in our model and due to the closure error of the energy balance in the data. In a sensitivity study, we found that the importance of plant competition on model outcomes increases with more nitrogen and water availability and may differ between soil types. We were thus able to illustrate the potential effect of plant competition in a coupled vegetation and atmospheric system and showed that it strongly influences this system, and therefore, we propose that competition should be considered in more vegetation-atmosphere models.

Key words: atmosphere-vegetation feedbacks, Leaf Area Index, modelling, optimality principle, plant competition

5.1 Introduction

Plants often grow in dense communities (e.g., forests or grasslands) where they share resources, such as light, water and nutrients, with neighbour plants and where competition for these resources is often an important selective force. As a result, through natural selection, vegetation stands have often become dominated by the best competitors, whose traits therefore strongly determine vegetation functioning (McNickle & Dybzinski 2013) and associated atmospheric interactions. However, even though inclusion of plant competition in atmospheric models has frequently been called for (Farrior 2014; Weng *et al.* 2015; Zhang *et al.* 2015), large atmospheric models usually do not include this (Sitch *et al.* 2003; Boussetta *et al.* 2013). Models that did include competition either used a Lotka-Volterra competition based approach (Zhang *et al.* 2015) or used a gap model (Moorcroft, Hurtt & Pacala 2001). In case of the Lotka-Volterra models, they assess whether competition between species is stronger than within species and then determine coexistence or exclusion. Gap models, on the other hand, predict the chance that an individual inhabits an empty area which was created by the death of others; thus, competition for light among individuals is considered. However, in contrast to those models we take an evolutionary game theoretical approach, by considering that natural selection favours plants that are the best competitors and not the ones that have the highest inherent performance. Plants asses the payoff of a given strategy (trait values) in relation to the characteristics of neighbouring plants (Riechert & Hammerstein 1983); the performance of one plant therefore depends on the characteristics of its neighbours.

It was shown for a variety of vegetation types that inclusion of competition between plants in a vegetation model using evolutionary game theory resulted in larger predicted leaf areas that were closer to observed values than when competition was not considered (Anten 2002; Lloyd *et al.* 2010). As leaves tend to have lower albedo than soil, such difference in estimates of leaf area may importantly impact estimates of the available radiative energy and its partitioning between evapotranspiration and sensible heat flux. Furthermore, inclusion of plant competition in a vegetation model also resulted in lower estimated photosynthetic CO_2 uptake and transpiration (Anten 2002; Van Loon *et al.* 2014) which in turn may impact carbon and water cycle projections, respectively. Here our aim is to investigate how the coupling between vegetation and the atmosphere is influenced by plant competition at diurnal scales during a whole growing season. That is, if plant traits and associated vegetation functioning evolved through natural selection on maximization of competitiveness rather than on maximization of inherent performance how would these affect vegetation-atmosphere interactions. Our hypothesis is that plant competition affects vegetation responses and thereby could strengthen or decrease certain feedback loops in the coupling of vegetation and atmosphere, resulting in changes in the atmospheric state variables. To study plant competition we use soybean (*Glycine max*). The choice for soybean is because this species is widely grown all over the world and might therefore have globally a large effect on

atmospheric processes. But we emphasize that we perform a simple and elementary analysis meant solely to assess the impact of competition on vegetation and atmospheric processes and not to develop a fully predictive climate model.

5.2 Material and Methods

Our methodology to quantify our hypothesis is based on a coupled vegetation-atmosphere model that includes explicitly a new representation of plant competition, which can be defined as an evolutionary game theoretical routine that models natural selection through competition. Our research strategy is to determine the impact of this new representation on surface and atmospheric processes, which include the LAI (Leaf Area Index, i.e., the leaf area per unit soil area), latent and sensible heat flux, net ecosystem exchange of CO_2, surface temperature, specific humidity and atmospheric CO_2. The coupled vegetation-atmosphere model we use was developed by Vilà-Guerau de Arellano *et al.* (2015), hereafter called CLASS-model. This model is a soil-water-atmosphere-plant model that predicts the energy, water and carbon balance on a daily time scale for the atmospheric boundary layer (ABL). This model explicitly includes the coupling of surface, heat and the exchange fluxes between the ABL and the troposphere. A short description of the CLASS-model is provided in paragraph 5.2.1. The vegetation part of the CLASS-model is replaced with the vegetation model of Van Loon *et al.* (2014). This vegetation model represents natural selection for canopy traits thereby relating photosynthesis to available nitrogen and has already been validated for soybean (Van Loon *et al.* 2014). A short description of the vegetation model is provided in paragraph 5.2.2, and in paragraph 5.2.3 it is explained how this model is coupled to the CLASS-model. We developed and explore two versions of this model: 1) $CLASS_{SimOpt}$: competition between plants is omitted, which is called the simple optimization model; and 2) $CLASS_{ComOpt}$: competition between plants is taken into account, which is called competitive optimization model. Here we will shortly explain the two model versions, in paragraph 5.2.4 we give a more elaborate description and explain how these model versions are incorporated in the vegetation-atmosphere model.

In the first model version, $CLASS_{SimOpt}$ it is assumed that plant traits are optimal simply when whole stand performance is maximized, meaning that the plants individual performance is optimized as long as it is in a monoculture without any invading strategies. The theory is based on the ecological concept that natural selection may have produced plants with optimal traits that maximize whole stand net photosynthesis independent of competition between plants (Dewar *et al.* 2009). We have chosen to optimize the LAI first because leaf area is an important trait driving photosynthesis, growth and competitive ability of plants and second, because LAI is a key vegetation parameter in many atmospheric models (Van den Hurk, Viterbo & Los 2003) and is generally thought to play an important role in vegetation-atmosphere feedbacks (Bounoua *et al.* 2000) due to its influence on the radiation balance and

evapotranspiration. The optimal LAI has been defined as the value at which, for a given total canopy N and fixed water availability, whole canopy photosynthesis is maximized (Schieving, Werger & Hirose 1992; Anten *et al.* 1995). The second model version, $CLASS_{ComOpt}$, uses a game theoretical approach assuming that plants compete for light through leaf overlap and that due to this the photosynthetic performance of one plant depends on the characteristics of its neighbours (Riechert & Hammerstein 1983). With this method the evolutionary stable LAI of a vegetation stand can be determined, which is defined as the LAI whereby no individual plant can increase its performance by a unilateral change in its LAI (Riechert & Hammerstein 1983). Thus, this method considers that natural selection favours plants that have a competitive advantage over their neighbours rather than those with optimal trait values for maximum performance.

Both $CLASS_{SimOpt}$ and $CLASS_{ComOpt}$ are validated against seasonal half hourly data from soybean collected in the year 1998 at the Ameriflux tower site located in Bondville, Illinois (see paragraph 5.2.5 and 5.2.6). By doing so, we compare the ability of the two model versions to reproduce the diurnal evolution of the essential components of the soil-vegetation-atmosphere system for soybean over a whole growing season, and we can determine the effects of inclusion of competition on surface and atmospheric processes. Finally, we complete the study by performing a sensitivity analysis on leaf nitrogen availability, soil type and soil water content in order to study the effect of competition on the coupling between surface and atmospheric processes under different environmental conditions, more explanation is provided in paragraph 5.2.7.

5.2.1 The soil-water-atmosphere-plant model (CLASS-model)

Here we briefly describe the CLASS-model, a full description of the CLASS-model can be found in Vilà-Guerau de Arellano *et al.* (2015). To ensure reproducibility, we list all parameter values, the variables mentioned in the main text, and of the initial conditions in Appendix Tables A5.1, A5.2 and A5.3 respectively. The model is a 0-dimension (in space) soil-water-atmosphere-plant system that can be used for studying the evolutions of the daily interactions between the main biophysical variables that control the surface, atmospheric boundary layer (ABL) and the carbon cycle. The main governing equations of the state variables, potential temperature, specific humidity, wind and carbon dioxide are according to the mixed layer theory. This theory assumes that these state variables are well mixed within the convective boundary layer (CBL) due to the intense convective turbulent motions. The interface between the top of the ABL - defined by the boundary layer height, h - and the free troposphere is characterized by a gradient (jump) in the state variables. The evolution of the ABL depends on the boundary layer growth, which is driven by surface fluxes of heat and moisture (buoyancy flux) and the entrainment flux of heat and moisture at the top of the CBL.

The general equation describing the diurnal evolution of an atmospheric state thermodynamic variable (potential temperature, specific humidity or wind) or atmospheric constituents (CO_2) ψ

$$\frac{\partial<\psi>}{\partial t} = \frac{\overline{w'\psi'}_s - \overline{w'\psi'}_e}{h} \quad (5.1)$$

where $\overline{w'\psi'}_s$ is the surface flux (e.g., sensible heat flux, latent heat flux and net ecosystem exchange of CO_2), $\overline{w'\psi'}_e$ the entrainment flux and h the atmospheric boundary layer height, and ψ is parameterized as a function of the entrainment velocity (dh/dt) and the jump of the variable at the inversion. Note that the boundary layer height modifies the dilution capacity of the ABL. Eqn (5.1) thus describes the connection between the surface conditions (represented by surface flux) and the atmospheric entrainment fluxes. The result is a variation in time of the specific variables in the ABL.

5.2.2 The vegetation model, $CLASS_{OPT}$

The vegetation part of the original CLASS-model is replaced by an optimality approach that allows to optimize LAI (Leaf Area Index) to maximize daily total canopy net photosynthesis rate (either at the individual plant or at vegetation level, see below) under the environmental constraints: total canopy leaf N content, incident light, temperature, atmospheric CO_2 and soil- and atmospheric water content. Here we give a brief summary of the vegetation model emphasizing equations that influence the atmospheric part of the model most; a full description of the model can be found in Van Loon *et al.* (2014).

From a whole stand a target plant is defined, whose leaves are within area, *A*. The ratio of the target plant's leaf area to the total leaf area (β) in the area *A* describes the degree to which canopies of plants are mixed, which in turn determines the degree to which plants influence each other's light climate (Fig 5.1).

$$\beta = \mathrm{LAI_i}/\mathrm{LAI_T} \quad (5.2)$$

where LAI_i is the LAI of the target plant and LAI_T the total LAI in area *A*. A β value of 1 means that in the area *A*, there are only leaves of the target plant and there is no mixture with leaves of neighbouring plants; therefore, the target plant is only influenced by its own light climate. This value of β is used for the simple optimization version of the model ($CLASS_{SimOpt}$). While a β value smaller than 1 means that in the area *A*, there is a mixture of leaves of the target plant with leaves of neighbouring plants, and this degree of mixture increases when β becomes smaller, indicating that the shading experienced by the target plant is mostly caused by leaves of neighbouring plants. The leaf area of the target plant and of its neighbours within the area *A* are assumed to be uniformly distributed, horizontally and vertically. Furthermore, all plants are assumed to be identical, in terms of height, LAI etc., but it is only the combined leaf area of the target plant and the neighbouring plants in the area *A* that matters. Thus competition between plants is taken into account in the competitive

optimization version of the model ($CLASS_{ComOpt}$). It is important to stress that β is fixed over the entire growing season, because the level of canopy mixing is the mean of the competitive environment a plant evolved in during natural selection. For example, trees with broad crowns would on average experience less overlap and thus have higher β values than herbaceous plants, and a similar distinction could be made for plants from sparse vs dense vegetation (see Discussion and also Anten & During (2011)). For further elaboration on the β values of the two model versions see paragraph 5.2.4.

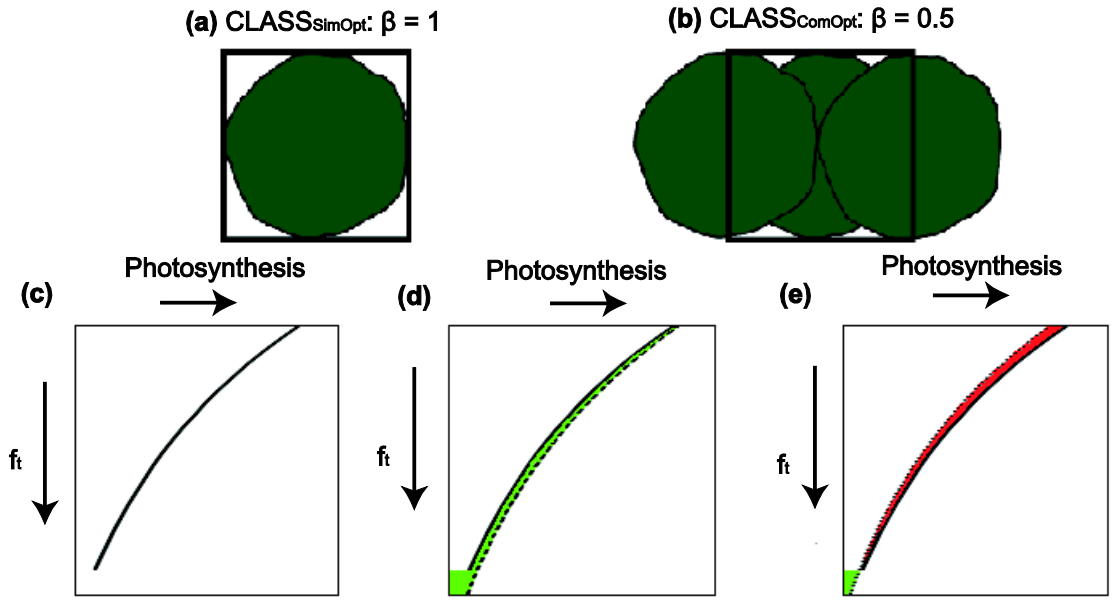

Fig 5.1. A value of β = 1 [Eqn (5.2)], leaves of the target plant in area *A* (black box) are not mixed with leaves of neighbouring plants, is the simple optimization model ($CLASS_{SimOpt}$) (a). β = 0.5, this is the competitive optimization model ($CLASS_{ComOpt}$) (b). In case of the simple optimization model, the target plant has an optimal LAI to maximize its photosynthesis (c). The continuous line shows the maximal photosynthesis of the target plant over the cumulative LAI (f_t). In case of the competitive optimization model, the stable LAI is determined. The target plant unilaterally increases its leaf area beyond the simple optimal LAI, therefore it captures a larger fraction of the available light at the cost of reducing its photosynthetic capacity per unit leaf area, because in the model we assume a constant canopy N content (d). The dashed line shows the photosynthesis of the target plant when only the target plant increases its LAI, the green area indicates the photosynthesis gain due to this increase in leaf area. When this resulted in an increase in the net photosynthesis of the target plant, the LAI of the neighbours was also increased (e). The dotted line shows the photosynthesis of the target plant when its neighbouring plants also increase their LAI, the red area indicates the photosynthesis loss due to this increase in leaf area, note that this red area is larger than the green area indicating that when all plants increase their leaf area photosynthesis is reduced. Panels a and b are redrawn from Van Loon *et al.* (2014)

For calculation of light (i.e., photosynthetically active radiation, PAR) partitioning within the canopy we follow the approach of (Spitters, Toussaint & Goudriaan 1986) that distinguishes between the distribution of direct solar beam and diffuse radiation. The leaf photosynthesis

(Farquhar, Von Caemmerer & Berry 1980) is a function of PAR (Spitters, Toussaint & Goudriaan 1986), nitrogen (Harley *et al.* 1992; Anten *et al.* 1995), temperature (Johnson, Eyring & Williams 1942; Farquhar, Von Caemmerer & Berry 1980), CO_2 and soil- and atmospheric water content Tuzet, Perrier & Leuning (2003). In this model the gross photosynthesis rate of a leaf (P_{gl}) is the minimum of the carboxylation or Rubisco limited photosynthesis rate P_{cl} and the electron transport limited photosynthesis rate P_{jl} (Farquhar, Von Caemmerer & Berry 1980). Net leaf photosynthesis (P_{nl}) is calculated as the gross photosynthesis rate of a leaf per unit ground area (P_{gl}) minus the leaf respiration rate (R_l). Integration of the leaf gross- and net daily photosynthesis rates over the cumulated LAI of the canopy and subsequently multiplying the integrands by β yields the canopy net photosynthesis rate (P_{nT}) and gross photosynthesis rate (P_{gT}) respectively.

We assumed a fixed total amount of leaf N (N_T), and because this is fixed results an increase in leaf area in a reduced leaf N content. As leaf photosynthetic capacity (i.e., the light saturated rate of photosynthesis) is strongly correlated with leaf N content an increase in LAI at fixed canopy N will thus entail a reduction in photosynthetic capacity per unit leaf area (Evans 1989). It is important though to note that roots are not represented in our model, but instead, we simply assume a given total N that plants can allocate to leaves.

We assumed a steady state of inflow of CO_2 into the plant and consumption of CO_2 by the plant. Meaning that the stomatal conductance times the difference in atmospheric and internal CO_2 is equal to the photosynthesis. The stomatal conductance of the canopy is described as (Tuzet, Perrier & Leuning 2003)

$$G_{sT} = G_{s0} + \frac{c \cdot P_{gT}}{(C_i - \Gamma^*)/Pa} \cdot g_\Psi \qquad (5.3)$$

where G_{s0} is the residual stomatal conductance; c is a scaling parameter and g_Ψ is an empirical logistic water stress function to describe the sensitivity of stomata to leaf water potential Ψ_l, C_i the internal CO_2, Γ^* the CO_2 compensation point and Pa the atmospheric pressure (Tuzet, Perrier & Leuning 2003).

Furthermore, we assumed a steady state of plant transpiration and plant water transport through the stem (Sterck & Schieving 2011). Meaning that the whole plant stomatal conductance times the vapour pressure difference between leaf and air is equal to the stem conductance times the difference between soil water potential and leaf water potential. The steady state assumptions of water transport and of CO_2 inflow and consumption were solved with the given parameters and for the given constraints (total canopy leaf N content, soil- and atmospheric water content, incident light, temperature and atmospheric CO_2).

5.2.3 Coupling of the CLASS model with the vegetation model

The ABL is influenced by vegetation in two ways: 1) vegetation determines the surface albedo, which influences how the net radiation available is partitioned between latent and

sensible heating (LE and SH respectively), and 2) vegetation controls the plant transpiration and therefore the moisture flux into the atmosphere. It is important to stress that the ABL hereby evolves over the day changing atmospheric moisture and potential temperature thereby feeding back on the net ecosystem exchange of CO_2 (NEE = - net photosynthesis rate + soil respiration rate), evapotranspiration and SH, and thus influencing the atmospheric processes [Eqn (5.1)]. Additionally, increase in vegetation coverage, reduces the surface albedo (except when the soil is very dark, as we will show), thereby influencing the energy balance, and this could increase the SH and in turn increase the temperature in the ABL. Finally, the photosynthesis is also calculated in a different way compared to the original CLASS model, now it relates to the available nitrogen, and this will thus affect NEE and thereby also atmospheric CO_2.

To study the vegetation-albedo feedback and in order to simulate seasonal changes in surface albedo, we calculated the overall albedo (α) combining the albedo's of pure soil (α_{soil}) and pure canopy (α_{canopy}), the LAI and the extinction coefficient (*k*) (e.g., Oguntunde *et al.* 2007; Zeng & Yoon 2009).

$$\alpha = \alpha_{soil} + \left(\alpha_{canopy} - \alpha_{soil}\right)e^{-k\frac{LAI_i}{\beta}} \quad (5.4)$$

Note that our model explicitly addresses the target plant and its interaction with neighbours, calculated as the ratio between the target plants' LAI (LAI_i) and its fraction presence in the vegetation (β) [Eqn (5.2)].

The soil vegetation coverage (c_{veg}) is a function of the LAI and the extinction coefficient (Sitch *et al.* 2003).

$$c_{veg} = 1 - e^{-k\frac{LAI_i}{\beta}} \quad (5.5)$$

5.2.4 The optimization model versions, $CLASS_{SimOpt}$ and $CLASS_{ComOpt}$

Our goal is to analyse two model versions of vegetation responses: 1) $CLASS_{SimOpt}$: a simple optimization approach that assumes that plant communities respond optimally to atmospheric influences such that net photosynthesis of the whole community is maximized, without including competition between plants; and 2) $CLASS_{ComOpt}$: a competitive optimization approach which assumes that vegetation stands will evolve through natural selection whereby the plant type with the highest plant-level photosynthesis prevails. It is thus assumed that through natural selection vegetation stands are dominated by the best competitors rather than by the ones that have the best inherent performance. Below we briefly describe their implementation.

$CLASS_{SimOpt}$: the optimization procedure determined the optimal LAI that maximized whole stand net photosynthesis (P_{nT}) for the given environmental constraints, and we thus assumed that there is no competition between plants [β = 1 Eqn (5.2), Fig 5.1a]. The

simulated photosynthesis is depending on the penetration of light within the canopy (Fig 5.1c). At the top of the canopy (cumulative LAI, $f_t = 0$) photosynthesis is highest while it decreases with increased cumulative LAI (f_t). In the simulation, leaf area of all plants in the vegetation is increased simultaneously until maximum net photosynthesis was reached which is then the optimal LAI. Such an optimal LAI exists, as light interception increases with LAI but with decreasing marginal returns while at fixed N increasing LAI also entails a reduction in leaf N content and thus in leaf photosynthetic capacity (Anten *et al.* 1995). The underlying assumption of simple optimization is that trait acclimation to atmospheric conditions will be such that whole stand performance is maximized.

$CLASS_{ComOpt}$: with this model the stable LAI of the stand, i.e., the LAI at which no individual can increase its performance with a change of its leaf area, is determined. Thus, plant competition is taken into account to determine the optimal trait values of individuals. In $CLASS_{ComOpt}$, the degree of mixture between target and neighbour plants, β, was set to 0.5 [Eqn (5.2), Fig 5.1b]; this values was chosen, because it has given satisfactory predictions of LAI of herbaceous stands in other studies (Anten 2002; Van Loon *et al.* 2014). After setting β to 0.5 the LAI of the target plant (LAI_i) was unilaterally increased by 5%, while the LAI of the neighbours was kept constant (Fig 5.1d). By this increase in its leaf area, the target plant captures a larger fraction of the available light at the cost of reducing its photosynthetic capacity per unit leaf area. When this resulted in an increased net photosynthesis rate of the target plant, the LAI of the neighbours was also increased by 5%, and as such LAI_T also increased by 5% (Fig 5.1e). This process was repeated until a value of LAI_T was found at which a further change in LAI_i did not increase the net photosynthesis rate of the target plant, which is the stable LAI for the given environmental constraints. This iteration process thus simulates the process of natural selection for evolutionary stable traits. In this calculation a lower β value means that a mutant plant has a relatively greater benefit of unilaterally increasing its leaf area, because it would get a greater fraction of the light that otherwise came available to neighbours; while if $\beta = 1$ the plant only shades itself. Thus, with declining β there is increased selection to produce larger leaf areas. As each day has different environmental constraints (e.g., atmospheric CO_2, N availability and soil water content; see Table A5.3) we determined the stable LAI for each day separately. Additionally, we set the constraint that all leaves must have a daily net photosynthesis above zero (Reich *et al.* 2009), meaning that each of the leaf layers in the model is not allowed to have a negative average daily net photosynthesis rate which sets a limit to leaf area production.

5.2.5 Vegetation and soil conditions

The input values used in defining the total canopy N content are summarized in Appendix Table A5.4 and all other input values can be found in Table A5.1. Below a description is

given of the estimation of the parameters of the albedo function, the total canopy N content and the parameters of the soil respiration.

For the albedo function [Eqn (5.4)] we estimated parameter values of the albedo of pure soil (α_{soil}) and pure canopy (α_{canopy}), from shortwave incoming and outgoing radiation data of soybean of the growing season 2002 of the Ameriflux tower in Bondville. The albedo is the average ratio of outgoing to incoming shortwave radiation during daytime, and if plotted against LAI we can obtain the parameter values.

In our case we find that, the albedo is lower without vegetation cover than with vegetation cover (Fig 5.2); this is because the soil is a very dark silt loam soil that is typically found throughout much of the Midwestern United States.

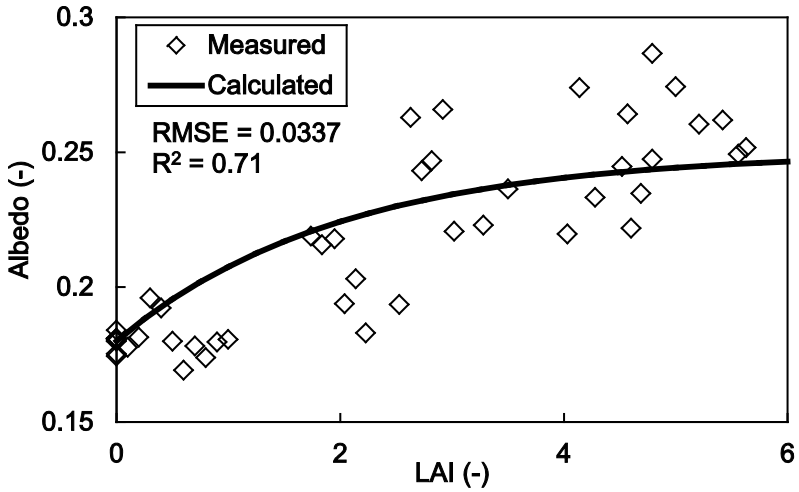

Fig 5.2. Measured LAI of soybean and albedo (average daily outgoing shortwave radiation/incoming shortwave radiation) during the growing season of the year 2002 (diamonds) and calculated LAI-albedo function (continuous line) and the root mean square error (RMSE) and R^2

From the data of the Ameriflux tower site there were no data available on total canopy N content (N_t). In order to estimate this, we interpolated the data of Dermody, Long & DeLucia (2006) (Table A5.4). The N data from Dermody, Long & DeLucia (2006) were used, because soybean was grown in a field close by the Ameriflux tower site; therefore, similar environmental conditions could be expected. From this data the LAI and N_t are known, while for the data of the Ameriflux tower site only the LAI data are available per day of the year. We interpolated the LAI-N_t data of Dermody, Long & DeLucia (2006) to determine N_t values for every LAI value in their data set. Then we used this relationship to determine the N_t values of Ameriflux per day of the year and used these N_t values as input in both $CLASS_{SimOpt}$ and $CLASS_{ComOpt}$ (Table A5.4).

The soil respiration rate (Resp) depends on a water stress function (f_w); whereby the soil respiration rate decreases with increasing soil water content, as it is assumed that in this case diffusive oxygen is limiting. Furthermore, the soil respiration rates depend on temperature according to a Q-10 relationship.

$$\text{Resp} = (1 - f_w)\, R_{10}\, e^{\left(\frac{E_0}{283.15\, R}\right)\left(1-\frac{283.15}{T_{soil}}\right)} \quad (5.6)$$

where R_{10} is the respiration rate at 10°C, E_0 the activation energy, R the universal gas constant and T_{soil} the soil temperature.

The parameter value R_{10} is estimated from data of CO_2 fluxes to the atmosphere (net ecosystem exchange, NEE). This is estimated from days without vegetation present, so CO_2 flux comes only from soil surface and is thereby only influenced by top soil layer temperature and soil moisture.

5.2.6 Data for model comparison

The model results of both $CLASS_{SimOpt}$ and $CLASS_{ComOpt}$ were compared with data of state variables and surface fluxes collected every half hour from soybean in the year 1998 at the Ameriflux tower site located in Bondville, Illinois (40^o latitude, -88^o longitude); in order to study if we get accurate predictions of the diurnal evolution of the main components, namely, LAI, LE, SH, NEE, surface temperature, specific humidity and atmospheric CO_2, of the soil-vegetation-atmosphere system for the soybean plot. These main components have been chosen to be adequate metrics to represent both vegetation responses as well as atmospheric responses. We selected 10 days during the whole growing season for this comparison. All input values per day can be found in Appendix Table A5.1. These 10 days have been chosen based upon the following criteria: cloudless days and with enough data available for use of input of initial and boundary conditions and for comparison with model results. The focus is on cloudless days, because the model assumptions are based on convective turbulent conditions [Eqn (5.1)] (Vilà-Guerau de Arellano *et al.* 2015). To provide some extra insight in the model results, we point out the results of three specific days of those ten days (one day in the beginning, middle and end of the growing season). To analyse how well the model predicts the observed values, we performed a linear regression and calculated the R^2, Root Mean Square Error (RMSE, standard deviation of the data about the regression line) and the average deviation between the observed and predicted values (S%)

$$S\% = \frac{100}{n} \sum_{i=1}^{n} \frac{y_{pr} - y_{obs}}{y_{obs}} \quad (5.7)$$

where n is the number of observations, y_{pr} the predicted value and y_{obs} the observed value.

5.2.7 Sensitivity analysis

For the sensitivity analyses we studied in detail one representative day in the growing season, namely DOY 213, as on this day the canopy was fully grown. We show the most representative outcomes of the model runs: these include the LAI, NEE and the evaporative

fraction (EF). The evaporative fraction is the LE divided by LE plus SH and is to quantify the partitioning of the surface energy balance.

With the coupled vegetation-atmosphere model we investigated the inclusion of plant competition on total canopy N content, because it is an important factor in regulating the total canopy photosynthesis rate and LAI and thus can have a large impact on the energy fluxes. Additionally, N input is also an anthropogenic forcing, with large spatial and temporal differences around the globe.

We also performed a sensitivity analysis on other soil types than silt loam, which was found on the location we had chosen, namely, sand and clay. We chose to do this sensitivity analysis, because the soil albedo for the silt loam soil is lower (albedo = 0.18) than the albedo of full canopy closure (albedo = 0.25, see Material and Methods: Vegetation and soil conditions), which is rather unusual as most soils have a higher albedo than the vegetation and this might therefore have large influences on the energy fluxes. The input values for the different soil types are shown in Table A5.5.

Next to this we also performed for each soil type a sensitivity analysis on the effect of changes in soil moisture index of the top and deeper soil layers. The soil moisture index is the water content of the soil (top or deeper soil layer) minus the water content at wilting point divided by the water content of at field capacity minus the water content at wilting point (soil moisture index, SMI $= \frac{w_2 - w_{wilt}}{w_{fc} - w_{wilt}}$). It reflects the ability of the soil to supply moisture to plants, a value of 0 means that there is no supply of water to plants while a value of 1 means that there is ample water available. This is simulated, because the water content of the soil in combination with the texture of the soil might also affect the energy fluxes. Additionally, the original experiment had relatively wet soils; therefore, it is also interesting to analyse how the effect of inclusion of competition will be on dryer soils.

5.3 Results and Discussion

5.3.1 Model validation with observations

Figs 5.3 and 5.4 show soybean data, from the Ameriflux Bondville tower, during the growing season of 1998 in comparison with predictions of the competitive optimization model ($CLASS_{ComOpt}$) and the simple optimization model ($CLASS_{SimOpt}$) for 10 selected days (see also Fig A5.1). This is shown to validate model outcomes and to investigate the influence of competition on the coupling between the vegetation and the atmosphere diurnal scales during a whole season. Fig 5.5 is a conceptual figure showing the effect of accounting for plant competition on modelled surface variables, by comparing the results obtained from the $CLASS_{SimOpt}$ with $CLASS_{ComOpt}$.

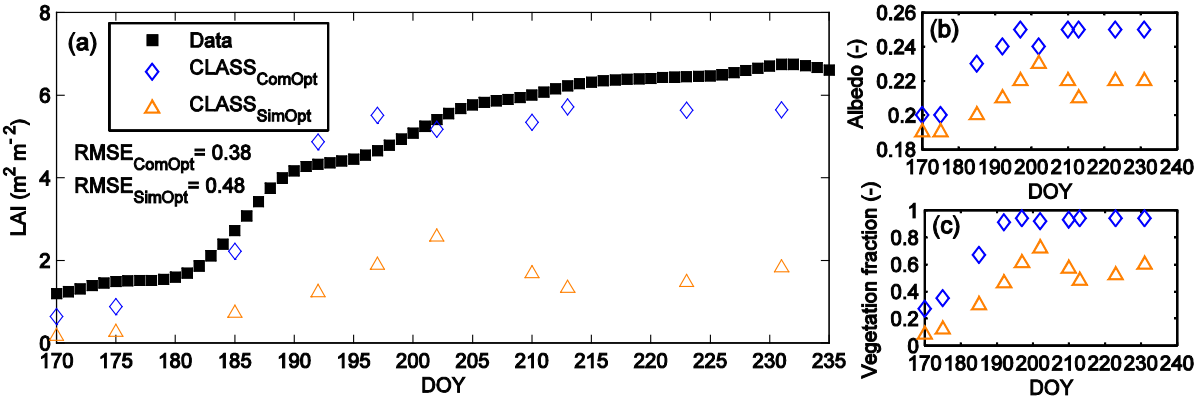

Fig 5.3. Soybean data on LAI from the Ameriflux Bondville tower site for the whole growing season (filled black squares) compared with the modelled LAI values of the competitive optimization model ($CLASS_{ComOpt}$, blue diamonds) and of the simple optimization model ($CLASS_{SimOpt}$, orange triangles) for the 10 selected days (a), and for these 10 days also the predicted albedo (b) and vegetation fraction (c)

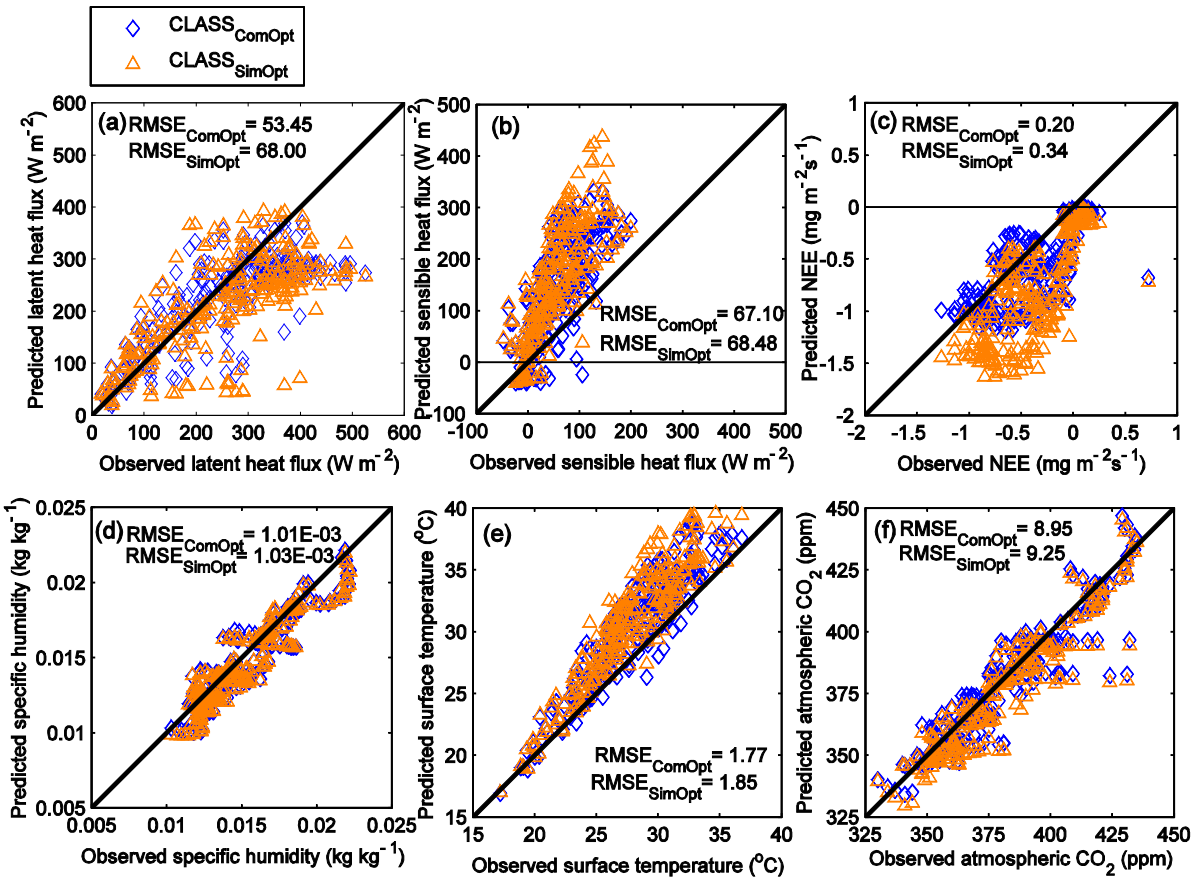

Fig 5.4. For the whole soybean growing season the half hourly predicted latent heat flux (a), sensible heat flux (b), net ecosystem exchange (NEE) (c), specific humidity air (d), surface temperature (e) and atmospheric CO_2 (f) for the competitive optimization model ($CLASS_{ComOpt}$) and the simple optimization model ($CLASS_{SimOpt}$) versus the observed values from Ameriflux 1998 Bondville for DOY 170, 175, 185, 192, 197, 202, 210, 213, 223 and 231 and the Root Mean Square Error of both the competitive optimization model and the simple optimization model ($RMSE_{ComOpt}$ and $RMSE_{SimOpt}$ respectively). All the results of the linear regression can be found in Table 5.1 and all the results over the days can be found in Fig A5.1

The inclusion of competition between plants in a coupled vegetation-atmosphere model resulted in a better agreement of the calculations of LAI (Leaf Area Index, i.e., the leaf area per unit soil area) with the data. $CLASS_{SimOpt}$ strongly underestimated the LAI observations for the whole growing season (Fig 5.3a). After DOY 202 the LAI simulated by $CLASS_{SimOpt}$ declined, the reason is a decrease in light intensity after this day. In contrast, $CLASS_{ComOpt}$ predictions are much more in line with the data observations (Fig 5.3a). The LAI increases during the beginning of the growing season and stabilizes after DOY 195 closely following the observed pattern (Fig 5.3a). The LAI values are 1.5, 3.6 and 4.4 m^2 m^{-2} higher for $CLASS_{ComOpt}$ compared to $CLASS_{SimOpt}$ on DOY 185, 197 and 213, respectively. Simulated albedo and vegetation fraction do also show clear differences between $CLASS_{ComOpt}$ and $CLASS_{SimOpt}$ (Fig 5.3b,c, respectively). Data on albedo and on vegetation fraction was not available.

The higher LAI for $CLASS_{ComOpt}$ compared to $CLASS_{SimOpt}$ can be explained according to game theoretical principles. Because plants compete for light, a unilateral increase in LAI of a given plant above the optimal LAI results in a relatively smaller increase in self-shading for that plant while it is able to capture a larger fraction of the available light. As a result, this plant can increase its carbon gain by increasing its LAI (Fig 5.1d) even if this reduces photosynthesis of the stand as a whole (Anten 2002)(Fig 5.1e). In the model the canopy N content remains constant, and production of extra leaf area to shade competitors therefore results in reduction of the leaf photosynthetic capacity. Consequently, $CLASS_{ComOpt}$ predicts a lower total canopy net photosynthesis rate than $CLASS_{SimOpt}$ while having a larger LAI. This suggests that natural selection under competition results in evolutionary stable communities that have a higher LAI than needed for maximization of whole stand photosynthesis (see also Anten 2002; Lloyd *et al.* 2010).

Here we show that inclusion of game theory to account for competition between plants not only improves simulations at the canopy level but also at the ecosystem level; as the modelled net ecosystem exchange rates of CO_2 (NEE = - net photosynthesis rate + soil respiration rate) by $CLASS_{ComOpt}$ are in clear agreement with the observations, while the NEE values from $CLASS_{SimOpt}$ are not (Fig 5.4c; Table 5.1). The NEE becomes 35%, 34% and 28% less negative for DOY 185, 197 and 213, respectively, with inclusion of competition between plants (negative entailing CO_2 being taken from the atmosphere). A less negative NEE is caused by a lower photosynthesis rate (Fig 5.5, arrow 2), as soil respiration only has a marginal influence. The soil respiration rate is only slightly reduced (Fig 5.5, arrow 14), which is due to lower soil temperature resulting from the higher albedo (Fig 5.5, arrow 10). In summary, including competition in a coupled vegetation-atmosphere model increases the LAI while it reduces whole stand photosynthesis, thus resulting in a less negative NEE.

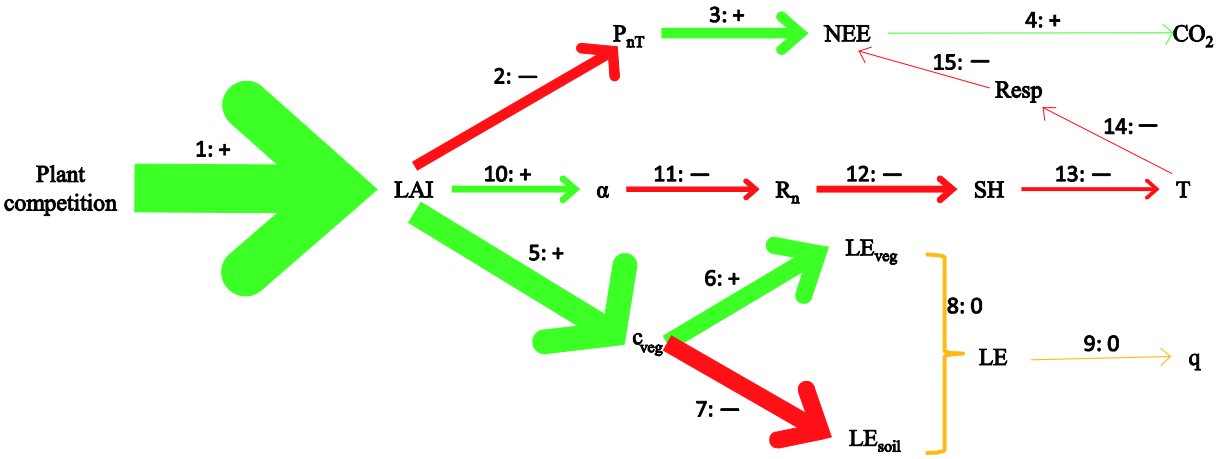

Fig 5.5. Conceptual diagram connecting the effect of accounting for plant competition on modelled surface variables. This effect can either be positive (green arrow with plus sign), negative (red arrow with minus sign), or no effect (yellow arrow with zero sign). The size of the arrow gives an indication about the size of the effect. Inclusion of plant competition results in a higher leaf area index, LAI (1), and a lower photosynthesis rate, P_{nT} (2). The lower photosynthesis rate increases the net ecosystem exchange of CO_2, NEE (indicates the removal of CO_2 from the atmosphere and it is a negative value, with a lower photosynthesis it becomes less negative) (3) and as a result the atmospheric CO_2 increases (4). The higher LAI also increases the fraction of vegetation, c_{veg} (5); resulting in a higher latent heat flux of the vegetation, LE_{veg} (6) while the soil heat flux, LE_{soil}, is reduced (7). These counterbalance each other and thereby the total latent heat flux, LE, is almost not changed (8) leading to also almost no change in specific humidity of the air, q (9). An increase in LAI also increases the albedo, α (10); and thereby reducing the total net radiation, R_n (11), sensible heat flux, SH (12) and temperature, T (13). The lower temperature reduces the soil respiration rate, Resp (14), but it only slightly reduces the NEE (15)

Although $CLASS_{ComOpt}$ predicted a higher LAI than $CLASS_{SimOpt}$, it resulted in an almost similar latent heat flux (LE) (Fig 5.4a; Fig 5.5, arrow 8), though RMSE and S% (average deviation between estimated values and observed values) of $CLASS_{ComOpt}$ are slightly lower than of $CLASS_{SimOpt}$ (Table 5.1). This is predicted, because of a high LAI, and thus, a high leaf coverage (the fraction of soil covered by vegetation is during most of the growing season above 0.9 for $CLASS_{ComOpt}$, see Figs 5.3c and 5.5, arrow 5) results in a high LE of the vegetation (Fig 5.5, arrow 6) but reduces soil LE (Fig 5.5, arrow 7), while it is the other way around for a low LAI. As a result, both the simple and the competitive optimization models estimate LE reasonably well compared to the observations (Fig 5.4a, Table 5.1). Thus, especially during the beginning of the growing season, when there is no full canopy closure, the LE is fully determined by the soil LE and at the end of the growing season by the LE of the vegetation (Figs 5.3c, A5.2). However, at the end of the growing season both model versions underestimate the maximum daily LE values obtained during noon (Fig A5.1b). On DOY 185, 197 and 213, the observed daily maximum LE values were 384, 410 and 525 W m^{-2}, respectively. Model predictions of daily maximum LE values for these days were 336, 294 and 275 W m^{-2} for $CLASS_{ComOpt}$ and 369, 271 and 297 W m^{-2} for $CLASS_{SimOpt}$, respectively. To conclude, while the LAI was thought to have a large impact on the water cycle (Eltahir &

Bras 1996), here we show that on the particular soil type in our experiment changes in LAI have almost no effect on the total LE and thereby also not on the atmospheric moisture content; in contrast, the soil LE has a large impact on the total LE.

Table 5.1 Results of the linear regression (slope, intercept, RMSE, R^2) with the competitive optimization model ($CLASS_{ComOpt}$) and the simple optimization model ($CLASS_{SimOpt}$) as a dependent variable and the observed values of Ameriflux 1998 Bondville for several days over the growing season (DOY 170, 175, 185, 192, 197, 202, 210, 213, 223 and 231) during daytime as the independent variables, and the average deviation between estimated values and observed values (S%).

	Model	Slope (S.E.)	Intercept (S.E.)	RMSE	R^2	S%
Atmospheric CO_2 (ppm)	**$CLASS_{ComOpt}$**	**0.923 (0.023)**	**26.720 (8.972)**	**8.95**	**0.87**	**1.7**
	$CLASS_{SimOpt}$	0.935 (0.024)	19.667 (9.267)	9.25	0.86	4.5
Ground heat flux (W m^{-2})	**$CLASS_{ComOpt}$**	**0.467 (0.029)**	**21.181 (1.297)**	**14.39**	**0.52**	**158.8**
	$CLASS_{SimOpt}$	0.484 (0.030)	23.682 (1.346)	14.93	0.52	171.1
LAI (-)	**$CLASS_{ComOpt}$**	**0.961 (0.103)**	**-0.182 (0.507)**	**0.64**	**0.92**	**18.9**
	$CLASS_{SimOpt}$	0.296 (0.076)	-0.027 (0.374)	0.47	0.65	72.8
Latent heat flux (W m^{-2})	**$CLASS_{ComOpt}$**	**0.575 (0.028)**	**76.444 (7.753)**	**52.92**	**0.64**	**27.4**
	$CLASS_{SimOpt}$	0.545 (0.036)	73.120 (10.022)	68.40	0.49	32.0
Net ecosystem CO_2 exchange (mg m^{-2} s^{-1})	**$CLASS_{ComOpt}$**	**0.724 (0.045)**	**-0.296 (0.024)**	**0.25**	**0.52**	**225.4**
	$CLASS_{SimOpt}$	0.986 (0.059)	-0.427 (0.032)	0.33	0.54	326.6
Net radiation (W m^{-2})	**$CLASS_{ComOpt}$**	**1.010 (0.015)**	**27.501 (6.194)**	**42.60**	**0.95**	**16.1**
	$CLASS_{SimOpt}$	1.038 (0.017)	29.566 (6.731)	46.29	0.94	19.4
Sensible heat flux (W m^{-2})	**$CLASS_{ComOpt}$**	**1.447 (0.082)**	**56.170 (6.272)**	**65.93**	**0.56**	**339.9**
	$CLASS_{SimOpt}$	1.604 (0.086)	67.235 (6.569)	69.05	0.59	375.9
Specific humidity (kg kg^{-1})	**$CLASS_{ComOpt}$**	**0.906 (0.023)**	**0.001 (0.000)**	**1.01E-03**	**0.87**	**6.0**
	$CLASS_{SimOpt}$	0.907 (0.023)	0.001 (0.000)	1.03E-03	0.87	6.2
Temperature air (°C)	**$CLASS_{ComOpt}$**	**1.066 (0.034)**	**-1.250 (0.910)**	**1.75**	**0.80**	**5.0**
	$CLASS_{SimOpt}$	1.085 (0.035)	-1.591 (0.934)	1.80	0.80	5.3
Temperature surface (°C)	**$CLASS_{ComOpt}$**	**1.102 (0.029)**	**-0.492 (0.824)**	**1.77**	**0.85**	**8.8**
	$CLASS_{SimOpt}$	1.165 (0.031)	-1.630 (0.860)	1.85	0.86	10.6

During the beginning of the season very high values of sensible heat flux (SH) were found (Fig A5.1c), as during this period there was little canopy coverage indicating that most of the SH was emitted by the soil (Bernacchi *et al.* 2007). Sensible heat fluxes were overestimated by both model versions with a factor of around 1.5 (Fig 5.4b). There could be several reasons for this. First, it could be that the representation of the surface energy balance in our model does not include all processes involved, such as heat storage within the canopy and horizontal advection of heat (Wilson *et al.* 2002). Second, the model underestimates the LE during the end of the growing season with around 5% (Fig A5.1b) leading to more energy available for SH and for the ground heat flux. The discrepancy between modelled and measured values could, however, also be related to uncertainty in observations as inaccuracies of 10-30% in

measurements are common (e.g., Wilson *et al.* 2002; Brotzge & Crawford 2003). This is further corroborated by the unbalance in the surface energy budget, as there is a gap in energy balance of the data between the net observed radiation and the sum of the surface heat fluxes (latent, sensible and ground heat flux); we found that the observed radiation is on average 25 W m^{-2} higher (16 W m^{-2} - 30 W m^{-2}, 95% confidence interval) compared to the observed sum of the surface heat fluxes (Fig A5.3). However, these measurement inaccuracies could at best explain about 60% of the difference between the model and observations.

Finally, both model versions ($CLASS_{ComOpt}$ and $CLASS_{SimOpt}$) calculate surface temperature, specific humidity and atmospheric CO_2 reasonably well (Table 5.1, Fig 5.4d-f), where RMSE and S% of $CLASS_{ComOpt}$ are always slightly better compared to $CLASS_{SimOpt}$ (Table 5.1). To conclude, for this location it was shown that inclusion of competition between plants ($CLASS_{ComOpt}$) greatly improves predictions of a number of key characteristics in the vegetation atmosphere system, especially LAI and NEE (Figs 5.3 and 5.4, Table 5.1). However, it is important to note that the value given to the degree to which plants are mixed and thus influence each other's light climate [β value, Eqn (5.2)] has a strong influence on predicted vegetation responses (Van Loon *et al.* 2014). Here we chose a β value of 0.5 as it was shown that it was a good value for the prediction of vegetation processes for soybean (Van Loon *et al.* 2014) as well as other herbaceous stands (Anten 2002). But the degree of interaction between plants strongly depends on the type of plant. Trees for example have relatively broader canopies and thus higher β than herbaceous plants (Anten & During 2011). This could entail that the coupling between vegetation and the atmosphere would be less affected by plant competition for forests than for herbaceous stands. More research is needed to assess how competition may affect vegetation-atmosphere coupling in different vegetation types.

5.3.2 Sensitivity analysis: total canopy N content

Here we show that the canopy N content (N_t) has a large impact on the LAI (Fig 5.6a), which is consistent with general findings (e.g., Reich 2012; Dewar *et al.* 2012). As LAI affects the surface albedo [Eqn (5.4)] and the canopy stomatal conductance (via affecting the photosynthesis rate, Eqn (5.3)] and thus the available radiative energy and the partitioning between the latent and the sensible heat flux, N_t indirectly influences the evaporative fraction (EF = LE / (LE + SH)) (Fig 5.6b). Canopy N content also had a large effect on the NEE (Fig 5.6c) due to its positive effect on photosynthesis and stomatal conductance; i.e., more nitrogen entails higher photosynthetic enzyme contents and associated photosynthetic activity in the canopy (Ollinger *et al.* 2008).

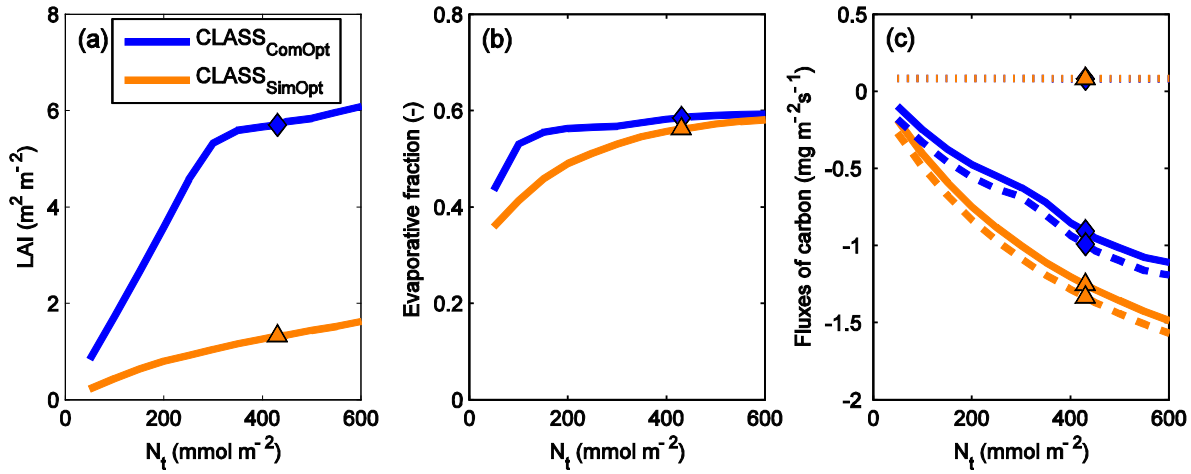

Fig 5.6. The LAI (a), evaporative fraction (LE / (SH + LE)) (b), and the fluxes of carbon represented by the contribution of CO_2 assimilation by photosynthesis (dashed lines), soil respiration (dotted lines) and net ecosystem exchange (continuous lines) (c) for different total canopy leaf N contents (N_t) for DOY 213 of the competitive optimization model (blue line; $CLASS_{ComOpt}$) and of the simple optimization model (orange line; $CLASS_{SimOpt}$). The blue diamond and the orange triangle in the panels indicate respectively for $CLASS_{ComOpt}$ and for $CLASS_{SimOpt}$ the original result corresponding to DOY 213

The effects of including plant competition on vegetation and atmospheric variables also depended strongly on N_t. The difference in LAI simulated by $CLASS_{ComOpt}$ and $CLASS_{SimOpt}$ increases with N_t (Fig 5.6a), because with more N availability, light becomes more limiting and there is a greater selective advantage of large leaf areas if light competition is considered (Fig 5.6a). This trend is consistent with the general consensus that light competition is weaker in habitats limited by nutrients as it limits growth (Grime 1973).

We also found that the net canopy photosynthesis (not shown) is increased by more N availability and that this increase is larger for $CLASS_{SimOpt}$ than for $CLASS_{ComOpt}$. This reflects the competitive effect where selective advantage of overinvesting in leaf area to compete with neighbours increases with N_t. Furthermore, an increase in N_t leads also to a decrease in soil respiration. This is because on our soil type LAI increases entail increases in surface albedo and thus a slightly lower soil temperature. We do note, however, that this simulation does not consider potential direct effects of N availability in the soil on microbial activity and thus soil respiration. $CLASS_{ComOpt}$ simulated a higher LAI than $CLASS_{SimOpt}$, resulting therefore in a lower soil respiration for $CLASS_{ComOpt}$. As a result of the increased net photosynthesis and decreased soil respiration when N_t increases, the NEE will become lower (Fig 5.6c), i.e., more CO_2 is extracted from the atmosphere. The photosynthesis increases more for $CLASS_{SimOpt}$ compared to $CLASS_{ComOpt}$ while having similar soil respiration rates, resulting in a more negative NEE for $CLASS_{SimOpt}$ (Fig 5.6c).

$CLASS_{ComOpt}$ simulated a higher EF than $CLASS_{SimOpt}$ at low N_t, but the values converged as N_t increased (Fig 5.6b). The higher LAI of $CLASS_{ComOpt}$ resulted in a larger surface albedo and thereby a lower SH and thus a higher EF at low N_t. With higher values of

N_t the predicted EF of $CLASS_{ComOpt}$ and $CLASS_{SimOpt}$ converge, because of similar SH and LE values. The converging SH values between the two model versions are explained by the fact that the albedo is a saturating function of LAI [Eqn (5.4)], and thus, at high N_t and associated LAI values, differences in LAI predicted by the two model versions do not impact the albedo very much. LE values are similar, because although $CLASS_{SimOpt}$ has a lower vegetation coverage and therefore a lower LE of the vegetation, this is compensated by the higher LE of the soil (Fig 5.6b). Thus, the inclusion of plant competition has a larger impact on the predicted LAI and NEE when N availability is high, while it has the largest impact on the EF for medium values of N. These interactive effects of competition and N availability on model outcomes are important as an increase in N deposition rates is forecasted (Galloway *et al.* 2004; IPCC 2014).

5.3.3 Sensitivity analysis: soil moisture index and soil types

Here we show that the effect of inclusion of plant competition on model outcomes strongly depends on the soil water content of both the top and the deeper soil layer. We conducted a sensitivity analysis on the soil moisture index of both the deeper and top soil layer (SMI; 0 means water level is at wilting point thus (almost) no water available, 1 means water level is at field capacity thus ample water available) and on the soil type. The original soil type is silt loam with a relatively high soil moisture content of both the top and deeper soil layer (SMI close to 1). Note that the water content of the deeper soil layer is constant over the day and that it determines plant water uptake and the drainage from top to the deeper soil layer. The effect of the SMI of the deeper soil layer is pointed out in Eqn (5.3), the stomatal conductance function, via a logistic water stress function. The water content of the top soil layer (first 2 cm) influences the soil evaporation.

Soil moisture index

The general pattern of the effects of increasing the SMI on the LAI, EF and NEE was similar across the three soil types (Fig 5.7). First, we will explain these general patterns and followed by a discussion of the sensitivity on the differences between the soil types. Very low values of SMI of the deeper soil layer strongly limit plant water uptake and thus stomatal conductance and thereby photosynthesis is strongly reduced, and NEE even becomes positive (Fig 5.7g,h,i). Therefore, the LAI is, for both $CLASS_{ComOpt}$ and $CLASS_{SimOpt}$, decreased (Fig 5.7a,b,c), and transpiration rate is also strongly reduced. When the SMI of the deeper soil layer is increased, both models predict an increase in LAI (Fig 5.7a,b,c). But this increase is stronger for $CLASS_{ComOpt}$ than for $CLASS_{SimOpt}$, because as water availability increases, plants can increase their LAI and thus competition for light also increases. This is in agreement with the general notion that light competition is less important in habitats with soil water deficit, because plant growth is then limited by water stress rather than by light (Grime

1977). This larger LAI for $CLASS_{ComOpt}$ than the optimal LAI simulated with $CLASS_{SimOpt}$ results in a lower photosynthesis, leading to less negative values of NEE (Fig 5.7g,h,i). The higher LAI for $CLASS_{ComOpt}$ also results in a higher vegetation fraction, and thus in a higher EF (Fig 5.7d,e,f).

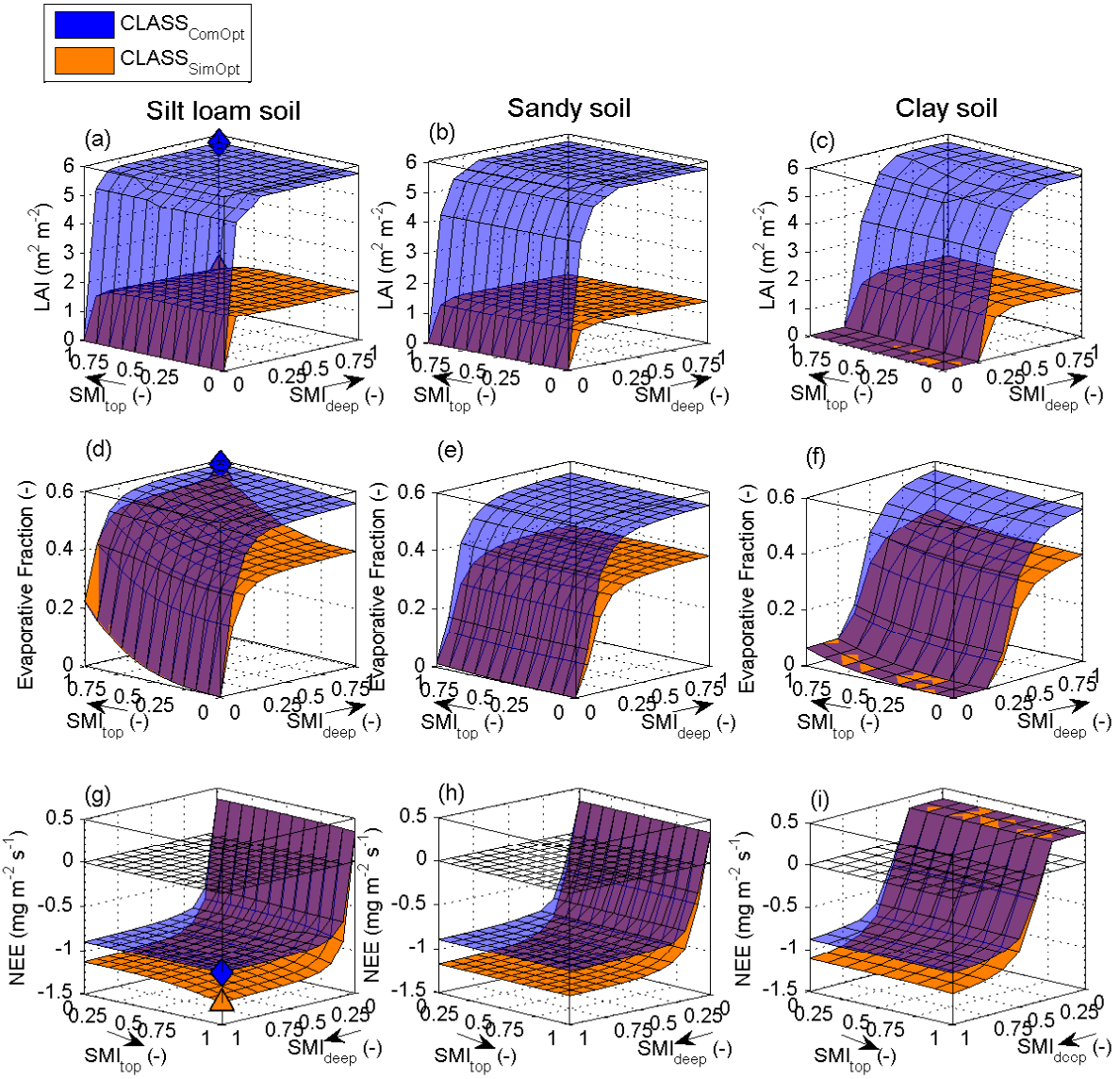

Fig 5.7. On a silt loam (left panels: a,d,g), sandy (middle panels: b,e,h) and on clay soil (right panels: c,f,i) the LAI (a-c), evaporative fraction (LE/(SH+LE)) (d-f) and the net ecosystem exchange (NEE) (g-i) for different soil moisture index (SMI) of the top soil layer (wc_{top}) and of the deeper soil layer (wc_{deep}) for DOY 213 of the simple optimization model ($CLASS_{SimOpt}$, orange surface) and the competitive optimization model ($CLASS_{ComOpt}$, blue surface). The blue diamond and the orange triangle on the panels for silt loam soil (a, d, g) indicates respectively for the competitive optimization model and for the simple optimization model the original result of DOY 213, note that for the evaporative fraction these points are very close (d)

Difference between the soil types

On a silt loam soil at low SMI of the deeper soil layer, both $CLASS_{SimOpt}$ and $CLASS_{ComOpt}$ predict a decrease in EF when the SMI of the top soil layer was reduced (Fig 5.7d). Due to the low LAI (Fig 5.7a) and thus the low vegetation coverage, the total LE is almost completely determined by the LE of the soil. A reduction in SMI of the top soil layer leads thus to a reduction of the soil LE and thereby also in total LE and EF (Fig 5.7d). This results in a reduction of the specific humidity of the air and thus an increase in the vapour pressure difference between leaf and air (D_s). This increased D_s caused a reduction in the leaf water potential, as a high D_s corresponds in general to plant water stress (Drewry *et al.* 2010) and thereby also a reduction of the stomatal conductance, which is in line with literature (e.g., Oren *et al.* 1999; Dekker, Bouten & Bosveld 2001). For plants, a high D_s in general corresponds to plant water stress, because stomatal closure usually occurs when atmospheric demands for water vapour increases due to rapid depletion of soil water content around the roots when atmospheric demand is high and thereby the soil is not able to supply the water (Denmead & Shaw 1962). In our model results, this reduced stomatal conductance under low SMI of the top soil layer resulted in a decrease in photosynthesis. Additionally, the soil respiration rate also increased because of the lower SMI (diffusive oxygen is not limiting) and thus resulting in a less negative NEE (Fig 5.7g), though we do note that we did not consider potential negative effects of soil drying on microbial activity and respiration which could somewhat mitigate the reduction in NEE.

On a sandy soil, the increase in EF with SMI of the top soil layer was much smaller compared to the other two soil types (Fig 5.7d,e,f). This is because on sandy soils, increasing the SMI of the top soil layer leads only to minor increase in soil LE, as the water content of the top soil layer is still quite low compared to other soil types. Although the albedo of a sandy soil is higher compared to a silt loam and clay soil and therefore a lower SH was found, the EF was still lower due to the low total LE resulting from the low soil LE (Fig 5.7e).

On the clay soil there was a much stronger effect of reducing the SMI on LAI, EF and NEE compared to the other soil types. This is because at low SMI the matric potential of a clay soil drops more rapidly compared to a sandy and silt loam soil [Fig A5.4, Eqn (A5.1), Table A5.5; Tuzet, Perrier & Leuning (2003)]. The ensuing greater water retention of clay soils entails that a reduction in SMI causes a stronger reduction in water availability to the plant and thus a greater stomatal closure (Tuzet, Perrier & Leuning 2003). Therefore LAI and EF increase less rapidly and NEE decreases less rapidly with an increase in SMI of the deeper soil layer (Fig 5.7c,f,i).

To summarize, independent of the type of soil the largest effect of including competition between plants on the EF and the NEE can be obtained on well-watered soils, top and deeper soil layer, and this also holds for changes in atmospheric state variables. However, there are

still some interesting and significant differences in atmospheric state variables between the soil types. The difference in LAI between $CLASS_{SimOpt}$ and $CLASS_{ComOpt}$ on a well-watered silt loam and clay soils caused on both soil types an increase in albedo of 12% and thereby led to a decrease in air temperature of 0.7°C. In comparison, Bounoua *et al.* (2000) showed with a coupled vegetation-atmosphere model that 3% increase in albedo, when the LAI increased, reduces the annual air temperature with 0.8°C. In contrast on a well-watered sandy soil increase up to 0.2°C. Here we also show that the effects of including competition for well-watered conditions were fairly similar across soil types, i.e. atmospheric CO_2 increased with 3, 2 and 2 ppm and specific humidity increased with $3.5E^{-4}$, $3.5E^{-4}$, and $3.9E^{-4}$ kg kg^{-1}, respectively, for silt loam, clay and sandy soil. Thus, independent of the type of soil, inclusion of plant competition led to an increase of the atmospheric CO_2.

Though it is important to note that the degree to which plants are mixed, the parameter β, was held constant during both the sensitivity analysis on the total canopy N content as well as on the soil water content. However, under natural conditions high water or N availability likely allows for denser stands and thus lower β values (β = 1 indicates that leaves of plants are not overlapping, and decreasing values of β indicates that the degree of overlap increases). Selection for competitive traits in such habitats may thus be stronger than what we assumed suggesting that the increased competition effect could also be larger than what we predicted.

5.4 Conclusions and Outlook

Here we show that the inclusion of plant competition for light through canopy overlap in a coupled vegetation-atmosphere model led to an improvement of the daily predictions of both a number of atmospheric state variables and vegetation responses throughout the whole growing season. Remarkably, including competition, thus considering that natural selection favoured plants with the highest competitive ability, results in an increase in LAI while this causes a reduction in whole stand photosynthesis (i.e., due to the assumed fixed total canopy N results an increase in leaf area in a reduced photosynthetic capacity), a less negative NEE and increased atmospheric CO_2 (+3 ppm). In addition, the increased LAI also caused a higher albedo for this site resulting in a slightly lower air temperature (-0.8°C). Our findings also indicate that the impact of competition on the coupling between vegetation and the atmosphere is sensitive to the available nitrogen content and the soil water content and to a lesser extent to the soil type. Regardless of the type of soil, we show that the largest effects of including plant competition on both vegetation as well as atmospheric processes can be obtained on well-watered soils with ample nitrogen available.

Our results thus indicate that plant competition may strongly influence vegetation and atmospheric processes, and we therefore strongly recommend including it in more coupled vegetation-atmosphere models. However, it should be emphasized that we performed a simple and elementary comparison meant solely to understand the impact of plant competition on the

coupling between vegetation and the atmosphere, by using a relatively simple parameter to describe plant competition. Several aspects could be considered in future studies. First as already noted, other plant types have a different degree of interaction, and therefore, the influence on the coupling between the vegetation and atmosphere could be altered. Second, our model does not consider root competition, while recent studies (e.g., Farrior *et al.* 2013; Farrior *et al.* 2015) showed that water limited conditions may result in overinvestment in fine roots drawing resources away from leaf area production.

5.5 Acknowledgements

All of the meteorological and flux data used in this study are freely available at http://cdiac.ornl.gov/ftp/ameriflux/data/Level1/Sites_ByName/Bondville/.
This work was financially supported by a Focus & Mass grant from Utrecht University awarded to N.P.R.A., M.R. and S.C.D..

Appendix

To ensure reproducibility of our model simulations, we list all parameter values, the variables mentioned in the main text, and the initial conditions in Tables A5.1 to A5.5. Fig A5.1 shows the model outcomes and observed values of both vegetation and atmospheric responses throughout the whole growing season. Fig A5.2 shows the model outcomes of soil and vegetation latent heat flux throughout the whole growing season. Fig A5.3 shows the imbalance of the surface energy budget of the data. Fig A5.4 shows the effect of changes in soil moisture index of the deeper soil layer on the water potential of the soil, this relationship is according to Eqn (A5.1) and input values of Table A5.5 are used.

Equation A5.1

The base water potential (Ψ_b) as a function of the water content of the deeper soil layer (W_2)

$$\psi_b = wp_{air}\left(\frac{w_{sat}}{w_2}\right)^b \qquad (A5.1)$$

where wp_{air} is the air entry water potential of the soil; W_{sat} the saturated volumetric water content; and b the Clapp and Hornberger retention curve parameter b

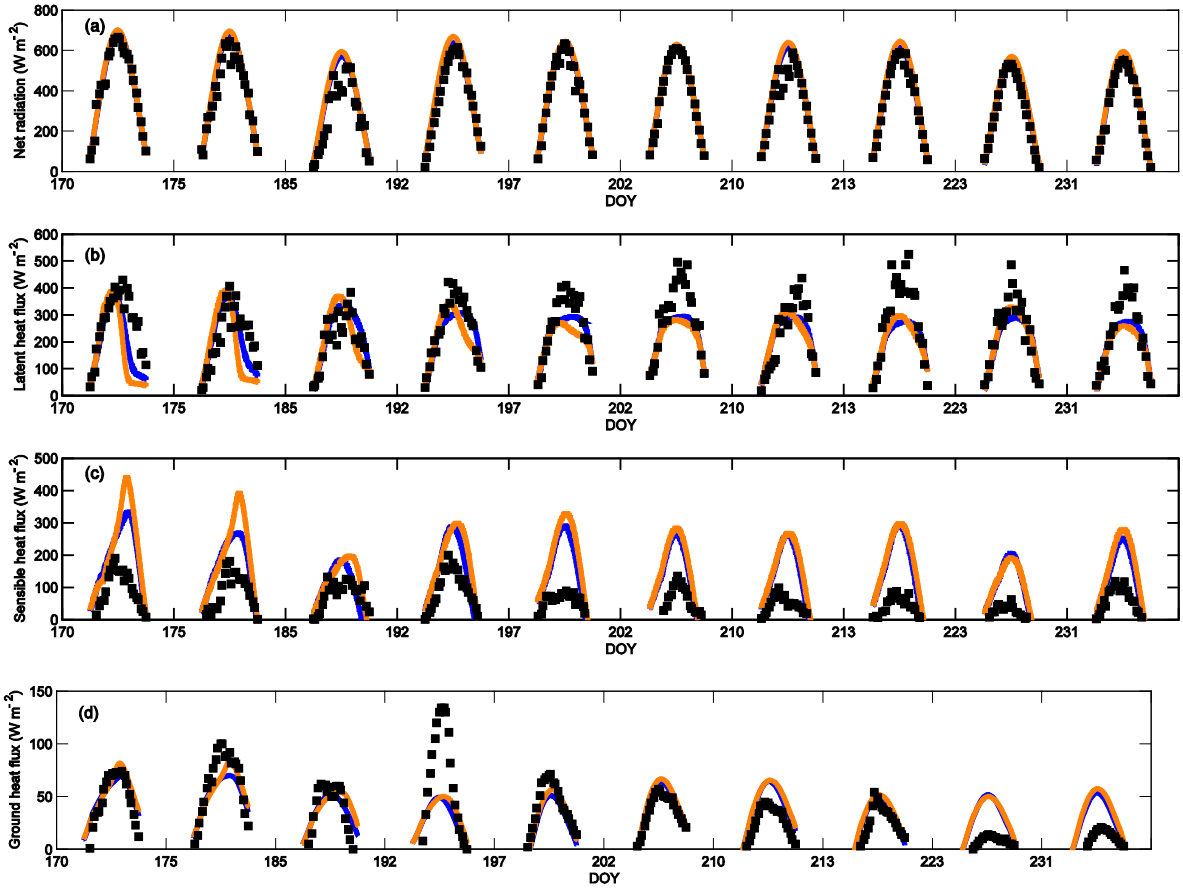

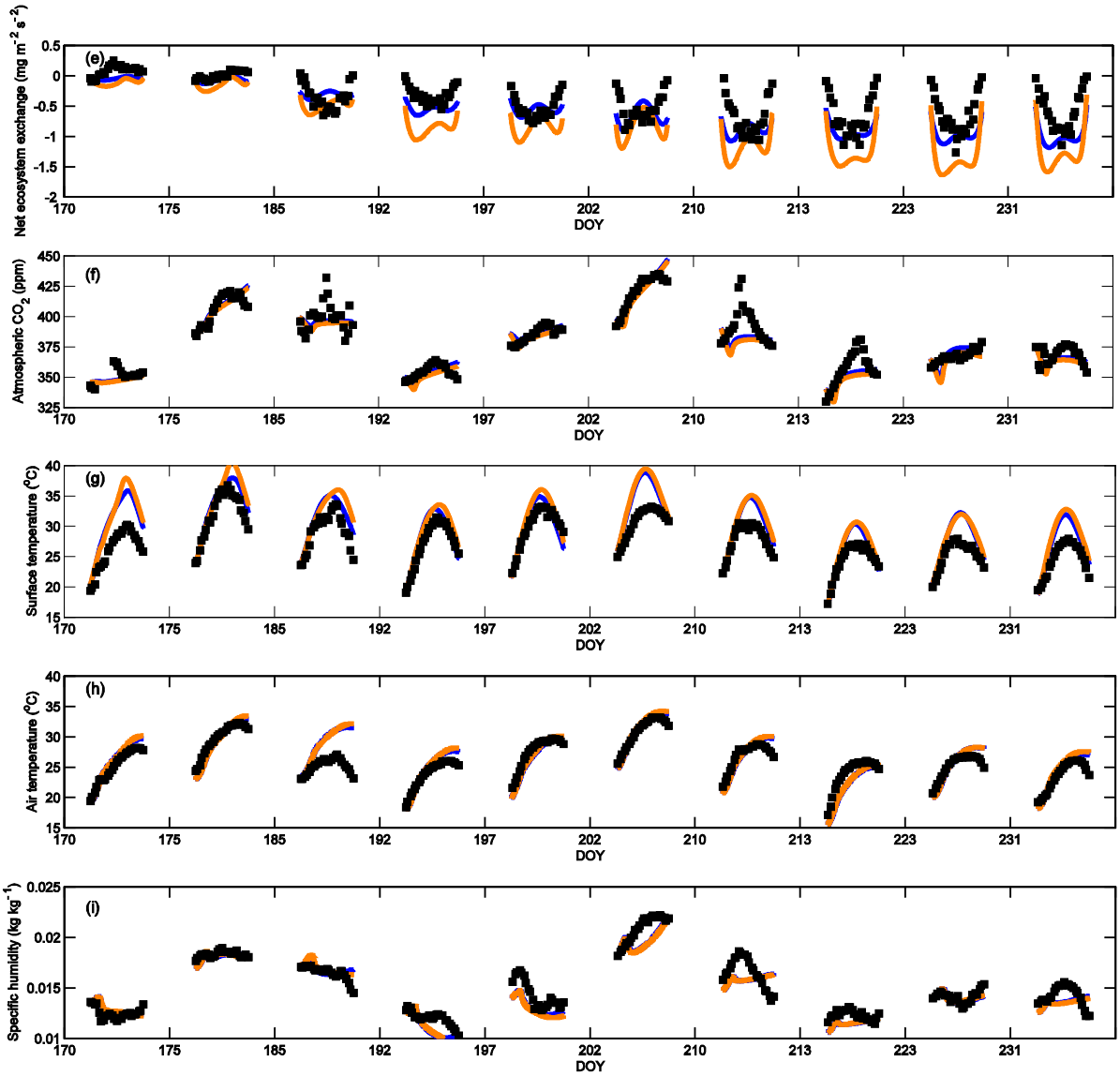

Fig A5.1 For the selected days within the growing season the half hourly observations from Ameriflux 1998 Bondville (black squares) versus predictions of the competitive optimization model (blue lines) and the simple optimization model (orange lines) for the net radiation (a), latent heat flux (b), sensible heat flux (c), ground heat flux (d), net ecosystem exchange (e), atmospheric CO_2 (f), surface temperature (g), air temperature (h) and specific humidity (i)

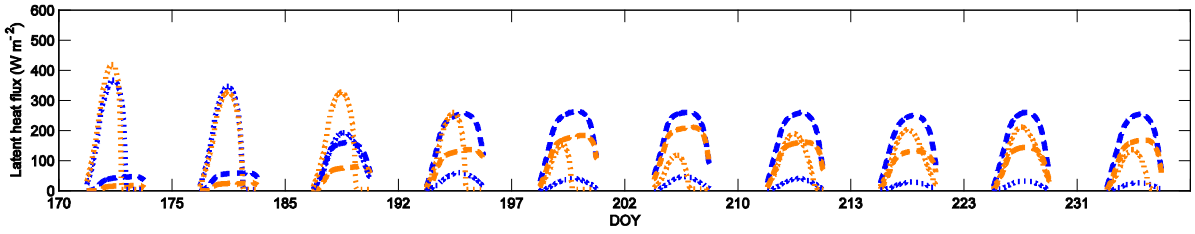

Fig A5.2 For the selected days within the growing season the predicted soil (dotted lines) and vegetation (dashed lines) latent heat flux by the competitive optimization model (blue lines) and the simple optimization model (orange lines)

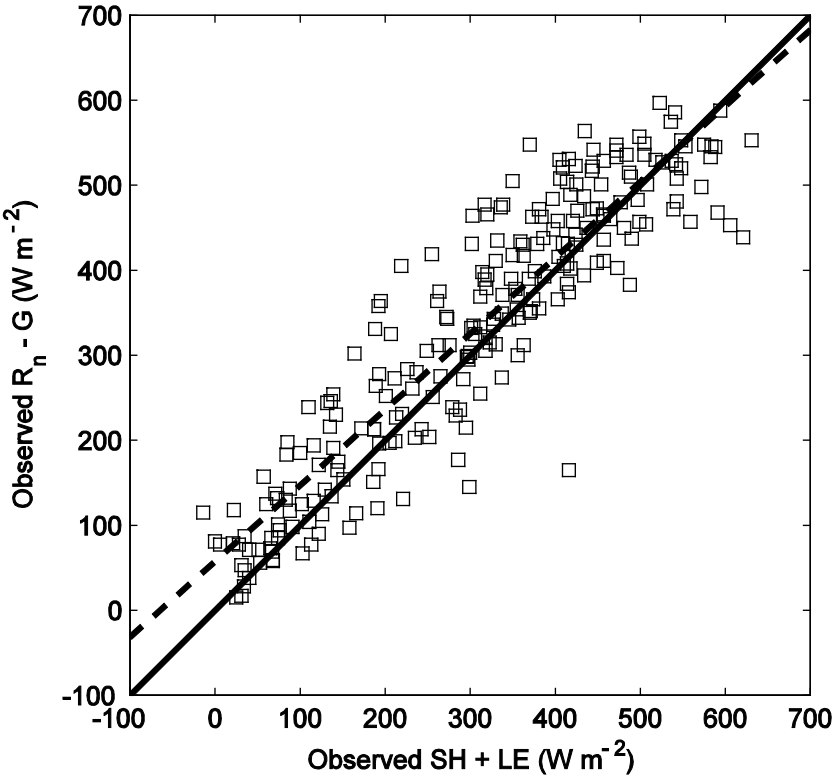

Fig A5.3 Sum of the observed sensible and latent heat flux (SH and LE respectively) versus the observed net radiation minus the ground heat flux (R_n and G respectively) (open squares) for DOY 170, 175, 185, 192, 197, 202, 210, 213, 223 and 231 from Ameriflux 1998 Bondville and the regression (dashed line) and one-to-one line (continuous line)

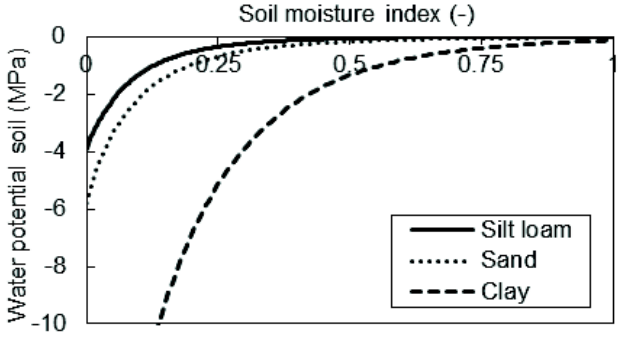

Fig A5.4 For silt loam, sand and clay soil type the relation between the soil moisture index (soil water content minus water content wilting point divided by water content field capacity minus water content field capacity) of the deeper soil layer with the soil water potential, as calculated with equation A5.1 and with the parameter values from Table A5.5

Table A5.1 List of symbols for the model parameters mentioned in the main text, with their unit, description of the parameter, input value and the source of the input value. The parameters are divided in three different categories: vegetation, soil, and other parameters. Within each category are the parameters given in alphabetic order.

Vegetation				
Symbol	Unit	Explanation	Input value	Source
A	m^2	The area in which an individual plant has its leaf area	1	
a_Ψ	MPa^{-1}	Slope parameter for the stomatal sensitivity function	3.2	11
a	Pa	Scaling parameter for calculation of stomatal conductance	2	11
c_{rl}	µmol m^{-2} s^{-1}	Intercept of the R_l N_l relation	0.388	1
G_{s0}	µmol d^{-1}	Residual stomatal conductance per unit ground area	0	10
H_a (of J_{max})	J mol^{-1}	Activation energy of J_{max}	58936	4
H_a (of K_{cmm})	J mol^{-1}	Activation energy of K_{cmm}	59400	4
H_a (of K_{omm})	J mol^{-1}	Activation energy of K_{omm}	36000	4
H_a (of R_l)	J mol^{-1}	Activation energy of R_l	24147	4
H_a (of V_{cmax})	J mol^{-1}	Activation energy of V_{cmax}	75794	4
H_a (of Γ^*)	J mol^{-1}	Activation energy of Γ^*	20970	4
H_d (of J_{max})	J mol^{-1}	Deactivation energy of J_{max}	199233	4
H_d (of V_{cmax})	J mol^{-1}	Deactivation energy of V_{cmax}	202022	4
K	kg MPa^{-1} d^{-1}	Stem conductance	1.1832	8
K_{cmm}(25˚C)	Pa	Michaelis-Menten constant for carboxylation at 25˚C	40.2	4
K_{df}	-	Extinction coefficient for diffuse PFD	0.747	1
K_n	-	Coefficient of leaf N allocation in a canopy	0.298	1
K_{omm}(25˚C)	Pa	Michaelis-Menten constant for oxygenation at 25˚C	56090	4
N_b	mmol m^{-2}	Leaf N concentration not associated with photosynthesis	29	1
O	Pa	Oxygen pressure in crown	20500	
q	µmol $µmol^{-1}$	Quantum yield (µmol electrons per photon)	0.25	
ΔS (of J_{max})	J mol^{-1}	Entropy term of J_{max}	647	4
ΔS (of V_{cmax})	J mol^{-1}	Entropy term of V_{cmax}	657	4
Wl	m	Equivalent water layer depth for wet vegetation	$1.4e^{-4}$	12
W_{max}	m	Thickness of water layer on wet vegetation	2e-4	12

Vegetation – continued				
Symbol	Unit	Explanation	Input value	Source
x_c	µmol CO_2 mmol N^{-1} s^{-1}	Slope of the V_{cmax} N_l-N_b relation	0.74	2
x_j	µmol CO_2 mmol N^{-1} s^{-1}	Slope of the J_{max} N_l-N_b relation	1.03	2
x_r	µmol CO_2 mmol N^{-1} s^{-1}	Slope of the R_l N_l relation	$9.9e^{-3}$	1
α_{canopy}	-	Albedo of full grown canopy	0.25	12
β	-	Degree of light interaction	0.5	3
γ_l	^{o}	Leaf inclination angle	26	
Γ^*(25˚C)	Pa	CO_2 compensation point in absence of mitochondrial respiration at 25˚C	5.1	4
θ	-	Curvature factor	0.9	6
λ_s	m^2 m^{-3}	Stem area density in the crown cylinder	$1.5e^{-5}$	
Σ	-	Leaf scattering coefficient	0.2	
Ψ_{ref}	MPa	Crown water potential at which the stomatal sensitivity function is half its maximum	-1.9	11
Soil				
Symbol	Unit	Explanation	Input value	Source
a	-	Clapp and Hornberger retention curve parameter b, silt loam soil	0.291	9
b	-	Clapp and Hornberger retention curve parameter b, silt loam soil	5.3	5
CG_{sat}	K m^{-2} J^{-1}	Saturated soil conductivity for heat	$3.6e^{-6}$	12
cp	J kg^{-1} K^{-1}	Specific heat of dry air	1005	12
d_1	m	Thickness top soil layer	0.02	12
E_0	kJ $kmol^{-1}$	Activation energy of soil respiration	$53.3e^3$	12
p	-	Clapp and Hornberger retention curve parameter c	12	12
R_{10}	mg CO_2 m^{-2} s^{-1}	Soil respiration at 10°C	0.035	
$rssoil_{min}$	s m^{-1}	Minimum resistance soil evaporation	50	12
w_{fc}	-	Volumetric water content field capacity, silt loam soil	0.36	7
wp_{air}	MPa	Air entry water potential of the soil	$-1.58e^{-3}$	11
w_s	m s^{-1}	Large scale vertical velocity	0	12
w_{sat}	-	Saturated volumetric water content, silt loam soil	0.48	5
w_{wilt}	-	Volumetric water content wilting point, silt loam soil	0.11	7
α_{soil}	-	Albedo of pure soil	0.18	
Other parameters				
Symbol	Unit	Explanation	Input value	Source
cp	J kg^{-1} K^{-1}	Specific heat of dry air	1005	12
f_c	m s^{-1}	Coriolis parameter	$1e^{-4}$	12
k	-	Von Karman constant	0.4	
Lat	°	Latitude	40.01	
Lon	°	Longitude	-88.29	

Other parameters – continued				
Symbol	Unit	Explanation	Input value	Source
L_v	J kg^{-1}	Heat of vaporization	$2.45e^{6}$	12
O	Pa	Oxygen pressure in crown	20500	
Pa	Pa	Atmospheric pressure	$1e^{5}$	
R	J K^{-1} mol^{-1}	Universal gas constant	8.315	
Rd	J kg^{-1} K^{-1}	Gas constant for dry air	287	
R_v	J kg^{-1} K^{-1}	Gas constant for moist air	461.5	12
S_0	W m^{-2}	Solar constant at the top of the atmosphere	1368	
w_s	m s^{-1}	Large scale vertical velocity	0	12
z_{0h}	m	Roughness length for scalars	0.01	12
z_{0m}	m	Roughness length for momentum	0.05	12
λ	-	thermal diffusivity skin layer	5.9	
ρ	kg m^{-3}	Density of air	1.2	
σ_{sb}	-	Bolzman constant	$5.67e^{-8}$	

Literature sources:

1) Anten *et al.* (1995)
2) Anten, Schieving & Werger (1995)
3) Anten, Werger & Medina (1998)
4) Cai & Dang (2002)
5) Clapp & Hornberger (1978)
6) Dermody, Long & DeLucia (2006)
7) Lambers, Chapin III & Pons (2008)
8) Maherali, Pockman & Jackson (2004)
9) Shao & Irannejad (1999)
10) Sterck & Schieving (2011)
11) Tuzet, Perrier & Leuning (2003)
12) Vilà-Guerau de Arellano *et al.* (2015)

Table A5.2 List of symbols for the model variables mentioned in the main text, with their unit, description of the variable and their equation number as mentioned in the main text. The variables are given in alphabetic order.

Symbol	Unit	Explanation	Equation
C_i	Pa	Internal CO_2	
c_{veg}	-	Vegetation fraction	(5.5)
LAI_i	-	Leaf area index of the target plant	
G_{sT}	µmol d^{-1}	Stomatal conductance of the plant to CO_2	(5.3)
g_Ψ	-	Describes stomatal sensitivity to water pressure at the focal point in the crown (-)	
H	W m^{-2}	Sensible heat flux	
LAI_i	-	Leaf area index of the individual	
LAI_T	-	Total leaf area index per unit of ground area of a stand	
LE	W m^{-2}	Total latent heat flux	
NEE	mg m^{-2} s^{-1}	Net ecosystem CO_2 exchange	
P_{cl}	µmol m^{-2} d^{-1}	Rubisco limited photosynthesis rate per unit ground area	
P_{jl}	µmol m^{-2} d^{-1}	Electron transport limited photosynthesis rate per unit ground area	
P_{gl}	µmol m^{-2} d^{-1}	Leaf gross photosynthesis rate per unit ground area	
P_{gT}	µmol d^{-1}	Whole plant gross photosynthesis rate	
P_{nl}	µmol m^{-2} d^{-1}	Leaf net photosynthesis rate per unit ground area	
P_{nT}	µmol d^{-1}	Whole plant net photosynthesis rate	
Resp	mg m^{-2} s^{-1}	Soil respiration rate	(5.7)
R_l	µmol m^{-2} d^{-1}	Leaf respiration rate	
α	-	Albedo	(5.4)
β	-	The ratio of the leaf area index of an individual to the total leaf area	(5.2)

Table A5.3 Initial conditions that are the same at the start of every day in the season and that differ per simulated day within the season (DOY).

Explanation	Unit	All days
Initial ABL height	M	175
Initial mixed-layer wind speed, horizontal component u-direction	m s^{-1}	5
Initial mixed-layer wind speed, horizontal component v-direction	m s^{-1}	0
Surface friction velocity	m s^{-1}	0.3

Explanation	Unit	DOY	170	175	185	192	197
Initial mixed-layer carbon dioxide	ppm		345	383	400	350	385
Total canopy N content	mmol N m^{-2}		38.4	52.8	128.2	269.2	299.3
Initial temperature deeper soil layer	K		294.34	296.24	297.68	297.04	296.94
Initial mixed-layer potential temperature	K		292.35	296.05	296.35	291.05	292.95
Initial surface temperature	K		291.79	294.78	296.33	291.31	292.73
Initial temperature top soil layer	K		291.55	294.87	295.93	290.32	302.17
Initial mixed-layer specific humidity	kg kg^{-1}		0.0135	0.0169	0.0172	0.0124	0.0140
Initial volumetric water content top soil layer	m^3 m^{-3}		0.41	0.41	0.4	0.36	0.29
Volumetric water content deeper soil layer	m^3 m^{-3}		0.4	0.41	0.41	0.41	0.41

Explanation	Unit	DOY	202	210	213	223	231
Initial mixed-layer carbon dioxide	ppm		396	391	340	365	375
Total canopy N content	mmol N m^{-2}		358.9	408.0	430.0	452.0	482.0
Initial temperature deeper soil layer	K		297.9	294.57	293.54	294.93	294.51
Initial mixed-layer potential temperature	K		297.75	293.75	288.45	293.05	291.25
Initial surface temperature	K		296.51	292.45	287.71	291.91	291.21
Initial temperature top soil layer	K		305.26	295.64	292.09	294.6	293.02
Initial mixed-layer specific humidity	kg kg^{-1}		0.0179	0.0147	0.0105	0.0141	0.0126
Initial volumetric water content top soil layer	m^3 m^{-3}		0.26	0.33	0.35	0.37	0.28
Volumetric water content deeper soil layer	m^3 m^{-3}		0.42	0.42	0.42	0.42	0.42

Table A5.4 Canopy leaf N content (N_t) and LAI as measured by Dermody, Long & DeLucia (2006) were used to estimate the canopy leaf N content over the growing season of the year 1998 of the Ameriflux tower site. LAI and canopy leaf N content of Dermody, Long & DeLucia (2006) were interpolated to estimate for several days within the growing season of the year 1998 (DOY) the canopy leaf N content from the measured values of LAI of that year.

Measured values by Dermody, Long & DeLucia (2006)		Measured and interpolated data from Ameriflux tower site, 1998		
Measured N_t	Measured LAI	DOY	Measured LAI	Interpolated N_t
21.2	0.89			
		170	1.19	38.4
44.7	1.30			
		175	1.48	52.8
80.2	2.09			
		185	2.72	128.2
153.3	3.05			
		192	4.32	269.2
		197	4.65	299.3
306.6	4.73			
		202	5.40	359.0
398.0	5.90			
		210	6.00	408.0
		213	6.22	430.0
		223	6.44	452.0
480.0	6.72			
		231	6.74	482.0

Table A5.5 Input values for different soil types.
See Table A5.1 for meaning parameter values.

	Soil types		
Parameter	Silt loam	Sand	Clay
a	0.291	0.627	0.083
b	5.3	4.1	11.4
w_{sat}	0.480	0.475	0.600
w_{fc}	0.36	0.15	0.44
w_{wilt}	0.11	0.04	0.28
wp_{air}	-0.00158	-0.00025	-0.00397
α_{soil}	0.18	0.35	0.2

Chapter 6

General discussion

The main aim of this thesis was to investigate how plant traits are altered by changes in the climate and how this is affected by plant competition, to identify how strong the associated feedbacks with the atmosphere are. First, I discuss the effects of competition on plant responses to climate change with regard to some model assumptions on competition. Then I discuss the choice of the objective function of an optimization model. This is followed by a discussion on the influence of the type and timing of plant responses to changes in environmental conditions. Finally, I discuss the consequences of including competition in a coupled vegetation-atmosphere model for the global carbon cycle. This chapter ends with some concluding remarks.

6.1 Effect of competition on plant responses

Plants often grow in dense communities, such as forests and grasslands; therefore, it has been thought that natural selection would favour plants that are good competitors (McNickle & Dybzinski 2013). As a consequence, it could be assumed that competition strongly influences plant responses and in doing so it determines vegetation functioning (Anten & Hirose 2001). The inclusion of competition, so considering that natural selection favours plants with the highest competitive ability, in a vegetation model was already shown to result in good predictions of LAI (Leaf Area Index, i.e., the leaf area per unit soil area) under current climate conditions (Anten 2002). In addition, we showed in **Chapter 3** that inclusion of competition results also in accurately predicted effects of elevated CO_2 on leaf photosynthesis, leaf N content and seasonal dynamics in LAI as observed in a large number of Free Air CO_2 Enrichment (FACE) experiments. Furthermore, we indicated that there is a strong influence of competition on plant responses to changes in environmental conditions. Namely, our model outcomes showed, when competition was considered the optimal response shifts to larger LAI, but with lower net photosynthesis, stomatal conductance and associated vegetation transpiration thereby leading to a lower water use efficiency (WUE, ratio of carbon gain to water loss) than when it was not considered.

The experimental results from **Chapter 4** also showed the importance of accounting for competition. In an experiment with *Plantago asiatica* we showed that when grown at elevated CO_2, plants originating from high CO_2 habitats (i.e., from natural CO_2 springs) only performed better than those originating from ambient CO_2 habitats when both genotypes competed and not when each was grown in mono stands. The reverse also held, plants native to ambient CO_2 habitats performed better at preindustrial CO_2, only when they competed with those from high CO_2 habitats and not when grown in mono stands. This indicates that changes in atmospheric CO_2 favoured genotypes that were the best competitors, and not those with the highest inherent performance. From the results in my thesis I can therefore conclude that when attempting to predict vegetation responses to climate change it is very important to

consider competition between plants under future climate scenarios, as it strongly modifies these responses.

6.1.1 Degree of interaction

The results from the vegetation model did show that the influence of competition on plant responses was strongly modified by the assumed degree of interaction between plants. To study the effect of competition we compared two model versions, one without competition (simple optimization model), and one with competition (competitive optimization model). Both model versions are the same, except for one parameter value, β, which is the degree of mixture between the target plant and neighbouring plants and thus the extent to which they influence each other's light climate. To be exact, β is defined as the ratio of the LAI of a target plant (LAI_i) divided by the total LAI within the area in which a target plant has its leaves (LAI_T).

$$\beta = LAI_i / LAI_T \quad (6.1)$$

For the simple optimization model the β values is 1, which entails canopies are not mixed and plants do not influence each other's light climate; therefore, a plant is only influenced by its own light climate (so, LAI target plant is equal to total LAI in the area of the target plant). For the competitive optimization model, I assumed a fixed β equal to 0.5. This means that there is mixture of leaves of the target plant and its neighbouring plants, and leaves of the target plants and those of neighbours equally contribute to the shading experienced by the target plant. There are two things that need more clarification: first, the assumption of a fixed β value, and second, why the value of 0.5 was chosen. Regarding the fixed value of β, it is important to know that β is as it were a historical value that depicts the mean of the competitive environment in which a given plant type evolved during natural selection. About the chosen value of β = 0.5, this value was chosen as it has given satisfactory predictions of LAI of herbaceous vegetation stands similar in structure to the soybean stands analysed here; as there was a strong correlation between the predicted and observed LAI value (R^2 = 0.8) and the slope of the regression line was not significantly different from 1 (Anten 2002). Yet, although we showed in **Chapter 3** that with this value of β the model predicts soybean responses to elevated CO_2 very well, we also showed that β has a large influence on the predicted LAI, net photosynthesis rate, stomatal conductance and transpiration rate.

So, I assumed a fixed β value of 0.5, but quantitative measurements of β are needed as it was postulated that the degree of interaction depends on the plant type (Anten & During 2011), the distance between the individuals (Givnish 1982), the size of the individual (Hikosaka & Hirose 1997) and the degree of mixing of leaves in space (Hikosaka *et al.* 2001). However, except for the study of Hikosaka *et al.* (2001) no quantitative measurements of the degree of interaction have been reported. Hikosaka *et al.* (2001) did quantify the degree of interaction

for a *Xanthium canadense* Mill. stand by measuring light interception. Yet, they had a different definition of the degree of interaction as compared to ours (i.e., theirs was the fraction of the intercepted light that penetrated the foliage of neighbours, while ours refers to the degree of mixture of leaves between the target plant and neighbouring plants) and their values can thus not directly be compared to the β parameter. They found that there was a high degree of interaction as light interception of a plant was more strongly influenced by the leaves of neighbouring plants than by its own leaves, 30% of the shading on a plant was caused by self-shading and the remainder was caused by non-self shading. But *Xanthium canadense* plants generally have very long petioles, and therefore they argued that the degree of interaction of other species with a shorter petiole would likely be lower.

6.1.2 Greenhouse experiment to quantify β

We showed that β has a strong effect on vegetation responses, and that this degree of interaction depends on several aspects like the distance between the individuals, therefore more work is needed to quantify β. For that reason, a greenhouse experiment was set-up with soybean (*Glycine max*) growing in different densities. A full description of the experiment can be found in Penning (2014), here a brief description of the experiment is given.

On 29 July 2013 we sow seeds in pots (0.21 by 0.21 m) filled with potting soil and placed them in a greenhouse (Wageningen, The Netherlands). Stands were established by putting four by four plants together, the middle four plants of each stand were used for measurements. Three different spacing's in-between the plants were created: 46 cm (low density), 31 cm (medium density) and 21 cm (high density). For each density there were three replicate stands.

On 9 October 2013, 72 days after sowing, light interception measurements were made with a SunScan Canopy Analysing System (Delta T Devices, Cambridge, UK). The total light interception of an individual plant within the stand (i.e., the target plant) (I_{tot}), and of only neighbours (without target plant) (I_{ns}) was measured. Additionally, leaf area was measured with a LICOR leaf area meter (LI3100 device, Lincoln NE, USA).

The degree of self to non-self shading (*s*/*ns*) of the target plant (i.e., ratio of the light interception of the target plant only, by the light interception with only neighbours) was calculated as:

$$s/ns = \left(1 - \frac{I_{\mathrm{ns}}}{I_{\mathrm{tot}}}\right) / \left(\frac{I_{\mathrm{ns}}}{I_{\mathrm{tot}}}\right) \qquad (6.2)$$

With the calculated degree of self to non-self shading and the measured total LAI of the stand, β could be calculated for each of the plants in the different stands.

Fig 6.1a shows for the three different densities the calculated β values and the corresponding LAI. It shows that β decreases as the LAI and the density increase. This is consistent with

what was expected, if plants grow closer together their canopies more strongly interact (lower β values). However, the LAIs that correspond with the β values were lower in the experiment than the model predictions of **Chapter 3**. The model predicted on average 55% higher LAI values than were observed. This can partly be explained by the lower canopy leaf N contents found in the experiment (on average 234 mmol N m^{-2} compared to 527 mmol N m^{-2}) (recall that canopy N is an important driver of LAI in my model). When we used the same canopy N content in the model as found in the experiment, then there was an improvement of the predicted LAI with the corresponding β values; namely, the average deviation between observed and predicted values [Eqn (5.7)] reduced with 59% compared to the higher canopy leaf N contents. On the other hand, the model is based on a number of simplified assumptions that can also partly explain the mismatch between observed and predicted LAIs for the corresponding β values. I will further discuss this in paragraph 6.2: Optimization, the objective function.

The results from the experiment indicate that the density plays an important role in determining the β value. Additionally, it was also found that when β was measured along the length of the stem its value tended to increase from the plant base towards the tip (Fig 6.1b). In other words, the degree of mixing between leaves of plants appeared to be higher at the bottom of the canopy than at the top. In contrast to this finding, in the model it is assumed that there is a uniform mixing of leaf area through the whole canopy (horizontally and vertically). As the importance of leaves for light competition increases with their height above the soil, therefore it should be considered to use different values of β over the height in the canopy in the model.

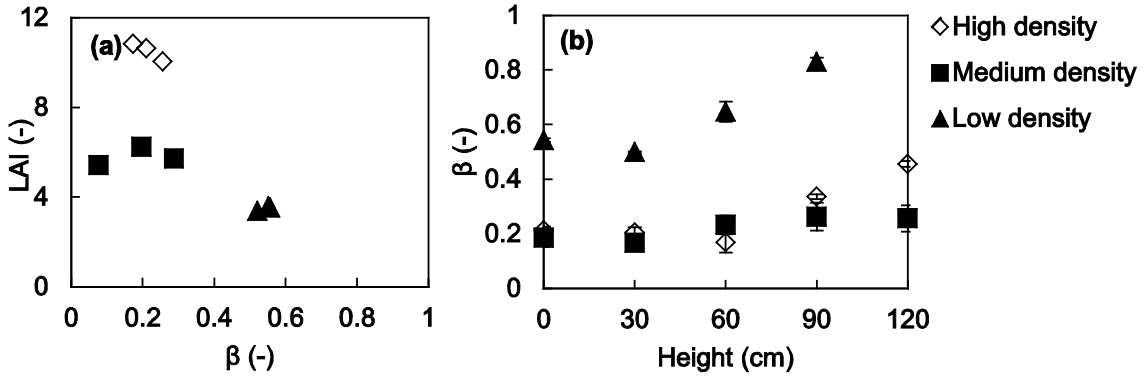

Fig 6.1 The degree of mixture between the target plant and neighbours, β, and its LAI (a) for different heights within the canopy (b) and for different sowing densities (high=21cm, medium=31cm and low=46 cm respectively)

To conclude, it is very important to consider competition between plants, as it strongly modifies vegetation responses. However, the predicted effects of competition strongly depend

on the assumed degree of interaction, which is among other dependent on the plant type, the density and the available N.

6.1.3 Competition for different resources

In this thesis, it was shown both with a model and experimentally (**Chapters 3 and 4** respectively) that competition has a strong influence on plant responses to elevated CO_2. It was also found that this influence of competition is less strong when nitrogen or water is limiting (**Chapter 5**), as competition for light is weaker because those factors are limiting growth. Furthermore, with the vegetation model it was shown that competition for light through natural selection (maximize competitiveness rather than maximization of inherent performance) leads to larger LAI, with lower net photosynthesis, stomatal conductance and transpiration compared to no competition. More studies suggest that plant responses are largely affected by selection acting through competition (e.g., Gersani *et al.* 2001; Beerling & Franks 2010). For example, experimental studies indicate that natural selection on competitive traits led to plants with a greater transpiration rate while having very high carbon construction costs for vein infrastructure (Beerling & Franks 2010). They indicate that although plants have a higher water loss they can support this, because in this way they can outcompete invading genotypes (Beerling & Franks 2010).

In my thesis the focus is on aboveground competition for light, while other studies indicate the importance of belowground competition. It has been suggested that plants respond to the presence of neighbours by increasing their root growth to acquire more resources, and that this results in greater root mass than would be optimal for vegetation level performance (Gersani *et al.* 2001), though this paper has been criticized (Hess & De Kroon 2007; Chen, During & Anten 2012). However, it has also been suggested that competition results in shallower roots compared to the optimal root distribution in absence of competition (Van Wijk & Bouten 2001). As with leaf production (Anten 2002) and other aboveground traits (see Falster & Westoby 2003b), this was framed as a tragedy of the commons. So, plants compete for both belowground and aboveground resources, and investment in capture of belowground resources goes at the expense of aboveground resource capture and vice versa. Putting it in a game theoretical perspective, plants play different games simultaneously. Therefore it might be needed to simulate both above- and belowground competition and its trade-offs simultaneously. Several game theoretical modelling studies did consider both aboveground and belowground resources. For example, model results reveal that competition for light and for N leads under N limited conditions to more leaf area and less fine root production when the N availability increases (Dybzinski *et al.* 2011). In contrast, in N saturated areas the leaf area production is independent of competition for N and only depends on competition for light (Dybzinski *et al.* 2011). In addition, model results that take into account competition for light and water show under water limited conditions that plants

overinvest in roots at the expense of leaf area production (Farrior *et al.* 2013). However, under elevated CO_2 it is predicted that woody plants increase their carbon storage as a result of competition for water (Farrior *et al.* 2015).

To conclude, the importance of competition in driving plant responses to environmental changes has clearly been shown. In this thesis only aboveground competition for light was considered, although several soil-based factors were considered in our model (e.g. water, N) competition for them was not included. But competition for these soil-based factors is much less important when levels are high; in contrast, at low levels they are more important than competition for light as in this case they trade-off for leaf area production. Including competition for those factors might alter the effect of competition on the relationship between LAI, net photosynthesis rate, and stomatal conductance when resources are limiting. Therefore, I recommend to further focus on how competition for both belowground and aboveground resources affects the relationship between LAI, photosynthesis and stomatal conductance under different environmental conditions.

6.2 Optimization, the objective function

In this thesis optimization models were frequently used. Optimization models maximize a goal or objective function to optimize plant functional traits given certain (physiological or environmental) constraints (Dewar *et al.* 2009). Thereby, it is assumed that natural selection led to optimized plant functional traits for maximizing fitness (Franklin *et al.* 2012). But real fitness (i.e., the transferral of ones genes to the next generation) is hard to quantify, therefore most optimization models use a performance measure as a proxy for fitness. In **Chapters 3 and 5** we chose to maximize net whole-plant photosynthesis (i.e., gross photosynthesis minus the leaf respiration rate), because photosynthesis supplies the energy for growth and reproduction (Bowes, Ogren & Hageman 1972) and might therefore be a good proxy for fitness. In general, other studies also use substitutes for fitness that are related to the carbon balance (Franklin 2007; Makela, Valentine & Helmisaari 2008; McMurtrie *et al.* 2008), but those models differ in the costs incorporated into the objective function (Dewar *et al.* 2009). For example, some models include costs for maintenance and growth respiration (Franklin 2007), while others also consider costs associated with foliage and fine root turnover (Makela, Valentine & Helmisaari 2008). On the other hand, our model does also not account for additional carbon construction costs of investment in leaves. Meaning that if this would be included, this could result in lower predictions of leaf area production for both the simple and the competitive optimization model, as the costs of (over)investing in leaf area would become higher.

It is therefore clear that net photosynthesis rate as a goal to maximize is a highly simplified proxy for fitness. Taking another more direct proxy for fitness like the number of offspring produced per individual in its lifetime (Parker & Maynard-Smith 1990) could be

more appropriate, but in this case it is more difficult to test experimentally (Franklin *et al.* 2012), as making a comparison between model predictions and real observations is more difficult (Schymanski *et al.* 2007). In general is the proper choice of the objective function debated (Dewar et al. 2009, 2012). In this debate it is mentioned that failure of optimization models in predicting observed values, is the result of incorrect specification of the objective function to be maximized and not that the optimality approach itself is invalid (Kull 2002; Dewar *et al.* 2012).

To conclude, the choice of the objective function of optimization models is still highly debated. Some opt for the use of a more direct measure of fitness, but this is more difficult to use as in most cases the outcomes are hard to validate against experimental data. Therefore, others generally use an objective function related to the carbon balance; which was also done in this thesis, were the objective function was to maximize net photosynthesis.

6.3 Type and timing of plant responses

Plant responses to climate change could be plastic, meaning that changes in traits occur during the lifetime of a plant and thus take place on a relatively short timescale. How fast plants can make these plastic responses to short term changes in environmental conditions is limited by the time it takes to make adjustments. Therefore, plants do not respond immediately to an environmental change, but are instead thought to respond to longer term average conditions (Chen *et al.* 1993). However, optimization models generally do not consider this timescale of response (Chen *et al.* 1993); that is, they implicitly assume that plants can track environmental changes optimally without delay. In **Chapter 2** we analysed optimal N allocation between ribulose-1,5-bisphosphate (RuBP) regeneration (process of transformation of light energy into the higher energy compounds ATP and NADPH) and RuBP carboxylation (the use of the higher energy compounds to bind CO_2 into complex sugar compounds) and calculated the extent to which the time lag between environmental change and this optimization affects simulated rates of photosynthesis. Our simulations showed that this time lag strongly affects predicted leaf photosynthesis, as even small changes in time lag between environmental change and optimal partitioning of N had a large negative effect on the simulated leaf photosynthesis. So, our results suggest that it is very important to consider this timescale of response in vegetation models.

Although the timescale of plant responses has such a large effect, we still did not take this into account when using the optimization approach in the other chapters; that is, we assumed in the other chapters that the LAI is optimized on a daily time scale. So, we optimized for a specific time interval, while plants are thought to respond to the average environmental conditions they evolved in, which might deviate from this daily time interval that we chose (Chen *et al.* 1993). For example, acclimation to changes in light through

changes in leaf anatomy require minimally a few days and in some cases several weeks (Pearcy & Sims 1994), as structural changes like changes in LAI are not reversible and thus take longer to realize. This indicates that our assumed daily optimization of the LAI might not be realistic. Therefore more research is needed to investigate the exact effect of the timescale of LAI optimization on predictions of whole-canopy level responses.

Current increase in atmospheric CO_2 is occurring on a relatively short time scale, therefore it is thought that if trait changes in response to elevated CO_2 occur primarily through short term plastic responses then a community may be able to keep up with these changes. Nevertheless, plastic responses alone are thought to be insufficient to keep up with the current changes in the climate and therefore genotypic responses (i.e., changes that take place over several generations) are also occurring (Visser 2008). However, if changes are mostly genotypic then it will take several generations of natural selection, and it could thus be expected that in this case plants face more difficulty to keep up to the current rapid increase in CO_2. As a result, it is likely that responses of many populations are inadequate to cope with the speed of climate change (Hoffmann & Sgrò 2011). For example, it is thought that species with long life cycles will not be able to adapt genotypically to climate change (Valladares 2008). Trees have a long life cycle and their trait adjustment to climate change will almost exclusively be through phenotypic plasticity. It is believed that the limitation on plasticity of trees will thus limit their ability to adequately cope with climate change (Valladares 2008). By contrast, annual plants have a short life cycle and therefore have more opportunities to adapt to climate change as in this case genotypic adaptation can go more rapidly (Jump & Penuelas 2005). Nevertheless, it has been shown that genotypic adaptations to climate change are frequently absent for several species (Hoffmann & Sgrò 2011).

The level of plastic and genotypic response thus determines how fast a species can adjust to climate change, while in optimization models this distinction is not considered. In **Chapter 4** we showed experimentally that responses of *Plantago asiatica* in e.g., whole-plant photosynthesis, specific leaf area (ratio of leaf area to dry weight) and stomatal conductance, to elevated CO_2 could mainly be attributed to plastic responses and not to genotypic adaptations. These findings imply that in short living plants the degree to which plants can cope with current climate change might be primarily depending on plastic responses.

To conclude, the timing of plant responses to climate change is very important, while this is generally not considered in optimization models. We showed that the timing of the response has a large impact on the leaf level response, and more research is needed on the canopy level. In addition, the type of response is also important, we showed for *Plantago asiatica* that responses to climate change occur mostly on the short term time scale.

6.4 The global carbon cycle and the role of plant competition

Plants may take up around 15% of the atmospheric carbon pool every year (Amthor 1995), and because this flux is so large any alterations of the plant's CO_2 exchange could significantly affect the global C cycle (Fig 6.2) (Amthor 1995). This is especially important under elevated CO_2, as plants are thought to increase their CO_2 uptake and thereby slowdown the rise in atmospheric CO_2, which constitutes an important negative vegetation-atmosphere feedback. Moreover, any global changes in plants C uptake might affect atmospheric CO_2 during years or even decades (Amthor 1995). Plant competition might strongly influence plant responses to climate change (Ziska 2011), because it is an important selective force and strongly determines vegetation functioning (McNickle & Dybzinski 2013). In **Chapter 5** we included plant competition, i.e., assuming that natural selection is on maximization of competiveness instead of inherent performance, in a coupled vegetation-atmosphere model. The inclusion of this new representation of competition in the model resulted in a reduction of the net photosynthesis rate, therefore a less negative net ecosystem exchange of CO_2 was projected, and resulting in an increased atmospheric CO_2 concentration compared to not taking competition into account. Whereas most coupled vegetation-atmosphere models do not take competition into account and thus might overestimate plants C uptake, this implies that with elevated CO_2 the negative vegetation feedback of uptake of CO_2 from the atmosphere by plants would be less strong than currently forecasted; which again would also play a role in final vegetation functioning.

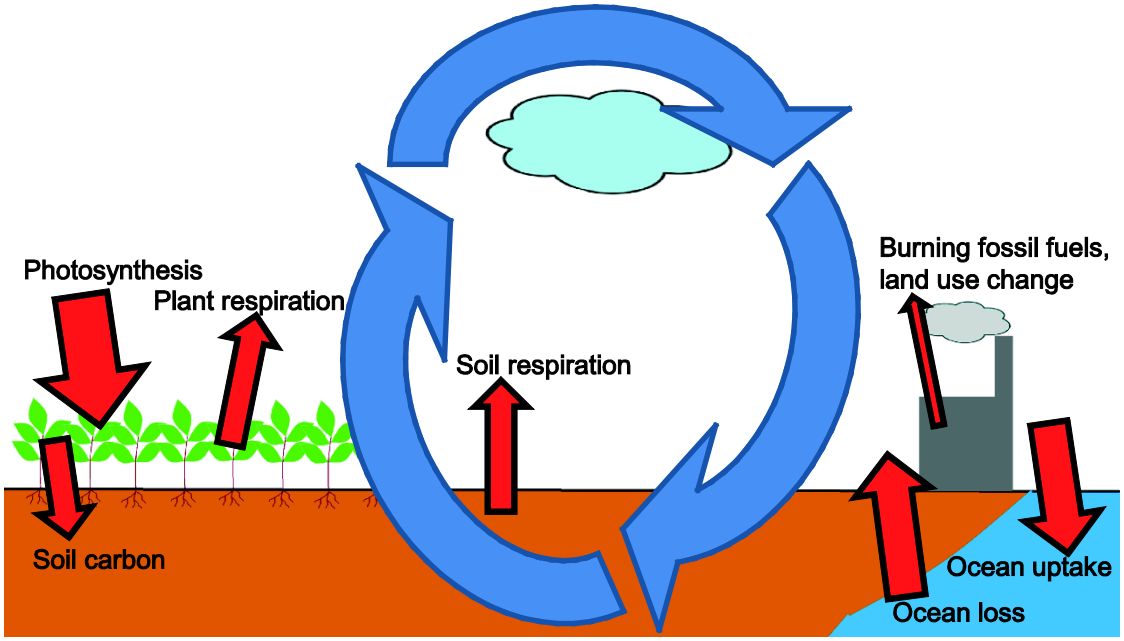

Fig 6.2 Conceptual diagram on the global carbon cycle, showing the fluxes of carbon between land, atmosphere and ocean (red arrows, size of the arrows indicates the size of the flux).

In line with our findings from **Chapter 5**, Weng *et al.* (2015) also suggests to include plant competition in atmospheric models. They incorporated height-structured competition for light and competition for water in a land model currently used in the earth system model. The height-structured formulation is based on the perfect plasticity approximation – i.e., each plant fills as much space as it can without growing into adjacent plants area, which is the result of plants individual plasticity. Meaning that, in contrast to the model used in this thesis, this model assumes that there is no mixture of leaves between plants. Furthermore, they assume that roots of competing plants are uniformly distributed in the horizontal plane. Their model did make reasonable predictions of diurnal and annual carbon and water fluxes, growth rates of trees when compared with data. This model predicts that due to competition plants will invest more in fine roots and less in wood when atmospheric CO_2 concentration increases, which they suggest would reduce the carbon sink caused by CO_2 fertilization.

So, including competition could diminish the reduction of carbon uptake by plants and thereby influence the carbon balance, as the slowdown of the rise of atmospheric CO_2 due to plants will be less. However, soil respiration rates can also have a large influence on the global C cycle (Fig 6.2) (Schlesinger & Andrews 2000). While current parameterizations for temperature and moisture dependencies of soil respiration rates are in general largely unknown (Moorcroft 2003). Although for our coupled vegetation-atmosphere model we used estimated temperature related parameters of the soil respiration rate based on data, the ability of these parameters to correctly characterize the response of below-ground ecosystems to long term environmental changes is still highly uncertain (Moorcroft, 2003). In addition, our coupled vegetation-atmosphere model was only applicable for local scales, and a next step would entail scaling this approach to the regional scales (e.g., including patches of different vegetation types each evolving a competitive scenario). But, take into consideration that vegetation feedbacks on atmospheric processes may function differently according to the regional characteristics of the climate (Levis, Foley & Pollard 2000).

6.5 Concluding remarks

It is important to stress that we used a canopy model that was based on a number of simplifications (e.g., no inclusion of: costs of leaf construction, limit to specific leaf area, growth-related processes for leaf area production) and is meant solely to understand the impact of plant competition on vegetation responses to climate change, and it was not our objective to produce a detailed model of vegetation functioning. So, although our model is based on a number of simplifications, our study on inclusion of trait acclimation in a competitive setting in vegetation (and coupled to atmosphere) models is ecologically realistic, as plants generally compete for resources, and can result in an improvement of the climate change predictions as also was suggested by Weng *et al.* (2015).

To conclude, the results presented in this thesis provided new insights in the type and timing of plant responses to changes in environmental conditions. We showed the importance of considering the time scale of leaf-level responses to environmental changes in optimization models. I therefore advocate to further explore the effect of the time scale of response on the level of the whole canopy. In addition, we showed that plants respond mostly on the short term time scale to elevated CO_2 and not on the long term time scale.

Lastly, the results presented in this thesis underline the importance of plant competition, i.e., considering that natural selection favours plants with the highest competitive ability, on vegetation functioning and its influence on atmospheric processes. We showed that the inclusion of competition in a vegetation model resulted in accurate predictions of the effect of elevated CO_2 on several plant traits. Furthermore, we found that there is a strong influence of competition on plant responses to changes in environmental conditions, when competition was considered this resulted in larger leaf areas, but with lower photosynthesis. Besides, our experimental results also showed the importance of accounting for competition. As changes in CO_2 favoured genotypes that were the best competitors and not those with the highest performance. Next to this, we showed with a coupled vegetation-atmosphere model that plant competition can also influence a number of atmospheric processes; namely, including competition resulted among others in reduced net ecosystem exchange of CO_2 and thereby implying that the negative feedback of plants extra carbon uptake under elevated CO_2 would be less strong. However, we emphasize that the magnitude of this effect might differ between plant types. It is therefore needed to further explore the effects of competition, for several plant types under different environmental conditions, on global atmospheric processes to define the impact on the climate.

References

Aerts R. (1999) Interspecific competition in natural plant communities: Mechanisms, trade-offs and plant-soil feedbacks. *Journal of Experimental Botany* 50, 29-37.

Aerts R. & Chapin III F.S. (1999) The mineral nutrition of wild plants revisited: A re-evaluation of processes and patterns. *Advances in Ecological Research* 30, 1-67.

Ainsworth E.A., Davey P.A., Bernacchi C.J., Dermody O.C., Heaton E.A., Moore D.J., Morgan P.B., Naidu S.L., Yoo Ra H., Zhu X., Curtis P.S. & Long S.P. (2002) A meta-analysis of elevated [CO_2] effects on soybean (*Glycine max*) physiology, growth and yield. *Global Change Biology* 8, 695-709.

Ainsworth E.A., Davey P.A., Hymus G.J., Osborne C.P., Rogers A., Blum H., Nösberger J. & Long S.P. (2003) Is stimulation of leaf photosynthesis by elevated carbon dioxide concentration maintained in the long term? A test with *Lolium perenne* grown for 10 years at two nitrogen fertilization levels under free air CO_2 enrichment (FACE). *Plant, Cell & Environment* 26, 705-714.

Ainsworth E.A. & Long S.P. (2005) What have we learned from 15 years of free-air CO_2 enrichment (FACE)? A meta-analytic review of the responses of photosynthesis, canopy properties and plant production to rising CO_2. *New Phytologist* 165, 351-372.

Ainsworth E.A., Rogers A., Leakey A.D.B., Heady L.E., Gibon Y., Stitt M. & Schurr U. (2007) Does elevated atmospheric [CO_2] alter diurnal C uptake and the balance of C and N metabolites in growing and fully expanded soybean leaves? *Journal of Experimental Botany* 58, 579-591.

Amthor J.S. (1995) Terrestrial higher-plant response to increasing atmospheric [CO_2] in relation to the global carbon cycle. *Global Change Biology* 1, 243-274.

Anten N.P.R., Hirose T., Onoda Y., Kinugasa T., Kim H.Y., Okada M. & Kobayashi K. (2004) Elevated CO_2 and nitrogen availability have interactive effects on canopy carbon gain in rice. *New Phytologist* 161, 459-471.

Anten N.P.R. (2005) Optimal photosynthetic characteristics of individual plants in vegetation stands and implications for species coexistence. *Annals of Botany* 95, 495-506.

Anten N.P.R. (2002) Evolutionarily stable leaf area production in plant populations. *Journal of Theoretical Biology* 217, 15-32.

Anten N.P.R. & During H.J. (2011) Is analysing the nitrogen use at the plant canopy level a matter of choosing the right optimization criterion. *Oecologia* 167, 293-303.

Anten N.P.R. & Hirose T. (2001) Limitations on photosynthesis of competing individuals in stands and the consequences for canopy structure. *Oecologia* 129, 186-196.

Anten N.P.R., Schieving F., Medina E., Werger M.J.A. & Schuffelen P. (1995) Optimal leaf area indices in C_3 and C_4 mono- and dicotyledonous species at low and high nitrogen availability. *Physiologia Plantarum* 95, 541-550.

Anten N.P.R., Schieving F. & Werger M.J.A. (1995) Patterns of light and nitrogen distribution in relation to whole canopy carbon gain in C_3 and C_4 mono- and dicotyledonous species. *Oecologia* 101, 504-513.

Anten N.P.R., Werger M.J.A. & Medina E. (1998) Nitrogen distribution and leaf area indices in relation to photosynthetic nitrogen use efficiency in savanna grasses. *Plant Ecology* 138, 63-75.

Asner G.P., Scurlock J.M.O. & Hicke J.A. (2003) Global synthesis of leaf area index observations: Implications for ecological and remote sensing studies. *Global Ecology and Biogeography* 12, 191-205.

Bazzaz F.A. & McConnaughay K.D.M. (1992) Plant plant interactions in elevated CO_2 environments. *Australian Journal of Botany* 40, 547-563.

Bazzaz F.A., Jasienski M., Thomas S.C. & Wayne P. (1995) Microevolutionary responses in experimental populations of plants to CO_2-enriched environments: Parallel results from two model systems. *Proceedings of the National Academy of Sciences of the United States of America* 92, 8161-8165.

Beerling D.J. & Franks P.J. (2010) Plant science: The hidden cost of transpiration. *Nature* 464, 495-496.

Bernacchi C.J., Leakey A.D.B., Heady L.E., Morgan P.B., Dohleman F.G., Mcgrath J.M., Gillespie K.M., Wittig V.E., Rogers A., Long S.P. & Ort D.R. (2006) Hourly and seasonal variation in photosynthesis and stomatal conductance of soybean grown at future CO_2 and ozone concentrations for 3 years under fully open-air field conditions. *Plant, Cell & Environment* 29, 2077-2090.

Bernacchi C.J., Morgan P.B., Ort D.R. & Long S.P. (2005) The growth of soybean under free air [CO_2] enrichment (FACE) stimulates photosynthesis while decreasing in vivo Rubisco capacity. *Planta* 220, 434-446.

Bernacchi C.J., Kimball B.A., Quarles D.R., Long S.P. & Ort D.R. (2007) Decreases in stomatal conductance of soybean under open-air elevation of [CO_2] are closely coupled with decreases in ecosystem evapotranspiration. *Plant Physiology* 143, 134-144.

Bonan G.B. (2008) Forests and climate change: Forcings, feedbacks, and the climate benefits of forests. *Science* 320, 1444-1449.

Bounoua L., Collatz G.J., Los S.O., Sellers P.J., Dazlich D.A., Tucker C.J. & Randall D.A. (2000) Sensitivity of climate to changes in NDVI. *Journal of Climate* 13, 2277-2292.

Boussetta S., Balsamo G., Beljaars A., Panareda A., Calvet J., Jacobs C., Van der Hurk B., Viterbo P., Lafont S., Dutra E., Jarlan L., Balzarolo M., Papale D. & Van der Werf G. (2013) Natural land carbon dioxide exchanges in the ECMWF integrated forecasting system: Implementation and offline validation. *Journal of Geophysical Research: Atmospheres* 118, 5923-5946.

Bowes G., Ogren W.L. & Hageman R.H. (1972) Light saturation, photosynthesis rate, RuDP carboxylase activity, and specific leaf weight in soybeans grown under different light intensities. *Crop Science* 12, 77-79.

Brotzge J.A. & Crawford K.C. (2003) Examination of the surface energy budget: A comparison of eddy correlation and bowen ratio measurement systems. *Journal of Hydrometeorology* 4, 160-178.

Brovkin V., Claussen M., Petoukhov V. & Ganopolske A. (1998) On the stability of the atmosphere-vegetation system in the Sahara/Sahel region. *Journal of Geophysical Research* 103, 31613-31624.

Buckley T.N., Cescatti A. & Farquhar G.D. (2013) What does optimization theory actually predict about crown profiles of photosynthetic capacity when models incorporate greater realism? *Plant, Cell & Environment* 36, 1547-1563.

Cai T. & Dang Q.L. (2002) Effects of soil temperature on parameters of a coupled photosynthesis-stomatal conductance model. *Tree Physiology* 22, 819-827.

Cao M. & Woodward F.I. (1998) Net primary and ecosystem production and carbon stocks of terrestrial ecosystems and their responses to climate change. *Global Change Biology* 4, 185-198.

Chen B.J.W., During H.J. & Anten N.P.R. (2012) Detect thy neighbor: Identity recognition at the root level in plants. *Plant Science* 195, 157-167.

Chen J.L., Reynolds J.F., Harley P.C. & Tenhunen J.D. (1993) Coordination theory of leaf nitrogen distribution in a canopy. *Oecologia* 93, 63-69.

Clapp R.B. & Hornberger G.M. (1978) Empirical equations for some soil hydraulic properties. *Water Resources Research* 14, 601-604.

Claussen M. (1997) Modeling bio-geophysical feedback in the African and Indian monsoon region. *Climate Dynamics* 13, 247-257.

Cook A.C., Tissue D.T., Roberts S.W. & Oechel W.C. (1998) Effects of long-term elevated [CO_2] from natural CO_2-springs on *Nardus stricta*: Photosynthesis, biochemistry, growth and phenology. *Plant, Cell and Environment* 21, 417-425.

Corlett R.T. (2011) Impacts of warming on tropical lowland rainforests. *Trends in Ecology & Evolution* 26, 606-613.

Cowan I.R. (1978) Stomatal behaviour and environment. *Advances in Botanical Research* 4, 117-228.

Cramer W., Bondeau A., Woodward F.I., Prentice I.C., Betts R.A., Brovkin V., Cox P.M., Fisher V., Foley J.A., Friend A.D., Kucharik C., Lomas M.R., Ramankutty N., Sitch S., Smith B., White A. & Young-Molling C. (2001) Global response of terrestrial ecosystem structure and function to CO_2 and climate change: Results from six dynamic global vegetation models. *Global Change Biology* 7, 357-373.

De Boer H.J., Lammertsma E.I., Wagner-Cremer F., Dilcher D.L., Wassen M.J. & Dekker S.C. (2011) Climate forcing due to optimization of maximal leaf conductance in subtropical vegetation under rising CO_2. *PNAS* 108, 4041-4046.

De Boer H.J., Eppinga M.B., Wassen M.J. & Dekker S.C. (2012) A critical transition in leaf evolution facilitated the cretaceous angiosperm revolution. *Nature Communications* 3, 1221.

De Pury D.G.G. & Farquhar G.D. (1997) Simple scaling of photosynthesis from leaves to canopies without the errors of big-leaf models. *Plant, Cell & Environment* 20, 537-557.

Dekker S.C., Bouten W. & Bosveld F.C. (2001) On the information content of forest transpiration measurements for identifying canopy conductance model parameters. *Hydrological Processes* 15, 2821-2832.

Dekker S.C., De Boer H.J., Brovkin V., Fraedrich K., Wassen M.J. & Rietkerk M.G. (2010) Biogeophysical feedbacks trigger shifts in the modelled vegetation-atmosphere system at multiple scales. *Biogeosciences* 7, 1237-1245.

Dekker S.C., Vrugt J.A. & Elkington R.J. (2012) Significant variation in vegetation characteristics and dynamics from ecohydrological optimality of net carbon profit. *Ecohydrology* 5, 1-18.

DeLucia E.H., George K. & Hamilton J.G. (2002) Radiation-use efficiency of a forest exposed to elevated concentrations of atmospheric carbon dioxide. *Tree Physiology* 22, 1003-1010.

Denmead O.T. & Shaw R.H. (1962) Availability of soil water to plants as affected by soil moisture content and meteorological conditions. *Agronomy Journal* 54, 385-390.

Dermody O., Long S.P. & DeLucia E.H. (2006) How does elevated CO_2 or ozone affect the leaf-area index of soybean when applied independently? *New Phytologist* 169, 145-155.

Dewar R.C., Franklin O., Makela A., McMurtrie R.E. & Valentine H.T. (2009) Optimal function explains forest responses to global change. *BioScience* 59, 127-139.

Dewar R.C., Tarvainen L., Parker K., Wallin G. & McMurtrie R.E. (2012) Why does leaf nitrogen decline within tree canopies less rapidly than light? An explanation from optimization subject to a lower bound on leaf mass per area. *Tree Physiology* 32, 520-534.

Diaz S., Hodgson J.G., Thompson K., Cabido M., Cornelissen J.H.C., Jalili A., Montserrat-Marti G., Grime J.P., Zarrinkamar F. & Asri Y. (2004) The plant traits that drive ecosystems: Evidence from three continents. *Journal of Vegetation Science* 15, 295-304.

Drewry D.T., Kumar P., Long S., Bernacchi C., Liang X. & Sivapalan M. (2010) Ecohydrological responses of dense canopies to environmental variability: 1.

Interplay between vertical structure and photosynthetic pathway. *Journal of Geophysical Research: Biogeosciences* 115, G04022.

Drewry D.T., Kumar P., Long S., Bernacchi C., Liang X. & Sivapalan M. (2010) Ecohydrological responses of dense canopies to environmental variability: 2. Role of acclimation under elevated CO_2. *Journal of Geophysical Research: Biogeosciences* 115, G04023.

Dukes J.S. & Mooney H.A. (1999) Does global change increase the success of biological invaders? *Trends in Ecology & Evolution* 14, 135-139.

Dybzinski R., Farrior C., Wolf A., Reich P.B. & Pacala S.W. (2011) Evolutionarily stable strategy carbon allocation to foliage, wood, and fine roots in trees competing for light and nitrogen: An analytically tractable, individual-based model and quantitative comparisons to data. *The American Naturalist* 177, 153-166.

Eltahir E.A.B. & Bras R.L. (1996) Precipitation recycling. *Reviews of Geophysics* 34, 367-378.

Evans J.R. (1989) Photosynthesis and nitrogen relationships in leaves of C_3 plants. *Oecologia* 78, 9-19.

Evans J.R. & Poorter H. (2001) Photosynthetic acclimation of plants to growth irradiance: The relative importance of specific leaf area and nitrogen partitioning in maximizing carbon gain. *Plant, Cell & Environment* 24, 755-767.

Falster D.S. & Westoby M. (2003a) Leaf size and angle vary widely across species: What consequences for light interception? *New Phytologist* 158, 509-525.

Falster D.S. & Westoby M. (2003b) Plant height and evolutionary games. *Trends in Ecology & Evolution* 18, 337-343.

Farquhar G.D., Von Caemmerer S. & Berry J.A. (1980) A biochemical model of photosynthetic CO_2 assimilation in leaves of C_3 species. *Planta* 149, 78-90.

Farrior C.E. (2014) Competitive optimization models, attempting to understand the diversity of life. *New Phytologist* 203, 1025-1027.

Farrior C.E., Dybzinski R., Levin S.A. & Pacala S.W. (2013) Competition for water and light in closed-canopy forests: A tractable model of carbon allocation with implications for carbon sinks. *The American Naturalist* 181, 314-330.

Farrior C.E., Rodriguez-Iturbe I., Dybzinski R., Levin S.A. & Pacala S.W. (2015) Decreased water limitation under elevated CO_2 amplifies potential for forest carbon sinks. *Proceedings of the National Academy of Sciences*201506262.

Field C.B., Jackson R.B. & Mooney H.A. (1995) Stomatal responses to increased CO_2: Implications from the plant to the global scale. *Plant, Cell & Environment* 18, 1214-1225.

Field C. (1983) Allocating leaf nitrogen for the maximization of carbon gain: Leaf age as a control on the allocation program. *Oecologia* 56, 341-347.

Fordham M., Barnes J.D., Bettarini I., Polle A., Slee N., Raines C., Miglietta F. & Raschi A. (1997) The impact of elevated CO_2 on growth and photosynthesis in *Agrostis canina* L. ssp. *monteluccii* adapted to contrasting atmospheric CO_2 concentrations. *Oecologia* 110, 169-178.

Frak E., Le Roux X., Millard P., Dreyer E., Jaouen G., Saint-Joanis B. & Wendler R. (2001) Changes in total leaf nitrogen and partitioning of leaf nitrogen drive photosynthetic acclimation to light in fully developed walnut leaves. *Plant, Cell & Environment* 24, 1279-1288.

Franklin O., Johansson J., Dewar R.C., Dieckmann U., McMurtrie R.E., Brannstrom A. & Dybzinski R. (2012) Modeling carbon allocation in trees: A search for principles. *Tree Physiology* 32, 648-666.

Franklin O. (2007) Optimal nitrogen allocation controls tree responses to elevated CO_2. *New Phytologist* 174, 811-822.

Friend A.D., Schugart H.H. & Running S.W. (1993) A physiology-based gap model of forest dynamics. *Ecology*792-797.

Friend A.D., Stevens A.K., Knox R.G. & Cannell M.G.R. (1997) A process-based, terrestrial biosphere model of ecosystem dynamics (hybrid v3. 0). *Ecological Modelling* 95, 249-287.

Friend A.D. & Cox P.M. (1995) Modelling the effects of atmospheric CO_2 on vegetation-atmosphere interactions. *Agricultural and Forest Meteorology* 73, 285-295.

Galloway J.N., Dentener F.J., Capone D.G., Boyer E.W., Howarth R.W., Seitzinger S.P., Asner G.P., Cleveland C.C., Green P.A., Holland E.A., Karl D.M., Michaelis A.F., Porter J.H., Townsend A.R. & Vorosmarty C.J. (2004) Nitrogen cycles: Past, present, and future. *Biogeochemistry* 70, 153-226.

Gersani M., O'Brien E.E., Maina G.M. & Abramsky Z. (2001) Tragedy of the commons as a result of root competition. *Journal of Ecology* 89, 660-669.

Givnish T.J. (1982) On the adaptive significance of leaf height in forest herbs. *The American Naturalist* 120, 353-381.

Goudriaan J. (1988) The bare bones of leaf-angle distribution in radiation models for canopy photosynthesis and energy exchange. *Agricultural and Forest Meteorology* 43, 155-169.

Goudriaan J. & Unsworth M.H. (1990) Implications of increasing carbon dioxide and climate change for agricultural productivity and water resources. *ASA Special Publication* 53, 111-130.

Grime J.P. (1977) Evidence for the existence of three primary strategies in plants and its relevance to ecological and evolutionary theory. *American Naturalist*1169-1194.

Grime J.P. (1973) Competitive exclusion in herbaceous vegetation. *Nature, UK* 242, 344-347.

Hardin G. (1968) The tragedy of the commons. *Science* 162, 1243-1248.

Harley P.C., Thomas R.B., Reynolds J.F. & Strain B.R. (1992) Modelling photosynthesis of cotton grown in elevated CO_2. *Plant, Cell & Environment* 15, 271-282.

Haworth M., Elliott-Kingston C. & McElwain J.C. (2013) Co-ordination of physiological and morphological responses of stomata to elevated [CO_2] in vascular plants. *Oecologia* 171, 71-82.

Haworth M., Elliott-Kingston C. & McElwain J.C. (2011) Stomatal control as a driver of plant evolution. *Journal of Experimental Botany* 62, 2419-2423.

Hess L. & De Kroon H. (2007) Effects of rooting volume and nutrient availability as an alternative explanation for root self/non-self discrimination. *Journal of Ecology* 95, 241-251.

Hikosaka K., Ishikawa K., Borjigidai A., Muller O. & Onoda Y. (2006) Temperature acclimation of photosynthesis: Mechanisms involved in the changes in temperature dependence of photosynthetic rate. *Journal of Experimental Botany* 57, 291-302.

Hikosaka K. & Terashima I. (1996) Nitrogen partitioning among photosynthetic components and its consequence in sun and shade plants. *Functional Ecology*335-343.

Hikosaka K., Yamano T., Nagashima H. & Hirose T. (2003) Light-acquisition and use of individuals as influenced by elevated CO_2 in even-aged monospecific stands of *Chenopodium album*. *Functional Ecology* 17, 786-795.

Hikosaka K. & Hirose T. (1997) Leaf angle as a strategy for light competition: Optimal and evolutionarily stable light-extinction coefficient within a leaf canopy. *Ecoscience* 4, 501-507.

Hikosaka K., Nagashima H., Harada Y. & Hirose T. (2001) A simple formulation of interaction between individuals competing for light in a monospecific stand. *Functional Ecology* 15, 642-646.

Hikosaka K. & Terashima I. (1995) A model of the acclimation of photosynthesis in the leaves of C_3 plants to sun and shade with respect to nitrogen use. *Plant, Cell & Environment* 18, 605-618.

Hikosaka K. (1997) Modelling optimal temperature acclimation of the photosynthetic apparatus in C_3 plants with respect to nitrogen use. *Annals of Botany* 80, 721-730.

Hikosaka K. & Hirose T. (1998) Leaf and canopy photosynthesis of C_3 plants at elevated CO_2 in relation to optimal partitioning of nitrogen among photosynthetic components: Theoretical prediction. *Ecological Modelling* 106, 247-259.

Hikosaka K. (2005) Leaf canopy as a dynamic system: Ecophysiology and optimality in leaf turnover. *Annals of Botany* 95, 521-533.

Hikosaka K., Ishikawa K., Borjigidai A., Muller O. & Onoda Y. (2006) Temperature acclimation of photosynthesis: Mechanisms involved in the changes in temperature dependence of photosynthetic rate. *Journal of Experimental Botany* 57, 291-302.

Hirose T., Ackerly D.D., Traw M.B., Ramseier D. & Bazzaz F.A. (1997) CO_2 elevation, canopy photosynthesis, and optimal leaf area index. *Ecology* 78, 2339-2350.

Hirose T. & Werger M.J.A. (1987) Maximizing daily canopy photosynthesis with respect to the leaf nitrogen allocation pattern in the canopy. *Oecologia* 72, 520-526.

Hirose T., Werger M.J.A., Pons T.L. & Van Rheenen J.W.A. (1988) Canopy structure and leaf nitrogen distribution in a stand of *Lysimachia vulgaris* L. as influenced by stand density. *Oecologia* 77, 145-150.

Hoffmann A.A. & Sgrò C.M. (2011) Climate change and evolutionary adaptation. *Nature* 470, 479-485.

Huh M.K. (2013) Genetic diversity and population structure in east Asian populations of *Plantago asiatica*. *Journal of Life Science* 23, 728-735.

Iio A., Hikosaka K., Anten N.P.R., Nakagawa Y. & Ito A. (2014) Global dependence of field-observed leaf area index in woody species on climate: A systematic review. *Global Ecology and Biogeography* 23, 274-285.

IPCC. (2014) Climate change 2014. impacts, adaptation and vulnerability. working group II contribution to the fifth assessment report of the intergovernmental panel on climate change. Cambridge University Press, Cambridge, United Kingdom.

IPCC. (2007) Summary for policymakers. in: Climate change 2007: The physical science basis. contribution of working group I to the fourth assessment report of the intergovernmental panel on climate change. Cambridge University Press, Cambridge.

Ishikawa K., Onoda Y. & Hikosaka K. (2007) Intraspecific variation in temperature dependence of gas exchange characteristics among *Plantago asiatica* ecotypes from different temperature regimes. *New Phytologist* 176, 356-364.

Johnson F.H., Eyring H. & Williams R.W. (1942) The nature of enzyme inhibitions in bacterial luminescence: Sulfanilamide, urethane, temperature and pressure. *Journal of Cellular and Comparative Physiology* 20, 247-268.

Jump A.S. & Penuelas J. (2005) Running to stand still: Adaptation and the response of plants to rapid climate change. *Ecology Letters* 8, 1010-1020.

Katul G., Manzoni S., Palmroth S. & Oren R. (2010) A stomatal optimization theory to describe the effects of atmospheric CO_2 on leaf photosynthesis and transpiration. *Annals of Botany* 105, 431-442.

Keenan T.F., Hollinger D.Y., Bohrer G., Dragoni D., Munger J.W., Schmid H.P. & Richardson A.D. (2013) Increase in forest water-use efficiency as atmospheric carbon dioxide concentrations rise. *Nature* 499, 324-327.

Körner C. & Miglietta F. (1994) Long term effects of naturally elevated CO_2 on mediterranean grassland and forest trees. *Oecologia* 99, 343-351.

Kull O. (2002) Acclimation of photosynthesis in canopies: Models and limitations. *Oecologia* 133, 267-279.

Lamarque J., Dentener F., McConnell J., Ro C.U., Shaw M., Vet R., Bergmann D., Cameron-Smith P., Dalsoren S., Doherty R., Faluvegi G., Ghan S.J., Josse B., Lee Y.H., MacKenzie I.A., Plummer D., Shindell D.T., Skeie R.B., Stevenson D.S., Strode S., Zeng G., Curran M., Dahl-Jensen D., Das S., Fritzsche D. & Nolan M. (2013) Multi-model mean nitrogen and sulfur deposition from the atmospheric chemistry and climate model intercomparison project (ACCMIP): Evaluation of historical and projected future changes. *Atmos.Chem.Phys* 13, 7997-8018.

Lambers H., Chapin III F.S. & Pons T.L. (2008) Plant physiological ecology. Springer, New York, USA.

Lammertsma E.I., De Boer H.J., Dekker S.C., Dilcher D.L., Lotter A.F. & Wagner-Cremer F. (2011) Global CO_2 rise leads to reduced maximum stomatal conductance in Florida vegetation. *PNAS* 108, 4035-4040.

Leakey A.D.B., Bernacchi C.J., Ort D.R. & Long S.P. (2006) Long-term growth of soybean at elevated [CO_2] does not cause acclimation of stomatal conductance under fully open-air conditions. *Plant, Cell & Environment* 29, 1794-1800.

Leakey A.D.B. & Lau J.A. (2012) Evolutionary context for understanding and manipulating plant responses to past, present and future atmospheric [CO_2]. *Philosophical Transactions of the Royal Society of London. Biological Sciences* 367, 613-629.

Levis S., Foley J.A. & Pollard D. (2000) Large-scale vegetation feedbacks on a doubled CO_2 climate. *Journal of Climate* 13, 1313-1325.

Lloyd J. & Farquhar G.D. (2008) Effects of rising temperatures and [CO_2] on the physiology of tropical forest trees. *Philosophical Transactions of the Royal Society B: Biological Sciences* 363, 1811.

Lloyd J., Patiño S., Paiva R.Q., Nardoto G.B., Quesada C.A., Santos A.J.B., Baker T.R., Brand W.A., Hilke I., Gielmann H., Raessler M., Luizão F.J., Martinelli L.A. & Mercado L.M. (2010) Optimisation of photosynthetic carbon gain and within-canopy gradients of associated foliar traits for Amazon forest trees. *Biogeosciences* 7, 1833-1859.

Long S.P. (1991) Modification of the response of photosynthetic productivity to rising temperature by atmospheric CO_2 concentrations: Has its importance been underestimated? *Plant, Cell & Environment* 14, 729-739.

Long S.P., Ainsworth E.A., Rogers A. & Ort D.R. (2004) Rising atmospheric carbon dioxide: Plants FACE the future*. *Annu.Rev.Plant Biol.* 55, 591-628.

Luo Y., Medlyn B., Hui D., Ellsworth D., Reynolds J. & Katul G. (2001) Gross primary productivity in duke forest: Modeling synthesis of CO_2 experiment and eddy-flux data. *Ecological Applications* 11, 239-252.

Lutze J.L. & Gifford R.M. (1998) Carbon accumulation, distribution and water use of *Danthonia richardsonii* swards in response to CO_2 and nitrogen supply over four years of growth. *Global Change Biology* 4, 851-861.

Maherali H., Pockman W.T. & Jackson R.B. (2004) Adaptive variation in the vulnerability of woody plants to xylem cavitation. *Ecology* 85, 2184-2199.

Makela A., Givnish T.J., Berninger F., Buckley T.N., Farquhar G.D. & Hari P. (2002) Challenges and opportunities of the optimality approach in plant ecology. *Silva Fennica* 36, 605-614.

Makela A., Valentine H.T. & Helmisaari H.S. (2008) Optimal co-allocation of carbon and nitrogen in a forest stand at steady state. *New Phytologist* 180, 114-123.

Manea A. & Leishman M.R. (2011) Competitive interactions between native and invasive exotic plant species are altered under elevated carbon dioxide. *Oecologia* 165, 735-744.

Maynard Smith J. (1974) The theory of games and the evolution of animal conflicts. *Journal of Theoretical Biology* 47, 209-221.

Maynard-Smith J. (1978) Optimization theory in evolution. *Annual Review of Ecology and Systematics* 9, 31-56.

McMurtrie R., Norby R.J., Medlyn B.E., Dewar R.C., Pepper D.A., Reich P.B. & Barton G.V.M. (2008) Why is plant-growth response to elevated CO_2 amplified when water is limiting, but reduced when nitrogen is limiting? A growth-optimisation hypothesis. *Functional Plant Biology* 35, 521-534.

McNickle G.G. & Dybzinski R. (2013) Game theory and plant ecology. *Ecology Letters* 16, 545-555.

Medlyn B.E. (1996) The optimal allocation of nitrogen within the C_3 photosynthetic system at elevated CO_2. *Functional Plant Biology* 23, 593-603.

Medlyn B.E., Duursma R.A., Eamus D., Ellsworth D.S., Prentice I.C., Barton C.V.M., Crous K.Y., de Angelis P., Freeman M. & Wingate L. (2011) Reconciling the optimal and empirical approaches to modelling stomatal conductance. *Global Change Biology* 17, 2134-2144.

Medvigy D., Wofsy S.C., Munger J.W. & Moorcroft P.R. (2010) Responses of terrestrial ecosystems and carbon budgets to current and future environmental variability. *Proceedings of the National Academy of Sciences of the United States of America* 107, 8275-8280.

Moorcroft P.R., Hurtt G.C. & Pacala S.W. (2001) A method for scaling vegetation dynamics: The ecosystem demography model (ED). *Ecological Monographs* 71, 557-586.

Moorcroft P.R. (2003) Recent advances in ecosystem-atmosphere interactions: An ecological perspective. *Proceedings. Biological Sciences / the Royal Society* 270, 1215-1227.

Nakamura I., Onoda Y., Matsushima N., Yokoyama J., Kawata M. & Hikosaka K. (2011) Phenotypic and genetic differences in a perennial herb across a natural gradient of CO_2 concentration. *Oecologia* 165, 809-818.

Nicotra A.B., Atkin O.K., Bonser S.P., Davidson A.M., Finnegan E.J., Mathesius U., Poot P., Purugganan M.D., Richards C.L., Valladares F. & van Kleunen M. (2010) Plant phenotypic plasticity in a changing climate. *Trends in Plant Science* 15, 684-692.

Niinemets Ü. (2010) A review of light interception in plant stands from leaf to canopy in different plant functional types and in species with varying shade tolerance. *Ecological Research* 25, 693-714.

Niinemets Ü. (2007) Photosynthesis and resource distribution through plant canopies. *Plant, Cell & Environment* 30, 1052-1071.

Niinemets Ü & Anten N.P.R. (2009) In *Photosynthesis in Silico* Packing the photosynthetic machinery: From leaf to canopy. pp. 363-399. Springer, Dordrecht, The Netherlands.

Norby R.J. & Zak D.R. (2011) Ecological lessons from free-air CO_2 enrichment (FACE) experiments. *Annual Review of Ecology, Evolution, and Systematics* 42, 181-203.

Oguchi R., Hikosaka K. & Hirose T. (2005) Leaf anatomy as a constraint for photosynthetic acclimation: Differential responses in leaf anatomy to increasing growth irradiance among three deciduous trees. *Plant, Cell & Environment* 28, 916-927.

Oguchi R., Hikosaka K. & Hirose T. (2003) Does the photosynthetic light-acclimation need change in leaf anatomy? *Plant, Cell & Environment* 26, 505-512.

Oguntunde P.G., Olukunle O.J., Ijatuyi O.A. & Olufayo A.A. (2007) A semi-empirical model for estimating surface albedo of wetland rice field. *International Commission of Agricultural Engineering* 9, .

Ollinger S.V., Richardson A.D., Martin M.E., Hollinger D.Y., Frolking S.E., Reich P.B., Plourde L.C., Katul G.G., Munger J.W., Oren R., Smith M.L., Paw U.K.T., Bolstad P.V., Cook B.D., Day M.C., Martin T.A., Monson R.K. & Schmid H.P. (2008) Canopy nitrogen, carbon assimilation, and albedo in temperate and boreal forests: Functional relations and potential climate feedbacks. *Proceedings of the National Academy of Sciences of the United States of America* 105, 19336-19341.

Onoda Y., Hirose T. & Hikosaka K. (2009) Does leaf photosynthesis adapt to CO_2-enriched environments? An experiment on plants originating from three natural CO_2 springs. *New Phytologist* 182, 698-709.

Onoda Y., Hirose T. & Hikosaka K. (2007) Effect of elevated CO_2 levels on leaf starch, nitrogen and photosynthesis of plants growing at three natural CO_2 springs in Japan. *Ecological Research* 22, 475-484.

Onoda Y., Hikosaka K. & Hirose T. (2005) The balance between RuBP carboxylation and RuBP regeneration: A mechanism underlying the interspecific variation in

acclimation of photosynthesis to seasonal change in temperature. *Functional Plant Biology* 32, 903-910.

Ordoñez J.C., Van Bodegom P.M., Witte J.M., Wright I.J., Reich P.B. & Aerts R. (2009) A global study of relationships between leaf traits, climate and soil measures of nutrient fertility. *Global Ecology and Biogeography* 18, 137-149.

Oren R., Sperry J.S., Katul G.G., Pataki D.E., Ewers B.E., Phillips N. & Schäfer K.V.R. (1999) Survey and synthesis of intra-and interspecific variation in stomatal sensitivity to vapour pressure deficit. *Plant, Cell & Environment* 22, 1515-1526.

Osada N., Onoda Y. & Hikosaka K. (2010) Effects of atmospheric CO_2 concentration, irradiance, and soil nitrogen availability on leaf photosynthetic traits of *Polygonum sachalinense* around natural CO_2 springs in northern Japan. *Oecologia* 164, 41-52.

Owensby C.E., Ham J., Knapp A. & Auen L. (1999) Biomass production and species composition change in a tallgrass prairie ecosystem after long-term exposure to elevated atmospheric CO_2. *Global Change Biology* 5, 497-506.

Parker G.A. & Maynard-Smith J.M. (1990) Optimality theory in evolutionary biology. *Nature* 348, 27-33.

Parmesan C. (2006) Ecological and evolutionary responses to recent climate change. *Annual Review of Ecology, Evolution and Systemetics* 37, 637-669.

Parmesan C. & Yohe G. (2003) A globally coherent fingerprint of climate change impacts across natural systems. *Nature* 421, 37-42.

Pearcy R.W. (1999) In Handbook of Functional Plant Ecology: Responses of plants to heterogeneous light environments. pp. 269-314. Marcel Dekker, New York, USA.

Pearcy R.W. & Sims D.A. (1994) In Photosynthetic acclimation to changing light environments: Scaling from the leaf to the whole plant. pp. 145-174. Academic Press, San Diego, USA.

Peltoniemi M.S., Duursma R.A. & Medlyn B.E. (2012) Co-optimal distribution of leaf nitrogen and hydraulic conductance in plant canopies. *Tree Physiology* 32, 510-519.

Penning K. (2014) The effect of density on the degree and type of light interception in different canopy heights of soybean (*Glycine max*). *MSc Thesis, Wageningen University, Wageningen, The Netherlands*.

Polle A., McKee I. & Blaschke L. (2001) Altered physiological and growth responses to elevated [CO_2] in offspring from holm oak (*Quercus ilex* L.) mother trees with lifetime exposure to naturally elevated [CO_2]. *Plant, Cell & Environment* 24, 1075-1083.

Poorter H. (1998) Do slow-growing species and nutrient-stressed plants respond relatively strongly to elevated CO_2? *Global Change Biology* 4, 693-697.

Poorter H. (1993) Interspecific variation in the growth response of plants to an elevated ambient CO_2 concentration. *Vegetatio* 104, 77-97.

Reich P.B., Wright I.J., Cavender-Bares J., Craine J.M., Oleksyn J., Westoby M. & Walters M.B. (2003) The evolution of plant functional variation: Traits, spectra, and strategies. *International Journal of Plant Sciences* 164, S143-S164.

Reich P.B., Falster D.S., Ellsworth D.S., Wright I.J., Westoby M., Oleksyn J. & Lee T.D. (2009) Controls on declining carbon balance with leaf age among 10 woody species in australian woodland: Do leaves have zero daily net carbon balances when they die? *New Phytologist* 183, 153-166.

Reich P.B. (2012) Key canopy traits drive forest productivity. *Proceedings.Biological Sciences / the Royal Society* 279, 2128-2134.

Riechert S.E. & Hammerstein P. (1983) Game theory in the ecological context. *Annual Review of Ecology and Systematics.* 14, 377-409.

Rietkerk M., Brovkin V., van Bodegom P.M., Claussen M., Dekker S.C., Dijkstra H.A., Goryachkin S.V., Kabat P., van Nes E.H., Neutel A., Nicholson S.E., Nobre C., Petoukhov V., Provenzale A., Scheffer M. & Seneviratne S.I. (2011) Local ecosystem feedbacks and critical transitions in the climate. *Ecological Complexity* 8, 223-228.

Rogers A., Allen D.J., Davey P.A., Morgan P.B., Ainsworth E.A., Bernacchi C.J., Cornic G., Dermody O., Dohleman F.G., Heaton E., Mahoney J., Zhu X.G., Delucia E.H., Ort D.R. & Long S.P. (2004) Leaf photosynthesis and carbohydrate dynamics of soybeans grown throughout their life-cycle under free-air carbon dioxide enrichment. *Plant, Cell & Environment* 27, 449-458.

Rogers G.S., Milham P.J., Gillings M. & Conroy J.P. (1996) Sink strength may be the key to growth and nitrogen responses in N-deficient wheat at elevated CO_2. *Functional Plant Biology* 23, 253-264.

Roumet C., Laurent G. & Roy J. (1999) Leaf structure and chemical composition as affected by elevated CO_2: Genotypic responses of two perennial grasses. *New Phytologist* 143, 73-81.

Running S.W. & Coughlan J.C. (1988) A general model of forest ecosystem processes for regional applications I. Hydrologic balance, canopy gas exchange and primary production processes. *Ecological Modelling* 42, 125-154.

Sage R.F. (1994) Acclimation of photosynthesis to increasing atmospheric CO_2: The gas exchange perspective. *Photosynthesis Research* 39, 351-368.

Scheffer M., Holmgren M., Brovkin V. & Claussen M. (2005) Synergy between small- and large-scale feedbacks of vegetation on the water cycle. *Global Change Biology* 11, 1003-1012.

Schieving F., Werger M.J.A. & Hirose T. (1992) Canopy structure, nitrogen distribution and whole canopy photosynthetic carbon gain in growing and flowering stands of tall herbs. *Vegetatio* 102, 173-181.

Schieving F. & Poorter H. (1999) Carbon gain in multispecies canopy: The role of specific leaf area and photosynthetic nitrogen-use efficiency in the tragedy of the commons. *New Phytologist* 143, 201-211.

Schlesinger W.H. & Andrews J.A. (2000) Soil respiration and the global carbon cycle. *Biogeochemistry* 48, 7-20.

Schmitt J., Dudley S.A. & Pigliucci M. (1999) Manipulative approaches to testing adaptive plasticity: Phytochrome-mediated shade-avoidance responses in plants. *The American Naturalist* 154, S43-S54.

Schymanski S.J., Roderick M.L., Sivapalan M., Hutley L.B. & Beringer J. (2007) A test of the optimality approach to modelling canopy properties and CO_2 uptake by natural vegetation. *Plant, Cell & Environment* 30, 1586-1598.

Sellers P.J., Dickinson R.E., Randall D.A., Betts A.K., Hall F.G., Berry J.A., Collatz G.J., Denning A.S., Mooney H.A., Nobre C.A., Sato N., Field C.B. & Henderson-Sellers A. (1997) Modeling the exchanges of energy, water, and carbon between continents and the atmosphere. *Science* 275, 502-509.

Shao Y. & Irannejad P. (1999) On the choice of soil hydraulic models in land-surface schemes. *Boundary-Layer Meteorology* 90, 83-115.

Sitch S., Smith B., Prentice I.C., Arneth A., Bondeau A., Cramer W., Kaplan J.O., Levis S., Lucht W., Sykes M.T., Thonicke K. & Venevsky S. (2003) Evaluation of ecosystem dynamics, plant geography and terrestrial carbon cycling in the LPJ dynamic global vegetation model. *Global Change Biology* 9, 161-185.

Song Q., Zhang G. & Zhu X. (2013) Optimal crop canopy architecture to maximise canopy photosynthetic CO2 uptake under elevated CO_2 – a theoretical study using a mechanistic model of canopy photosynthesis. *Functional Plant Biology* 40, 108-124.

Spitters C.J.T., Toussaint H.A.J.M. & Goudriaan J. (1986) Separating the diffuse and direct component of global radiation and its implications for modeling canopy photosynthesis part I. Components of incoming radiation. *Agricultural and Forest Meteorology* 38, 217-229.

Sterck F., Markesteijn L., Schieving F. & Poorter L. (2011) Functional traits determine trade-offs and niches in a tropical forest community. *Proceedings of the National Academy of Sciences* 108, 20627-20632.

Sterck F. & Schieving F. (2011) Modelling functional trait acclimation for trees of different height in a forest light gradient: Emergent patterns driven by carbon gain maximization. *Tree Physiology* 31, 1024-1037.

Tetens O. (1930) Über einige meteorologische begriffe z. *Geophysics* 6, 297-309.

Tor-ngern P., Oren R., Ward E.J., Palmroth S., McCarthy H.R. & Domec J. (2015) Increases in atmospheric CO_2 have little influence on transpiration of a temperate forest canopy. *New Phytologist* 205, 518-525.

Trouwborst G., Hogewoning S.W., Harbinson J. & van Ieperen W. (2011) Photosynthetic acclimation in relation to nitrogen allocation in cucumber leaves in response to changes in irradiance. *Physiologia Plantarum* 142, 157-169.

Tuzet A., Perrier A. & Leuning R. (2003) A coupled model of stomatal conductance, photosynthesis and transpiration. *Plant, Cell and Environment* 26, 1097-1116.

Valladares F. (2008) A mechanistic view of the capacity of forest to cope with climate change. *Managing Forest Ecosystems* 17, 15-40.

Van den Hurk B.J.J.M., Viterbo P. & Los S.O. (2003) Impact of leaf area index sesonality on the annual land surface evaporation in a global circulation model. *Journal of Geophysical Research* 108, 4191-4199.

Van Heerwaarden C.C., Vilà-Guerau de Arellano J., Moene A.F. & Holtslag A.A.M. (2009) Interactions between dry-air entrainment, surface evaporation and convective boundary-layer development. *Quarterly Journal of the Royal Meteorological Society* 135, 1277-1291.

Van Heerwaarden C.C., Vilà-Guerau de Arellano J., Gounou A., Guichard F. & Couvreux F. (2010) Understanding the daily cycle of evapotranspiration: A method to quantify the influence of forcings and feedbacks. *Journal of Hydrometeorology* 11, 1405-1422.

Van Ittersum M., Leffelaar P., Van Keulen H., Kropff M., Bastiaans L. & Goudriaan J. (2003) On approaches and applications of the Wageningen crop models. *European Journal of Agronomy* 18, 201-234.

Van Loon M.P., Schieving F., Rietkerk M., Dekker S.C., Sterck F. & Anten N.P.R. (2014) How light competition between plants affects their response to climate change. *New Phytologist* 203, 1253–1265.

Van Wijk M.T. & Bouten W. (2001) Towards understanding tree root profiles: Simulating hydrologically optimal strategies for root distribution. *Hydrology and Earth System Sciences Discussions* 5, 629-644.

Vermeulen P.J. (2015) On selection for flowering time plasticity in response to density. *New Phytologist* 205, 429-439.

Vilà-Guerau de Arellano J., van Heerwaarden C.C., Van Stratum B.J.H. & Van den Dries K. (2015) Atmospheric boundary layer: Integrating air chemistry and land interactions. Cambridge: Cambridge University Press, .

Vincent T.L. & Brown J.S. (1984) Stability in an evolutionary game. *Theoretical Population Biology* 26, 408-427.

Violle C., Navas M., Vile D., Kazakou E., Fortunel C., Hummel I. & Garnier E. (2007) Let the concept of trait be functional! *Oikos* 116, 882-892.

Visser M.E. (2008) Keeping up with a warming world; assessing the rate of adaptation to climate change. *Proceedings. Biological Sciences / the Royal Society* 275, 649-659.

Vodnik D., Pfanz H., Maček I., Kastelec D., Lojen S. & Batič F. (2002) Photosynthesis of cockspur [*Echinochloa crus-galli* (L.) beauv.] at sites of naturally elevated CO_2 concentration. *Photosynthetica* 40, 575-579.

Von Caemmerer S. (2000) Biochemical models of leaf photosynthesis. Csiro publishing, Collingwood, Victoria, Australia.

Von Caemmerer S., Ghannoum O., Conroy J.P., Clark H. & Newton P.C.D. (2001) Photosynthetic responses of temperate species to free air CO_2 enrichment (FACE) in a grazed new zealand pasture. *Functional Plant Biology* 28, 439-450.

Weiner J. (1990) Asymmetric competition in plant populations. *Trends in Ecology & Evolution* 5, 360-364.

Weng E.S., Malyshev S., Lichstein J.W., Farrior C.E., Dybzinski R., Zhang T., Shevliakova E. & Pacala S.W. (2015) Scaling from individual trees to forests in an earth system modeling framework using a mathematically tractable model of height-structured competition. *Biogeosciences* 12, 2655-2694.

Westoby M., Cornwell W.K. & Falster D.S. (2012) An evolutionary attractor model for sapwood cross section in relation to leaf area. *Journal of Theoretical Biology* 303, 98-109.

Wilson K., Goldstein A., Falge E., Aubinet M., Baldocchi D., Berbigier P., Bernhofer C., Ceulemans R., Dolman H., Field C., Grelle A., Ibrom A., Law B.E., Kowalski A., Meyers T., Moncrieff J., Monson R., Oechel W., Tenhunen J., Valentini R. & Verma S. (2002) Energy balance closure at FLUXNET sites. *Agricultural and Forest Meteorology* 113, 223-243.

Wong S.C., Cowan I.R. & Farquhar G.D. (1979) Stomatal conductance correlates with photosynthetic capacity. *Nature*.

Woodrow I.E. (1994) Optimal acclimation of the C_3 photosynthetic system under enhanced CO_2. *Photosynthesis Research* 39, 401-412.

Xu C., Fisher R., Wullschleger S.D., Wilson C.J., Cai M. & McDowell N.G. (2012) Toward a mechanistic modeling of nitrogen limitation on vegetation dynamics. *PloS One* 7, e37914.

Yamori W., Noguchi K., Hikosaka K. & Terashima I. (2010) Phenotypic plasticity in photosynthetic temperature acclimation among crop species with different cold tolerances. *Plant Physiology* 152, 388-399.

Yamori W., Noguchi K., Hikosaka K. & Terashima I. (2009) Cold-tolerant crop species have greater temperature homeostasis of leaf respiration and photosynthesis than cold-sensitive species. *Plant and Cell Physiology* 50, 203-215.

Yin X. & Struik P.C. (2010) Modelling the crop: From system dynamics to systems biology. *Journal of Experimental Botany* 61, 2171-2183.

Zeng N. & Yoon J. (2009) Expansion of the world's deserts due to vegetation-albedo feedback under global warming. *Geophysical Research Letters* 36, .

Zhang Z., Xue Y., MacDonald G., Cox P.M. & Collatz G.J. (2015) Investigation of north American vegetation variability under recent climate: A study using the SSiB4/TRIFFID biophysical/dynamic vegetation model. *Journal of Geophysical Research: Atmospheres* 120, 1300-1321.

Ziska L.H., Reeves J.B. & Blank B. (2005) The impact of recent increases in atmospheric CO_2 on biomass production and vegetative retention of cheatgrass (*Bromus tectorum*): Implications for fire disturbance. *Global Change Biology* 11, 1325-1332.

Ziska L.H. (2011) Global climate change and carbon dioxide: Assessing weed biology and management. In *Handbook of Climate Change and Agroecosystems: Impacts, Adaptation, and Mitigation* Global climate change and carbon dioxide: Assessing weed biology and management. pp. 191-208. Imperial College Press, London.

Ziska L.H., Faulkner S. & Lydon J. (2004) Changes in biomass and root: Shoot ratio of field-grown Canada thistle (*Cirsium arvense*), a noxious, invasive weed, with elevated CO_2: Implications for control with glyphosate. *Weed Science* 52, 584-588.

Summary

The climate has changed drastically over the past century and is expected to continue to change in the future. The atmospheric CO_2 concentration is predicted to rise in the future, and partly as a result of this, global temperature will increase. It is important to know how plants respond to these changes, as this determines future biodiversity and food production. Besides, plants have a large influence on atmospheric processes that influence the climate, so there are vegetation-atmospheric feedbacks.

Responses of plants to climate change, and associated atmospheric feedbacks, will depend on overall environmental conditions in which plants grow. Notably, plants often grow in dense communities where they share resources with neighbouring plants, and competition for these resources is often an important selective force. Thereby, plant competition may also strongly influence plant responses to climate change. So, it is very important to know how plants respond to changes in the climate and how this is affected by plant competition to identify how strong the associated feedbacks with the climate are.

To study the effect of plant responses to climate change and the potential effect on the coupling between vegetation and the atmosphere, two optimization approaches were used. The first is simple optimization, here natural selection leads to optimize plant functional traits (i.e. an attribute that has the potential to significantly influence plants performance; like leaf area, stomatal conductance) to maximize fitness. This approach implicitly assumes that optimal trait values of one plant are independent of the trait values of its neighbours, so ignoring that plants strongly compete for resources. Nevertheless, on the leaf scale simple optimality can still be a valid approach, as on this scale there is no influence of competition. The second approach is competitive optimization (or evolutionary game theory). This approach assumes that natural selection results in vegetation stands that are dominated by the best competitors and not necessarily by the best inherent performers. In this case it is assessed to which extent a plant playing a certain strategy (i.e. with a trait value) can be invaded by an individual, playing another strategy. By comparing the simple optimization approach with the competitive optimization approach the effect of competition can be determined.

In **Chapter 2** we start by focussing on optimal leaf level responses to environmental change. It is believed that plants optimize allocation of nitrogen, a key component of the photosynthetic machinery, between ribulose-1,5-bisphosphate (RuBP) regeneration (P_{jl}) and RuBP carboxylation (P_{cl}) to maximize photosynthesis, which occurs when P_{cl} and P_{jl} co-limit photosynthesis. An analytical solution for the optimal N distribution is provided.

We showed that the simulated response of leaf photosynthesis to changes in atmospheric CO_2 and temperature differ substantially when plants are allowed to distribute N optimally within the leaf, compared to the situation where allocation is assumed to be constant. Simulating increasing CO_2 reduced the fraction of N allocated to P_{cl}, while

increasing temperature increased the N fraction allocated to P_{cl}. The simulated increase in leaf photosynthesis with CO_2 elevation was considerably higher when N allocation responded optimally than when this allocation was fixed. A similar but weaker trend was found for warming.

Our simulations also showed that the rate of acclimation – i.e., the time lag between environmental change and trait optimization – may strongly affect predicted photosynthesis, indicating that more research on this time lag and variation therein is needed.

In **Chapter 3** we scale up to the vegetation canopy level. We develop a canopy model with which we investigate how vegetation functioning and structure is influenced by climate change and to which extent competition may modify these effects. To study the effect of competition between plants in a canopy, a comparison of the simple optimality with the competitive optimality approach was made. So, considering different degrees of light competition between neighbouring plants through canopy mixing (simple optimization no mixing versus competitive optimization with mixing). Soybean (*Glycine max*) was used as a reference system.

The model predicts increased net photosynthesis and reduced stomatal conductance and transpiration under atmospheric CO_2 increase. When CO_2 elevation is combined with warming, photosynthesis is increased more, but transpiration is reduced less. When competition is considered the optimal response shifts to produce a larger LAI (leaf area index, i.e. leaf area per unit ground area), but with lower canopy photosynthesis, stomatal conductance and associated vegetation transpiration than when competition was not considered. The evolutionary game theory can explain this, when plants compete for light, a unilateral increase in LAI of a given plant above the optimal LAI results in a relatively smaller increase in self-shading for that plant while it is able to capture a larger fraction of the available light. As a result, this plant can increase its carbon gain by increasing its LAI even if this reduces photosynthesis of the stand as a whole. In the model the canopy N content remains constant, and production of extra leaf area to shade competitors therefore results in reduction of the leaf photosynthetic capacity. Furthermore, inclusion of competition resulted in accurate predictions of the effects of elevated CO_2 on LAI and the seasonal dynamics in LAI as observed in a large number of Free Air CO_2 Enrichment (FACE) experiments. Together, our results illustrate how competition between plants may modify vegetation responses to climate change.

Our experimental results from **Chapter 4** further showed the importance of accounting for competition when considering climate change effects on plant communities. Here we determined the relative contribution of plastic versus genotypic responses to elevated CO_2 on plant performance and define the extent to which these patterns are modified by competition.

To investigate this we grew *Plantago asiatica* seeds originating from three independent natural CO_2 springs and from ambient CO_2 in mono stands of plants origins as well as mixtures of both origins. These plants were grown in CO_2 controlled walk-in climate rooms, under a CO_2 of 270, 450 and 750 ppm. A model was used for upscaling from leaf to whole-plant photosynthesis and for quantifying the influence of plastic and genotypic responses.

We showed that plant performance was mainly determined by plastic and not by genotypic response to changes in growth CO_2. We further found that when grown at elevated CO_2, plants originating from high CO_2 habitats only performed better than those originating from ambient CO_2 habitats when both genotypes compete. Likewise, plants from ambient CO_2 habitats performed better at low CO_2, also only when both genotypes compete. No difference in performance was found in mono stands. So, our results indicate that natural selection in our species under increasing CO_2 might be mainly driven by competitive interactions.

In **Chapter 5** we scale up to a higher aggregation level and study how the coupling between vegetation and the atmosphere is influenced by competition. We used a coupled vegetation-atmosphere model and include a game theoretical procedure to incorporate plant competition and compare the model results against diurnal data from Ameriflux Bondville site over a growing season. We showed that inclusion of competition improved predictions of vegetation and atmospheric processes. A lower photosynthesis was predicted due to plant competition selecting for larger leaf areas, resulting in a less negative net ecosystem exchange of CO_2. We further found that the importance of plant competition on vegetation and atmospheric processes increases with more nitrogen and water availability and may differ between soil types. So, we were able to illustrate the potential effect of plant competition in a coupled vegetation and atmospheric system and showed that it strongly influences this system.

To conclude, the results presented in this thesis show the importance of considering the time scale of leaf-level responses to environmental changes in optimization models. I therefore advocate to further explore the effect of the time scale of response on the level of the whole canopy. In addition, we showed that plants respond mostly on the short term time scale to elevated CO_2 and not on the long term time scale.

More generally, the results presented in this thesis underline the importance of plant competition on vegetation functioning and its influence on atmospheric processes. However, it should be taken into account that the magnitude of this effect might differ between plant types. Furthermore, our results strongly imply that the negative feedback of plants extra carbon uptake under elevated CO_2 would be less strong, and therefore I recommend to further explore the implications of competition on global atmospheric processes to define the effects on the climate.

Samenvatting

Het klimaat is de afgelopen decennia drastisch veranderd en de verwachting is dat deze veranderingen in de toekomst door zullen zetten. Zo wordt er verwacht dat de concentratie CO_2 in de atmosfeer in de toekomst verder toeneemt, en deels als gevolg daarvan zal de temperatuur wereldwijd toenemen. Het is van groot belang om te bepalen hoe planten zullen reageren op deze klimaatveranderingen, dit vanwege de belangrijke rol die planten spelen in de voedselvoorziening en biodiversiteit. Verder hebben planten ook een erg grote invloed op atmosferische processen die het klimaat beïnvloeden. Dit komt door de invloed die ze hebben op de water-, stikstof-, koolstof- en energie stromingen. Er zijn dus tweeweg interacties tussen vegetatie en de atmosfeer, de vegetatie-atmosferische terugkoppelingen.

De reactie van planten op klimaatsverandering, en de terugkoppeling die ze daarbij op de atmosfeer zullen geven, hangt af van de omgeving waarin planten groeien. Meestal groeien planten in een dichte vegetatie, waar ze dus grondstoffen met hun buren moeten delen. In deze milieus oefent competitie voor grondstoffen dan ook een grote selectiedruk uit. Daarom wordt gedacht dat sommige eigenschappen die planten hebben (zoals de hoogte, het bladoppervlak, en de stomataire geleidbaarheid van planten) in hoge mate onder invloed van competitie geëvolueerd zijn, en deze eigenschappen bepalen op hun beurt weer het functioneren van vegetaties. Op deze manier heeft competitie tussen planten dus een grote invloed op hoe vegetaties gaan reageren op klimaatsverandering. Vandaar dat het erg belangrijk is om te weten hoe planten reageren op veranderingen in het klimaat, en hoe competitie tussen planten deze reactie beïnvloedt, om daarmee uiteindelijk vast te stellen hoe sterk de terugkoppeling van met elkaar concurrerende planten op het klimaat is.

In dit proefschrift worden twee optimalisatie methodes gebruikt om te onderzoeken hoe planten op klimaatsverandering reageren, en om het potentiele effect te bepalen van wat ze daarmee hebben op de koppeling tussen vegetatie en de atmosfeer. De eerste methode die gebruikt wordt is simpele optimalisatie, deze methode veronderstelt dat natuurlijke selectie leidt tot optimale eigenschappen van planten waarmee fitness gemaximaliseerd wordt. Hierbij wordt impliciet aangenomen dat de optimale eigenschappen die een plant heeft onafhankelijk zijn van de eigenschappen van de buurplanten, en er wordt dus niet meegenomen dat planten sterk met elkaar concurreren om de beschikbare grondstoffen. Maar als gekeken wordt naar het blad, dan kan simpele optimalisatie nog steeds een goede methode zijn, omdat er op dit schaalniveau minder invloed is van competitie. De tweede methode die in dit proefschrift gebruikt wordt is competitieve optimalisatie, dat een concept is uit de speltheorie. Het is een “spel” waarbij de strategie van een individuele plant afhangt van de strategie die door zijn concurrent “gespeeld” wordt. Het spel wordt gespeeld, omdat de fitness van een individu afhangt van de eigenschappen van het individu zelf, de eigenschappen van de concurrenten en van de omgevingsfactoren. Er wordt gekeken of een vegetatie opstand met planten die een bepaalde strategie spelen (dus met bepaalde specifieke planteneigenschappen) kan worden

geïnvadeerd door een plant die een andere strategie speelt (door andere planteneigenschappen te hebben). Een bepaalde strategie van een populatie die niet meer geïnvadeerd kan worden door een alternatieve strategie, omdat deze geen hogere fitness oplevert voor de concurrenten, is een (evolutionaire) stabiele strategie. Bij competitieve optimalisatie wordt, in tegenstelling tot de simpele optimalisatie, dus aangenomen dat natuurlijke selectie resulteert in een vegetatie opstand die wordt gedomineerd door degene die de het beste kunnen concurreren en dit is dus niet perse degene die de hoogste wezenlijke fitness hebben. Door het vergelijken van de simpele en de competitieve optimalisatie methodes is het mogelijk om het effect van competitie zichtbaar te maken.

Hoofdstuk 2 richtte zich op het niveau van het blad, hierbij keken we naar optimale reacties op veranderende milieuomstandigheden. De grondgedachte is dat planten de allocatie van stikstof naar de verschillende onderdelen van het fotosynthese apparaat optimaliseren om zo de fotosynthese te kunnen maximaliseren. Dit wordt aangenomen, omdat stikstof een erg belangrijk onderdeel is van het fotosyntheseapparaat en omdat stikstof in veel gebieden een beperkende factor is. Het meest gebruikte fotosynthesemodel neemt aan dat de fotosynthese gelimiteerd wordt door één van twee processen. Het eerste is de elektronen transport, P_{jl}, waarbij lichtenergie wordt omgezet tot de hogere energiecomponenten ATP en NADPH, en dit proces is limiterend voor de ribulose-1,5-bisphosphate (RuBP) regeneratie. Het tweede proces is RuBP carboxylatie, P_{cl}, en dit gebruikt deze hogere energiecomponenten om atmosferische koolstof te binden en het vervolgens om te zetten in meer complexere suikercomponenten. Wanneer beide processen de fotosynthese co-limiteren dan heeft de plant een maximale fotosynthese. In hoofdstuk 2 wordt een analytische oplossing voor de optimale stikstof allocatie naar deze beide processen gegeven.

In dit hoofdstuk laten we ook zien dat de bladfotosynthese snelheid onder veranderende atmosferische CO_2 en temperatuur heel anders is wanneer planten hun stikstof verdeling optimaal aapassen in vergelijking met een constante verdeling. Een toename van de CO_2 concentratie in de atmosfeer zorgde ervoor dat de fractie stikstof die naar P_{cl} wordt gealloceerd afnam, terwijl met een toename van de temperatuur die fractie juist toenam. Door de toename in atmosferische CO_2 concentratie nam de bladfotosynthese snelheid toe, en deze toename was een stuk groter wanneer de N verdeling optimaal was in vergelijking met een constante verdeling. Een vergelijkbare maar minder sterke trend werd gevonden voor temperatuurtoename.

Naast de eerder genoemde optimale N verdeling, is ook de snelheid waarmee deze verdeling gerealiseerd kan worden van belang voor de uiteindelijke bladfotosynthese. Dat wil zeggen, er kan een bepaalde tijd zitten tussen een verandering in milieuomstandigheden en het moment dat een plant zijn eigenschappen weer optimaal heeft aangepast. Het is het meest voordelig wanneer planten zich net zo snel aanpassen zodat ze de verandering in

milieuomstandigheden precies kunnen bijhouden. Maar over het algemeen worden planten beperkt door de snelheid waarmee ze zich anatomisch aan kunnen passen, en daardoor passen planten zich waarschijnlijk aan langdurigere gemiddelde omstandigheden aan. Wij lieten in dit hoofdstuk zien dat dit vertragingseffect grote consequenties kan hebben voor de uiteindelijke voorspelde bladfotosynthesesnelheid, en daarom zou hier meer onderzoek naar gedaan moeten worden.

In **hoofdstuk 3** schaalden we op naar het vegetatie opstand niveau. We ontwikkelde een vegetatie opstand model en hiermee onderzochten we hoe het functioneren en de structuur van een vegetatie wordt beïnvloed door klimaatsverandering en in welke mate competitie deze effecten kan veranderen. Om het effect van competitie tussen planten in een opstand te bestuderen vergeleken we de simpele en de competitieve optimalisatie methodes. In het geval van simpele optimalisatie werd er aangenomen dat er geen menging is tussen verschillende planten, hier wordt het lichtklimaat van een plant alleen beïnvloed door zelfbeschaduwing en niet door beschaduwing van buren. Terwijl bij de competitieve optimalisatie er wel menging was tussen verschillende planten, waarbij het lichtklimaat van een plant dus zowel door zelfbeschaduwing als door niet-zelfbeschaduwing wordt bepaald. Voor het model gebruikten we sojaboon (*Glycine max*) als referentiesysteem.

Het model voorspelde dat met een toename van CO_2 concentratie in de atmosfeer, de fotosynthese van de vegetatie zal toenemen en de stomataire geleidbaarheid en de transpiratie af zullen nemen. Wanneer zowel de CO_2 concentratie als de temperatuur toenemen, dan voorspelde het model dat de fotosynthese meer zal toenemen, maar tegelijkertijd zal de transpiratie minder afnemen. Als we competitie in het model meenamen dan resulteerde dit in de productie van meer bladoppervlak, maar met daarnaast een lagere fotosynthesesnelheid, stomataire geleidbaarheid en daaraan gerelateerde lagere vegetatietranspiratie, in vergelijking met wanneer competitie niet werd meegenomen. De speltheorie kan verklaren waarom je met een groter bladoppervlak toch een lagere fotosynthese van de vegetatie kunt krijgen. Wanneer planten met elkaar concurreren om licht, dan resulteert voor een individuele plant een toename in bladoppervlak boven het optimale bladoppervlak in een kleinere toename in zelfbeschaduwing voor die plant, terwijl de plant een grotere fractie van het beschikbare licht ontvangt. Hierdoor kan een groter bladoppervlak resulteren in een hogere fotosynthese voor de individuele plant terwijl dit de fotosynthese van de hele vegetatie opstand juist vermindert. Dit komt omdat in het model de totale hoeveelheid stikstof van de vegetatie opstand constant blijft, productie van extra bladoppervlak om buren te beschaduwen resulteerde dus in een afname van het blad stikstof gehalte en daarmee van de bladfotosynthesecapaciteit. Met het model vonden we ook dat het meenemen van competitie ervoor zorgt dat je goede voorspellingen krijgt van de effecten van verhoogde CO_2 op de hoeveelheid bladoppervlak en op de seizoendynamiek van het bladoppervlak zoals geobserveerd in een groot aantal

experimenten [Free Air CO_2 Enrichment (FACE) experimenten]. Al deze resultaten laten dus zien dat competitie tussen planten de reactie van planten op klimaatsverandering kan beïnvloeden.

De experimentele resultaten uit **hoofdstuk 4** lieten ook het belang zien van het rekening houden met competitie wanneer we keken naar de effecten van klimaatsverandering op plantengemeenschappen. In dit hoofdstuk bepaalden we de relatieve bijdrage van plastische en genotypische reacties op verhoogde CO_2 op het functioneren van planten, en we bepaalden ook de mate waarin dit wordt veranderd door competitie. Om dit te onderzoeken hebben we *Plantago asiatica* planten opgekweekt die afkomstig zijn uit drie onafhankelijke natuurlijke CO_2 bronnen (bron planten) en uit gebieden nabij die bronnen waarbij het CO_2 gehalte de normale huidige waarde heeft (niet-bron planten). Met deze planten creëerden we experimentele opstanden waarin bron planten en niet-bron planten alleen groeiden in zgn. mono-opstanden of samen in mengteelt. Deze planten werden opgekweekt in klimaatkamers met CO_2 niveaus van 270, 450, of 750 ppm. Ook werd een model gebruikt om op te schalen van bladfotosynthese naar de fotosynthese van de hele plant en om hiermee vervolgens de invloed van plastische en genotypische reacties te kwantificeren.

De resultaten lieten zien dat de groei en bladoppervlakte productie van planten vooral bepaald werd door plastische en niet door genotypische reacties op verandering in CO_2 concentratie. Daarnaast vonden we bij de midden-hoge en hoge CO_2 behandelingen (450 en 750 ppm) dat de bronplanten het alleen beter deden dan de niet-bron planten wanneer planten van beide herkomsten met elkaar concurreerden en niet wanneer ze apart opgekweekt werden. Overeenkomstig, deden niet-bron planten het beter onder lage CO_2 alleen wanneer deze met bron planten concurreerden en niet wanneer ze apart werden opgegroeid. Onze resultaten suggereren dus dat natuurlijke selectie in onze soort onder verhoogde CO_2 voornamelijk wordt gedreven door competitieve interacties.

In **hoofdstuk 5** schaalden we verder op, en bestudeerde we hoe de koppeling tussen vegetatie en de atmosfeer wordt beïnvloed door competitie. Hiervoor gebruikten we een gekoppeld vegetatie-atmosfeer model, en voegden hieraan een speltheoretische procedure toe die competitie tussen planten meeneemt. De resultaten van dit model vergeleken we met data van Amerixflux Bondville over een heel groeiseizoen.

We lieten zien dat de toevoeging van competitie voor een verbetering zorgt van de voorspelling van vegetatie en atmosferische processen. Een lagere fotosynthesesnelheid was voorspeld doordat competitie tussen planten resulteert in selectie op meer bladoppervlak, wat resulteerde in een minder negatieve netto ecosysteem uitwisseling van CO_2 (minder CO_2 onttrokken van de atmosfeer, doordat de fotosynthese lager is). Daarnaast lieten we zien dat het belang van competitie op vegetatie en atmosferische processen toeneemt wanneer er meer

stikstof en water beschikbaar is, en dat dit ook afhangt van het type bodem. Hiermee hebben we dus het potentiele effect van competitie tussen planten in een gekoppelde vegetatie en atmosferisch systeem geïllustreerd en lieten daarnaast ook zien dat competitie dit systeem erg sterk beïnvloedt.

Concluderend, de resultaten uit dit proefschrift laten het belang zien van het meenemen van de tijdschaal van acclimatiseren op bladniveau op veranderingen in milieuomstandigheden in optimalisatiemodellen. Het is daarom nodig om dit effect van deze tijdschaal verder te onderzoeken op het niveau van de gehele vegetatie opstand. Daarnaast lieten we ook zien dat planten meestal op de korte termijn reageren op verhoogde CO_2 en niet op de lange termijn.

Daarnaast onderstrepen de resultaten uit dit proefschrift het belang van competitie tussen planten op het functioneren van de vegetatie en de invloed op atmosferische processen. Maar wat wel overwogen moet worden is dat de grootte van het effect anders kunnen zijn bij andere type planten dan de door ons onderzochte soorten. Onze resultaten suggereren sterk dat de negatieve terugkoppeling, waar planten voor zorgen door de extra koolstof opname, onder verhoogde CO_2 minder sterk is dan wordt gedacht; daarom raad ik aan om verder onderzoek te doen naar de implicaties van competitie op globale atmosferische processen om zo het exacte effect op het klimaat beter te bepalen.

Dankwoord

Ten eerste wil ik iedereen bedanken van zowel E&B in Utrecht als CSA in Wageningen. Ik heb me altijd erg thuis gevoeld bij beide groepen.

Ik wil Feike in het bijzonder bedanken, de discussies die ik met Feike heb gehad zijn voor mij heel erg belangrijk geweest, omdat ik hierdoor het model kon ontwikkelen en de uitkomsten daarvan ook beter kon begrijpen. Daardoor zou zonder de bijdrage van Feike mijn proefschrift nooit zo zijn geworden zoals het nu is. Daarom ben ik Feike erg dankbaar dat hij altijd tijd had om met mij te praten.

Maar na een tijdje moest ik toch met “echte” planten gaan werken. Thijs Pons heeft toen meegedacht over de opzet van het experiment en Heinjo over de uitwerking van het experiment, beide wil ik daarvoor bedanken. Tijdens het oogsten van mijn Weegbree experiment heb ik van onder andere van Ambra, Betty, Bin, Meindert, Peter, Simone en Stefan hulp gehad en hun wil ik natuurlijk bedanken. Bin wil ik in het bijzonder bedanken voor zijn hulp met het opkweken en de vermeerdering van de zaden: Bin thank you for all the help not only during the *Plantago* experiment, but alsof or your company during the rest of my PhD. Het onderzoek aan de huidmondjes en vaten wat Ambra tijdens mijn experiment deed vond ik erg interessant, en ik ben daarom erg blij dat Ambra dit gedaan heeft: thank you Ambra for all the work that you did and I also enjoyed your company. En daarmee wil ik ook Hugo bedanken die ervoor heeft gezorgd dat Ambra al dit werk aan de huidmondjes en vaten kon doen.

Natuurlijk wil ik mijn begeleiders Stefan, Max en Niels bedanken, zo ben ik erg blij dat Stefan zich toentertijd bij het team heeft toegevoegd. Ondanks de soms wat lastige begeleiders constructie heb ik veel aan ze gehad. Ze moesten daardoor regelmatig op en neer reizen (naar Wageningen of naar Utrecht), toch maakten ze daar altijd tijd voor vrij.

Als laatste wil ik mijn familie en Meindert bedanken voor al hun morele steun. Zo ben ik erg blij dat ze mij kwamen opzoeken toen ik fotosynthesemetingen aan het doen was in de Kerstvakantie.

Affiliations of co-authors

Niels P.R. Anten
Centre for Crop Systems Analysis, Wageningen University, Wageningen, the Netherlands

Stefan C. Dekker
Department of Environmental Sciences, Copernicus Institute for Sustainable development, Utrecht University, Utrecht, the Netherlands

Daniel Falster
Department of Biological Sciences, Macquarie University, Sydney, Australia

Kouki Hikosaka
Graduate School of Life Sciences, Tohoku University, Aoba, Japan

Max Rietkerk
Department of Environmental Sciences, Copernicus Institute for Sustainable development, Utrecht University, Utrecht, the Netherlands

Feike Schieving
Ecology and Biodiversity Group, Utrecht University, Utrecht, the Netherlands

Frank Sterck
Forest Ecology and Forest Management Group, Wageningen University, Wageningen, the Netherlands

Miki U. Ueda
Graduate School of Life Sciences, Tohoku University, Aoba, Japan

Jordi Vilà-Guerau de Arellano
Meteorology and Air Quality Section, Wageningen University, Wageningen, the Netherlands

Xinyou Yin
Centre for Crop Systems Analysis, Wageningen University, Wageningen, the Netherlands

Curriculum vitae

Marloes van Loon was born on 18 October 1988 and grew up in Kaatsheuvel. In 2006 she graduated from secondary school in Waalwijk and began a 3 year BSc in Plant Sciences at Wageningen University, with the specialisation Plant Production, Ecology and Management. In 2009 she received her BSc degree and continued studying at Wageningen University with a 2 year MSc in Plant Sciences, with the specialisation Crop Science. During her MSc thesis at the Plant Production System group she focussed on adapting and using the bio-economic model FSSIM to assess the impact of agricultural policies on sustainable development of arable farming in Taihu Basin, China. Afterwards, she did an internship at the Netherlands Environmental Assessment Agency in Bilthoven where she compared different models for the calculation of excretion rate of dairy cows. In 2011 she received her MSc degree and started a PhD research at Utrecht University in the Ecology and Biodiversity group. Under the supervision of Niels Anten, Max Rietkerk and Stefan Dekker. Later she was also working on her PhD research at Wageningen University in the Crop and Weed Ecology group. The details of her PhD research can be found in this thesis.